Spatio-temporal variation assessment of zinc concentrations and loads and its source identification in rivers

(河川における亜鉛濃度•負荷量の時空間変動評価と発生源の特定)

July 2021

Doctor of Philosophy (Engineering)

Pertiwi Andarani

ペルティィウィアンダラニ

Toyohashi University of Technology

Abstract

Zinc (Zn) is crucial for life and plays a vital part in organisms' biological activities (humans, animals, and plants). Zn, the fourth-most frequent metal in usage, is widely used in the industrial sector to create products. Zn is the third-most produced non-ferrous metal in Japan and the third-most released chemical in water bodies. Zn has become one of the most critical considerations concerning worldwide water quality, including in Japan, with the role of preserving aquatic life. Since 2003, the Japanese Ministry of the Environment has established an environmental quality standard (EQS) for Zn in surface water (0.030 mg/L) to conserve aquatic life. However, multiple Japanese rivers still could not comply with the EQS in 2019. Therefore, this study aimed to assess the spatial and temporal variation and the source identification of Zn in near-neutral rivers.

This study was conducted in two rivers, affected mainly by urban areas (manufacturing industries) and agriculture located in the vicinity of Aizumame River and the Umeda River, Aichi, Japan. This study consisted of three survey types, i.e., monthly baseflow survey (on sunny days), hourly baseflow survey (on sunny days during weekday and weekend), and hourly stormflow survey (during a rain event). The monthly baseflow survey and the hourly baseflow survey were undertaken in the Aizumame River and the Umeda River. Because a further investigation of the possible Zn source and the underlying factors of the Zn variability was needed, more detailed water parameter measurement was conducted in the Umeda River. Water parameters [Zn, Fe (iron), particulate organic carbon (POC), temperature, pH, electroconductivity, cations, and anions] and riverbed sediments (Zn, Fe, and POC in fine sand, medium sand, and coarse sand) were measured accordingly. The metal content was measured using atomic absorption spectrometry. Hierarchical cluster analysis (HCA), flow analysis, pearson correlation, principal component factor loading analysis (PCFA), load and discharge curve (L-Q model), and end member mixing analysis (EMMA) were performed to assess the association among the parameters and to identify the potential Zn sources.

In the Aizumame River, at the two downstream sampling stations (A4 = 0.059 mg/L; A5 = 0.055 mg/L), the EQS was breached in 2017. Zn levels considerably varied from undetected to 0.139 mg/L. Throughout the year, Zn concentrations along the Umeda River fluctuated in spatial and temporal, ranging from 0.002 to 0.090 mg/L. At the most downstream part of the Umeda River, the annual mean concentration value of 0.031 mg/L exceeded the EQS. Anthropogenic activities have likely influenced the riverine Zn levels in Umeda River.

Most of the Zn concentrations in the river water and wastewater were presented in a dissolved phase in the Umeda River. Seasonal variation also affected the Zn fluctuation in water, in which the highest level was found during the winter and spring. By contrast, in summer and autumn, the Zn concentrations in the riverbed sediment were relatively higher than in other seasons.

The HCA of observation revealed that the middle-lower reach of the Aizumame River and Umeda River has been polluted by Zn. Based on the flow analysis, the industrial area at the downstream section contributed 44% (in summer) to 88% (in winter) of total Zn loading in the Aizumame River. However, in the Umeda River, the industrial Zn input (61%) was clearly observed only in spring. A further data analysis of water parameters in the Umeda River was thus conducted to whether the variability was affected by the water parameters. According to the HCA of variable in the Umeda River, the cations and anions presence are generally less significant in term of metal transport and behavior compared to parameters such as pH, organic matter, and the particulate Fe. The dissolved Zn was grouped together with pH, POC, and HCO_3^-. Furthermore, results of cluster variable analysis were verified by PCFA, which shows that the dissolved Zn (together with pH, Na^+, Cl^-, HCO_3^-, POC, Ca^{2+}, and Mg^{2+}) contributed to a varifactor (industrial point sources) which explains about 15% of the total variance. Meanwhile, particulate Zn participated in the varifactor (agricultural sources), representing 17% of total variance. Moreover, particulate Zn and Fe were also involved in the varifactor (inorganic fraction of SS), constituting 8% of the total variance.

The source identification was also confirmed by the hourly survey. The hourly survey conducted in the baseflow during weekday and weekend revealed that the Zn levels were remarkably higher during weekday, indicating that the industrial point sources contributed to the riverine Zn levels both in the Aizumame River (57%) and the Umeda River (67%). The Fe was potentially originated from natural occurrences. During the stormflow, the Fe concentrations were mainly governed by the suspended solids. The Zn concentrations remained high following the discharge fluctuation in the stormflow and had four subsequent peaks indicating the sources were ubiquitous. Nevertheless, at the end of the stormflow, the Zn source might have been relatively reduced, as shown by lower concentrations. Although the Zn was likely from non-point sources according to the L-Q model, several data points did not fit the prediction interval of the regression line. Using the baseflow and stormflow loads comparison and the EMMA, approximately 74% of the Zn loadings were released from point sources and the rest was originated from non-point sources. Not only industrial discharges but also anthropogenic non-point sources should be adequately managed in order to maintain the Zn level below the toxic threshold level to the aquatic organisms.

Acknowledgements

In the name of Allah SWT, the most gracious the most merciful

It is a genuine pleasure to express my deep sense of gratitude to our honorable laboratory head, Prof. Takanobu Inoue for his excellent guidance, providing many invaluable experiences and opportunities, and kind supports during my PhD study. His meticulous scrutiny, timely advice, scholarly advice and scientific approach have helped me to accomplish this work.

Similarly, sincere gratitude goes to my supervisor Assoc. Prof. Dr. Kuriko Yokota for the support and guidance to achieve the study's objectives. I also would like to thank Prof. Shigeru Kato for the constructive comments and suggestion which greatly improved this dissertation. I am grateful to other members: Dr. Makoto Saga who sacrificed his time to guide me performing analytical procedures using atomic absorption spectroscopy; and Assist. Prof. Dr. Nguyen Minh Ngoc for her kind support and guidance to conduct particulate organic carbon measurements.

I am really grateful to the Japanese Ministry of Education, Culture, Sports, Science, and Technology (MEXT) for the PhD scholarship which gave me opportunities to conduct research that I always dream of.

I would like to thank the Diponegoro University Board and my colleagues at Department of Environmental Engineering (Faculty of Engineering) for the endorsement and encouragement. I sincerely thank my colleagues in the Water Environment Conservation Engineering Laboratory. Special mention to Hardianti Alimuddin for her dedication to accomplish the laboratory works and Moliya Nurmalisa for her useful advice and huge supports. I would like to thank Widyastuti, Aemilia, Samim, and Suzuki for a part of sampling and laboratory works; Jane, Fatin, Husna, Ashkani, Ting, Cavan, Edo, Safira, Mrs. Mega Mutiara S., Mr. Rizal, Adrian, Angelin, Mrs. Farida, Mr. Alex, Mrs. Isti, Mr. Qidun, Aiman, Mr. Fengky, Mr. Lolo, Mr. Ali, and all of Indonesian Student Association fellows for the friendship and supports.

This PhD journey would not be completed without the support of my family. I am indebted to my beloved husband (Mr. Wiwik) and son (Arshaka) for continuous encouragement, supports, and prayers over the year. I would like to dedicate this dissertation to my late father who always support me even in his difficult time and also my mother who always prays for me the best.

Pertiwi Andarani

Contents

List of figures

List of tables

List of abbreviations

Ca	calcium
CRM	certified reference material
CV	coefficient of variation
D-Zn	zinc (Zn) in dissolved phase
D-Fe	iron (Fe) in dissolved phase
EQS	environmental quality standards
EMMA	end member mixing analysis
Fe	iron
H	water level
HCA	hierarchical cluster analysis
L	load
N	eigenvector
Na	natrium
n.d.	not detected (Fe ≤ 0.01 mg/L, Zn ≤ 0.0005 mg/L)
NES	national effluent standards
Mg	magnesium
PC	principal component
PCFA	principal component factor loading analysis
POC	particulate organic carbon
PRTR	pollutant release and transfer register
P-Fe	Fe in particulate phase
P-Zn	Zn in particulate phase
Q	river discharge
RBS	riverbed sediment
SD	standard deviation
SS	suspended solids
st.	sampling station or sampling point
Temp.	temperature
UK	United Kingdom
US-EPA	United States - Environmental Protection Agency
USA	United States of America
WFD	Water Framework Directive
VF	varifactor
ww	industrial wastewater
Zn	zinc

Chapter 1 General introduction

1.1 Background of the study

Depending on the geological setting, heavy metals is natural element occurred in the environment, including surface water. Those heavy metals presents in the environment through rock weathering, surface runoff, and erosion (Dalai et al., 2004). Zinc (Zn) is a trace element that is usually found as the 24th most prevalent element in the earth's crust and is typically classed as a heavy metal. Zn presents on earth while all life developed. However, it should be noted that Zn metal does not occur in the natural environment, instead, it is present only in the divalent state, Zn(II) (Simon-Hertich et al., 2001). The Zn levels in nature, including rock, soil, and surface water vary over wide range from less than 0.01 mg/L and more than 0.2 mg/L in rivers (International Zinc Association, 2014). In soil and rock, it typically ranges from 10 mg/kg to 300 mg/kg. In river systems, metals carried at low and high flows may cause distinct burdens. Sediment-rich water (Jain et al., 2004) generated mostly by natural erosion and atmospheric deposition during storm events may be the source of elevated heavy metal pollution. Sea salt is the most significant source of natural Zn emissions on a worldwide scale, followed by soil particle load (Richardson et al., 2001).

Nonetheless, in United Kingdom (Gozzard et al., 2011), China (Ke et al., 2017), Taiwan (Vu et al., 2017), Canada (Mansoor et al., 2018), and Japan (Mohiuddin et al., 2012; Naito et al., 2010; Shikazono et al., 2008). Zn is increasingly acknowledged as a water quality issue. The Tsurumi River, an urbanized river that flows into Tokyo Bay, has been contaminated by Zn, with anthropogenically contributed Zn accounting for 80.2% of the total (Mohiuddin et al., 2012). On Tsushima Island, Japan, Zn pollution occurs as a result of mining activities and natural exposure of ores and sediments (Shikazono et al., 2008).

Zn has become one of the most important concerns in Japan's water quality, with the goal of protecting aquatic life. Since 2003, the Japanese Ministry of the Environment has legislated an environmental quality standard (EQS) for Zn in surface water (0.03 mg/L) to conserve aquatic life. This number was calculated using laboratory toxicity studies and confirmed using field data on the effects of Zn on aquatic communities (Matsuzaki, 2011).

Due to its large industrial region, Aichi Prefecture on Honshu Island is one of the “Zn elevated sites” (Naito et al., 2010). Manufacturing accounts for 30% of Aichi's overall industrial structure, which is substantially more than the national average (Tachibana et al., 2008).. After 2002, no obvious trends for Zn reduction were identified in this prefecture, suggesting that the implementation of the Zn EQS had

little impact on Zn concentrations (Naito et al., 2010).. However, there are few peer-reviewed publications in this field that quantify Zn in water bodies. It is critical to estimate why Zn concentrations in Japanese river water are elevated.

1.2 Role of Zn in organisms and anthropogenic activities

Zn is necessary for life, since it is involved in a variety of biological processes in humans, animals, and plants, including cell division, protein synthesis, the immune system, and growth (Chasapis et al., 2012; International Zinc Association, 2014; Schroeder et al., 1967; Smith et al., 1973). Because Zn has advantageous qualities such as high durability, anti-corrosion, and wear resistance capabilities (Guo et al., 2010), it is widely used in the industrial sector to produce things from galvanized metal, brass, and die casting (Guo et al., 2010; Tabayashi et al., 2009).

After copper and aluminum, zinc is the third most commonly produced non-ferrous metal in Japan (Ministry of Environment of Japan, 2021). According to statistics from the Pollutant Release and Transfer Register (PRTR), about 608 tons of Zn compounds (water-soluble) are released into public bodies of water in Japan each year (Ministry of Environment of Japan, 2021). It is the third most often emitted chemical in these bodies of water (Ministry of Environment of Japan, 2021). Galvanizing, which protects steel against corrosion, accounts for more than half of the Zn produced annually, followed by Zn oxide, die casting, a vulcanizing agent for tire rubber, and other applications to manufacture brass, tiles, ceramics, glass (Jones et al., 2014), dyes (Oguntade et al., 2015), battery (Mansoorian et al., 2014), and electronic products (Wahaab and Alseroury, 2019). Furthermore, Zn wastewater discharges are caused by the paper and pulp sectors (Carolin et al., 2017). Unlike other heavy metal pollutants, Zn does not represent a health concern to individuals who are exposed to it indirectly through the environment, however direct exposure to Zn oxide (ZnO) and Zn chloride ($ZnCl_2$) does (Autrup et al., 2007; Bodar et al., 2005). Humans, animals, plants, and even microbes, on the other hand, require Zn for development and growth, making it essential to life processes (Chasapis et al., 2012). However, when it exceeds a certain level, which occurs frequently as a result of Zn contamination, it causes persistent toxicity in aquatic life (Amoatey and Baawain, 2019; Bodar et al., 2005; Hatakeyama, 1989; Jensen et al., 2016; Seto et al., 2013).

1.3 Toxicity of Zn in organisms

Even though Zn is a necessary trace mineral, excessive amounts may induce anemia or damage to the kidneys and pancreas in humans (Gyorffy and Chan, 1992; Hein, 2003). High Zn concentrations are hazardous to aquatic species, according to previous studies (Hatakeyama, 1989), including salmonids, crustaceans, and algae (Li et al., 2020), a possible risk to aquatic species (Jensen et al., 2016) and plants (Bhatti et al., 2018). Zn is a significant environmental risk and a harm to aquatic life (Itahashi et al.,

2014; Tsushima et al., 2010). Multiple European nations and Japan's regulatory bodies are apprehensive about Zn toxicity in aquatic ecosystem.

Zn has been assessed as providing intolerable risks in both local and regional scenarios, according to the EU risk assessment study, although the only human health concerns from Zn have been identified as Zn oxide from welding fumes (Autrup et al., 2007). Furthermore, because Zn occurs naturally, its environmental impact cannot be measured in the same way that other human-made chemical compounds. Because Zn occurs naturally, removing it from the environment would be impossible and might potentially have negative consequences across an ecosystem (International Zn Association, 2014).

Statistical data and equations for estimating Zn discharges to surface waters were used to conduct an exposure and risk assessment of Zn in the aquatic environment of Japan (Naito et al., 2010). Due to large biologically available percentages of metals, site-specific risk assessment is particularly important for rivers highly contaminated with metals, particularly rivers influenced by metal industry and mining (Han et al., 2013).

The effect of water physiochemistry on metal toxicity is related to metal bioavailability. A metal is considered bioavailable when it is free for uptake by an organism and can react with its metabolic machinery, which may result in a toxic effect. The main idea behind the bioavailability concept is that the toxic effect of a metal does not only depend on the total (or dissolved) concentration of that metal in the surrounding environment but also on the complex interactions between physiochemical and biological factors.

1.4 Environmental quality standards of Zn

In riverine ecosystems, Zn is typically present in its most ecotoxic form, i.e., Zn^{2+} (Hem 1972; International Zn Association 2014; US-EPA 1980). Consequently, in European countries, stringent environmental quality standards (EQS) on the total fraction of Zn have set the range from 0.008 to 0.125 mg/L, depending on the water hardness (Water Framework Directive, 2010). Specifically, in the UK and Wales, the standards for dissolved bioavailable Zn have been set at 10.9 µg/L, plus ambient background concentrations that depend on catchments/groups thereof (Water Framework Directive, 2015). Meanwhile, in order to protect freshwater aquatic life, the US Environmental Protection Agency set the criterion for total recoverable Zn to 0.047 mg/L as a 24-hour average (US-EPA, 1980).

Two methods for establishing Zn environmental quality standards (EQS) have been adopted by European nations. Water hardness is one of the approaches, because toxicological levels of Zn rise as water hardness decreases. The EQS ranges from 0.008 mg/L (0–50 mg/L $CaCO_3$) to 0.125 mg/L (>250 mg/L $CaCO_3$) for total Zn annual mean concentration (Water Framework Directive, 2010). Because of the large amounts of Zn that are discharged into the water, the United Kingdom considers it a probable

"specific pollutant" (Comber et al., 2008). Another method for predicting bioavailable Zn concentrations, developed specifically in the UK and Wales, is the biotic ligand model (Heijerick et al., 2002). Furthermore, under the WFD, Comber et al. (2008) proposed a tiered approach to the application of metal EQS. Despite greater Zn concentrations during low flow and the fact that these sources produced adverse pollution even when point sources were remediated, Gozzard et al. (2011) showed that high-flow EQS exceedances outnumbered low-flow EQS exceedances generated by non-point sources.

To protect the aquatic ecosystem, in 2003, Japan has enacted an EQS for Zn, namely 0.03 mg/L. The current EQS was the first standard in Japan for protection of aquatic organisms and was enacted in 2003. Before the current EQS of Zn was developed, Zn standards had been administered under the limits for industrial wastewater (5 mg/L) which is more than 100 times higher compared to the current EQS (Matsuzaki, 2011), while the current effluent standards of Zn were set at 2 mg/L in 2006 (Yamagata et al., 2010). The current EQS was developed using laboratory toxicity tests and has been validated using field data by Matsuzaki (2011). However, EQS based on total metal concentrations and laboratory toxicity data for conditions unrepresentative of field situations may both under protect and overprotect (Bass et al., 2008).

Based on the Ministry of Environment of Japan (2020), Zn levels in 1.6% of 1,203 Japanese rivers still breached the EQS in 2019. By contrast, all of monitored points in lakes and sea were below the EQS value (Ministry of the Environment of Japan: Water and Air Environment Bureau, 2020). Based on the PRTR Data (Ministry of Environment of Japan, 2021), from 2001 to 2019, Aichi Prefecture had the fourth largest Zn discharges to the public water bodies (approximately 38 tons/year) to the public water bodies. The first highest Zn discharging prefecture was Osaka, followed by Tokyo, and Kanagawa Prefecture.

1.5 Fate and pathway of Zn in the environment

Figure 1.1 shows the cycle of Zn in the environment. Zn is originally extracted from mineral ore bodies (mainly sphalerite, ZnS) and going through refinery into metallic state. This metal containing products generally have a long-life span and could be recovered and recycled at the end of life. However, if the products exposed to the atmosphere, corrosion may occur which results in Zn leaching into the environment (International Zn Association, 2014).

Zn compounds [ZnO, $ZnCl_2$, $Zn_3(PO_4)_3$] uses may also contribute small non-point release. Tyres that made of ZnO contained rubber is an important non-point source of Zn into the environment (tyre wear). Along with natural processes (erosion and weathering), various Zn compounds are mobilized into the environment. The Zn interaction with other components of water, sediments, and soil will define the fate of Zn in the environment. The forms (fractions) of Zn depend on interactions with the existing

components as well as where it will ultimately end up. Most of the Zn will return to the stable chemical form (often ZnS) from which it was originally mined (International Zn Association, 2014). This "mineralization" back into stable chemical forms closes the "natural cycle" (International Zn Association, 2014). This stable form has exceptionally low solubility and potential uptake by organisms. Therefore, the concern regarding Zn pollution is often focused on the complex interactions among Zn and the various environmental compartments because Zn is considered as bioavailable for uptake by organisms.

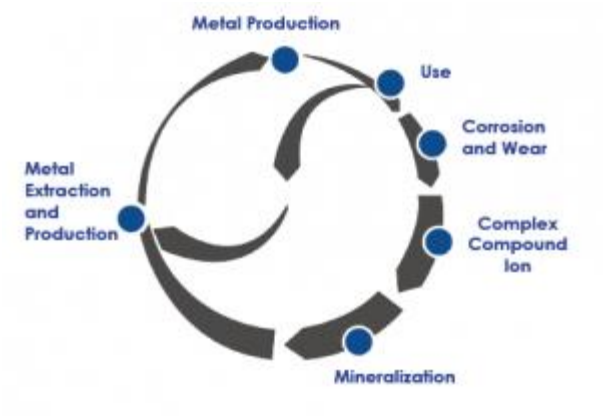

Figure 1.1 Zn cycle in the environment
(Source: International Zn Association, 2014)

1.6 Zn origins and factors affecting the variability of Zn in rivers

Zn may originate from various sources both natural occurrences and anthropogenic sources. Figure 1.2 shows the potential sources of Zn which may also involve point sources and non-point sources. Zn rarely occurs in the natural environment in its metallic state, but it is present in Zn(II) contained in minerals as a major component. In the soil environment, Zn concentrations vary by three or four orders of magnitude (Simon-Hertich et al., 2001). In Canada, a mean value of 80 mg/kg for stream sediments was reported (Simon-Hertich et al., 2001). The Zn-rich surface sediment is also a possible source of Zn in the river, particularly during the stormflow when the river water level is elevated (Gozzard et al., 2011). In the suspended sediment of world rivers, the average concentration is 208 ± 237 mg/kg (Viers et al., 2009). Mineral weathering may result in Zn release to water as soluble compounds. The global load of Zn to water through erosion was estimated at 915,000 t/year (GSC, 1995). Meanwhile, annual global emissions to air were estimated to be 19,000 t (windborne soil particles), 9600 t (igneous emissions), and 7600 t (forest fire) (Simon-Hertich et al., 2001). By including the biogenic emissions from volcanic activity, Simon-Hertich et al. (2001) estimated Zn input to atmosphere at 350,000 t/year. However, the uncertainties involving these data are quite high, thus it is difficult to estimate a ratio of natural to anthropogenic emissions into air for Zn (Simon-Hertich et al., 2001).

Total Zn concentrations in natural waters span six orders of magnitude and are heavily influenced by human activities (Hogstrand, 2011). However, in most surface water, Zn concentrations in total fraction rarely exceed 0.05 mg/L (Naito et al., 2010). Municipal and industrial effluents provide major sources contribution of Zn to surface water (Naito et al., 2010). In the European countries, mining and abandoned mines are one of the significant Zn contributors in the surface water (Gozzard et al., 2011; Resongles et al., 2015; Rudall and Jarvis, 2012). As shown in Figure 1.3, Zn loadings to surface water in Japan are highly influenced by the anthropogenic activities. Atmospheric corrosion of Zn products (galvanized materials and Zn alloys) is one of the largest anthropogenic Zn sources accounted for 30% of the total Zn loads in Japan (Naito et al., 2010) and the Netherlands (Bodar et al., 2005). Zn loadings from non-point sources are significant, but the non-point sources impact on Zn concentrations are limited during normal surface water levels or in the baseflow (Naito et al., 2010). Zn is one of the most abundant transition metals in road runoff (Legret and Pagotto, 1999). Therefore, considerable amount of Zn originates from point and non-point sources associated with human activities.

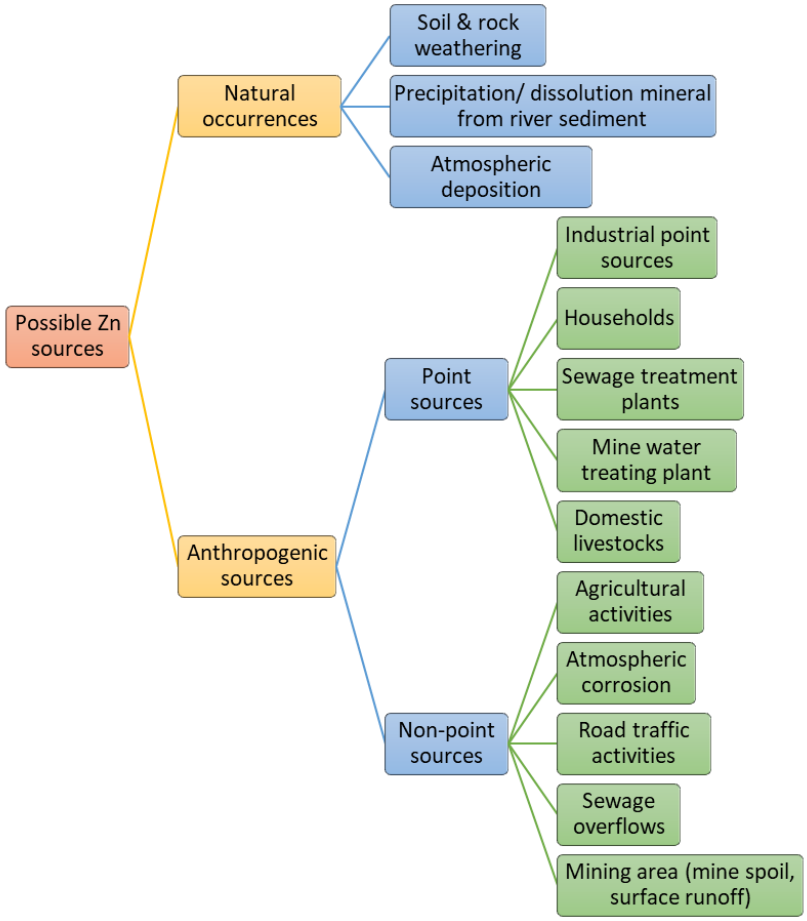

Figure 1.2 Zn possible origins, i.e. from natural occurrences and anthropogenic sources which including both point sources and non-point sources

These various Zn sources, particularly the natural occurences deposited in the environment in particulate phase or larger deposits, are leached by rainfall, resulting in water runoff with elevated Zn concentrations. Moreover, the potential anthropogenic sources such as the atmospheric corrosion will eventually release Zn into the river water system. In urbanized river, previous research reported that the Zn was mostly transported in dissolved form which potentially has higher bioavailability to aquatic organisms (Le Pape et al., 2012). River catchment plays a key role in the water cycle, capturing and storing enormous quantities of water, which ultimately supply a large part of the available freshwater on Earth. Thus, controlling Zn concentrations in surfacewater is a major environmental issue.

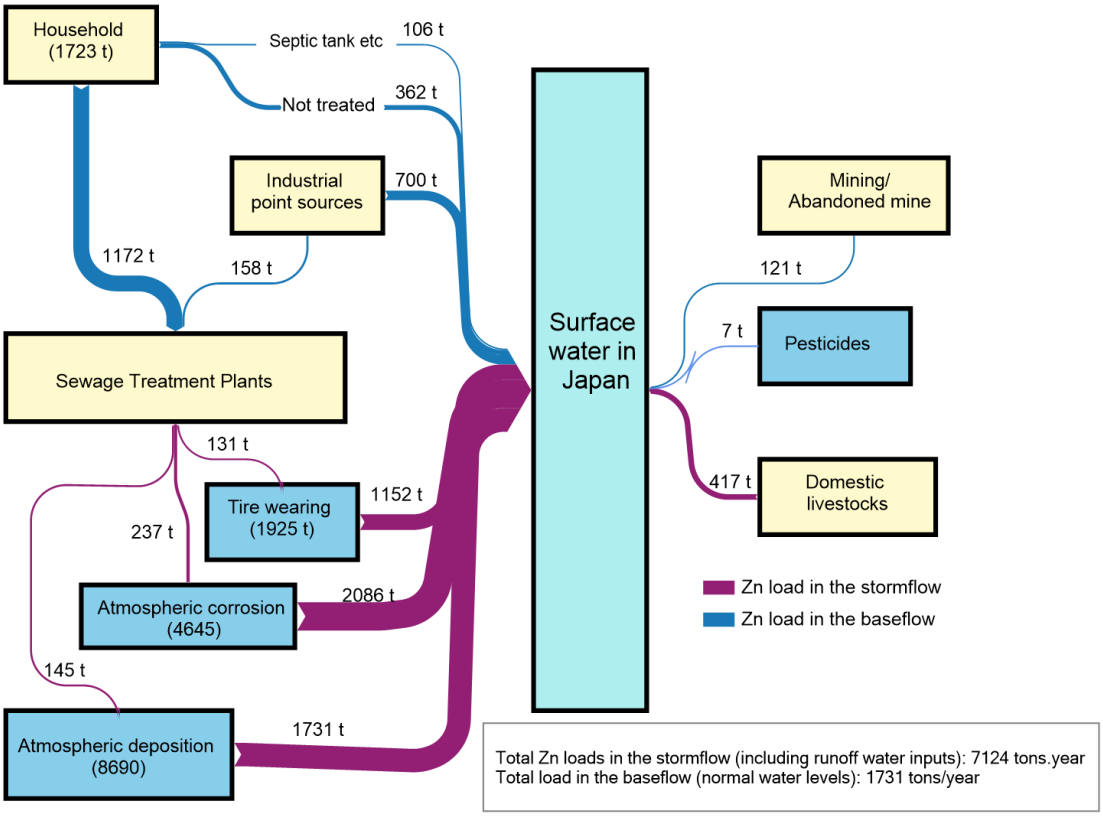

Figure 1.3 Total Zn loads to surface water in Japan: domestic livestocks estimation has relatively high uncertainty
[Adapted from Naito et al. (2010)]

Zn is a conservative element, and its toxicity depends on the chemical form, i.e. the speciation. The speciation strongly affects Zn mobility during variations of river physico-chemical conditions (Le Pape et al., 2012). Chemical forms of Zn in aqueous phase occur such as cationic, inorganic and/or organometallic forms, incorporated into crystalline structures, adsorbed onto mineral surfaces (iron, manganese oxides, and clays), or metal alloys (Manceau et al., 2002). In the water column, ions are partitioned between particulate and dissolved fraction but are mainly carried by the solid phase, apart

from Ca, Mg, K, and Na (Viers et al., 2009). For trace element, i.e. Zn, this partition depends both on total loads and physico-chemistry of the river system. Speciation of Zn in waters is modulated by pH and by the concentration of organic and inorganic ligands in solution (Hogstrand, 2011; Le Pape et al., 2012). The size of suspended and riverbed sediment also play important role in the partition. Within the particulate phase, Zn is usually associated with iron or manganese oxy(hydro)oxides and organic matter (Gammons et al., 2015; Nimick et al., 2011; Parker et al., 2007), in calcite or sulfide minerals (Priadi et al., 2011), or clay components (Jacquat et al., 2009). In most natural waters the free Zn^{2+} ion is the dominant inorganic Zn species. The diel physico-chemical properties changes may also affect the diel variability of Zn which are illustrated in Figure 1.4. The important processes that may cause diel cycles in rivers are changes in river discharges, sewage/industrial treatment effluent discharges, photosynthesis and respiration, inorganic photochemical reactions, reductive dissolution of hydrous metal oxides (Fe or Mn), pH and temperature dependent adsorption, pH and temperature dependent mineral solubility and biological assimilation (absorption) (Gammons et al., 2015). In near neutral rivers, previous researches revealed that only dissolved Zn exhibited diel fluctuation (Bourg and Bertin, 1996; Gammons et al., 2015; Nimick et al., 2011, 2003; Shope et al., 2006). Photosynthesis depends on sunlight and typically peaks when the sun is overhead, while respiration consumes O_2 and releases CO_2 and nutrients to the river water. The simplified reactions are written as follows (Gammons et al., 2015):

Photosynthesis : $CO_2 + H_2O + \text{sunlight} \rightarrow CH_2O\ (\text{org.}) + O_2$ (1.1)

Respiration : $CH_2O\ (\text{org.}) + O_2 \rightarrow CO_2 + H_2O$ (1.2)

The respiration is usually accompanied by pH decrease due to CO_2 release. Respiration occurs throughout the day and night but is still dependent on temperature in which faster in warm than in cold water. Thus, on sunny days, the rate of photosynthesis is commonly higher than respiration resulting dissolved oxygen and pH increase. The pH is affected primarily because of the CO_2 release, a weak acid, which drives the following reaction to the right, increasing activity of H^+:

$CO_2\ (aq) + H_2O = HCO_3^- + H^+$ (1.3)

In contrast, because photosynthesis does not occur at night, only respiration persists resulting in DO and pH decrease. However, it should be noted that diel pH cycles amplitude are usually less than 1 pH unit (Gammons et al., 2015). Among previously mentioned processes that influence diel Zn variation, it is likely that pH and temperature dependent adsorption is important process that influences the mobility of Zn in natural water as long as suitable mineral or organic surface present in the river system. Most adsorption reactions are kinetically fast unlike dissolution-precipitation of mineral so that the equilibrium could be maintained during parts of the day-night hours when pH and temperature of the water are swiftly changing (Gammons et al., 2015). The Zn cycles in near-neutral to alkaline rivers have highest concentrations at or shortly after down whereas lowest levels in the afternoon (Nimick et al.,

2011). In contrast to Zn that has positive charge, diel As cycles usually has the opposite pattern of the Zn cycles because As has negative charge.

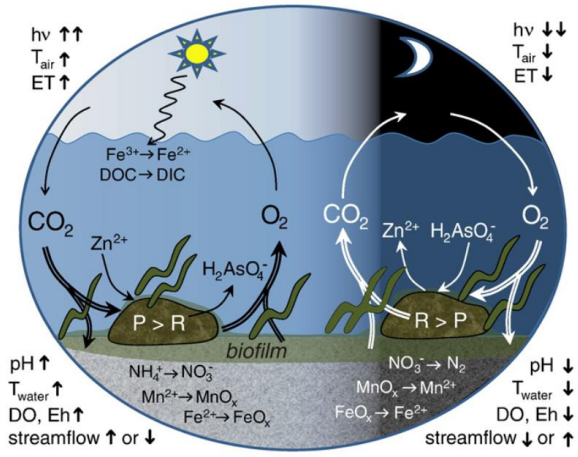

Figure 1.4 Diagram showing key diel biogeochemical processes affecting aqueous chemistry of streams with neutral to alkaline pH: bold arrows indicate increase (↑) or decrease (↓). DIC = dissolved inorganic C. DO = dissolved O_2. DOC = dissolved organic C. Eh = oxidation–reduction potential. ET = evapotranspiration. $H_2AsO_4^-$ = common aqueous species of As. hν = photons. P = photosynthesis. R = respiration. T = temperature. Zn^{2+} represents cationic trace metals and rare earth elements.
(Source: Nimick et al. 2011)

As depicted in Figure 1.5, it is obvious that the Zn variability in both phases is associated with the sources, seasons and weather, and catchment characteristics, i.e. catchment area, river discharges, geochemical settings, and surrounding landuses which eventually affects the physico-chemistry of the river. Thus, this dissertation addresses the Zn issue primarily about the Zn variability in dissolved and particulate phase in different sampling events which are shown in Figure 1.6. The spatial variation refers to two different catchments in Aichi prefecture, namely Aizumame River and Umeda River. In each river catchment, several sampling stations were appointed based on the possible sources and the land uses in the vicinity of sampling stations. Basically, two different sampling campaigns are conducted, i.e., in highflow (in this dissertation referred to as stormflow) when the samples collected during rain events and lowflow (referred to as baseflow) when sampling campaigns conducted on sunny days. The baseflow comprised the monthly survey and hourly survey which has different specific objectives. To identify the seasonal variation, it is important to undertake monthly survey which also addressed the issue of agricultural river catchment when the irrigation and non-irrigation scheduled over the year. Diel variability of Zn affected by the diel changes of physico-chemistry is also discussed in the hourly sampling events.

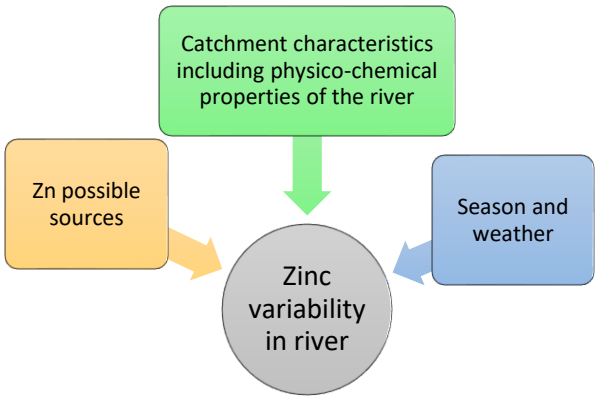

Figure 1.5 Factors involving Zn variability in river

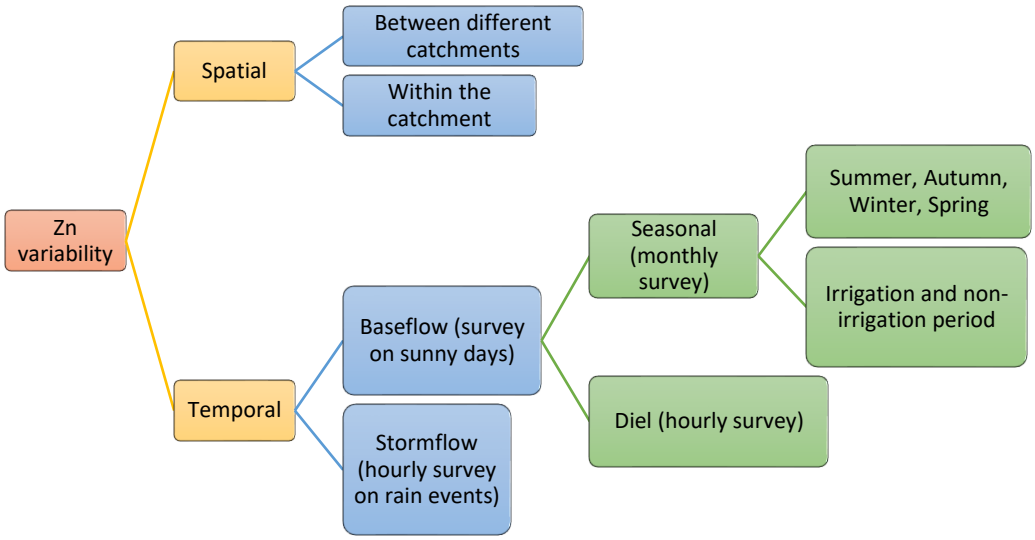

Figure 1.6 Problem formulation on the Zn variability in river

1.7 Aim and objectives

The aim of this study was to assess the spatial and temporal variation and source identification of Zn in near-neutral rivers located in Aichi Prefecture, Japan. The Zn dynamics in the river system could be different in each sampling event. To characterize the contamination tendency and their potential implications on the river system, it is necessary to analyze both dissolved and particulate concentrations of Zn. However, first of all, a general trend of Zn contamination in total fraction should be assessed. Table 1.1 and Table 1.2 show the objectives that would be addressed in this dissertation. The table also includes the parameters, survey type, sampling period, and sampling location (Aizumame River or Umeda River).

Specifically, the objectives were:

1. To analyze Zn variations in different sampling stations and seasons in the Aizumame River and the Umeda River
2. To analyze temporal variability of Zn concentrations and to compare Zn levels during weekday and weekend in the Aizumame River and the Umeda River
3. To analyze Zn variations and related parameters in different sampling stations and seasons in the Umeda River
4. To analyze Zn variations in the riverbed sediment in different sampling stations and seasons and the grain size effect in the Umeda River
5. To compare the diel D-Zn, P-Zn, D-Fe, P-Fe, and POC concentrations during weekday and weekend in the baseflow
6. To evaluate the variability of Zn concentrations and loads in the stormflow
7. To analyze Zn transport in the Umeda River
8. To identify cluster of sampling locations and water parameters related to the Zn variability in the Aizumame River and the Umeda River
9. To estimate the underlying factors governing the variability of water parameters, including Zn, in the Umeda River
10. To analyze Zn load balances during irrigation and non-irrigation period as well as the seasonal variation in the Aizumame River and the Umeda River
11. To estimate the Zn loads from point sources and non-point sources in the Umeda River
12. To determine the contribution of industrial point sources affected the riverine Zn loads in the Umeda River

The interactions between Zn and other components in the river systems exhibit a complex phenomenon. It was hypothesized that the Zn concentrations vary between seasons and sampling locations. Due to a dense industrial area, it is possible that the industrial wastewater contributes significant Zn loading into the river. However, the proportion of Zn and the speciation are still unknown. Iron (for inorganic substance) and POC (for organic substance) was considered as a suitable indicator for Zn dynamics because adsorption of Zn is favorable in a near-neutral river (Gammons et al., 2015; Nimick et al., 2003). Each event's major sources of Zn contamination were determined. In addition, amounts of Zn contribution from point and non-point sources to river water were estimated using a simple end member mixing analysis.

1.8 Organization of the thesis

A total of five sampling campaigns and followed by laboratory analyses was conducted to address the above hypothesis. The organizations of the thesis entitled "Spatio-temporal variation assessment of zinc concentrations and loads and its source identification in rivers", including the location involved, parameters, survey type, sampling time and conditions, is described in Table 1.1 and Table 1.2. The chapters are as follows:

- Chapter 1 is designed to highlights the background and general introduction to this study. The summarized literature reviews are presented to clarify this work in the context of previous studies and literatures. The significance of this study is presented to fill in the knowledge gap of Zn studies, particularly in monitoring assessment.
- Chapter 2 describes the study areas, sampling collection, river discharge measurement, analytical methods as well as its quality assurances and quality control, and finally the statistical analyses including the descriptive statistics, Pearson correlations, and multivariate analytical statistics.
- Chapter 3 discusses the Zn concentrations in total fraction and its loadings in the Aizumame River and the Umeda River both in the monthly survey and the weekday-weekend survey.
- Chapter 4 highlights an assessment of aqueous Zn levels (both in dissolved and particulate phase) and Zn levels in the riverbed sediments (fractionated to three grain sizes) in the Umeda River through a regular sampling campaign undertaken monthly in a year. More extended water quality parameters (temperature, pH, EC, SS, Fe, POC, cation and anion) were measured to analyze the Zn behavior in the river system.
- Chapter 5 presents an evaluation of high-resolution temporal samplings conducted in the Umeda River in the baseflow on sunny days (weekday and weekend) and in rain event (in the stormflow). The samples were collected hourly. The comparison of weekday and weekend surveys is presented to identify the possible sources both during weekday and weekend using the additional parameters such as Fe and POC.
- Chapter 6 highlights the factors influence Zn transport within the river system. The multivariate analytical statistics were applied to clarify the correlations among sampling stations, seasons as well as the Zn sources or underlying factors in the baseflow. The average mass balances are presented to distinguish the Zn load trend between the irrigation period and non-irrigation period, seasonal variation, and weekday-weekend comparison. Lastly, the ratio of baseflow and stormflow levels as well as the weekday and weekend revealed the contributions of point sources and non-point sources, specifically industrial point sources.
- Chapter 7 concludes the findings throughout this study.

Table 1.1 Chapters of results and discussions grouping based on the objectives

Chapter	Objectives	Data analysis	River	Compartment	Parameter	Survey Type	Sampling time and condition
Chapter 3	**Monthly survey:**				T-Zn		
Spatial and temporal variability of T-Zn concentrations and loads	To analyze Zn variations in different sampling stations and seasons	Spatial and temporal variability		Water	Q	Monthly	on weekday, during baseflow, monthly from May 2016 to December 2017 (20 months)
			Aizumame		T-Zn	Weekday-Weekend	**September–October 2017 survey (for 48 hours):**
	Weekday and weekend survey:			Water	Q	(hourly sampling)	**Weekday**: 17:00 (14 Sep) – 16:00 (15 Sep) 2017
	To analyze the temporal variability of Zn concentrations	Temporal variability					**Weekend**: 17:00 (30 Sep) – 16:00 (1 Oct) 2017
	To compare Zn levels during weekday and weekend	Comparison between weekday and weekend Zn levels		Water	T-Zn	Monthly	on weekday, during baseflow, monthly from August 2019 to July 2020 (12 months)
					Q		
			Umeda	Water	T-Zn	Weekday-Weekend	**February 2020 survey (for 50 hours):**
					Q	(hourly sampling)	**Weekday**: 17:00 (5 Feb)–17:00 (6 Feb)
							Weekend: 17:00 (8 Feb)–17:00 (9 Feb)

Table 1.1 Chapters of results and discussions grouping based on the objectives *(Continued)*

Chapter	Objectives	Data analysis	River	Compartment	Parameter	Survey Type	Sampling time and condition
Chapter 4.1 Spatial and temporal variability of Zn in particulate, dissolved phase, and riverbed sediment in the Umeda River	To analyze Zn variations and related parameters in different sampling stations and seasons	Spatial and temporal variability of Zn in particulate and dissolved phase Descriptive statistics of the water parameters	Umeda	Water	pH, EC, Temp.	Monthly	on weekday, during baseflow
					Q		Monthly survey for 9 months:
					D-Zn		2019: Aug, Oct, Nov
					D-Fe		2020: Jan, Feb, Mar, Apr, May, Jun
					HCO_3^-		
					major anion and cation		
				SS	P-Zn		
					P-Fe		
					POC		
Chapter 4.2 Zn levels in the river bed sediments	To analyze Zn variations in different sampling stations and seasons	Spatial and temporal variability of weighted average values	Umeda	**River bed sediment**		Monthly	on weekday, during baseflow
				fine sand (<300 µm)	Zn 0.3		
					Fe 0.3		Survey for 7 months:
					POC 0.3		2019: Jul, Aug, Sep, Nov
				medium sand (300–600 µm)	Zn 0.6		2020: Jan, Mar, May
	To identify the effect of grain size in Umeda River	Variability among respective grain sizes			Fe 0.6		
					POC 0.6		
				coarse sand (600–1000 µm)	Zn 1.0		
					Fe 1.0		
					POC 1.0		

Table 1.1 Chapters of results and discussions grouping based on the objectives *(Continued)*

Chapter	Objectives	Data analysis	River	Compartment	Parameter	Survey Type	Sampling time and condition
Chapter 5 Assessment of Zn in surface water through high-resolution temporal sampling in Umeda River	To compare the diel D-Zn, P-Zn, D-Fe, P-Fe, and POC concentrations during weekday and weekend in the baseflow	Temporal variability of Zn, Fe, and POC every hour	Umeda	Water SS	Q D-Zn D-Fe P-Zn P-Fe POC	Weekday-weekend (hourly sampling)	**February 2020 survey (for 50 hours):** **Weekday**: 17:00 (5 Feb)–17:00 (6 Feb) **Weekend:** 17:00 (8 Feb)–17:00 (9 Feb) **October 2020 survey (for 102 hours):** **Weekday**: 08:00 (1 Oct)–23:00 (2 Oct) and 00:00 (5 Oct)–13:00 (5 Oct) **Weekend:** 00:00 (3 Oct)–23:00 (4 Oct)
	To evaluate the variability of Zn concentrations and loads in the stormflow	Temporal variability of Zn, Fe, and POC every hour		Water SS	Q D-Zn D-Fe P-Zn P-Fe POC	Stormflow (hourly sampling)	**September 2020 survey (for 42 hours):** 14:30 (6 Sep)–07:30 (8 Sep)

Table 1.2 Chapters of results and discussions grouping based on the objectives (Chapter 6)

Chapter	Objectives	Data analysis	Dataset
Chapter 6 Identification of possible Zn sources and underlying factors governing the Zn concentrations variability	**1.** To identify clusters of stations and seasons that have similar tendency	Cluster observations (mean value at each stations)	Dataset presented in Chapter 4
	2. To compare Zn load flow analysis during irrigation and non-irrigation period, as well as the seasonal variation	Flow analysis of T-Zn and Q (irrigation vs non-irrigation period; spring vs summer vs autumn vs winter)	Dataset presented in Chapter 3
	3.1 To estimate the mobility of Zn using log ratio of D-Zn and P-Zn as well as Fe	Log ratio of dissolved and particulate concentration	Dataset presented in Chapter 4
	3.2 To estimate underlying factors governing the variability of water parameters, including Zn, using pearson correlation and principal component factor loading analysis	Pearson correlation and principal component factor loading analysis	Dataset presented in Chapter 4
	4.1 To determine how much industrial point sources affected the riverine Zn loads using weekday and weekend loads	Zn loadings calculation and its ratios	Dataset presented in Chapter 5
	4.2 To estimate the Zn loads from point sources and non-point sources between during the baseflow and the stormflow	Zn and Fe load ratios	Dataset presented in Chapter 5

Chapter 2 Materials and methods

2.1 Description of the study area

Japan, located in East Asia, has a warm and humid climate. In 2020, the daily mean temperature varied from 7.9 °C in December–January to 28.9 °C in August in Toyohashi City. The humid climate is resulted from the high precipitation during *Tsuyu* (in June and July) except on Hokkaido, typhoons (in September and October), and snowfall on the north side of the archipelago. The annual mean precipitation is expected to be around 1600 mm, according to the Japan Meteorological Agency (2021). The lowest precipitation quantity (about 50 mm per year) occurs in January, while the maximum precipitation amount (roughly 100 mm per year) occurs in September or October (approximately 200 mm). As a result, rivers have different seasonal flow patterns (Yoshimura et al., 2005). According to Japan Meteorological Agency (2021), the months representing summer, autumn, winter, and spring are June–August, September–November, December–February, and March–May, respectively. The study was conducted in two rivers in Aichi Prefecture, Japan, namely Aizumame River and Umeda River. The locations of these rivers are illustrated in Figure 2.1.

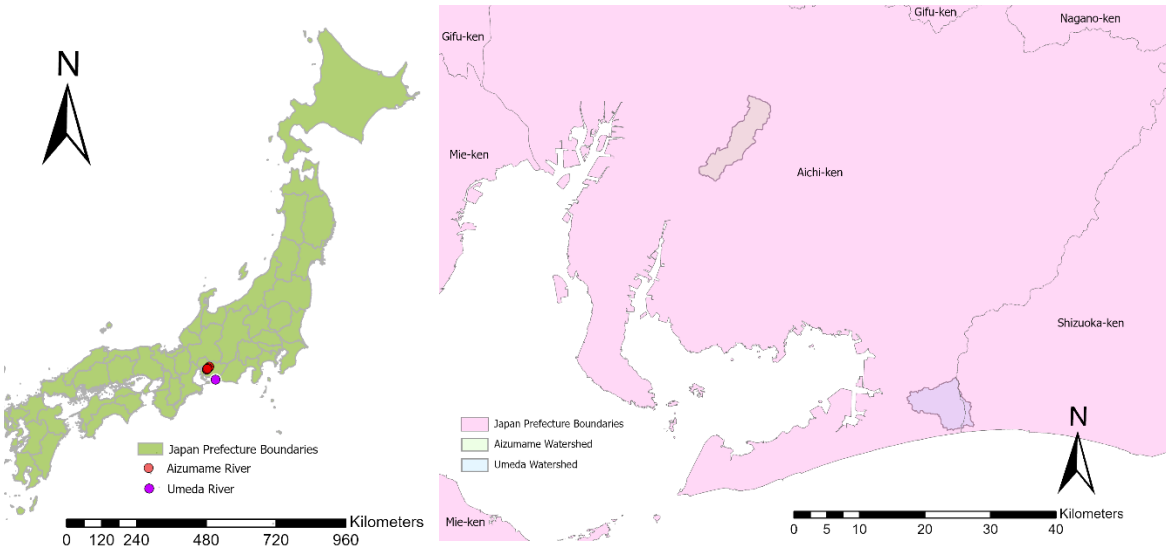

Figure 2.1 Location of two study areas in Aichi Prefecture: Aizumame River and Umeda River

As shown in Figure 2.2, the major soil types in the Chubu area of Japan are andosols and cambisols, with acrisols also found in the Aizumame River and Umeda River catchments (Kanda et al., 2018; Matsuyama et al., 1994),. The fine component of andosol is made up of allophane, imogolite, and ferrihydrite, as well as Fe- and Al-organic matter complexes. They have a low bulk density, high organic matter levels, variable charge (Kögel-Knabner and Amelung, 2014), and significant heavy metal

concentrations due to their unusual mineralogy (Levard and Basile-Doelsch, 2016). Acrisols (Britannica, 2021) and cambisols (Driessen and Deckers, 2001), on the other hand, have very few weatherable minerals.

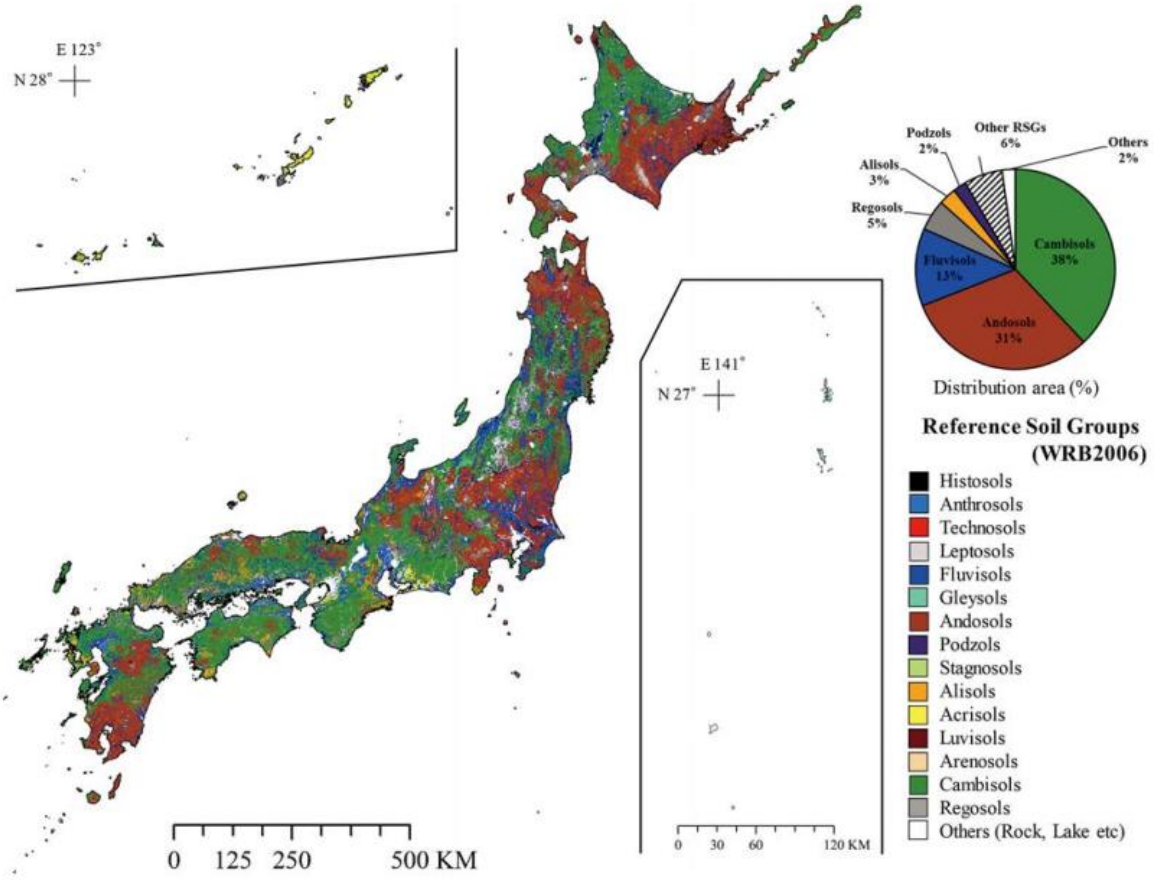

Figure 2.2 The 1:200,000 soil map of Japan with mapping units based on the reference soil groups of the World Reference Base for Soil Resources 2006
(Source: Kanda et al., 2018)

2.1.1 Aizumame River

This study focused on the Aizumame River (137°7'15"E 35°7'49"N – 137°3'29"E 34°59'58"N and 137°2'11"E 35°1'40"N – 137°9'19"E 35°6'43"N), in Aichi Prefecture located in the middle region of Honshu Island. Toyota City is traversed by the Aizumame River. Prior to its confluence with the Aizumao River, the river is about 20.8 kilometers long. Upstream of the confluence of tributaries, five sample sites were set on the mainstem of the Aizumame River. Figure 2.3. depicts the position of the sample locations. There were four sample sites in the tributaries. The sample locations were about 15–80 meters before the confluence of the two rivers (Figure 2.4). Station A1 depicts the area farther upstream where no Zn contamination was predicted. A2 was found around 7 kilometers downstream of where a tributary of A11 enters. A21 is a tributary where effluent from a few industrial locations was

released. A3 was established after around 760 meters, just before a tributary where several industrial sites discharged effluent (A31). Many industrial operations discharge effluent into a nearby tributary (A41). The position of A4 was located at the mainstem river before the intersection with the A41. Finally, A5 was the location further downstream before the Aizumao River's confluence. The weekday-weekend study was conducted at the most downstream station on A5 (Komashin Bridge).

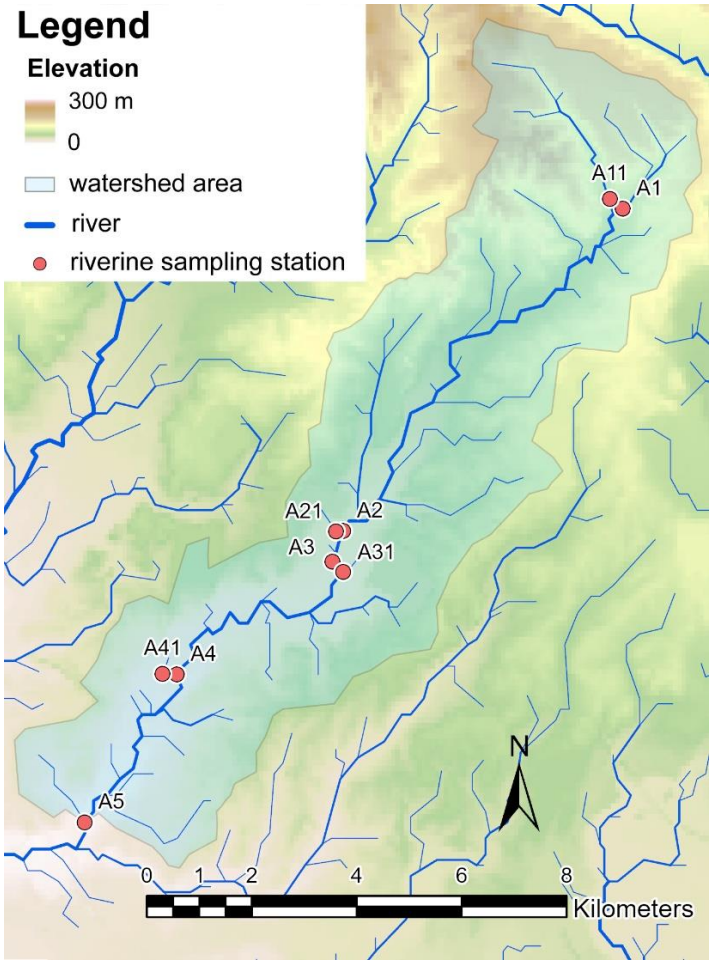

Figure 2.3 Sampling stations in the Aizumame River

The watershed area at the most downstream sampling station is 44.8 km^2. A general illustration of land use and land cover in the Aizumame River catchment area can be seen in Figure 2.5. As illustrated inFigure 2.6, land use in the Aizumame River watershed includes urban sites (42.2%), paddy fields (12.4%), crop land (30.0%), bamboo (4.7%), forest (4.3%), grassland (2.9%), bareland (2.0%), solar panel (0.8%), and river (0.7%).

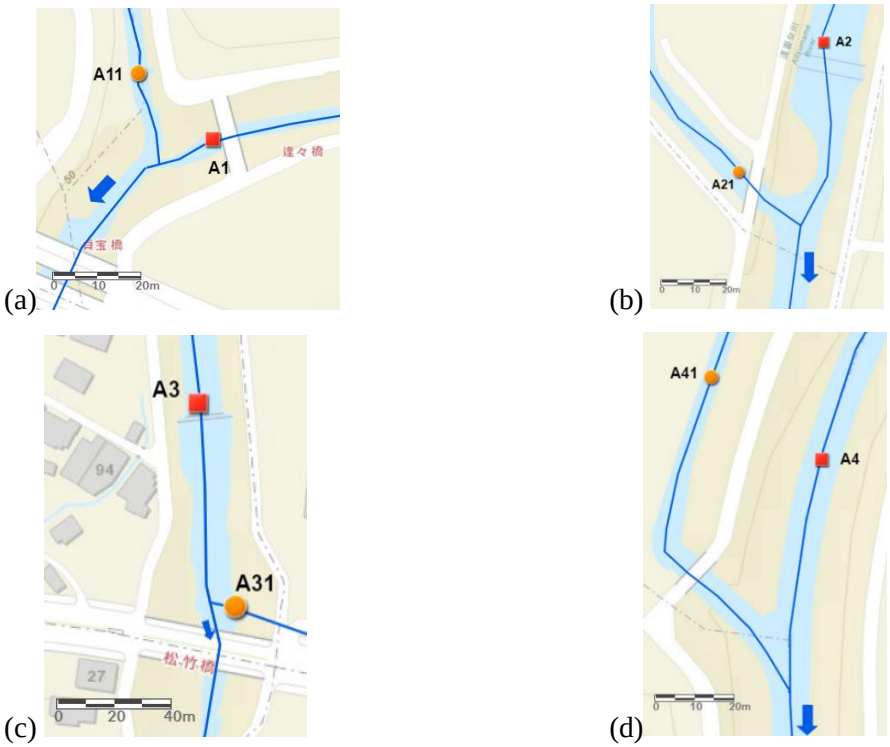

Figure 2.4 Details of the sampling station in the mainstream located just before the confluence with the respective tributary: (a) A1 and A11; (b) A2 and A21; (c) A3 and A31; (d) A4 and A41

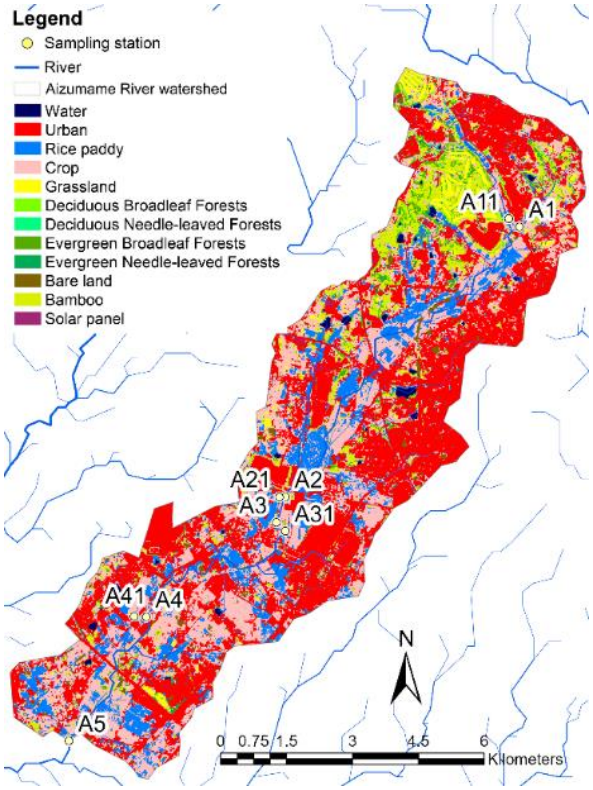

Figure 2.5 Land use and land cover in the Aizumame River catchment area
[Land use and land cover maps are provided by ALOS-2/ALOS Science Project (JAXA, 2021)]

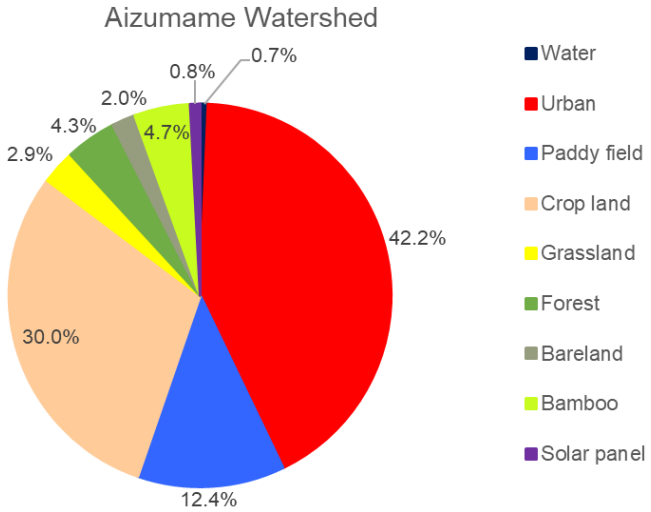

Figure 2.6 Land use and land cover of the Aizumame River watershed at A5

The geology consists of sedimentary rocks and accretionary complexes (Geological Survey of Japan, 2021). The catchment has mud, sand and gravel (Geological Survey of Japan, 2021).

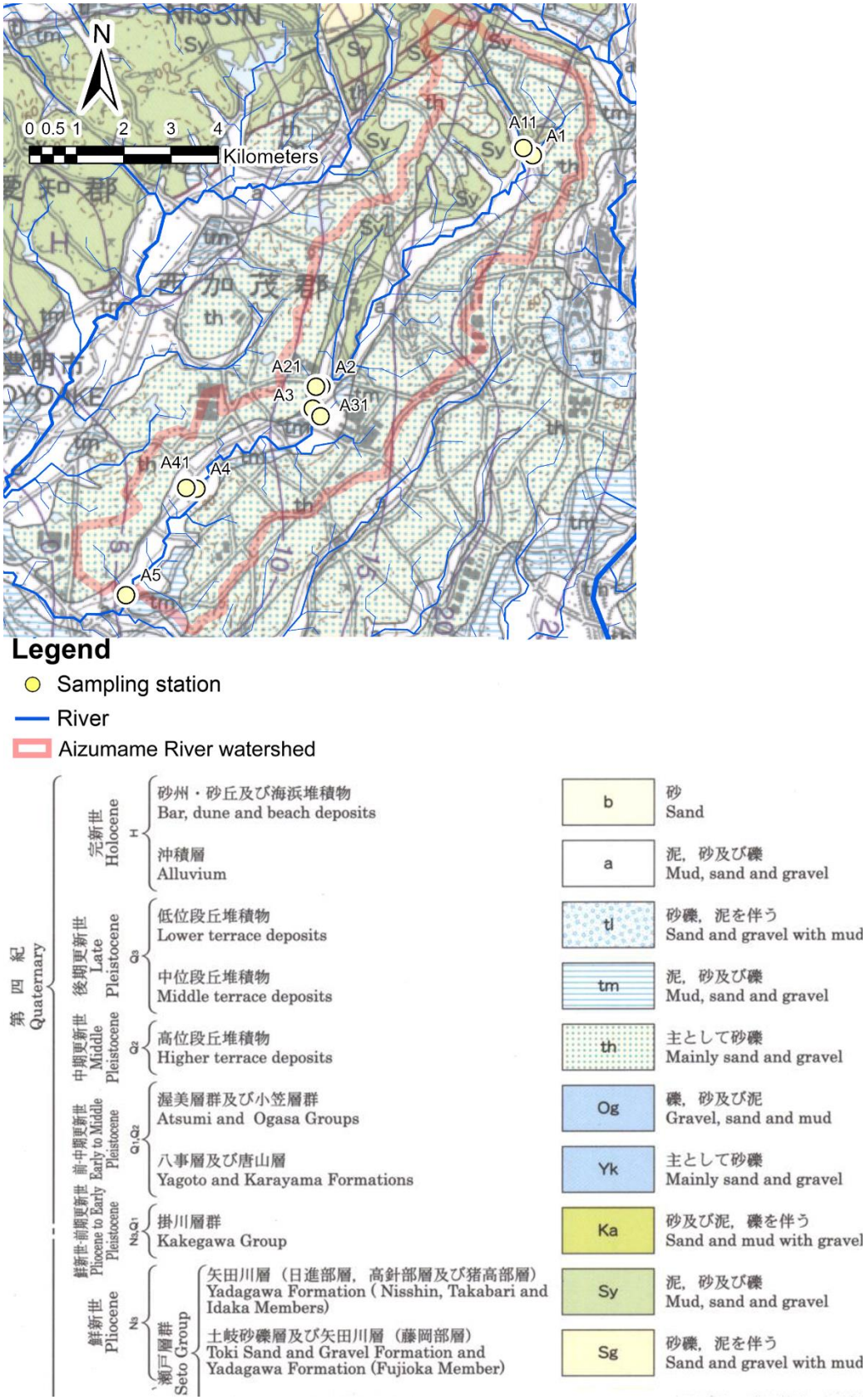

Figure 2.7 Geological map in the vicinity of Aizumame River
(Basemap source: Geological Survey of Japan, 2021)

2.1.2 Umeda River

This research was conducted in the Umeda River located in Toyohashi City, which flow into Mikawa Bay. U1 through U5 represent five sample stations in the Umeda River's mainstream, as shown in Figure 2.8. The Umeda River length is approximately 11.7 km from the upstream to the most downstream station (U5). The water samples were also collected in one tributary sampling stations located in Ochiai River (U31) and three stations in Sakai River (U21 to U23). The manufacturing industries are located surrounding Sakai River which indicated by ww-A, ww-B, and ww-C. The details of the location of each tributary are shown in Figure 2.9.

The river catchment area at U5 is approximately 43.7 km^2, located at 137°28'3"E 34°44'41"N–137°28'20"E 34°40'41"N and 137°23'42"E 34°42'44"N–137°30'17"E 34°41'19"N. Agricultural areas (48.8%), including paddy fields (5.8%), cabbage, tea, and other crops (43.0%), are the most common uses of the surrounding land, as shown in Figure 2.10 and Figure 2.11. Commercial, industrial, and residential areas (urban) account for 29.6% of the catchment area, while forests, rivers, and barren land account for 7.8%, 5.8%, and 1.8%, respectively.

The sampling station U5 was established below Hatakeda Bridge, at the furthest downstream location where there was no tidal effect. The monthly survey, the weekday-weekend survey, and the stormflow survey all used this station as a sampling site.

The geology setting in the Umeda River watershed consists of sedimentary rocks and accretionary complexes (Geological Survey of Japan, 2021). The catchment also has mud, sand and gravel, mélange with blocks of basalts, chert and limestone, mudstone and sandstone (Geological Survey of Japan, 2021).

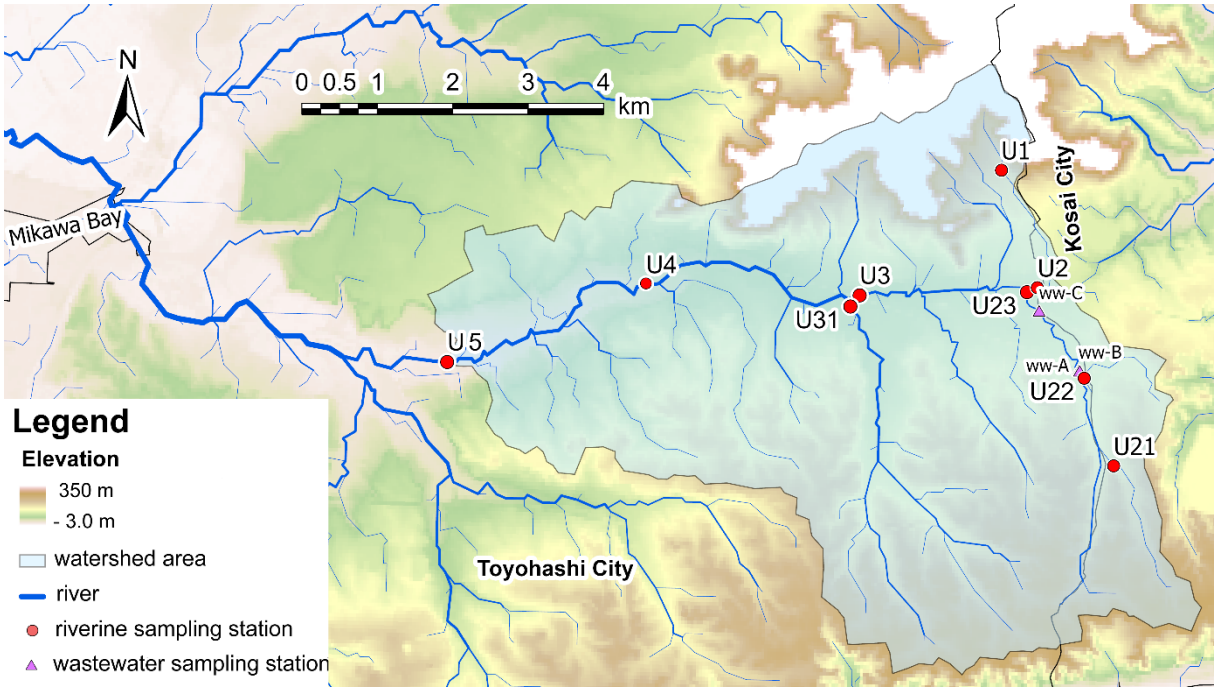

Figure 2.8 Sampling stations located in the Umeda River

(a)

(b)

(c)

Figure 2.9 Details of the sampling station in the mainstream located just before the confluence with the respective tributary: (a) U2 and U23; (b) Sakai River; (c) U3 and U31

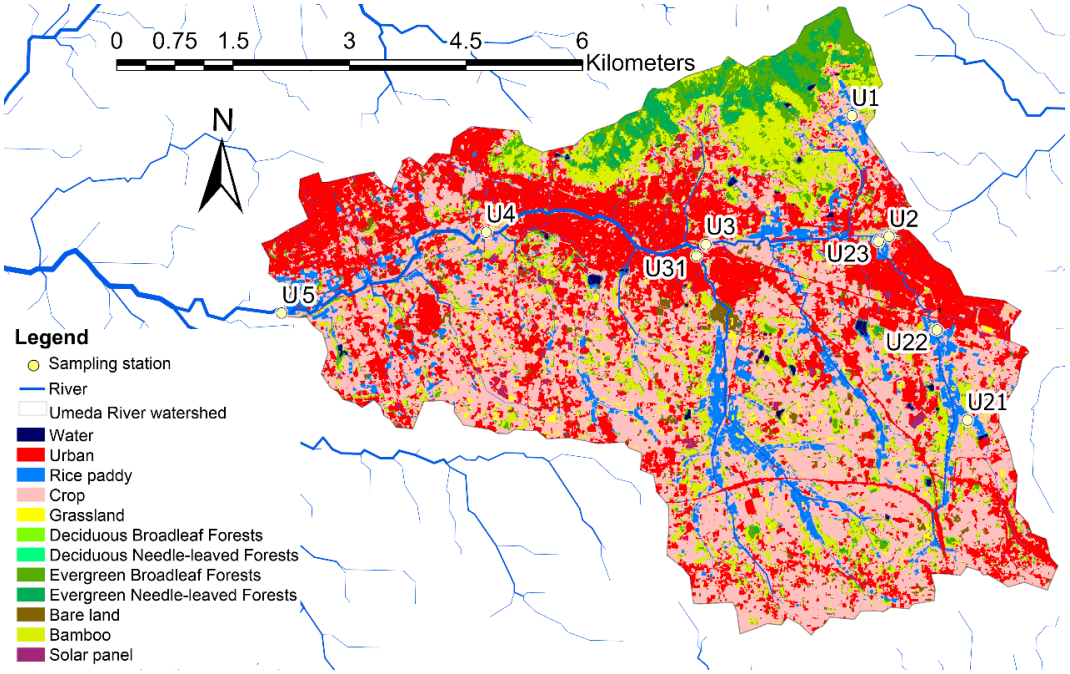

Figure 2.10 Land use and landcover in the Umeda River catchment area
[Land use and land cover maps are provided by ALOS-2/ALOS Science Project (JAXA, 2021)]

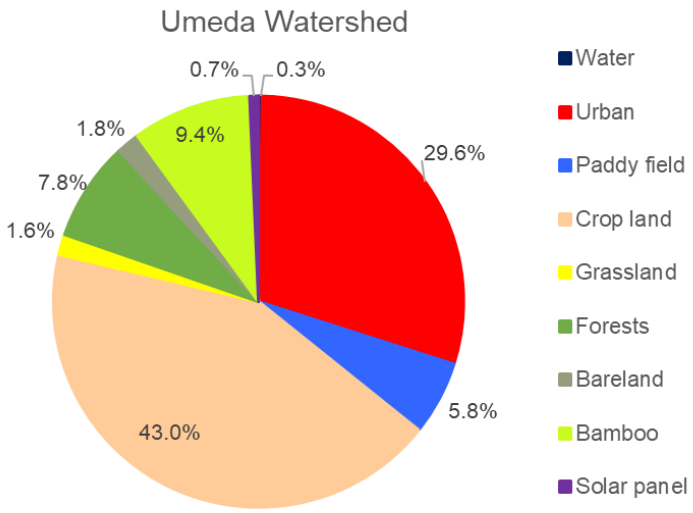

Figure 2.11 Land use and land cover of the Umeda River watershed at U5

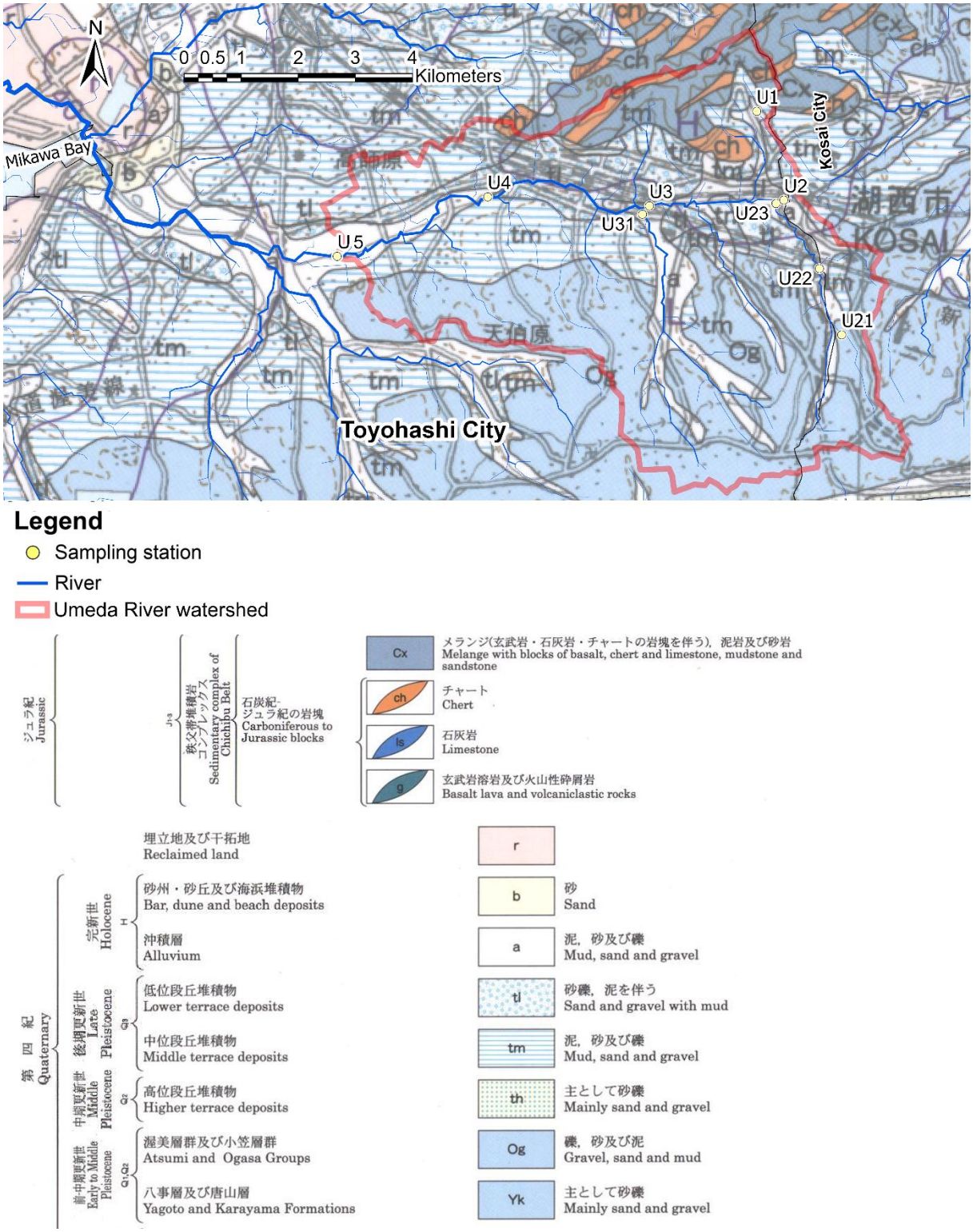

Figure 2.12 Geological map in the vicinity of Umeda River

(Basemap source: Geological Survey of Japan, 2021)

2.2 Sampling time and condition

2.2.1 Aizumame River

Two kinds of survey were conducted in the Aizumame River. The summary of these surveys is shown in Table 2.1.

Monthly survey

Water sampling and river discharge measurements were conducted monthly in the daytime from May 2016 until December 2017 (twenty months) on sunny days. The previous day of each sampling event was also fine weather.

Weekday-weekend survey

The majority of industrial plants do not operate on weekends. In the baseflow, water samples were collected over the following 24 hours. For comparison, the weekday-weekend survey was performed on both weekends and weekdays. This investigation was conducted to determine the impact of industrial effluent discharged into tributaries and eventually into the Aizumame River's main channel.

Table 2.1 Summary of survey type, parameters, sampling time and condition in the Aizumame River

Survey type	Monthly	Hourly
Compartment	water	water
Parameters	T-Zn, Q	T-Zn, Q
Condition	Baseflow, on weekday	Baseflow, on weekday and weekend
Sampling time	monthly from May 2016 to December 2017 (for **20 months**)	September–October 2017 survey **(for 48 hours):** **Weekday**: 17:00 (14 Sep) – 16:00 (15 Sep) 2017 **Weekend**: 17:00 (30 Sep) – 16:00 (1 Oct) 2017

2.2.2 Umeda River

The monthly and hourly survey were undertaken in the Umeda River. Several parameters were measured in order to analyze the spatio-temporal variations and the source identification which can be seen in Table 2.2.

Monthly survey

The survey was performed every month for a year, from August 2019 to July 2020. The surveys were conducted on sunny days (daytime) when there had been no precipitation in the previous two days. For 12 months, in water samples, pH, electroconductivity (EC), temperature (temp), suspended solid (SS), T-Zn, P-Zn, D-Zn, T-Fe, P-Fe, D-Fe, and particulate organic carbon (POC) were measured. Bicarbonate (HCO_3^-), major cation, and anion Meanwhile, bimonthly (in August, October, November 2020, January,

February, March, April, May, and June 2020), riverbed sediment samples were collected to measure Zn, Fe, and POC in each fraction, i.e., fine sand, medium sand, and coarse sand.

Weekday-weekend survey in the baseflow

In the first week of February 2020 (winter), clear sunny weather events on weekdays (Wednesday–Thursday) and weekends (Saturday–Sunday) were monitored in the downstream part of the Umeda River. Winter has the lowest precipitation levels of the year, implying that point sources may have a significant impact on Zn loading into the stream.

In order to verify the diel cycles of riverine Zn concentrations, a baseflow survey for 102 hours including weekday and weekend was undertaken in autumn. The weekday was represented by the samples collected from 08:00 (1st October 2020) to 23:00 (2nd October 2020) and from 00:00 (5th October 2020) to 13:00 (5th October 2020). Meanwhile, weekend survey was conducted from 00:00 (3rd October 2020) to 23:00 (4th October 2020).

Stormflow survey

This study evaluated a high-resolution temporal sampling undertaken in the stormflow or during a rainy event. Because of the significant precipitation, the stormflow study was performed in September. To determine the impact of non-point sources of Zn, a stormflow survey was undertaken. The stormflow survey was performed between 14:30 on September 6, 2020, and 07:30 on September 8, 2020.

Table 2.2 Summary of survey type, parameters, sampling time and condition in the Umeda River

Survey type	Monthly	Monthly	Bimonthly	Hourly	Hourly	Hourly
Compartment	water	water	riverbed sediment	water	water	water
Parameters	pH, EC, Temp., SS, T-Zn, P-Zn, D-Zn, T-Fe, P-Fe, D-Fe, POC	HCO_3^-, major cation and anion	Zn, Fe, POC in fraction: fine sand, medium sand, coarse sand	T-Zn, P-Zn, D-Zn, T-Fe, P-Fe, D-Fe, SS, Q	T-Zn, P-Zn, D-Zn, T-Fe, P-Fe, D-Fe, SS, Q	T-Zn, P-Zn, D-Zn, T-Fe, P-Fe, D-Fe, SS, Q
Condition	Baseflow, on weekday	Baseflow, on weekday	Baseflow, on weekday	Baseflow, on weekday and weekend	Baseflow, on weekday and weekend	Stormflow
Sampling time	Monthly survey for **12 months**: 2019: Aug, Sep, Oct, Nov, Dec 2020: Jan, Feb, Mar, Apr, May, Jun, Jul	Monthly survey for **9 months**: 2019: Aug, Oct, Nov 2020: Jan, Feb, Mar, Apr, May, Jun	Bimonthly survey for **7 months:** 2019: Jul, Aug, Sep, Nov 2020: Jan, Mar, May	**February** 2020 survey (for **50 hours**): **Weekday**: 17:00 (5 Feb)–17:00 (6 Feb) **Weekend**: 17:00 (8 Feb)–17:00 (9 Feb)	**October** 2020 survey (for **102 hours**): **Weekday**: 08:00 (1 Oct)–23:00 (2 Oct) and 00:00 (5 Oct)–13:00 (5 Oct) **Weekend**: 00:00 (3 Oct)–23:00 (4 Oct)	**September** 2020 survey (for **42 hours**): 14:30 (6 Sep)–07:30 (8 Sep)

2.3 Samples collection and pre-treatment

When a tributary or drainage route runs into a river, it quickly mixes with the water in the river. However, it is dependent on the river's size and an uniform ratio of mainstream and confluent water in the transverse direction. Prior to full mixing, more wastewater frequently outflows into urban rivers. As a consequence, observing the effect of tributaries in the mainstream following the introduction of tributary water is difficult. Even if it is not always uniform in the transverse direction upstream of the inflow point, the central channel is recognized as the typical location for collecting water samples.

2.3.1 Monthly survey in the Aizumame River

A two hundred and fifty milliliter water sample was collected from each sampling station (A1–A5, A11, A21, A31, and A41) for measuring total fraction Zn. A 2.5 ml concentrated HNO_3 was added to the water samples, then the samples were stored at 4 $^{\circ}$C until Zn measurement.

2.3.2 Monthly survey in the Umeda River

Water samples collection

At riverine sampling stations (U1–U5, U31, and U41–43) and industrial wastewater sampling locations, about two liters of water were collected manually using acid-cleaned polypropylene bottles (ww-A, ww-B, and ww-C). One hundred milliliters water sample represents for total fraction of metals in the monthly survey. It was immediately preserved using 1% concentrated HNO_3 (ultrapure analytical reagent, Tamachemicals Co., Ltd., Japan) after each sampling event. Then, all water samples were stored at 4 °C until analyses.

Riverbed sediment samples collection

Riverbed sediment samples were collected at a depth of 0–15 cm using acid-cleaned polypropylene bottle. Three sediment samples were taken separately for the triplicate analysis. After transported to the laboratory, the samples were oven dried at 40 °C for three days to evaporate the water content. Drying at relatively low temperature (40 °C) was necessary to prevent organic matter to evaporate. The samples were then stored at 4 °C to minimize any chemical reactions until grain size distribution analysis.

2.3.3 The weekday-weekend survey in the baseflow and the stormflow survey

A Teledyne ISCO-6712 autosampler (USA) was used, which was configured to take one-liter samples every hour. For each sample occasion, twenty-four polypropylene bottles (containing up to a liter of water) were collected. To minimize cross-contamination, water samples were collected using polypropylene pipe and conveyed using a peristaltic pump with a purge phase. In case of the February survey in the Umeda River, on the second day, a one-liter water sample was manually collected using polypropylene bottles at 17:00 in order to acquire data for a total of 50 hours. Before each sampling

procedure, the autosampler and polypropylene sample containers were triple-rinsed with deionized water. After all of the samples were collected in autosampler bottles, the water samples were taken and filtered at the laboratory within 48 hours.

2.4 On-site measurements

Temperature, pH, and EC are necessary to be measured on-site (field measurements). These parameters were measured on the field using EC and pH meter (WM-32EP, DKK-TOA Corporation, Japan). The device was calibrated prior to each sampling event.

2.5 River discharges

2.5.1 River discharge direct measurement

The velocity area method was used to determine river discharge values. The cross-sectional region was partitioned up into multiple subsections depending on the river's width. At the midpoint width of each subsection and 40% of depth from the bottom, the flow velocity of each subsection area was measured using an electromagnetic current meter CKK-LP30 (Kenek Co., Ltd., Japan). Finally, the overall river discharge was determined by adding all of the subsection's calculated river discharges.

2.5.2 River discharge and water level model

The river discharges were estimated using a water level–discharge (H–Q) model (Yokota et al., 2013). In the Aizumame River, the River Division of the Aichi Prefectural Construction Bureau monitored the water level at Komashin Bridge. In the Umeda River, the water levels at the Hamamichi Station were monitored. This study's survey was conducted at Hatakeda Bridge, which is about one kilometer from Hamamichi Station. To estimate river discharge, the H–Q model was used, which included converting the water level from Hamamichi Station to Hatakeda Bridge.Water level every hour was used for the weekday–weekend survey in the Aizumame River (September–October 2017) and Umeda River (in February 2020). Meanwhile, water level every 10 minutes was used to determine the river discharges in the weekday–weekend survey (in October 2020) and the stormflow in the Umeda River so that the discharge fluctuation could be assessed more frequently.

2.6 Analytical methods

2.6.1 Suspended solids (SS)

The SS was obtained using two types of membranes: GF/F membranes and cellulose acetate membranes. Particulate organic carbon (POC) was obtained using the GF/F (0.7 m, glass microfiber filters, Whatman^{TM}, UK) membrane, whereas cellulose acetate membrane (Advantec®, Japan) was employed

to obtain filtrate as a dissolved fraction of Zn (D-Zn) and Fe (D-Fe). To extract the particulate Zn and Fe fraction, the SS on the cellulose acetate membrane was further digested.

One hundred milliliters water samples were filtered using wash-dried and pre-weigh GF/F membranes to quantify suspended solids (SS) concentrations. Before filtering the samples, the GF/F membranes were oven-dried at 400°C. The concentrations were calculated by subtracting the weight of the SS-coated membrane (oven-dried at 105 °C) from the pre-weight divided by the filtered volume. This filtration was done three times, and the average values were derived for this study's purposes.

2.6.2 Water sample

2.6.2.1 Acid digestion for total fraction of metals

One hundred milliliters water samples for total fraction of elements Zn and Fe were immediately acidified by adding 1.0 ml of concentrated HNO_3 (ultrapure analytical reagent, Tamachemicals Co., Ltd., Japan). On top of a hotplate, a 20-ml sub-sample was heated to 205 °C in a fluorine bottle, then filtered through a 0.45 µm syringe filter using cellulose acetate membrane (Advantec Co., Ltd., Japan). In order to prevent contamination, the first five milliliters of the filtrate were removed to avoid contamination. Then, the acid digested samples were stored at 4 °C until metal analysis procedures.

2.6.2.2 Acid digestion for dissolved metals

A cellulose acetate membrane (0.2 m, Advantec®, Japan) was used to filter 500 milliliters of water. Before filtering each sample, the filter container was thrice washed with deionized water. To avoid cross-contamination, the first 100 mL of filtrate were removed. In the case of D-Zn and D-Fe, 100 ml of filtrate was mixed with 1.0 ml of concentrated HNO_3 (ultrapure analytical reagent, Tamachemicals Co., Ltd., Japan) and digested. The digestion required 20 minutes of heating the samples on a hotplate to a temperature of 205 °C. The acid digested samples were kept at 4 °C until metal analysis performed.

2.6.2.3 Acid digestion for particulate metals

Metals in suspended particles were measured using US-EPA Method 3050B, which included the addition of concentrated HCl (suprapure guaranteed reagent, Wako Pure Chemical Corporation, Japan).

2.6.2.4 Cation and anion measurement

Major cation (Ca^{2+}, Mg^{2+}, K^{+}, and Na^{+}) and anion (Cl-, NO_3^{-}, SO_4^{2-}) concentrations were measured by ion chromatography (881 Compact IC Pro, Metrohm AG, Switzerland). Prior to measurement, the filtered and unacidified samples were diluted to achieve EC less than 10 mS/m. HCO_3^{-} concentrations were measured using titration against 0.005 N sulphuric acid (H_2SO_4) until the end-point pH of 4.8 (APHA, 2018).

2.6.3 Riverbed sediments (RBS)

2.6.3.1 Grain size distribution analysis

The homogenized RBS samples were sieved into three size categories, i.e. medium sand (300–600 µm), coarse sand (600–1000 µm), and fine sand (<300 µm). Mechanical shaker (MVS-1, AS ONE, Japan), was used to separate the sediment particles.

2.6.3.2 Acid digestion methods

About 0.1 gram (dry weight) of the RBS sample was acid digested with additions of HCl according to EPA method 3050B. After heated up on hot plate at 95 °C and diluted to a final volume of 50 mL To eliminate the sediment particles, the samples was centrifuged at 2,300 rpm for ten minutes then decanted. The samples were stored in acid-cleaned polypropylene bottles at 4 °C until metal measurement.

2.6.4 Metal analysis using atomic absorption spectrometry

The total fraction of Zn and Fe concentrations was measured using a flame Atomic Absorption Spectrometry (AAS) (AA-7000, Shimadzu Corporation, Japan) instrument with four calibration standard solutions. For water samples, the detection limits were 0.005 mg/L for Zn and 0.01 mg/L for Fe. It should be noted that Zn measurement of Aizumame's water samples in 2016 has a detection limit of 0.01 mg/L. As for other water samples, the samples were re-measured using graphite furnace AAS (GFAAS) with a detection limit of 0.0005 mg/L if the Zn level was less than 0.005 mg/L. The detection limits of sediment samples were 2.5 mg/kg for Zn and 25 mg/kg for Fe. The Zn measurement using graphite furnace AAS for sediment samples was not undertaken because the HCl might interfere the AAS instrument.

2.6.5 Particulate organic carbon measurement

POC concentrations of suspended solids and riverbed sediment were measured using an NC analyzer instrument (Sumigraph NC-22A, Sumika Chemical Analysis Service, Ltd., Japan) combusted at a temperature of 600 °C. The POC in suspended solids on the GF/F membrane were measured for each sampling station. Approximately 0.1 gram (dry weight) of the riverbed sediment for each grain size category was used to measure POC.

2.6.6 Quality assurance and quality control (QA/QC)

Standard solutions were made using ultrapure (milli-Q) water, and all of the reagents were ultrapure grade. For the elemental analysis, all glass and plasticware were immersed in a 3% alkali detergent solution (SCAT 20X, Dai-ichi Kogyo Seiyaku, Co., Ltd., Japan) for at least 3 hours and then in 1% HNO_3 solution (ultrapure reagent, Kanto Chemical, Co., Inc., Japan) overnight. Afterward, they were triple-rinsed with ultrapure water and the glass and plasticware were dried before use.

Prior to the analysis, the calibration was completed. Every six samples, the standard solutions were measured, and each sample was also measured three times for Quality Assurance/Quality Control. The mean values were derived as the measurement findings for this study's subsequent assessment.

For quality assurance and quality control (QA/QC) purposes, re-validation of the standard solutions every six sample measurements for the calibration curves was required. The procedure blanks and a set of six samples were examined together. According to the method blank, the Zn and Fe in the procedures and reagents were not identified. The coefficient of variation (CV) for both Zn and Fe concentrations in water samples was less than 7% in a triplicate analysis of all samples. The CVs of particle sample measurements ranged from 8% to 12%. A certified reference material (CRM) for trace elements (National Metrology Institute of Japan, CRM 7202-c No. 0356) was used to verify the analytical method. The analytical method had recovery rates of 84–92% for Zn and 93–99% for Fe.

As for the POC measurement, to establish the calibration curves, the acetalinide standard (Wako Pure Chemical Industries, Japan) was analyzed. The sample measurement required less than 30 μm of drift and zero noise of the instrument baselines. Thereafter, the triple measurement was performed for quality assurance and control purposes.

2.7 Data analyses

2.7.1 Statistical description

2.7.1.1 Case study of the Aizumame River

General statistical description

In the study presented in Chapter 3, Zn concentrations in water samples and river discharges, as well as Zn load, were evaluated using descriptive statistics such as mean and standard deviation. As suggested by the US-EPA (2006), samples with undetectable Zn concentrations were considered to have a concentration of 0.005 mg/L (half of the detection limit). Furthermore, total fraction Zn contamination in the river is a major concern, particularly at levels that exceed the EQS (0.03 mg/L T-Zn).

Multivariate statistical analyses

In Chapter 6, the hierarchical cluster analysis was performed for the Aizumame River dataset using Ward's linkage method and the Euclidean distance. Euclidean distance calculates the square root of the sum of squared differences. The variables used for this analysis were total fraction of Zn (T-Zn) and river discharge (Q). This cluster reveals the interrelations among sampling stations as well as the sampling period. A dendogram was used to present the clustering processes and the groups, and their proximity.

2.7.1.2 Case study of the Umeda River

General statistical description and bivariate statistical analyses

In the study described in Chapter 3, 4 and 5, the mean, standard deviation, and range of values were utilized in the statistical description to describe the study results. To elucidate the link between the factors, a Minitab® 19 was utilized to do a Pearson correlation (*r*) analysis and regression. A statistically significant association was defined as a probability (*p*) value of less than 0.05. With respect to the statistical analyses, the undetected Zn concentrations (below 0.0005 mg/L) was assumed to have concentration of its detection limit 0.0005 mg/L as the worst case scenario.

Multivariate statistical analyses

In the Chapter 6, Hierarchical cluster analysis (HCA) was conducted on the dataset of water analysis in the Umeda River using Minitab® 19. Previously, the parameter values were standardized by subtracting the mean and divided by the parameter's standard deviation, hence, the standardized values had a mean of 0 and standard deviation of 1. The data used for HCA were pH, EC, particulate Fe (P-Fe), dissolved Fe (D-Fe), particulate Zn (P-Zn), dissolved Zn (D-Zn), particulate organic carbon (POC), cation (Ca^{2+}, Mg^{2+}, K^{+}, and Na^{+}), and anion $(NO_3)^{-}$, $(HCO_3)^{-}$, $(SO_4)^{2-}$. Two kinds of HCA were performed, namely cluster observations and cluster variables. The cluster observation implemented Ward's linkage method and the Euclidean distance. The Ward's method shows a tendency to generate clusters that have similar number of observations. Euclidean distance calculates the square root of the sum of squared differences. This cluster showed the interrelations among sampling stations and their respective sampling time. The results of both cluster analyses were presented in dendrograms providing a clustering processes, the groups, and their proximity.

Meanwhile, cluster variables analysis highlighted the interrelations among the water quality variables analyzed (Gogoi et al., 2016). Similar variables (correlated) were grouped together. Ward's method was also employed in this analysis. As for the distance measure, correlation method. Absolute correlation method was implemented to give distances between 1 and 0 because the strength of the correlation is necessary in considering distance and not the sign (negative or positive).

In addition, principal component factor loading analysis was also performed for 16 parameters in aqueous phase (both dissolved and particulates). The analysis aimed to estimate the possible sources and the underlying factors determining the variation of the parameters.

2.7.2 Load calculations

Zn loads were calculated according to the following equation:

$$L = C \times Q \tag{2.1}$$

where L represents load or load, C denotes concentrations and Q is river discharge.

Total daily load in the hourly survey was calculated by summing up all of Zn load every hour.

The load (L)-discharge (Q) equation model was used to both baseflow and stormflow datasets to determine the Zn load (Kunimatsu et al., 2006). The hourly loads were estimated using high-resolution temporal sampling during the baseflow and stormflow sampling campaigns by multiplying Zn concentration and river discharge. The L-Q equation may be expressed as follows (Kunimatsu et al., 2006):

$$L = aQ^n \tag{2.2}$$

where a and n are coefficients derived from non-linear regression. By adjusting parameter estimations to minimize the residual error of sum of squares, the Levenberg–Marquardt algorithm (Levenberg and Arsenal, 1943; Marquardt, 1963) was used to solve the non-linear regression of the L-Q model.

2.7.3 Flow analyses of Zn loadings and the end member mixing analysis in the river water

By using Sankey diagrams (*e!*Sankey®calc version 4.5.3), flow analyses during the monthly survey in the Aizumame River and the Umeda River were performed to identify any load increases or load losses in the Zn flow, as well as the river discharges. The diagram could reveal the variation both spatially and temporally.

The Sankey diagrams showing the loading flow of total fraction of Zn (in g/day and percentage by the most downstream sampling station at the respective catchment, i.e. A5 and U5) and the river discharges were divided by:

1. Seasonal variations (spring, summer, autumn, and winter)
2. Irrigation and non-irrigation period

An end member mixing analysis (EMMA) (Barthold et al., 2011) was performed using two tracers, namely Zn from point sources and Zn from non-point sources, to determine the fraction of Zn load from both point and non-point sources. The daily load was computed by summing the hourly metal loads from each sample period. To calculate the non-point source load ratio of Zn, a natural source element from non-point sources is required. According to the baseflow survey campaign evaluation, Fe is deemed a natural source element originating from non-point sources in this circumstance. The EMMA

equation indicating Zn release estimation the point sources (F_{PS}) and non-point sources (F_{NPS}) is written as follows:

$$1 = F_{PS} + F_{NPS} \tag{2.3}$$

$$\text{total ratio of Zn} = F_{PS} \times R_{Zn\_PS} + F_{NPS} \times R_{Zn\_NPS} \tag{2.4}$$

where R_{Zn_PS} is the Zn ratio from PS whereas R_{Zn_NPS} is Zn ratio from non-point or diffuse sources. Subsection 6.4.2 describes the values of current estimation using baseflow and stormflow load ratios.

Chapter 3 Spatial and temporal variability of Zn in total fraction concentrations and loads

Summary

Zn remains a concern in Japan since numerous locations with high Zn concentrations have been discovered, and aquatic life is expected to be vulnerable to high Zn concentrations. This study investigated total Zn (T-Zn) concentrations and load in the Aizumame River and the Umeda River located in Aichi Prefecture.

Throughout 2017, the EQS of 0.03 mg/L was violated at the Aizumame River's two downstream stations (A4 = 0.059 mg/L; A5 = 0.055 mg/L). T-Zn levels considerably varied from <0.005 mg/L to 0.139 mg/L. The highest concentration was found at A4 in June 2017. During winter, the T-Zn concentrations constantly increased toward the downstream, whereas in other seasons the level attenuated from the most upstream to 8.1 km downstream, then eventually hiked at the most downstream station. Apart from the highest concentration (0.139 mg/L) found in June, winter's T-Zn levels were the highest among other seasons. Irrigation water from the downstream area impacted the Aizumame River's mainstream. The water released to the river, allowing it to discharge at a greater rate than during the non-irrigation time. Dilution along the river was exacerbated by the high river discharge, leading to a lower concentrations. Given that the largest land use area was industries and the river discharges that were not associated with T-Zn, it is possible that the elevated T-Zn concentration in the Aizumame River might be caused by industrial point sources. The industrial point source input into the river was confirmed by the weekday-weekend loading assessment.

Total Zn concentrations along the Umeda River fluctuated from 0.002 to 0.090 mg/L throughout spatial and temporal throughout the year. In February, during the winter season, all sample locations exhibited quite high values ranging from 0.021 mg/L to 0.062 mg/L. At the most downstream part of the Umeda River, the annual mean concentration value of 0.031 mg/L exceeded the EQS (0.030 mg/L). Although the river discharges during irrigation and non-irrigation period were similar, the T-Zn concentrations were considerably higher during non-irrigation period than those in irrigation period. During the fall and winter seasons, the greatest quantities were observed, with concentrations typically increasing downstream. According to the weekday-weekend survey, anthropogenic activities have impacted the Umeda River, as seen by higher T-Zn levels during the weekday.

The weekday-weekend surveys comparing concentrations during the weekday and weekend in the Aizumame River and the Umeda River showed that industry largely delivered Zn inputs into the

mainstream and accounted for the higher concentrations during the weekday than the weekend. Other major Zn sources, particularly during the irrigation period when river flows were relatively high, should be considered.

3.1 Introduction

Zn is required for both biological processes (such as cell division, immune system function, growth, and cell division) and basic necessities. Zn, on the other hand, has negative effects on aquatic organisms. Despite the fact that Japan has set a new environmental quality standards (EQS) of 0.03 mg/L for total Zn fraction (T-Zn) on annual average value, monitoring data in Aichi Prefecture revealed no clear trends for Zn reduction (Naito et al., 2010). The Zn reduction might be difficult to achieve because Aichi Prefecture has significantly higher proportion of manufacturing industries than average for Japan. As the first step, it is necessary to analyze the T-Zn concentrations in rivers which might affected by the industrial wastewater. Thus, this chapter highlights the concentrations of T-Zn and its seasonal variation as well as the influence of the land use area, particularly paddy field. The detail of sampling sites, sampling collections, chemical analyses, are thoroughly described in Chapter 2.

3.2 Aizumame River

Aizumame River watershed is dominated by constructed area such as industrial area by 42.2%, followed by crop land (30.0%) and paddy fields (12.4%). Both industries and agriculture might have contributed to Zn concentrations into the Aizumame River. It was hypothesized that the Zn loadings from industrial input might outweigh the agricultural activities. The Zn concentrations and river discharges were measured and then the Zn loads were calculated over 20 months from May 2016 to December 2017. Meanwhile, the weekday and weekend T-Zn levels in the most downstream sampling station were assessed to verify the industrial discharges.

3.2.1 Zn concentration and load in river water

T-Zn concentrations varied both spatially and temporally. Concentrations at sample sites tended to rise in a downstream direction. The T-Zn concentrations in the Aizumame River are illustrated in Figure 3.1 (mainstream) and Figure 3.2 (tributaries). In 2017, the means of Zn concentrations in the Aizumame River ranged from 0.019 mg/L (A1) to 0.059 mg/L (A4), whereas the downstream tributaries A31 (0.284 mg/L) and A41 (0.232 mg/L) has substantially higher level than those in the upper stream sampling stations (A11: 0.012 mg/L; (A21: 0.025 mg/L). According to the annual average, the downstream section in the mainstream (A4 = 0.059 mg/L; A5 = 0.055 mg/L) and tributaries of A31, A41 breached the EQS of T-Zn in 2017.

From the upstream location at A1 (0.010–0.031 mg/L), in December 2016, the Zn level (0.031 mg/L) was already above the environmental quality standard (EQS) of 0.03 mg/L. The A2 sample station (0.010–0.045 mg/L) is located just before a tributary that flows through an industrial sector. T-Zn concentrations at A2 exceeded the EQS from January to March. Because river flows were very modest compared to other months, there may have been no diluting impact during these months (see Figure 3.3 for the mainstream discharges and Figure 3.4 for tributaries discharges). The A3 sampling station (<0.01–0.042 mg/L) showed a lower concentration than A2's (May 2016–March 2017 and August 2017). The concentration at A3 was the greatest of any month (e.g. 0.042 mg/L) in February. The EQS was only exceeded at A3 in February, March, and December 2017. Figure 3.1 shows that A4 (0.010–0.139 mg/L) had greater T-Zn concentrations than A5 (0.012–0.086 mg/L), especially in September, December, and March, when the EQS was violated. It should be emphasized that the river discharge in September was higher than in December-March. The T-Zn concentrations exhibited lower values in relatively high discharge owing to dilution effect. However, there was a strong probability of elevated T-Zn loadings owing to runoff from nearby land use and roads. In 2017, EQS exceedance is more often at A5, the most downstream station, than at other sampling stations.

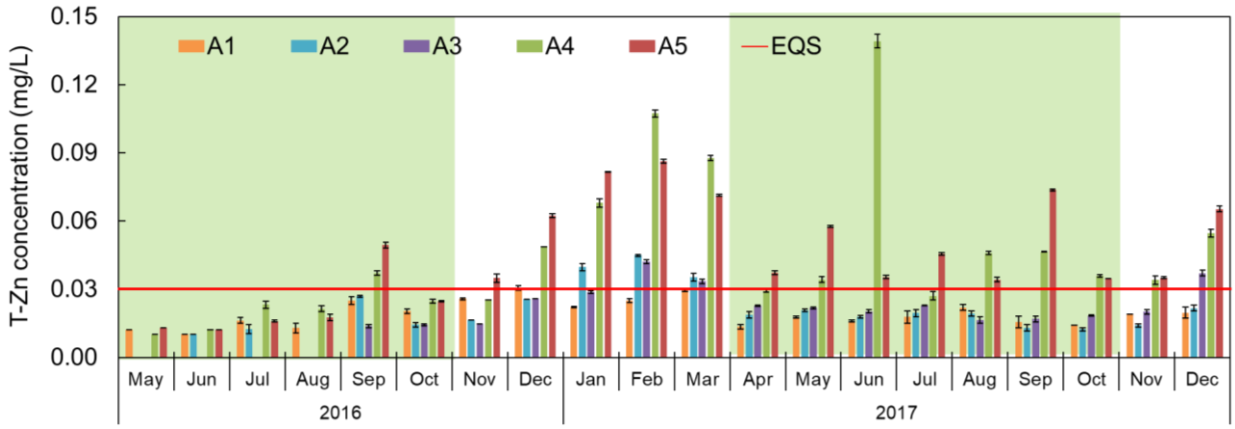

Figure 3.1 T-Zn concentrations in mainstream of the Aizumame River in the monthly baseflow survey: the error bars reflect the data series' SDs. Green shaded area represents irrigation period

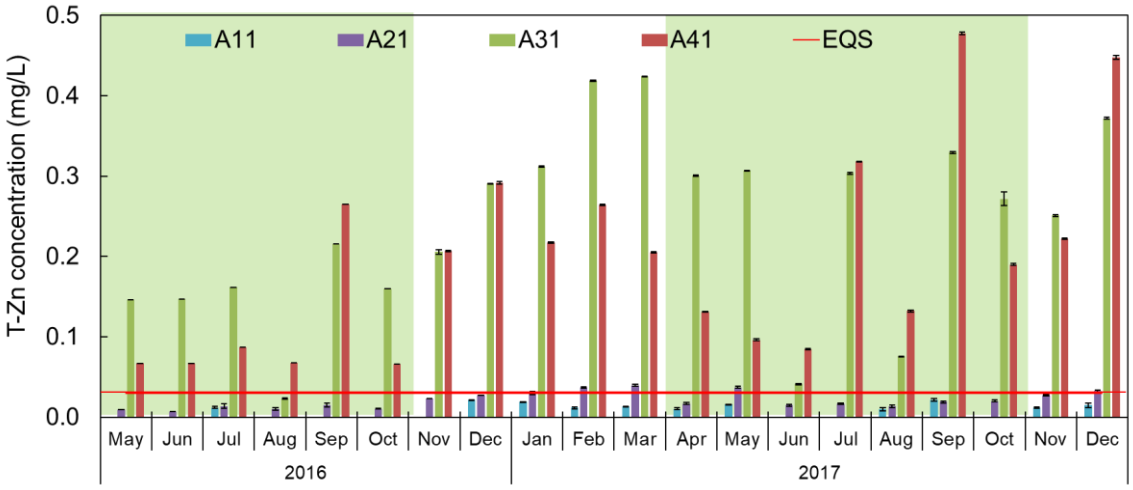

Figure 3.2 T-Zn concentrations in tributary of the Aizumame River in the monthly baseflow survey: the error bars reflect the data series' SDs. Green shaded area represents irrigation period

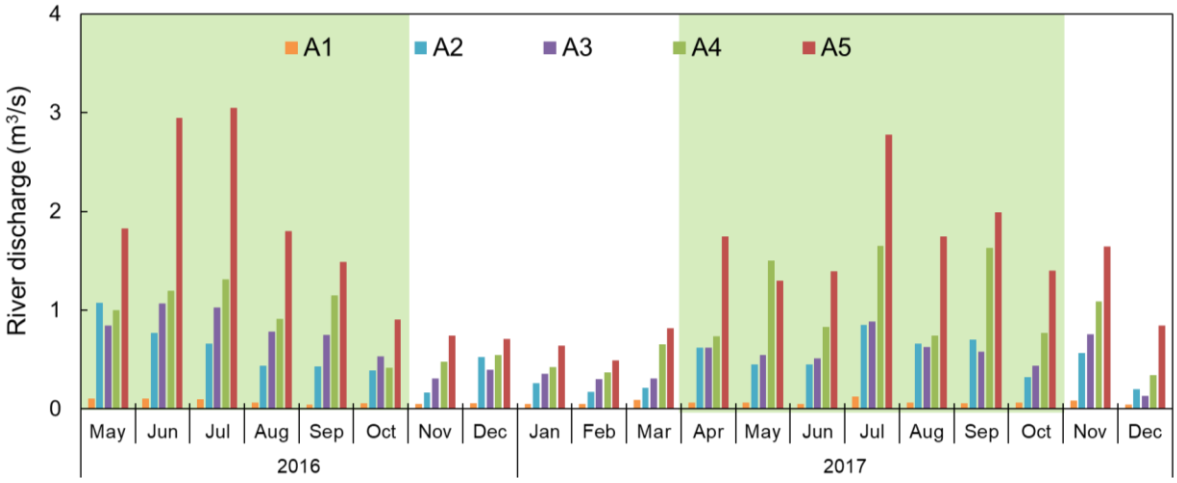

Figure 3.3 River discharge in the mainstream of Aizumame River during the monthly survey: green shaded area represents irrigation period

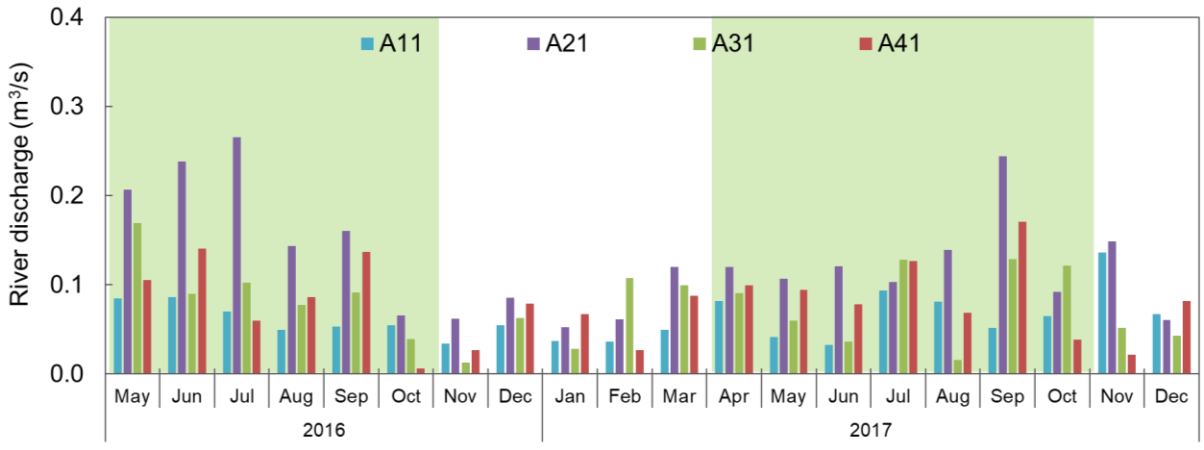

Figure 3.4 River discharge in the tributaries of Aizumame River during the monthly survey: green shaded area represents irrigation period

Figure 3.1 demonstrates that the concentrations at four sample locations surpassed the EQS from January to March, with the exception of January, when A3's concentration did not exceed the allowable limit. The monthly concentration value was compared to the EQS in this investigation. The observed values at the most downstream sample site were up to five times higher than those at the most upstream monitoring point between May 2016 and December 2017. T-Zn concentrations are high in both A4 and A5, which are found in the downstream portion. A4 (0.046 mg/L) had the highest average concentration across all sampling events (2016–2017), whereas A5 (0.045 mg/L) had the lowest. Surprisingly, instead of the upper-stream sampling point, the lowest concentration was recorded at A3 (0.006 mg/L).

T-Zn concentrations were greater between December and March than in other months. Furthermore, in June 2017, A4 had an unusually high concentration (0.139 mg/L). The T-Zn concentrations in the same months of 2017 were greater than the values from May to December of 2016. As demonstrated in Figure 3.2, the greater T-Zn concentration in 2017 might have occurred from a higher input of T-Zn concentration from the tributaries. Manufacturing industries are found in lesser numbers in the tributaries A11 (0.005–0.022 mg/L) and A21 (0.007–0.040 mg/L) than in the tributaries A31 (0.023–0.424 mg/L) and A41 (0.066–0.478 mg/L). Furthermore, river flows in May-December 2016 were greater than in 2017, implying that the T-Zn concentration in 2016 was diluted more than in 2017.

Figure 3.5 depicts the load of T-Zn along the mainstem river. Except in June 2017 and December 2017, the higher the T-Zn load, the further downstream you go. Even though the loading rate from A31 was minimal, there was a peak T-Zn load at A4 in June 2017 (Figure 3.6). Other Zn sources must have existed in June 2017 and contributed to the mainstream at A4. Because of the heavy precipitation in June and July, it is possible that the excessive Zn loading was caused by a non-point source. The T-Zn loading from the tributaries was low in the previous month (May 2017), but it was greater in the following month (July 2017) than in both May and June, as shown in Figure 3.6.

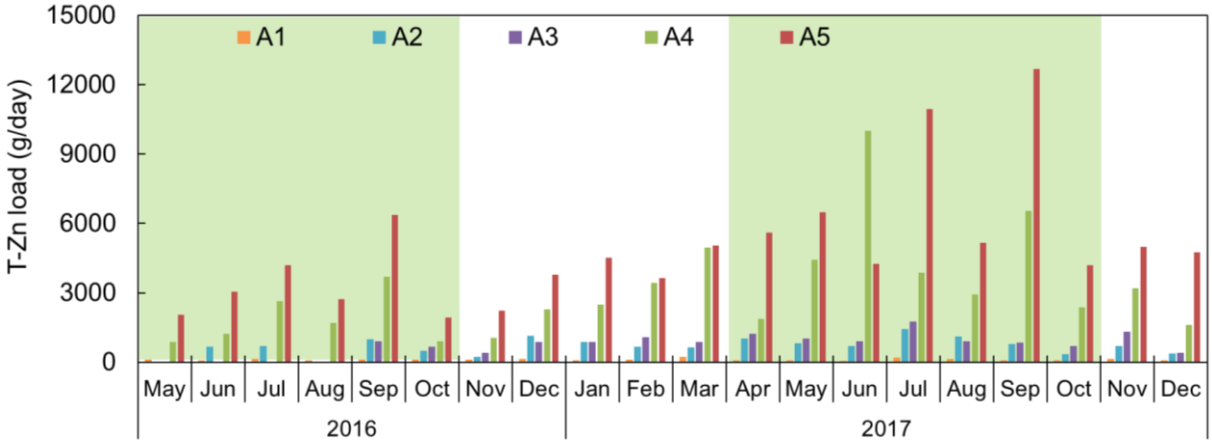

Figure 3.5 T-Zn loads in mainstream of the Aizumame River: green shaded area represents irrigation period

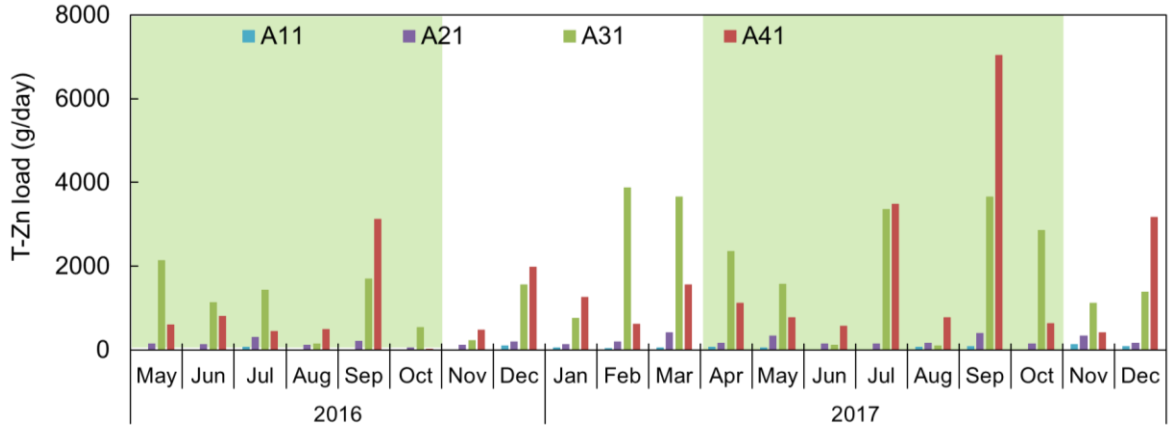

Figure 3.6 T-Zn loads in tributaries of the Aizumame River: green shaded area represents irrigation period

3.2.2 Total fraction of Zn concentration comparison among seasons

The seasonal average values of T-Zn concentrations and river discharges were calculated. According to Japan Meteorological Agency, the months representing summer, autumn, winter, and spring are June–August, September–November, December–February, and March–May, respectively. Based on Figure 3.7, the river discharges in summer were distinctively higher than other seasons, followed by spring, autumn, and lastly winter.

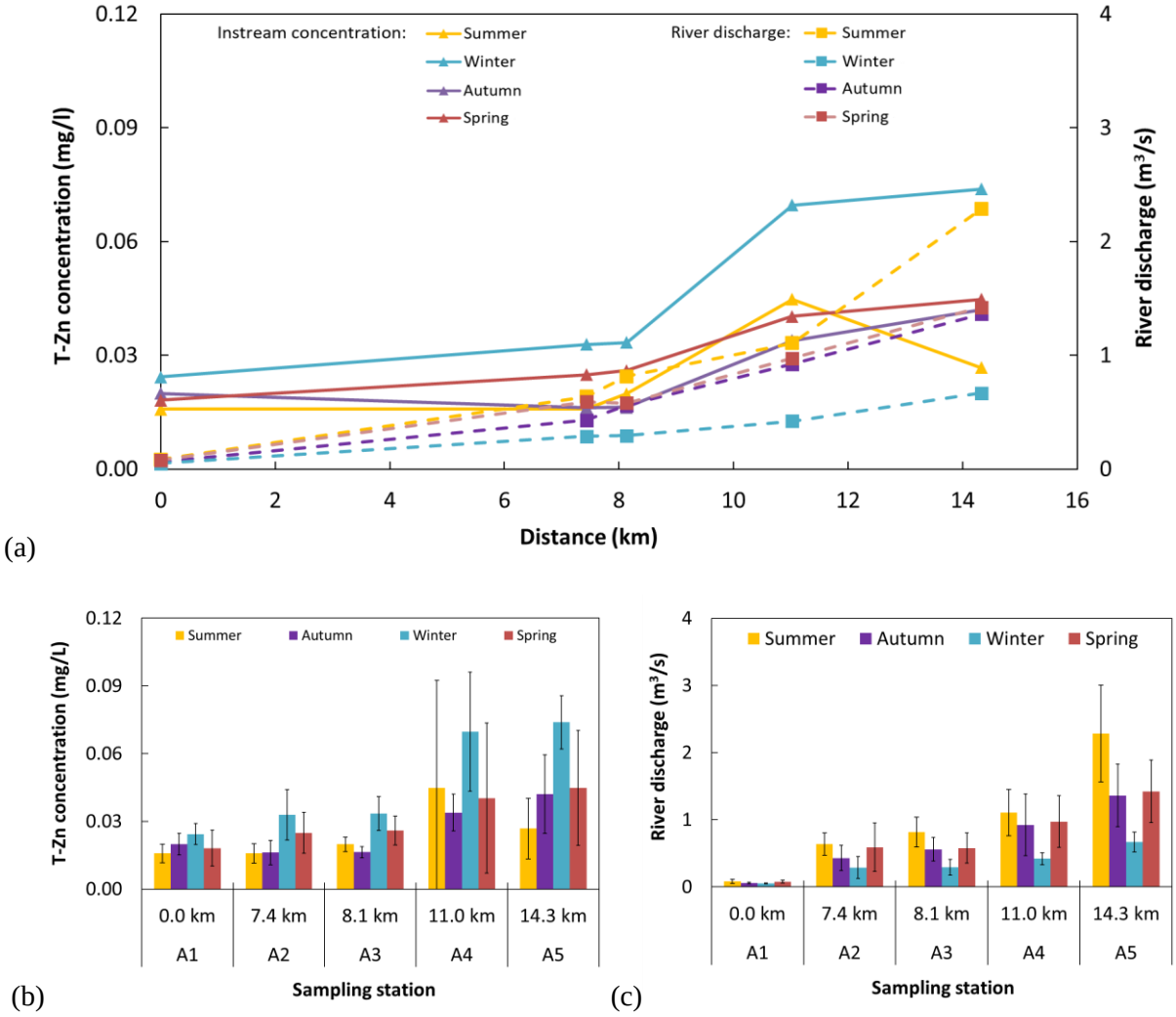

Figure 3.7 Average value of T-Zn concentrations and river discharges in the Aizumame River in each season: (a) T-Zn fluctuation over the distance (0 km to 14.3 km); (b) average values of T-Zn concentrations and error bar represents standard deviation; (c) average values of river discharges; error bar represents standard deviation.

The T-Zn plot over the distance clearly revealed that the highest T-Zn concentrations at all sampling stations were in winter. Autumn and spring levels exhibited nearly the same values until 14.3 km toward the downstream. The T-Zn concentrations slightly attenuated from the upstream to 8.1 km downstream, except during the winter which constantly increasing. Dilution effect was clearly shown during the summer from 11.0 km to 14.3 km downstream, where the T-Zn level significantly decreased when the river discharge was considerably higher.

3.2.3 Total fraction of Zn concentration comparison between non-irrigation and irrigation period

Rice cultivation has changed the environment of Japan, converting alluvial plains into paddy fields that are often connected to nearby rivers and streams (Yoshimura et al., 2005). Irrigation has a considerable impact on the river flow of the mainstream since paddy fields are the second most dominant land use in the area of the Aizumame River basin. Irrigation takes place from April to October, therefore November to March is the non-irrigation period. Around A5 (downstream), the paddy field area was significantly bigger than the upper stream region, ranging from 0% at A1 to 30% at A5. In instance, the greatest paddy field area in the vicinity of A5 is around 13 km^2. Between the survey events, the river discharges displayed temporal and spatial fluctuation. During the irrigation term, the river discharge progressively surged from A1 to A5, as illustrated in Figure 3.8. During the winter, the river discharge grew steadily downstream, but during the summer, the river discharge increased significantly after A3 and continued to increase until A5.

Figure 3.8 shows that average concentrations were lower during the irrigation period than during the non-irrigation period. Dilution may have resulted in lower concentrations during the irrigation period. Figure 3.8 clearly indicates that the concentration rose from 8.14 km downstream (A3) to around 11.0 km downstream during the irrigation period (A4). Furthermore, mild attenuation from 0.037 to 0.035 mg/L was detected at 11.0 km downstream at the most downstream site (A5). The dilution of T-Zn was enhanced by the greater river discharge at A5. The industrial point source might impact T-Zn concentrations primarily up to A4, as evidenced by an increase in concentration from 0.029 to 0.061 mg/L during the non-irrigation period. At A5 (0.062 mg/L), however, the concentration rose modestly. Other point and non-point sources might include road runoff (Hüffmeyer et al., 2009), wet and dry Zn deposition (Sörme and Lagerkvist, 2002), agricultural processes (Ke et al., 2017), and residential sources (Naito et al., 2010).

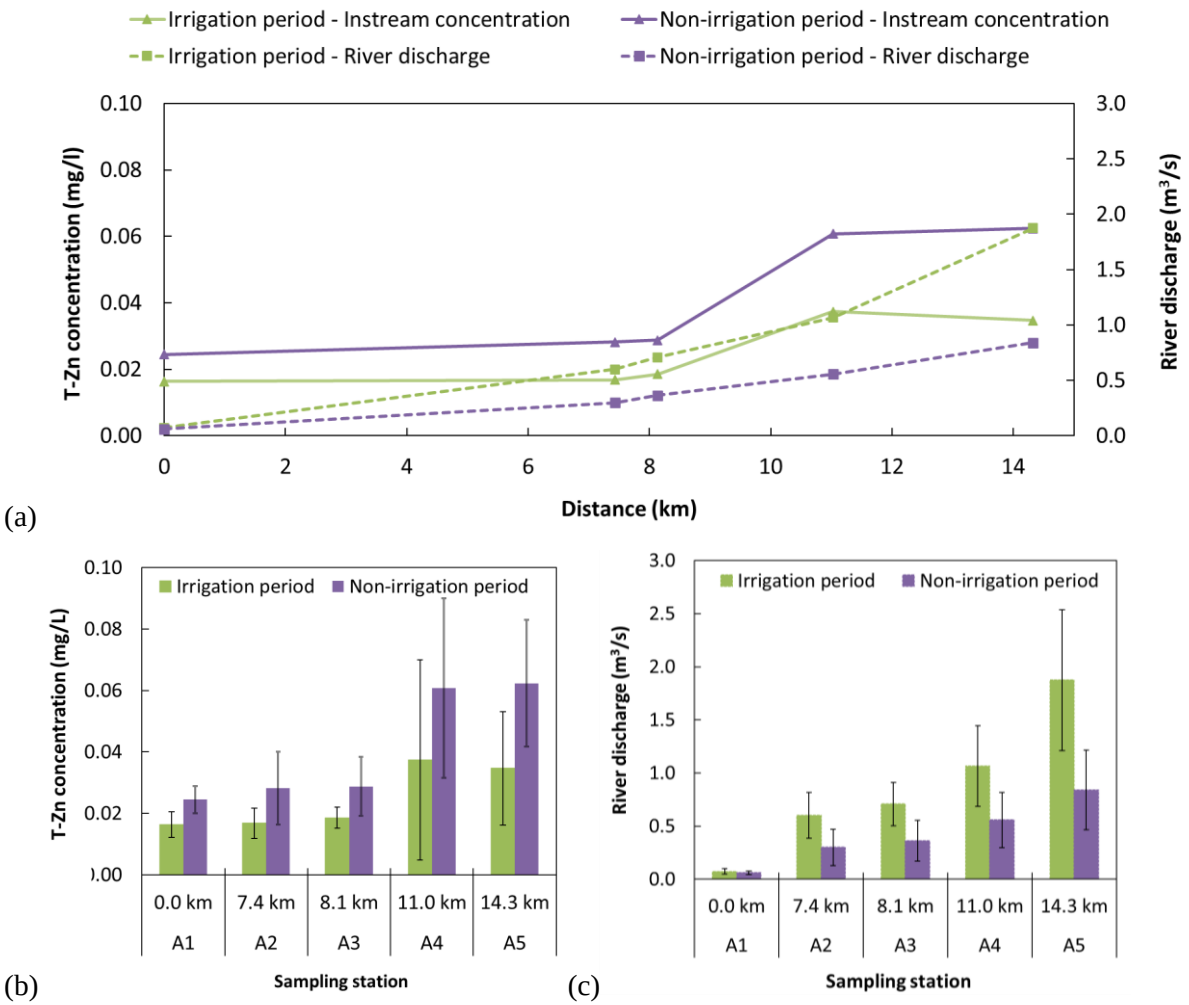

Figure 3.8 Average T-Zn concentrations and river discharges between irrigation and non-irrigation period in the Aizumame River: (a) T-Zn fluctuation over the distance (0 km to 14.3 km); (b) average values of T-Zn concentrations and error bar represents standard deviation; (c) average values of river discharges; the error bar represents standard deviation.

The larger the area and quantity of paddy fields, the further downstream the sample sites are. Agricultural activities might be to responsible for the substantial concentration increase observed during the irrigation period. Although the use of Zn in fertilizer can boost agricultural yields (Montalvo et al., 2016), excessive fertilizer usage can lead to an increase in Zn runoff into water bodies (Hüffmeyer et al., 2009; Naito et al., 2010). Elevated Zn levels have also been linked to agricultural activities in several studies (Ke et al., 2017; Maanan et al., 2015; Zhang et al., 2017). Another research of Zn runoff from highways found that inputs from tire wear might be substantially larger than those from atmospheric sources (Councell et al., 2004). Zn particles were also detected in brake pad emissions, according to Lough et al. (2005). However, if tire wear is the primary contributor, the connection between river discharge and Zn content should be strong. Unlike Mansoor et al. (2018), the current research found no

link between river discharge and Zn content as depicted in Figure 3.9. This implies that in the Aizumame river basin, Zn contribution from tire wear may be minimal.

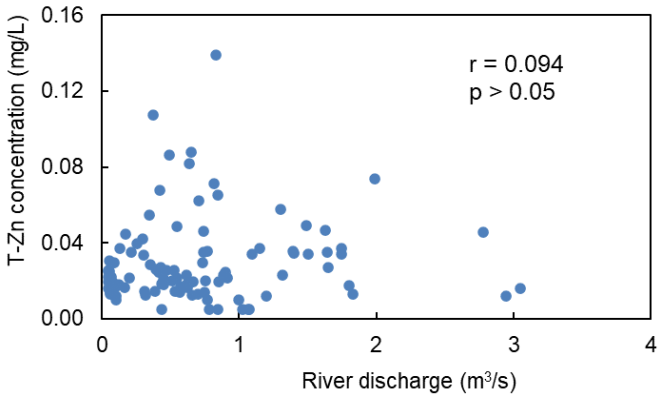

Figure 3.9 The correlation between T-Zn concentrations and river discharges during all sampling events

3.2.4 Total fraction of Zn concentrations comparison between weekday and weekend

Given the greater river discharge and Zn concentrations in the downstream part of the Aizumame River, it is critical to evaluate the contribution of industrial point sources by comparing working days (weekday) and weekends, so that the contribution to the mainstream might well be addressed properly. Samples were collected hourly for 24 hours on weekdays and weekends for the weekday-weekend survey. There are variations between weekday and weekend concentrations, as seen in Figure 3.10.

The greatest concentration difference was recorded from 13:00 to 15:00. T-Zn concentrations were much higher at A5 (0.025-0.060 mg/L) on weekday, than those during weekend (0.021-0.039 mg/L). River discharges during both sampling events were relatively stable at 0.20 m^3/s indicating that the T-Zn fluctuation did not relate to the river discharge. Other sources of T-Zn might contribute to these tributaries, although industry are the primary source of T-Zn in this area. The levels at A5 throughout the weekday have clearly exceeded EQS, although during the weekday at night the concentration also breached the EQS from 02:00 to 06:00 and 08:00 to 10:00. Further discussion including the T-Zn loadings and the contribution of industrial point sources is presented in Chapter 6.

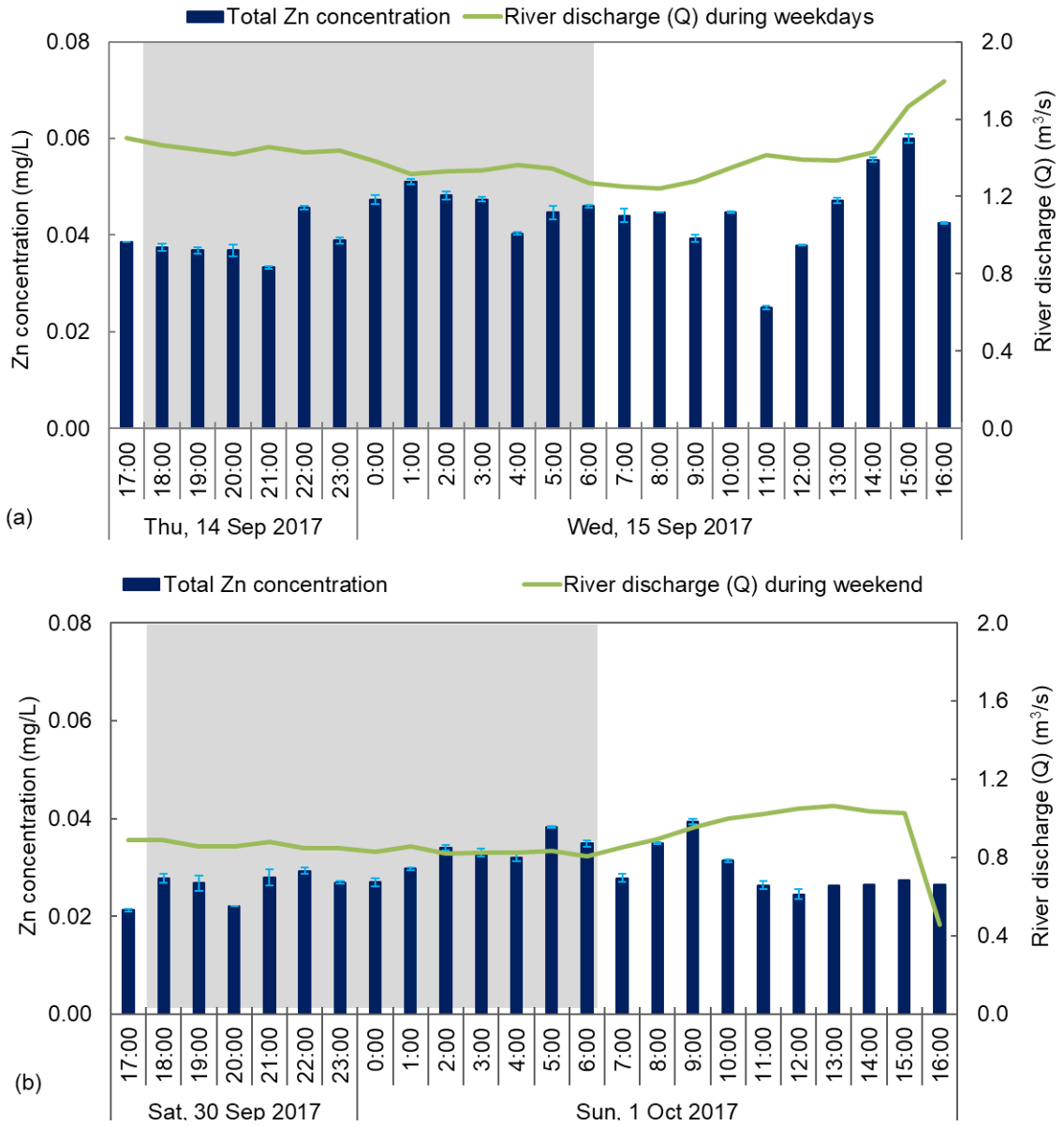

Figure 3.10 T-Zn levels on weekday and weekend in the Aizumame River: (a) weekday and (b) weekend

3.3 Umeda River

Compared to the Aizumame River, the Umeda River has smaller area of manufacturing industries (21.8%). Furthermore, the watershed area is dominated by agricultural crop land (66.6%). However, the paddy fields only accounted for 17.5%. It is necessary to identify the seasonal Zn levels variation and its fluctuation during irrigation and non-irrigation period. The watershed characteristic difference between the Aizumame River and the Umeda River may result in distinguished variation of Zn levels in each month over the year. The monthly survey was conducted from August 2019 to July 2020 (12 months in total). This section highlights the evaluation of Zn levels during irrigation period and non-

irrigation period, seasonal variation, and weekend-weekday levels comparison in the Umeda River, aiming at assessing the spatiotemporal variation of Zn levels for 12 months in surface water of the Umeda River, Aichi Prefecture, Japan.

3.3.1 Zn concentrations and loads in river water

The total Zn concentrations in surface water of Umeda River and its tributaries in a year are illustrated in Figure 3.11 and Figure 3.12. During the research period, Zn concentrations ranged from 0.11 mg/L (U1) to 0.031 mg/L (U5). The annual mean of T-Zn concentrations at U5 (0.031 mg/L) exceeded the EQS from August 2019 to July 2020, according to the Environmental Quality Standards (EQS) in Japan, whereas the average concentrations at U1, U2, U3, and U4 were 0.011 mg/L, 0.023 mg/L, 0.028 mg/L, and 0.029 mg/L, respectively. In the tributaries, the annual mean values were 0.014 mg/L (U31), 0.015 mg/L (U21), 0.007 mg/L (U22), and 0.026 mg/L (U23). The annual mean of Zn concentrations in U3, U4, and U23 almost exceeded the EQS. These findings highlight the need of determining the sources of Zn in the Umeda River basin.

In general, Zn concentrations rose as distance increased from upstream. Low values (0.005–0.026 mg/L) were sometimes undetectable (0.005 mg/L) at the highest upstream sites (U1). The U2 was situated right before the Sakai River's confluence (U21, U22, and U23). Beginning in October, Zn concentrations at U2 (0.005–0.062 mg/L) started to rise, eventually exceeding 0.030 mg/L in February and April 2020. The Zn concentrations at U2 might well be affected by an air conditioner dumped at the confluence in January 2020.

Except in November and April, concentrations at U3 before to the confluence with the Ochiai River (U31) were greater (0.010–0.062 mg/L) than those at U2. Point sources from industrial regions around the Sakai River might be to responsible for the increased Zn concentrations in U3. The Zn loading reaching the river might well be increased by point source input from the industrial zone adjacent to the river. Figure 3.13 illustrates that all Zn values in industrial wastewater (0.036–0.079 mg/L) were still below the National Effluent Standards of 2.0 mg/L, which were enacted in 2006. After U22, industrial wastewaters were released, affecting concentrations in U23. In August–September 2019, November 2019–January 2020, April, and July 2020, Zn concentrations at Station U22 are below the detection limit. In April 2020, the Sakai River's highest upstream station (U21) showed high concentrations on occasion, even exceeding the EQS. The agricultural and residential land usage around U21 may have contributed to the higher concentrations.

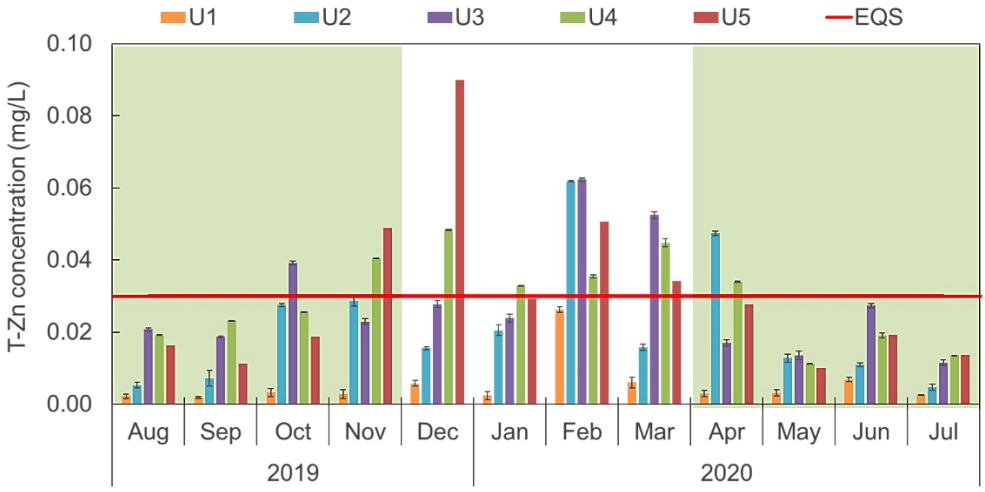

Figure 3.11 T-Zn concentrations in the mainstream of the Umeda River

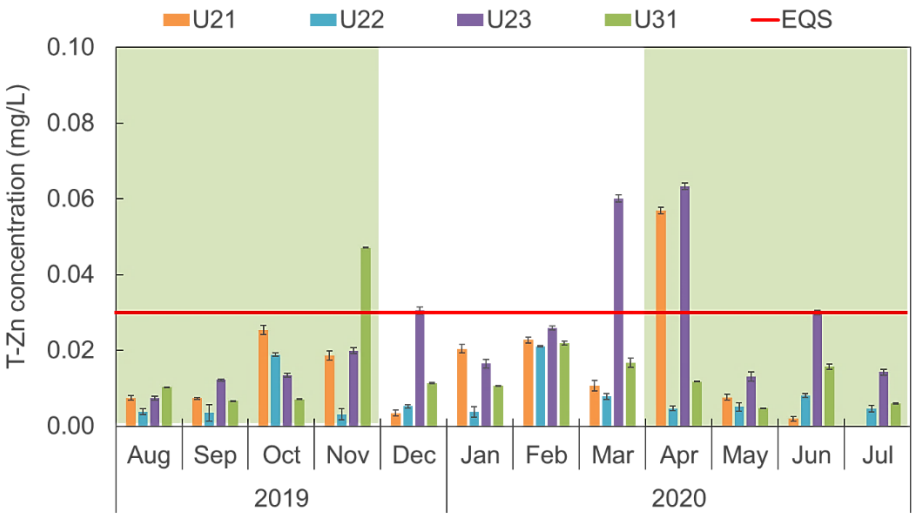

Figure 3.12 T-Zn concentrations in tributaries of the Umeda River

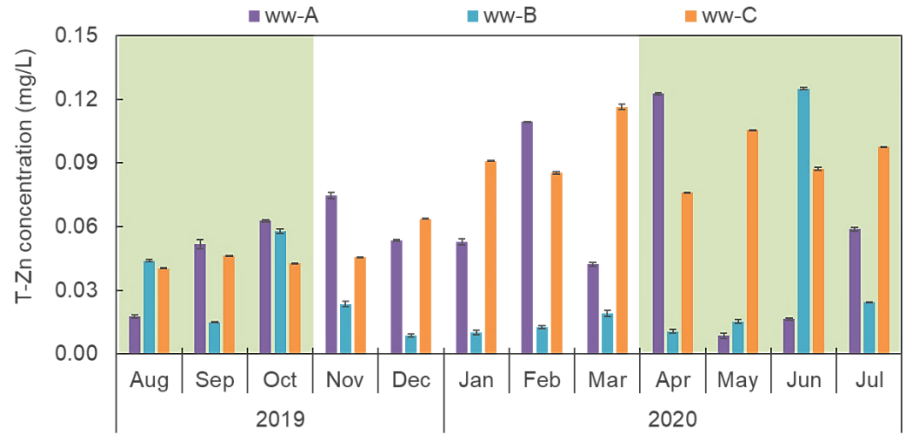

Figure 3.13 T-Zn concentrations of industrial wastewater located in the vicinity of Sakai River, a tributary of the Umeda River

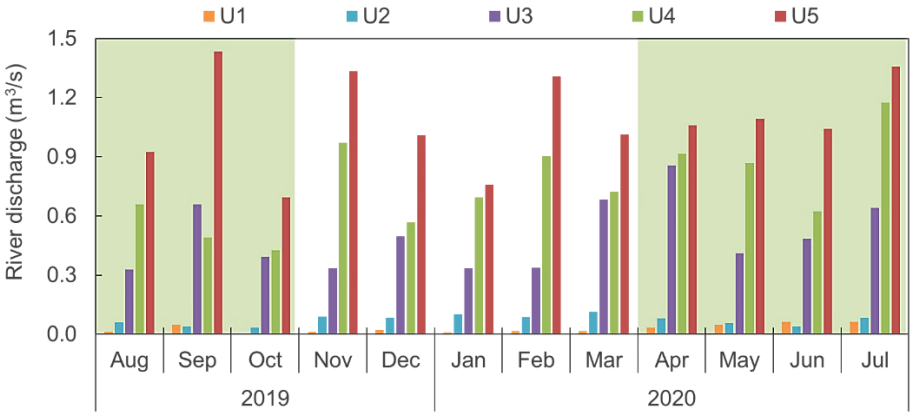

Figure 3.14 River discharges of mainstream of the Umeda River

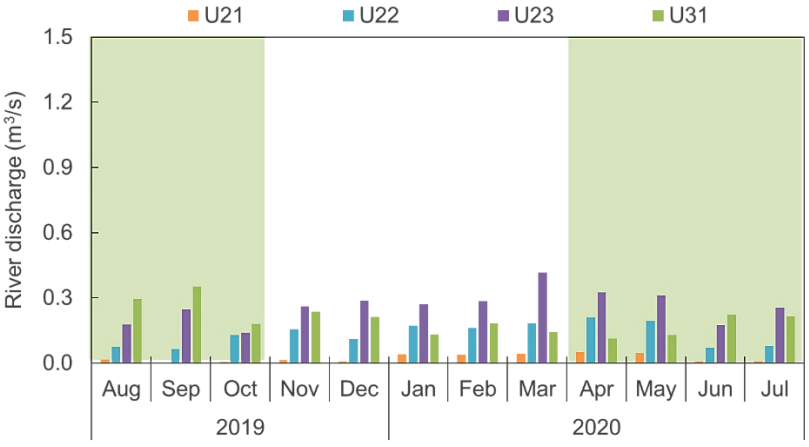

Figure 3.15 River discharges of tributaries of the Umeda River

Except for August, October, February 2019, and June 2020, Zn concentrations at U4 were typically greater than at U3. The amounts of Zn in the samples ranged from 0.011 to 0.048 mg/L. As a non-point

source, the U4 might add Zn load due to its proximity to trains, highways, and the Zoo and Botanical Park. The Umeda River's U5 segment was the farthest downstream. The Zn values at U5 were much higher (0.010–0.090 mg/L) than at other sample locations. In November, December 2019, February, and March 2020, total Zn values are higher than 0.030 mg/L. According to the annual mean value of total Zn concentration at U5, the EQS was violated, as previously stated. Anthropogenic activities may have a significant influence on the Zn concentrations in the region farther downstream.

The Zn concentrations in the Umeda River were greater from January to April 2020 than in other months, which might be due to industrial zone activities, which was reflected in wastewater Zn concentration data. In comparison to other seasons, Zn concentrations increased in the fall (September-November) and winter (December-February) (spring and summer). The highest concentration (0.090 mg/L) was found in December, whereas all sample sites in February had greater amounts (0.021–0.062 mg/L) than in previous months. Other anthropogenic causes might be to responsible, given that Zn contents in wastewater were low in December (Figure 3.13). Furthermore, due to minimal precipitation during the winter season, river discharges were reduced, potentially raising instream Zn concentrations. Figure 3.14 and Figure 3.15 depicted the values of river discharges for each sample occasion.

Total Zn and river discharges had a weak Pearson correlation ($r = 0.275$, $p < 0.05$). If non-point sources account for the majority of Zn load, the higher the river discharge, the higher the overall Zn concentration, particularly the particle component, as shown in the Gozzard et al. (2011).

Figure 3.16 and Figure 3.17 depict the total Zn load in Umeda River water samples from June 2019 to July 2020. The maximum Zn load occurred in November, December, February, and April, as can be shown. At the most downstream sample location, the Zn loading ranged from 954 to 7,833 g/day (U5). The upper stream section (U1–U4), on the other hand, had lower loads ranging from 2 to 3,551 g/day. Because of dilution and precipitation, total Zn loading might decrease down the stream, i.e. in July 2019, October 2019, and March 2020. The overall Zn loading in the Umeda River, on the other hand, typically increased downstream. The total Zn loading of U5 reached approximately 1.06 t from August 2019 to July 2020, and subsequently flowed to Mikawa Bay.

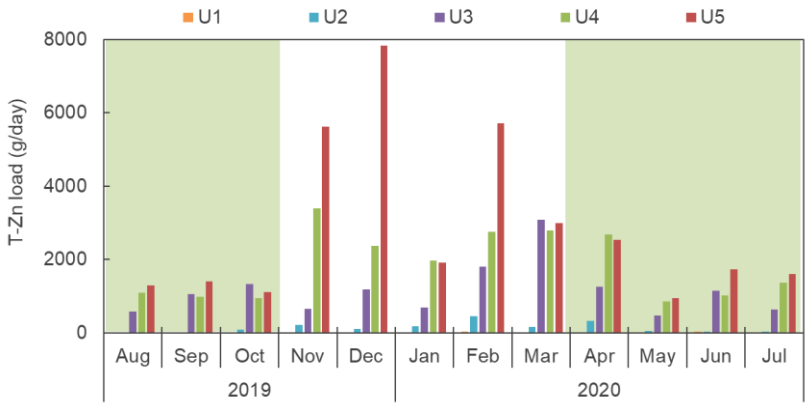

Figure 3.16 T-Zn loads in the mainstream of Umeda River

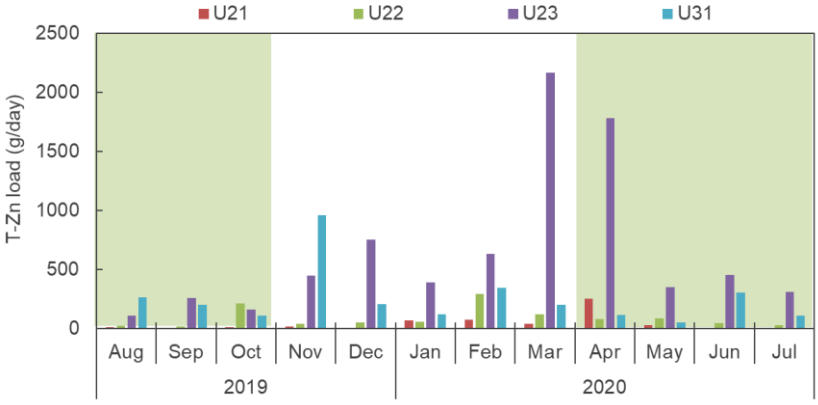

Figure 3.17 T-Zn loads in the tributaries of Umeda River

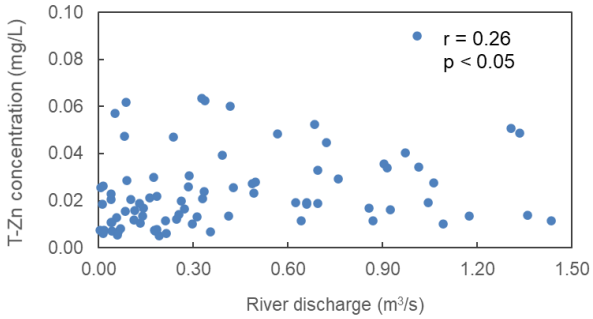

Figure 3.18 Scatterplot of river discharges and T-Zn concentrations

Different from the Aizumame River, there was a low correlation ($r = 0.26$, $p < 0.05$) between T-Zn and the river discharge at all sampling stations during the monthly survey. It may indicate that not only point sources, but also non-point sources contributed to the instream T-Zn concentrations along the Umeda River.

3.3.2 Total fraction of Zn concentration comparison among seasons

The river discharges of the Umeda River were not significantly affected by the seasons as illustrated in Figure 3.19. The river discharges in autumn were initially the lowest at the upstream, but eventually became the highest at the most downstream point [remarkably increased from 0.63 m^3/s at (7.6 km) to 1.15 m^3/s (10.5 km)]. Although winter did not have the lowest river discharge, the T-Zn levels at all sampling stations were also the highest among other seasons, a similar case to the Aizumame River. The concentrations from the most upstream to 10.5 km downstream were 0.016–0.057 mg/L (winter), 0.004–0.024 mg/L (spring), 0.003–0.026 mg/L (autumn), and 0.004–0.016 mg/L (summer). This tendency of T-Zn concentrations (winter>spring=autumn>summer) is nearly the same as the Aizumame River's case.

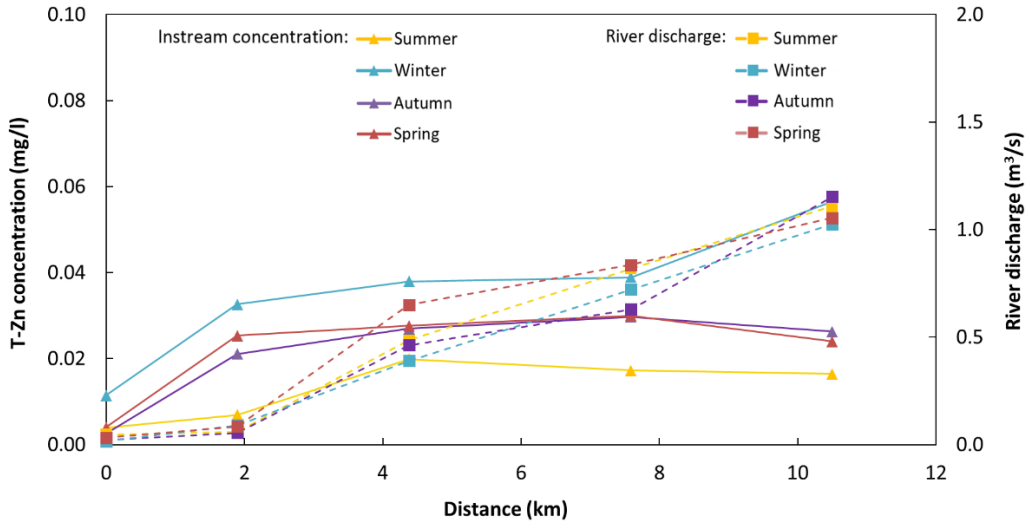

(a)

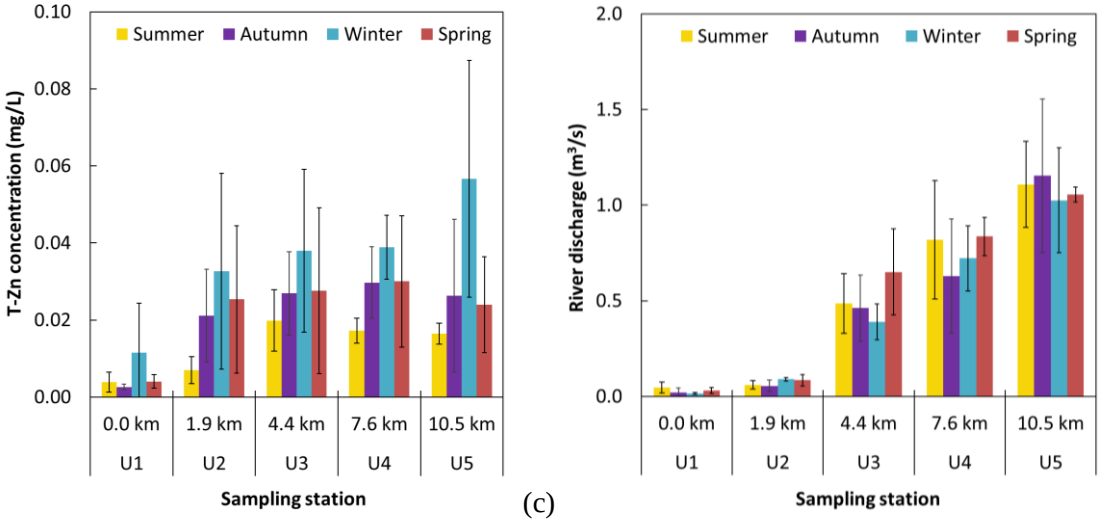

(b) (c)

Figure 3.19 Average value of T-Zn concentrations and river discharges in the Umeda River in each season: (a) T-Zn fluctuation over the distance (0 km to 10.5 km); (b) average values of T-Zn concentrations and error bar represents standard deviation; (c) average values of river discharges; error bar represent standard deviation.

3.3.3 T-Zn concentrations comparison between non-irrigation and irrigation period

Figure 3.20 shows the average values of instream T-Zn concentration and river discharge trends during irrigation period and non-irrigation period. The T-Zn exhibited distinguished concentrations during both periods in which non-irrigation period exhibit higher concentrations than during irrigation period. However, paddy fields only accounted for 17.5% of total area mainly dominated in the lower reach of Umeda River, thus, might cause indifferent river discharges between two periods, apart from U3 when irrigation period has slightly higher discharge. The instream T-Zn concentrations from upstream to downstream sampling stations increased gradually from 0.009 mg/L to 0.051 mg/L during non-irrigation period. However, in the period irrigation, T-Zn slightly attenuated from 4.4 (0.021 mg/L) km to 10.5 km (0.017 mg/L) downstream.

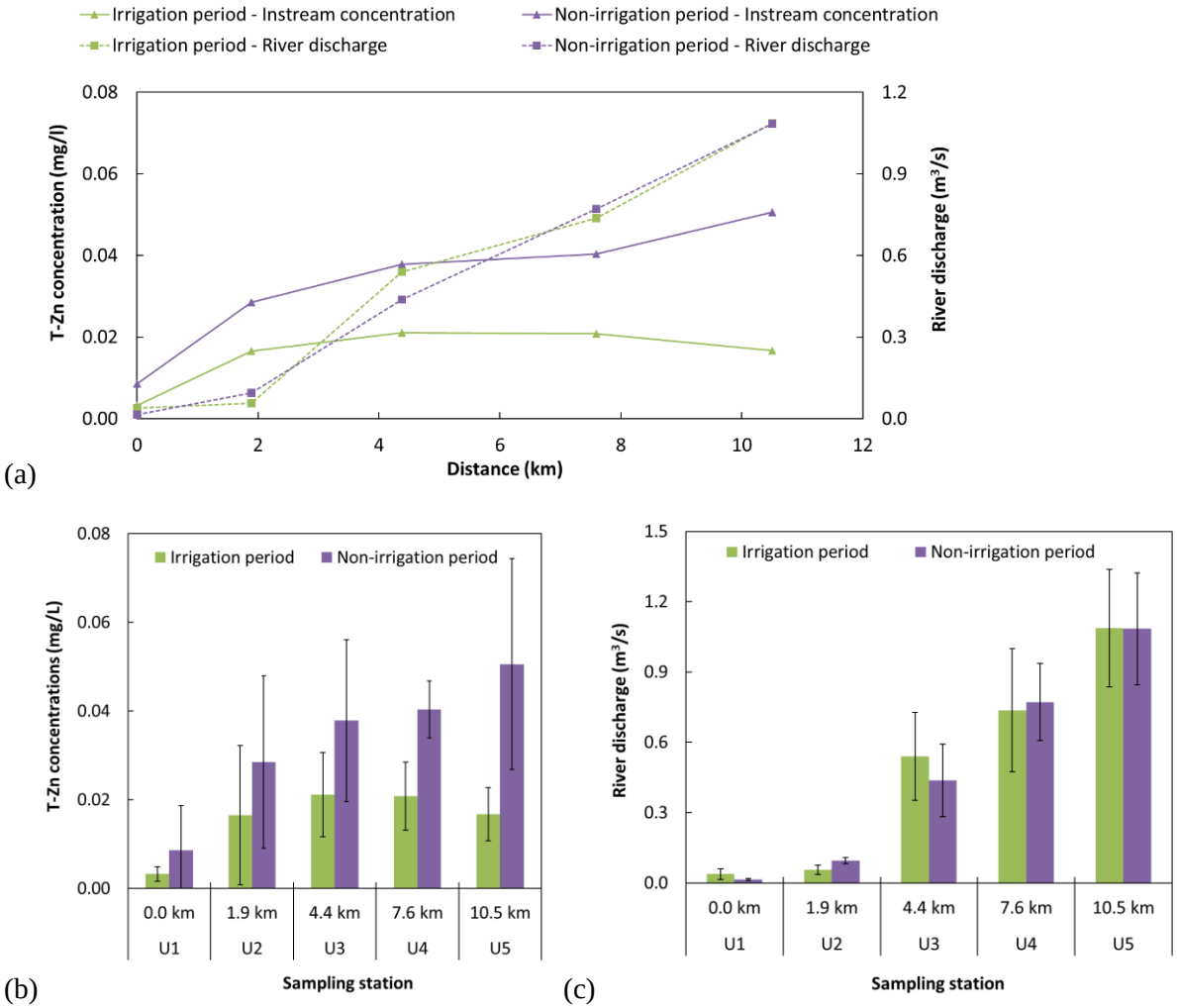

Figure 3.20 Average value of T-Zn concentrations and river discharges in the Umeda River in irrigation and non-irrigation period: (a) T-Zn fluctuation over the distance (0 km to 10.5 km); (b) average values of T-Zn concentrations and error bar represents standard deviation; (c) mean values of river discharges; error bar represents standard deviation.

3.3.4 Total fraction of Zn concentrations comparison between weekday and weekend

Figure 3.21 shows the Zn concentrations for 25 hours during weekday and weekend. In February, there was a significant variation in Zn concentration between weekdays and weekends (during the winter season). Weekday Zn concentrations (mean: 0.034 ± 0.008 mg/L, range: 0.019–0.051 mg/L) were greater than weekend Zn values (mean: 0.016 ± 0.006 mg/L, range: 0.001–0.029 mg/L).. The Zn concentrations showed that they were fluctuating (up to 392% in amplitude from the minimum to the maximum level). Regardless of river discharge variations, Zn concentrations were much greater at night than during the day. Except at 18:00, the EQS was significantly exceeded during the weekday evenings. These findings suggest that the increased Zn concentrations were caused by human activities that occurred exclusively on weekdays.

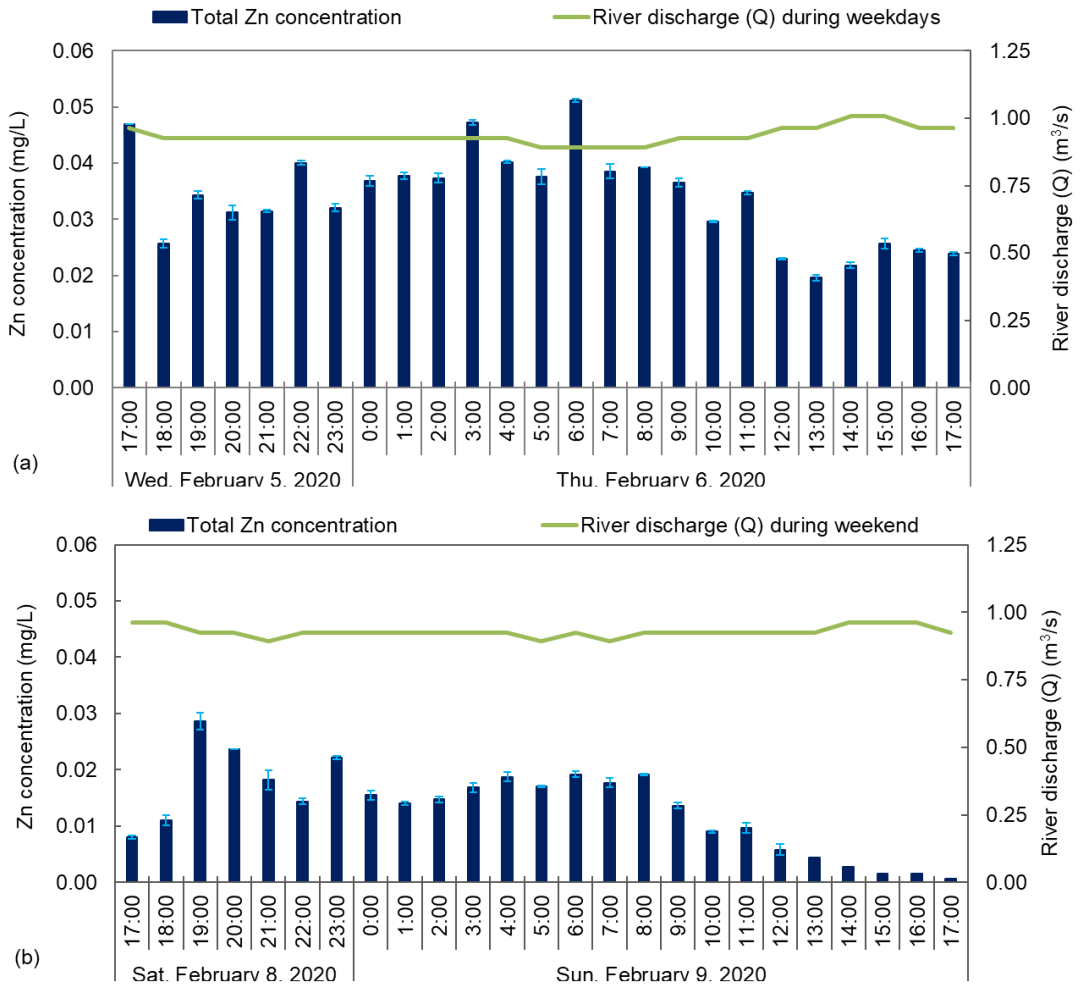

Figure 3.21 T-Zn concentrations on weekday and weekend in the Umeda River: (a) weekday; (b) weekend. The error bars depict standard deviations.

Chapter 4 Spatial and temporal variability of Zn in particulate, dissolved phase, and riverbed sediment in the Umeda River

Summary

This chapter assessed the spatial and temporal variations of Zn and Fe for nine months in the Umeda River in Japan's Aichi Prefecture. The increasing Zn levels were observed from upstream to downstream section of the Umeda River. The industrial wastewater point sources were identified in the Ochiai River and Sakai River, the tributaries of the Umeda River. However, only the Sakai River contributed a significant Zn input to the Umeda River. It is also revealed that the most common phase in Zn in the Umeda River is in dissolved form, although the river water pH is near-neutral. The Zn also exhibited seasonal variation where the highest concentration occurred in the winter season (December). However, the Zn concentrations in the mainstream were relatively high from October to March.

This chapter also provide detail information about the dissolved water parameters such as pH, EC, temperature, suspended solids, HCO_3^-, major cation (Ca^{2+}, Mg^{2+}, Na^+, K^+) and major anion (Cl^-, NO_3^-, SO_4^{2-}). The major cation and anion concentrations were apparently influenced by anthropogenic activities, indicated by high concentration of K^+, NO_3^-, and SO_4^{2-}.

The riverbed sediment provided more information about the Zn concentration in the Umeda River. The results showed that the Zn presence in the coarse sand (0.6–1.0 mm) was relatively higher than other grain size categories [fine sand (<0.3 mm) and medium sand (0.3–0.6 mm)]. Compared to the Zn concentrations in river water, the Zn in riverbed sediment did not exhibit an obvious seasonal variation. Indeed, the concentration in summer (May and July) was relatively lower than other seasons. Other riverbed sediment parameters (i.e. Fe and POC) measurement results are also presented in this chapter.

4.1 Introduction

This chapter gives insights about the Zn pollution in the Umeda River by assessing the water parameters such as pH, EC, temperature, suspended solids, HCO_3^-, major cation (Ca^{2+}, Mg^{2+}, Na^+, K^+) and major anion (Cl^-, NO_3^-, SO_4^{2-}, HCO_3^-). Fe is a naturally occurring abundant element in river (Guo and Barnard, 2013) and Fe hydroxides may adsorb the Zn in the surface water (Gammons et al., 2015; Nimick et al., 2003). It is also possible that adsorption of Zn on organic matter occur in the river, thus, measuring particulate organic carbon (POC), as the organic ligand, is necessary to verify whether the Zn is associated with POC. Particulate and dissolved phase of Zn and Fe were measured because ions in water column are divided by dissolved phase and particulate phase (Le Pape et al., 2012). The sampling campaigns of these parameters are the same as the monthly sampling in the Umeda River. However, only water samples for nine months (August, October, November 2019, January–June 2020) were measured for the HCO_3^-, major cations, and anions.

Furthermore, riverbed sediment quality has brought significant concern. The sediment could play a key role as a reservoir of a pollutant (i.e. Zn) and directly interacts with water quality affected by various factors (Fu et al., 2014; Liao et al., 2017). As described in Table 1.1, the sampling campaign collecting riverbed sediment samples was the monthly survey in Umeda River, but the sediment samples were collected bimonthly for seven months (July, August, September, November 2019, January, March, May 2020).

The details of samples collection and water analyses are described in Chapter 2. The Chapter 4 aims to analyze Zn variations, both in aqueous phase (dissolved and particulate) and riverbed sediment, and related parameters across the sampling stations in different seasons.

4.2 Water column

4.2.1 Spatial and temporal variation of dissolved and particulate Zn concentrations

The results of Zn concentrations in the main stem of the Umeda River during the monthly survey from August 2019 to July 2020 are illustrated in Figure 4.1 (mainstream of the Umeda River), Figure 4.2 (tributary), and Figure 4.3 (industrial wastewater). Table 1 shows a summary of all metrics (SS, Zn, Fe, POC, and river discharge). Zn levels varied significantly across seasons, as evidenced by substantial CVs (50–155% for P-Zn; 33–202% for D-Zn). The Zn levels, which were mostly in dissolved form, tended to rise downstream. U5, U4, U3, and U23 were all found to have significant Zn concentrations. Three manufacturing industries around U23 release their effluent into the Sakai River. Figure 4.3 depicts the detailed wastewater measurement results (Zn). The overall proportion of Zn concentrations in the wastewater did not exceed the national effluent standards (NES), as shown in Figure 4.3. However, Zn levels in the Umeda River's downstream section remained elevated. During the preliminary survey, no further point sources of Zn were discovered. In December 2019 and February 2020, Zn concentrations

in U5, U4, and U3 surpassed the environmental quality standards (EQS). EQS exceedances were also seen in U4 (February, March), U3 (February, March), and U23 in March 2020. (February). Zn concentrations were found to be relatively high in virtually all sample locations from December 2019 to April 2020. Figure 4.1 and Figure 4.2 demonstrate that Zn levels were much greater in the winter and spring than in the summer.

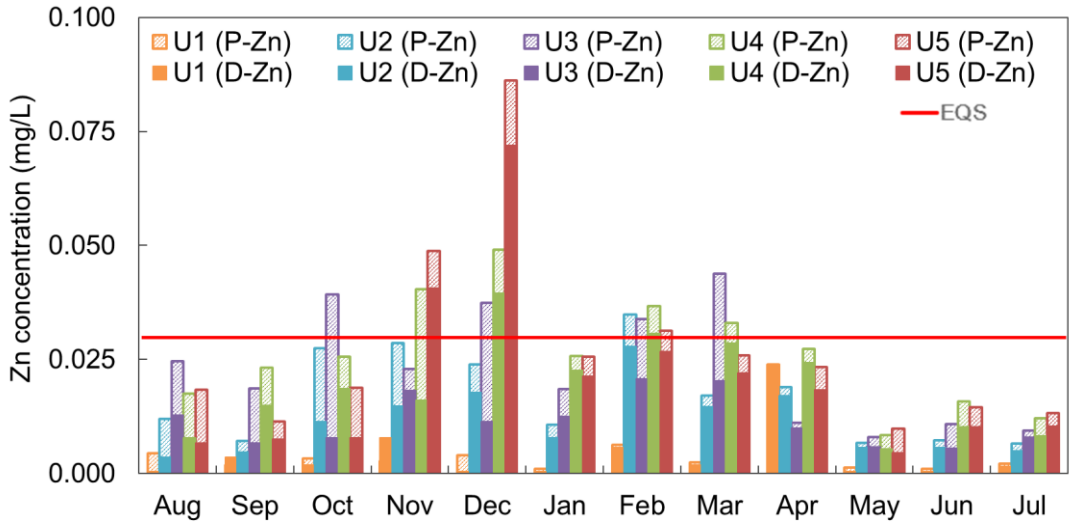

Figure 4.1 Zn concentrations in particulate (P-Zn) and dissolved (D-Zn) phase in the mainstream of the Umeda River

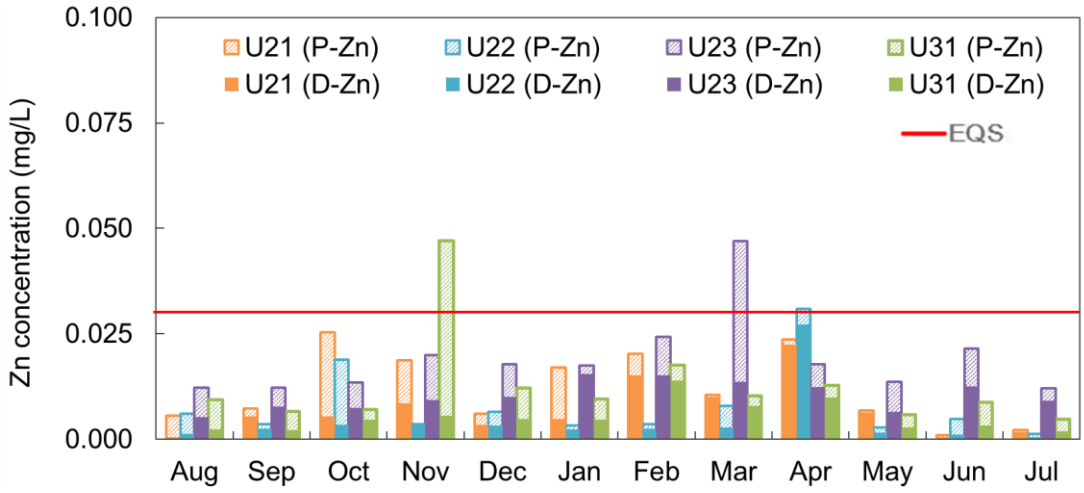

Figure 4.2 Zn concentrations in particulate (P-Zn) and dissolved (D-Zn) phase in the tributaries of the Umeda River: U31 was located in the Ochiai River whereas U21–U23 were located in the Sakai River

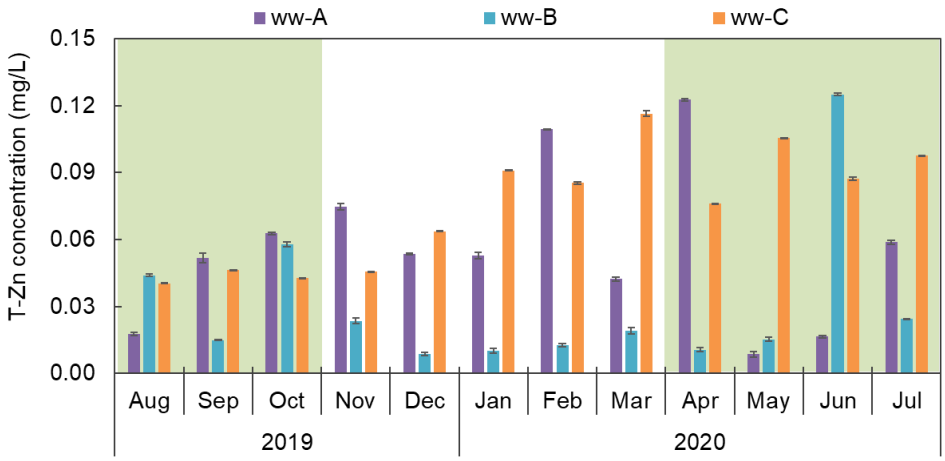

Figure 4.3 Zn concentrations in particulate (P-Zn) and dissolved (D-Zn) phase in the industrial wastewaters located in the vicinity of the Sakai River

4.2.2 Spatial and temporal variation of dissolved and particulate Fe concentrations

As a potential natural element in river water, Fe measurement is required. Figure 4.4 depicts the findings of Fe measurements in the Umeda River's main channel, Figure 4.5 depicts the tributaries, and Figure 4.6 illustrates the industrial effluent. The inorganic component of SS could be regarded Fe, whereas the organic portion of SS represents POC (Figure 4.7). During the monthly survey, the Fe levels did not show any apparent downstream trends. There was no seasonal change in Fe levels. Nonetheless, in June 2020 (summer), quite high Fe concentrations were detected in the mainstream.

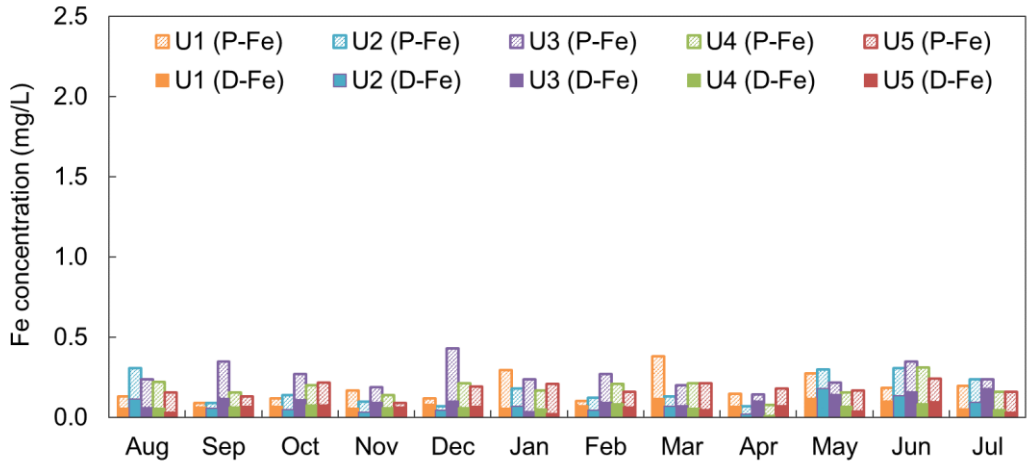

Figure 4.4 Fe concentrations in particulate (P-Fe) and dissolved (D-Fe) phase in the mainstream

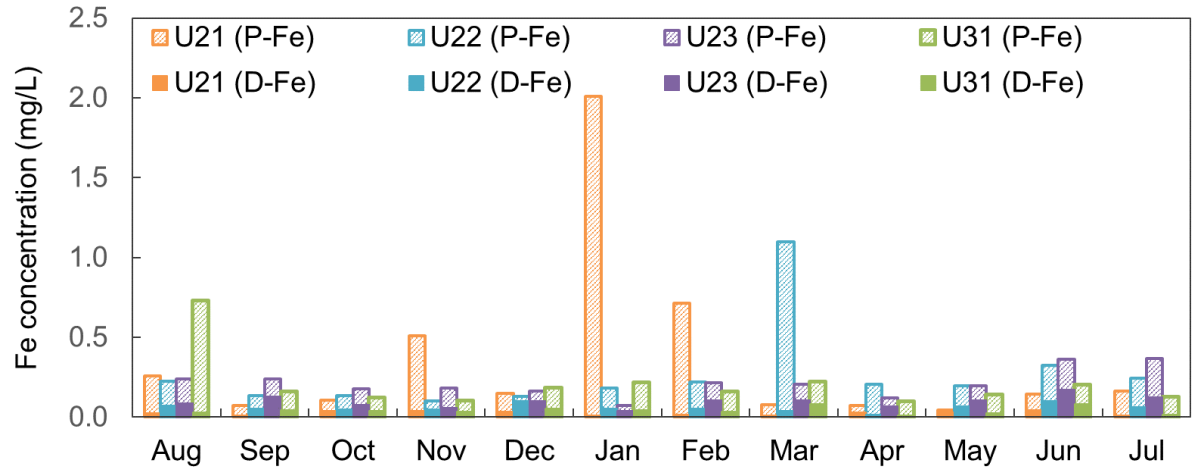

Figure 4.5 Fe concentrations in particulate (P-Fe) and dissolved (D-Fe) phase in the tributaries

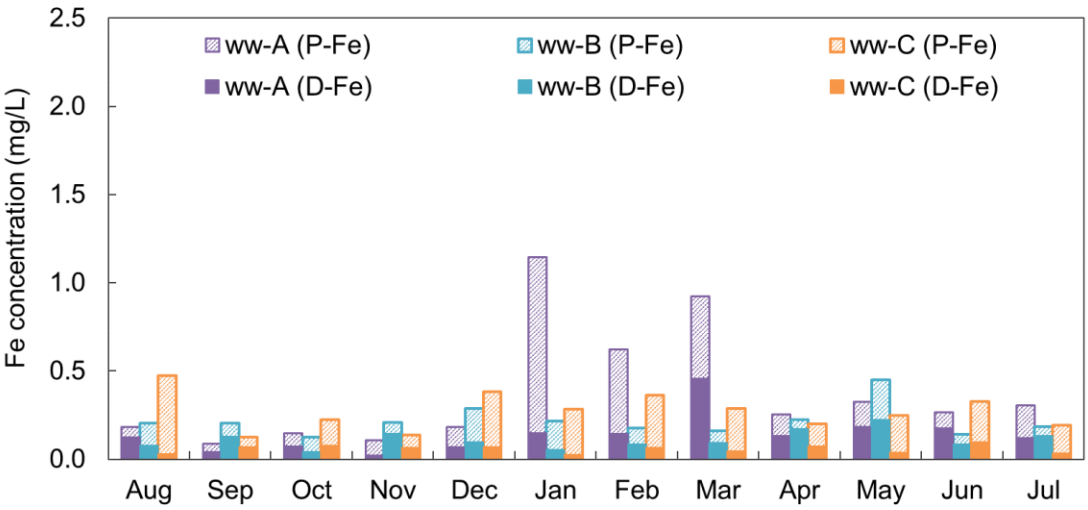

Figure 4.6 Fe concentrations in particulate (P-Fe) and dissolved (D-Fe) phase in the industrial wastewaters discharged from the industrial areas in the vicinity of the Sakai River

Wastewater discharge or leaching from soil or sediment might affect the dynamic of Zn and Fe concentrations in river water. Changes in physiochemical characteristics may cause metal redistribution between particulate and solution fractions. The pH was near neutral (7.17 ± 0.17) and rather constant (CV 6%), suggesting that pH may not be the primary driver of monthly Zn variability.

4.2.3 Spatial and temporal variation of particulate organic carbon (POC)

Particulate organic carbon (POC) concentrations varied from 27 to 281 mg/g (U1), 25 to 528 mg/g (U2), 24 to 283 mg/g (U3), 66 to 297 mg/g (U4), 62 to 283 mg/g (U5), 77 to 330 mg/g (U21), 95 to 207 mg/g (U22), 117 to 422 mg/g (U23), and 60 to 312 mg/g (U31). U23 has the largest POC level among other sampling stations. U23 also has a relatively higher Zn concentration. Although the CV did not vary (29–

57%) as high as those of Zn, based on Figure 4.7, it is obvious that in February and March, the POC exhibited relatively higher concentrations than in other months. However, it should be noted that August and May when the Zn in river water did not have high concentration, the POC also has relatively high concentrations. June, July, September, and October have relatively low levels of POC which might be due to the high frequency of rainfall (thus potential higher river discharge).

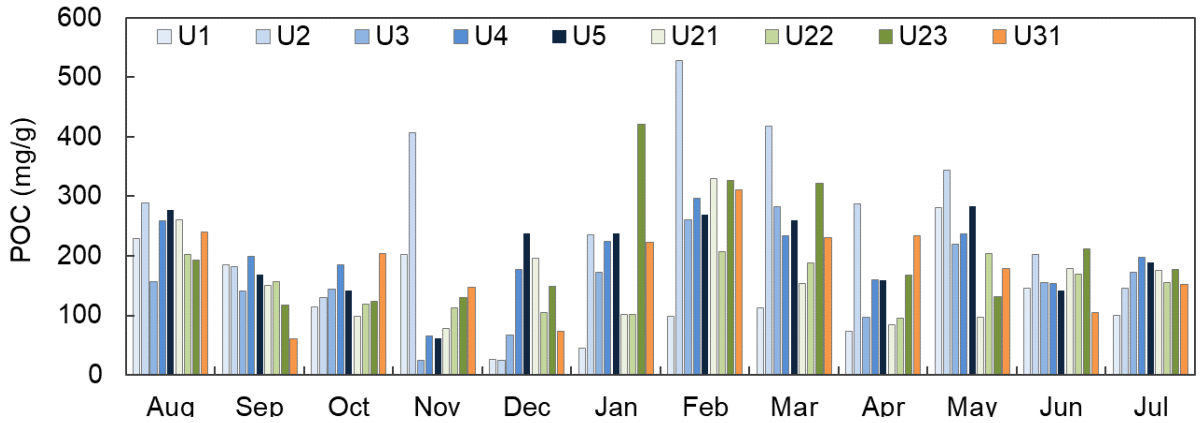

Figure 4.7 Particulate organic carbon (POC) concentrations in suspended solids (SS) in the river water

4.2.4 Other water parameters measurement results

The summary of all measurement results in the aqueous phase are described in Table 4.1 and Table 4.2

4.2.4.1 On-site measurement (temperature, pH, EC)

The water temperature is an important parameter because most of biochemical reaction are temperature dependent, namely solubility of dissolved oxygen in water column, rates of metabolism and growth of aquatic organisms, rate of photosynthesis). The results of temperature measurement in the Umeda River are illustrated in Figure 4.8a. The lowest temperatures were in winter (January 2020, 7.5–10.6 °C), whereas the highest temperatures occurred in summer (August 2019, 27.7–32.2 °C). May (spring), June and July (summer) have relatively similar temperature ranges. At high temperature, the aquatic plants may grow and die faster which eventually leaving behind organic matter that require oxygen for decomposition. The temperature may also affect the diel cyclicity of other several water parameters (Nimick et al., 2011). The coefficient of variance (CV) in temperatures varied from 35% (at U22 and U23) to 49% (at U21). c. As the temperature increases, the surface water temperature will likely increase, although the change in water temperature may be lower than change in air temperature (Morrill et al., 2001).

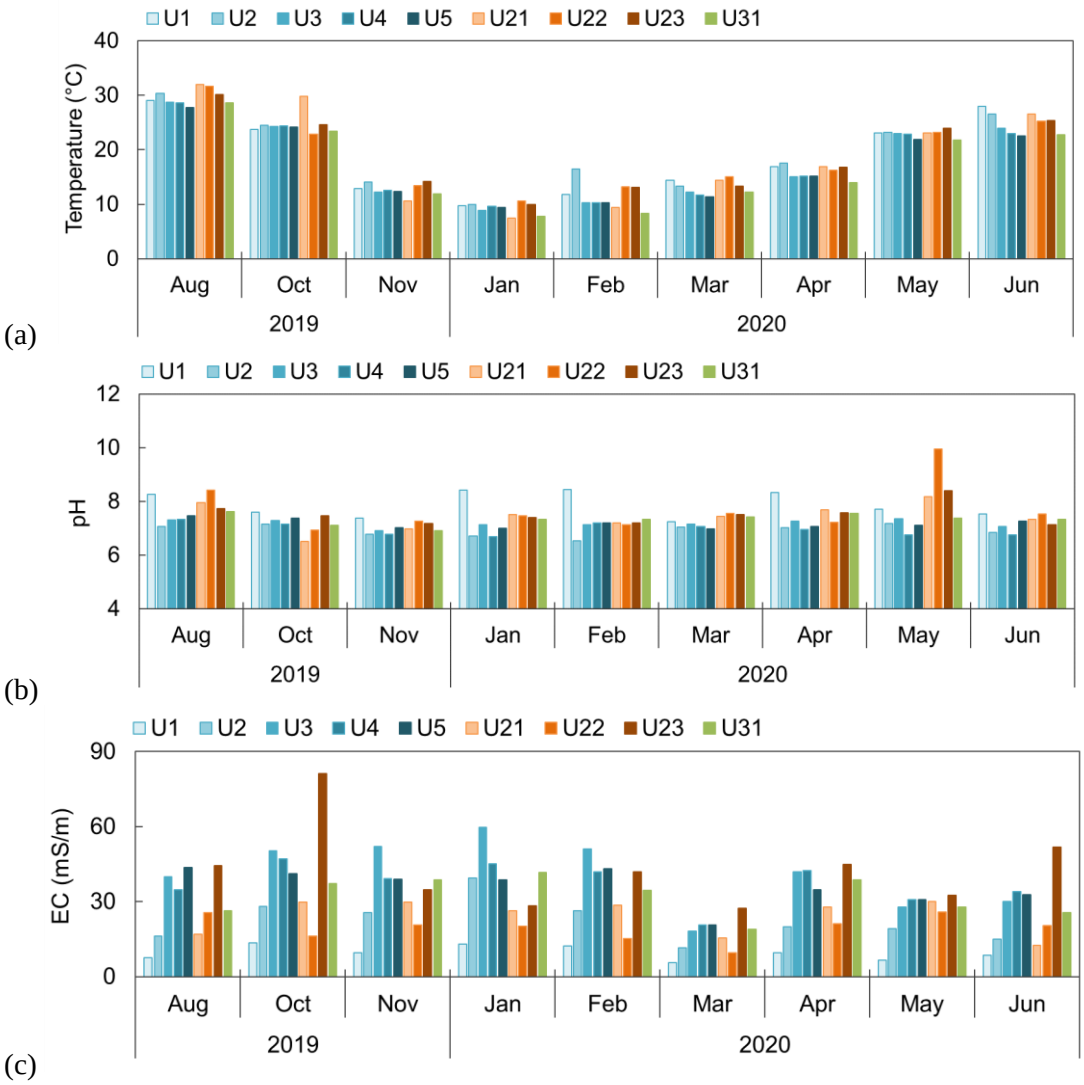

Figure 4.8 On-site measurement (temperature, pH, and EC) in the Umeda River and its tributaries: (a) Temperature; (b) pH; (c) EC

The pH value is determined by taking the negative logarithm of the molar concentration of hydrogen ion (H^+). The pH measurement in river water is to determine how acidic or basic the water is on scale from 0 to 14. The results of pH measurement in the Umeda River are shown in Figure 4.8b. The Umeda River had a near neutral pH ranging from 6.54 to 8.43. The pH did not exhibit remarkable seasonal variation in this case. The pH value play a key role in determining the speciation of Zn (Gammons et al., 2015; Gogoi et al., 2016). No seasonal variation was observed in pH.

Electroconductivity (EC) is a measure of the water ability to transfer an electrical current which is influenced by the presence of inorganic dissolved anions (that carry a negative charge) and cations (that carry a positive charge). Temperature also affects EC. The warmer the water temperature, the higher the conductivity, thus conductivity is reported as EC at 25 °C. As shown in Figure 4.8c, the EC generally

increased toward downstream direction in the Umeda River. EC at U23 was extremely high affected by K^+ and SO_4^{2-}. March has the lowest EC compared to other months, whereas January has the highest EC in all sampling stations.

4.2.4.2 Major cations (K^+, Na^+, Ca^{2+}, Mg^{2+})

The concentrations of major cations can be seen in Figure 4.9. Kalium (K^+) is the common cation in river water. It is released from silicate minerals like potassium feldspar and mica. The overall lowest concentrations exhibited in May. Generally, the higher concentration found in U2 then decreased along the Umeda River until U1. In Sakai River, the K^+ is extremely high in October along with sulphate (see Subsection 4.2.4.4). Relatively high concentrations in U23 were always found during all sampling events, apart from November, January, and May.

Natrium (Na^+) is usually related to chloride ions. Rocks containing NaCl are the most common source of the natrium found in river water. Sewage, fertilizers, and road salt are common sources of Na^+ in river water. The natrium concentrations in October and February were relatively higher compared to other months. It is also revealed that U23 was the highest during all sampling events. No obvious seasonal variation was observed in natrium.

Calcium (Ca^{2+}) is the abundant cation found in the world´s rivers. It is released by the weathering of sedimentary carbonate rocks and is often grouped with magnesium (Mg^{2+}) to describe the water hardness. Both calcium and magnesium in the Umeda River and its tributaries showed a similar tendency. In the Umeda River, the higher concentration, the higher the distance downstream, but in the Sakai River, U21 was the highest. U22 and U23 could be the highest interchangeably.

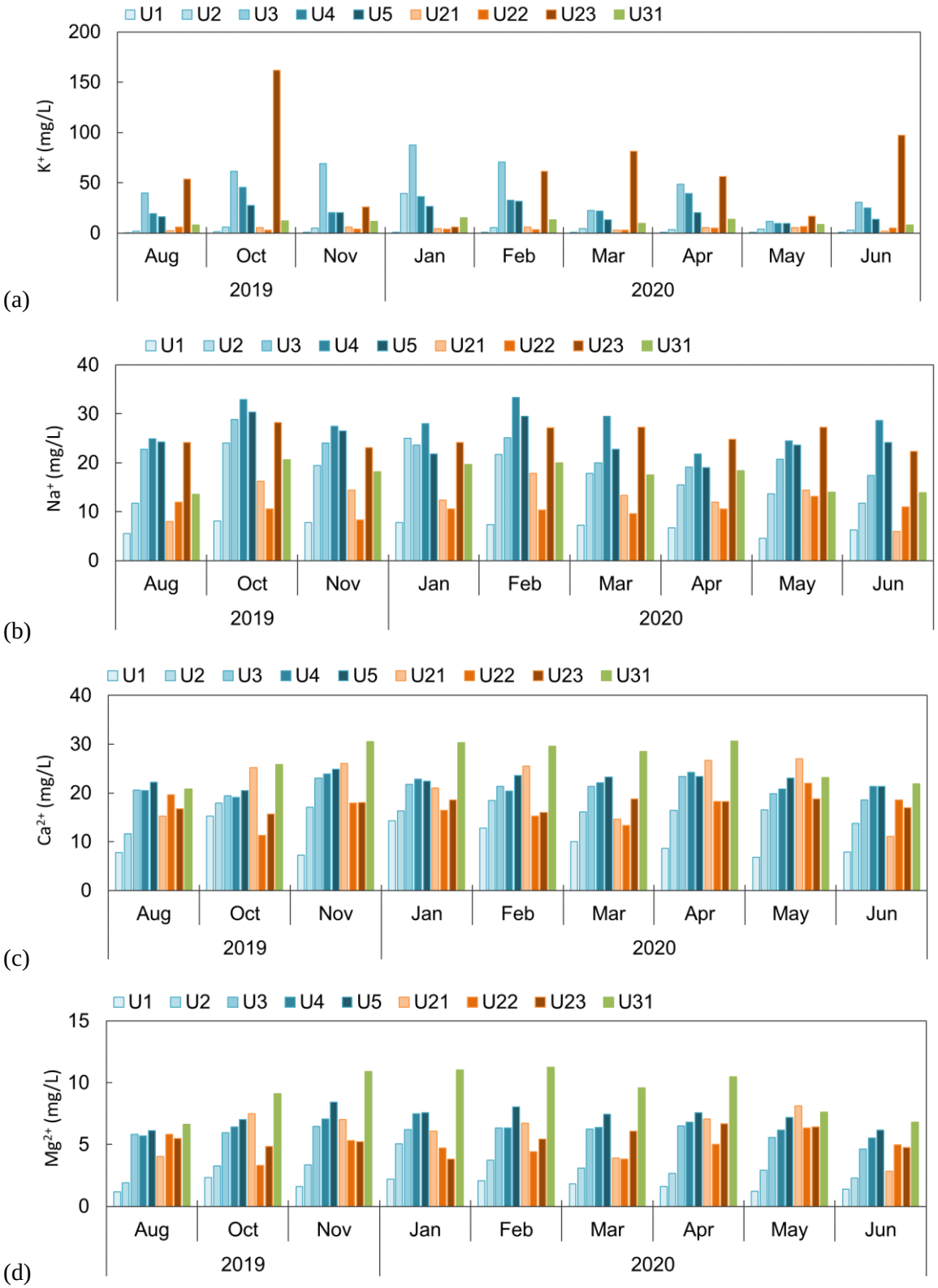

Figure 4.9 Major cation concentrations in the Umeda River and its tributaries: (a) K^+; (b) Na^+; (c) Ca^{2+}; (d) Mg^{2+}

4.2.4.3 Major anions (HCO_3^-, Cl^-, NO_3^-, SO_4^{2-})

Zn forms complexes with bicarbonate (HCO_3^-), chloride (Cl^-), nitrate (NO_3^-), and sulfate (SO_4^{2-}). The complexes with sulfate and phosphate are the most important regarding total Zn in solution. Under neutral or alkaline conditions, The formation of carbonates is also possible (Simon-Hertich et al., 2001), and is probably an important factor in explaining some of the retention of Zn at high pH values. The concentrations of major anions are illustrated in Figure 4.10.

Bicarbonate (HCO_3^-) may originate from rocks and soil weathering, salts, certain plant, and industrial wastewater discharges. Carbonate rocks (limestone, $CaCO_3$) are the main source, thus, often associated with the hardness. Moreover, the process of respiration which indirectly generates bicarbonate (HCO_3^-). The respiration continuously produces CO_2 which eventually encourage the generation of HCO_3^-. Figure 4.10a shows that the HCO_3^- increased to the downstream in the Umeda River in August, November, March, April, May, June. However, in Sakai River, U22 showed lowest concentration in October, November, February, March, April, May. However, overall, there was no obvious seasonal variation in HCO_3^-.

Chloride ions (Cl^-) could be generated from weathering of rocks and soil. However, pollutant may be a key source in wastewater contaminated rivers. It may also form a soluble Zn (ZnCl) which is one of the concerned compounds in Japan. Figure 4.10b shows that October has the lowest range of Cl^-. In the Umeda River, the trend of Cl^- showed U2 > U3 > U1 and U5 > U4 > U3 in November, January, February, March, April and June. Other trend shows that the concentration increased with increasing distance downstream. In Sakai River, U23 has relatively higher concentration than those in upstream section. The levels of Cl^- at U31 were also relatively high.

Nitrate (NO_3^-) is found naturally in environment and is a necessary plant nutrient. Nitrate can reach the river because of agricultural activity, such as excess application of inorganic nitrogenous fertilizers and manures, and from wastewater discharges. In October, November, January, February, March, and April, the nitrate concentrations were extremely high at U31, which might indicate agricultural activities in the vicinity of Ochiai River. U21, the most upstream in Sakai River, also showed higher concentrations compared to U23 which was the downstream of Sakai River. In the Umeda River, U2 (in November, February, March, and May) and U5 (in August, January, April, and June) has the highest concentrations in the respective months.

In natural environment, sulphate (SO_4^{2-}) is derived from rocks weathering. However, it may also originate from anthropogenic pollutants, i.e., fertilizers, wastewater, and mining. Sulphate sources may include acidified rainfall which may show elevated concentrations compared to overall ionic concentrations. In the Sakai River, there is also a battery and electronic manufacturers which discharge wastewater which potentially increasing sulphate in the water bodies. Extremely high concentrations

found in U23 after wastewater input as shown in Figure 4.10c, particularly in August, October, March, and June. The overall highest concentrations in the Umeda River were in January, despite the lower concentration of sulphate in U23. Nevertheless, the sulphate concentrations in U1, U21, U22, and U31 were always low.

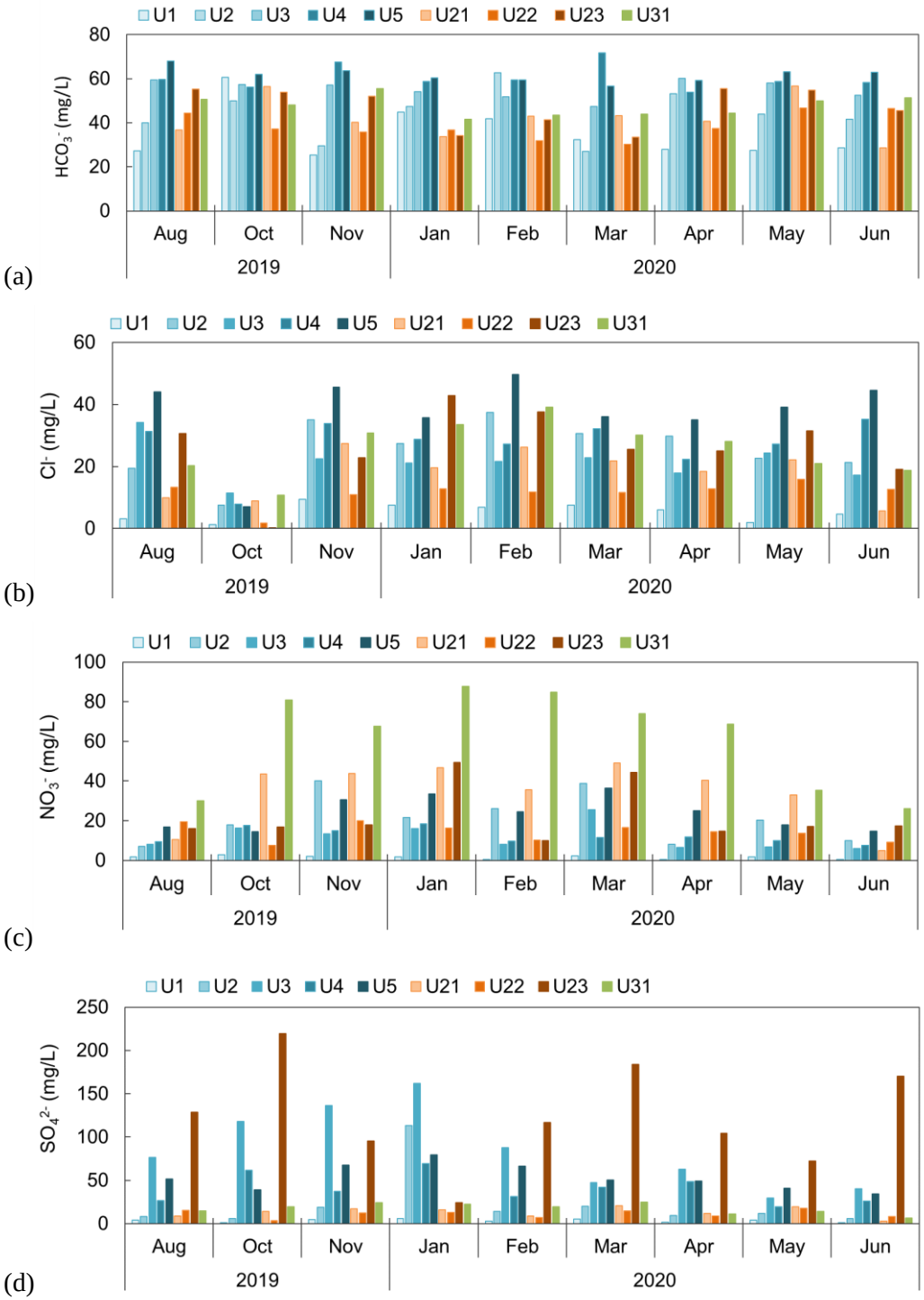

Figure 4.10 Major anion concentrations in the Umeda River and its tributaries: (a) HCO_3^-; (b) Cl^-; (c) NO_3; (d) SO_4^{2-}

Table 4.1 Summary of water parameters measurement in the mainstream of the Umeda River

st.		T (°C)	pH	EC (mS/m)	Cl^- (mg/L)	NO_3^- (mg/L)	SO_4^{2-} (mg/L)	Na^+ (mg/L)	K^+ (mg/L)	Ca^{2+} (mg/L)	Mg^{2+} (mg/L)	HCO_3^- (mg/L)	D-Zn (mg/L)	P-Zn (mg/kg)	D-Fe (mg/L)	P-Fe (mg/kg)	POC (mg/g)	SS (mg/L)	Q (m^3/s)
U1	min	9.7	7.23	5.5	0.35	0.88	1.16	4.55	0.61	6.8	1.18	25.4	n.d.	34	0.06	3146	45	2.3	0.004
	max	29.1	8.43	13.4	9.42	2.86	6.82	8.09	1.35	15.2	2.32	60.7	0.0236	864	0.12	45141	281	15.7	0.063
	mean	18.8	7.88	9.5	3.59	1.93	4.7	6.82	0.93	10.1	1.71	35.1	0.0048	200	0.08	18663	145	7.8	0.024
	CV	39%	6%	30%	100%	32%	35%	17%	24%	32%	24%	34%	158%	130%	31%	83%	54%	73%	82%
U2	min	10	6.54	11.5	7.47	5.81	5.77	11.69	2.16	11.7	1.92	29.5	0.0036	177	0.02	1752	130	3.1	0.034
	max	30.3	7.17	39.4	35.03	40.22	113.16	25.06	39.35	18.4	5.05	269	0.0278	2492	0.18	33179	528	51.8	0.115
	mean	19.6	6.92	22.4	20.8	19.47	29.65	17.84	8.13	16	3.15	70.8	0.0121	822	0.08	17234	315	11.3	0.074
	CV	35%	3%	38%	49%	65%	111%	29%	145%	13%	29%	106%	63%	99%	66%	58%	39%	136%	38%
U3	min	8.9	6.9	5.2	6.01	6.91	17.2	17.44	11.43	18.6	4.62	47.3	0.0056	100	0.04	2656	24	5.6	0.33
	max	28.7	7.36	59.7	34.12	87.76	162.02	28.89	87.71	23.4	6.53	60.3	0.0207	3713	0.16	34710	283	35	0.857
	mean	17.6	7.18	36	17.43	30.85	69.74	22.42	49.12	21.1	5.98	55.3	0.0127	1383	0.1	21384	168	10.8	0.463
	CV	42%	2%	48%	56%	90%	80%	16%	51%	8%	10%	8%	47%	89%	39%	54%	48%	86%	40%
U4	min	9.6	6.68	20.6	7.56	9.5	19.68	21.76	9.43	19.1	5.54	53.8	0.0055	363	0	4806	66	5.2	0.426
	max	28.6	7.33	47.2	33.93	48.4	69.34	33.39	45.27	24.3	7.52	71.8	0.0308	1633	0.09	38679	297	15.8	0.972
	mean	17.6	6.96	37.3	21.14	20.87	37.99	27.9	27.66	21.7	6.44	60.5	0.0183	879	0.06	20302	202	7.8	0.754
	CV	41%	3%	22%	54%	61%	46%	14%	41%	8%	10%	9%	50%	53%	42%	49%	34%	42%	23%
U5	min	9.4	6.98	20.7	7.12	14.34	34.97	19.02	9.8	20.5	6.11	56.7	0.0046	589	0.03	2144	62	3.6	0.693
	max	27.7	7.47	43.7	45.61	66.4	79.58	30.42	31.63	24.9	8.44	68	0.0407	2014	0.1	31420	283	10	1.333
	mean	17.2	7.16	36.1	30.23	33.29	51.01	24.69	19.97	22.7	7.29	61.7	0.0176	1038	0.06	20292	204	6.4	1.025
	CV	40%	2%	20%	44%	50%	28%	15%	37%	6%	11%	5%	66%	43%	40%	42%	39%	33%	21%

n.d. : not detected (detection limit: 0.0005 mg/L for Zn and 0.01 mg/L for Fe)

CV, coefficient of variation; D-Zn, Zn in dissolved phase; D-Fe, Fe in dissolved phase; POC, particulate organic carbon; P-Fe, Fe in particulate phase; P-Zn, Zn in particulate phase; SD, standard deviation; SS, suspended solids; st., sampling station

Table 4.2 Summary of water parameters measurement in the tributaries of the Umeda River

st.		T (°C)	pH	EC (mS/m)	Cl^- (mg/L)	NO_3^- (mg/L)	SO_4^{2-} (mg/L)	Na^+ (mg/L)	K^+ (mg/L)	Ca^{2+} (mg/L)	Mg^{2+} (mg/L)	HCO_3^- (mg/L)	D-Zn (mg/L)	P-Zn (mg/kg)	D-Fe (mg/L)	P-Fe (mg/kg)	POC (mg/g)	SS (mg/L)	Q (m^3/s)
U21	min	7.5	6.5	12.4	4.94	3.06	5.65	6	2.07	11.1	2.85	28.6	n.d.	21	n.d.	2245	77	1.3	0.006
	max	32	8.18	30.1	40.47	49.18	26.25	17.8	6.11	27	8.14	56.7	0.0224	3811	0.05	343247	330	23.3	0.051
	mean	18.9	7.42	24.1	21.21	27.81	16.31	12.72	4.53	21.4	5.93	42.1	0.0082	1365	0.03	65110	154	7.9	0.029
	CV	49%	7%	29%	57%	68%	38%	29%	35%	29%	31%	22%	86%	108%	55%	169%	58%	91%	62%
U22	min	10.6	6.92	9.6	1.76	7.14	3.36	8.29	2.8	11.3	3.29	30.3	0.0012	137	0.02	13654	95	2.7	0.069
	max	31.7	9.95	25.8	15.83	19.95	17.64	13.17	6.57	22	6.33	46.8	0.0273	3369	0.1	181955	207	19.1	0.208
	mean	19.1	7.72	19.4	11.14	13.1	12.59	10.66	4.44	17	4.86	38.6	0.0051	904	0.06	42593	156	5.8	0.15
	CV	37%	12%	26%	37%	40%	31%	13%	31%	19%	19%	16%	162%	119%	41%	124%	31%	89%	33%
U23	min	10	7.13	27.4	0.31	15.93	19.14	22.32	5.98	15.7	3.82	33.5	0.0052	253	0.04	5471	124	4.7	0.138
	max	30.1	8.4	81.1	42.94	170.22	219.52	28.21	161.94	18.8	6.67	55.5	0.0154	2998	0.17	33234	422	18.1	0.417
	mean	19.1	7.51	43	21.75	61.46	89.55	25.37	62.34	17.5	5.42	47.4	0.0109	1319	0.09	18921	226	8.4	0.262
	CV	37%	5%	38%	59%	91%	83%	8%	77%	7%	17%	19%	35%	67%	41%	46%	47%	52%	33%
U31	min	7.8	6.9	18.8	10.73	6.29	14.3	13.55	7.93	20.8	6.65	41.7	0.0024	272	n.d.	13621	105	1.4	0.113
	max	28.6	7.62	41.7	84.7	87.63	39.17	20.6	15.04	30.6	11.25	55.5	0.0139	5500	0.08	120546	312	20.2	0.296
	mean	16.8	7.33	32.2	36.2	45.79	22.9	17.31	11.11	26.8	9.28	47.7	0.0061	1497	0.04	31503	208	7.7	0.181
	CV	45%	3%	24%	67%	69%	33%	16%	23%	15%	20%	10%	62%	140%	62%	107%	29%	65%	33%

n.d. : not detected (detection limit: 0.0005 mg/L for Zn and 0.01 mg/L for Fe)

CV, coefficient of variation; D-Zn, Zn in dissolved phase; D-Fe, Fe in dissolved phase; POC, particulate organic carbon; P-Fe, Fe in particulate phase; P-Zn, Zn in particulate phase; SD, standard deviation; SS, suspended solids; st., sampling station

4.3 Riverbed sediment

4.3.1 Grain size fractionation

About 563 riverbed sediment samples were collected and fractionated by sieving, namely fine sand (<300 µm), medium sand (300–600 µm), and coarse sand (600–1000 µm). Figure 4.11 shows the fractionation of the grain size categories. The highest proportion of grain size was medium sand (45 ± 10%), followed by coarse sand (39 ± 15%) throughout the year during the 7-month sampling event. Meanwhile, low proportion of fine sand presented in the riverbed sediment (17 ± 11%). The Umeda River's water level was considered shallow (less than one meter) and relatively fast flowing which most of fine particulates transported away by the current, thus, resulting in coarser particles resisted on the bed sediment (Tessier et al., 1982; Whitney, 1975). In the upper-stream section, the fine particles portion tend to remain in the bed sediment in most sampling events apart from September and January.

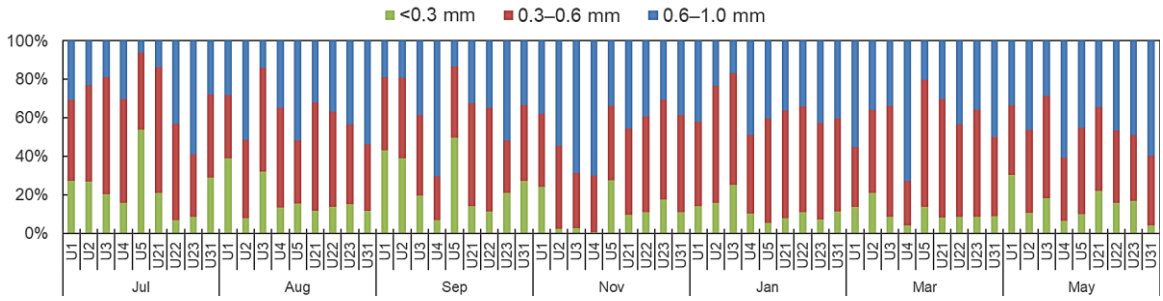

Figure 4.11 Grain size fractionation of the riverbed sediment

4.3.2 Spatial and temporal Zn concentrations in the riverbed sediment

In each size fraction, Zn, Fe, and POC concentrations were measured. The spatial, temporal, and related grain size variations for Zn levels can be seen in Figure 4.12 (in the mainstream) and Figure 4.13 (in tributaries). Compared to the Zn concentrations in water, the levels in riverbed sediment were relatively stable over the season. Relatively higher concentrations were revealed during August–September 2019 (summer and autumn), in contrast to those in water levels. The Zn concentrations in water were relatively higher during winter and spring (December and March).

In terms of spatial variation, downstream of the Umeda River (U4 and U5) and Sakai River (U23) tended to have higher concentrations than those at other sites. U31 (Ochiai River) did not exhibit elevated Zn concentrations. Furthermore, the most upstream station (U1) also revealed relatively low concentrations. However, the Sakai River showed elevated Zn concentration in a downstream direction during all sampling events. The weighted average of Zn concentrations is illustrated in Figure 4.14.

The Zn measurements in each grain size fractionation mostly revealed that the larger the particles, the higher the concentrations. This finding may not in accordance in most geochemical studies in which the smaller particle will have higher concentration as the surface area is also higher (Guan et al., 2016; Jain and Ram, 1997; Singh et al., 1999; Tansel and Rafiuddin, 2016). However, previous studies also reported a similar tendency as the present study results (Alomary and Belhadj, 2007; Maslennikova et al., 2012; Parizanganeh, 2008; Tessier et al., 1982). As aforementioned in subsection 4.4.1, oxide deposition is preferred in shallow and relatively rapid flowing section due to prevalence of oxidizing conditions (Whitney, 1975). Thus, it is likely that the coarse particles have more duration being exposed at the sediment/water sites than smaller particles and the Fe oxides are a common adsorbent in the river system (Tessier et al., 1982).

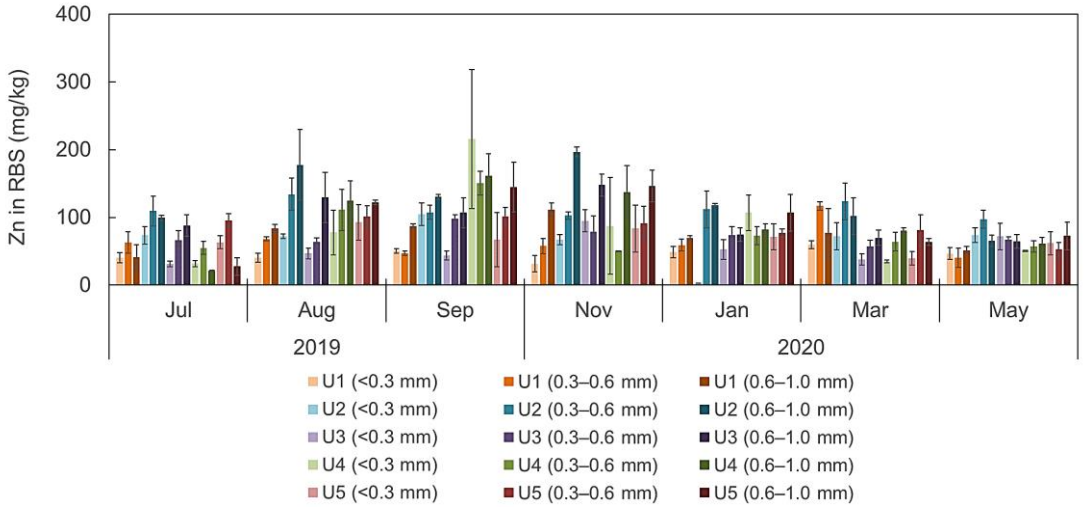

Figure 4.12 Zn concentrations in the fractionated riverbed sediment

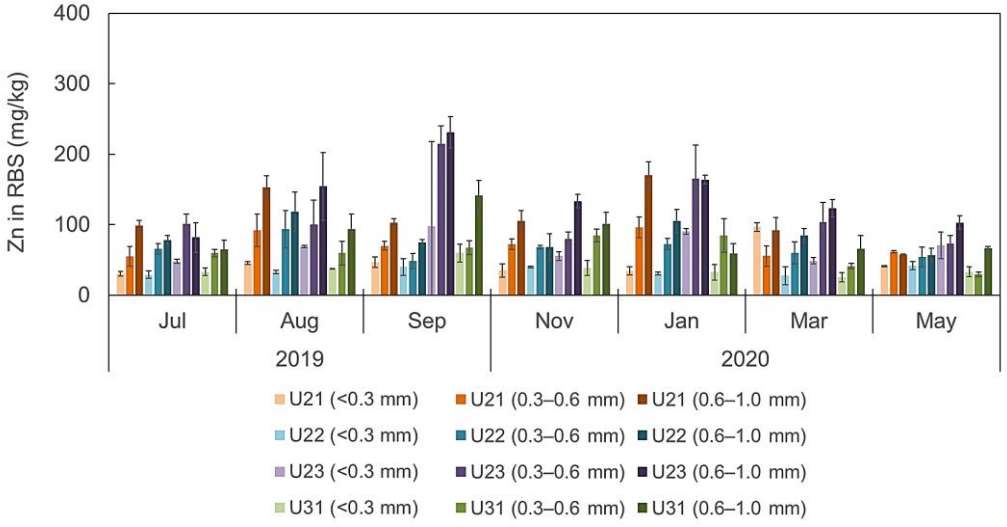

Figure 4.13 Zn concentrations in the fractionated riverbed sediment of the tributaries

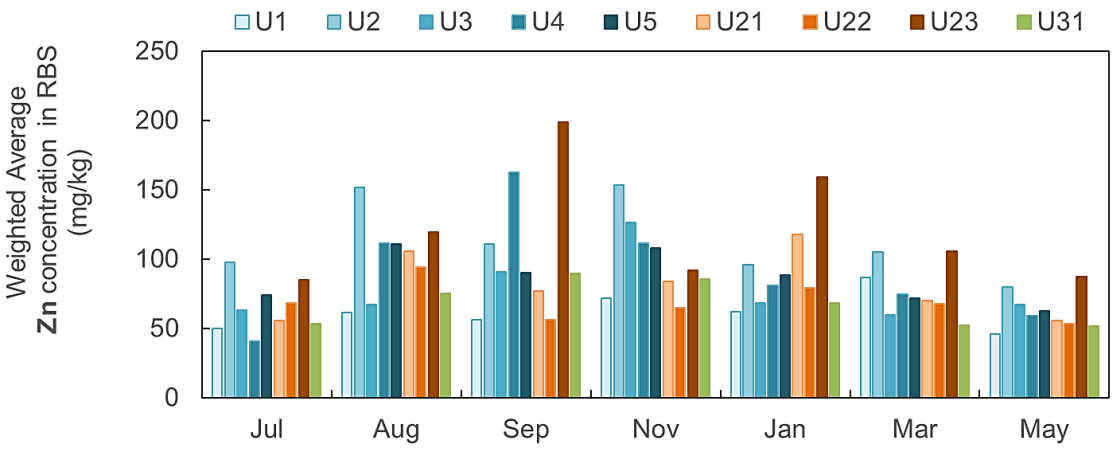

Figure 4.14 Weighted average of Zn concentrations of the riverbed sediment

4.3.3 Spatial and temporal Fe concentrations in the riverbed sediment

Figure 4.15 and Figure 4.16, shows Fe concentrations in fractionated grain size in the Umeda River and its tributaries. Figure 4.17 illustrated the weighted average of Fe concentrations. Fe concentrations in August clearly presented a larger level than in other months. It is also obvious that the concentrations from March and May were relatively lower than other months. The variability of Fe concentrations across the sampling stations shows that mostly the upper stream section has higher level of Fe levels. It is clearly shown in Figure 4.17.

With respect to the grain size, the result is generally the same as Zn fractionated concentrations. Anomaly elevated concentrations of Fe in the medium and coarse sand fractions. This might be due to the exposed time duration following shallow river. The larger particles may be exposed for a longer time at the sediment/water interface where the oxidizing conditions are most effective for oxide deposition (Tessier et al., 1982; Whitney, 1975).

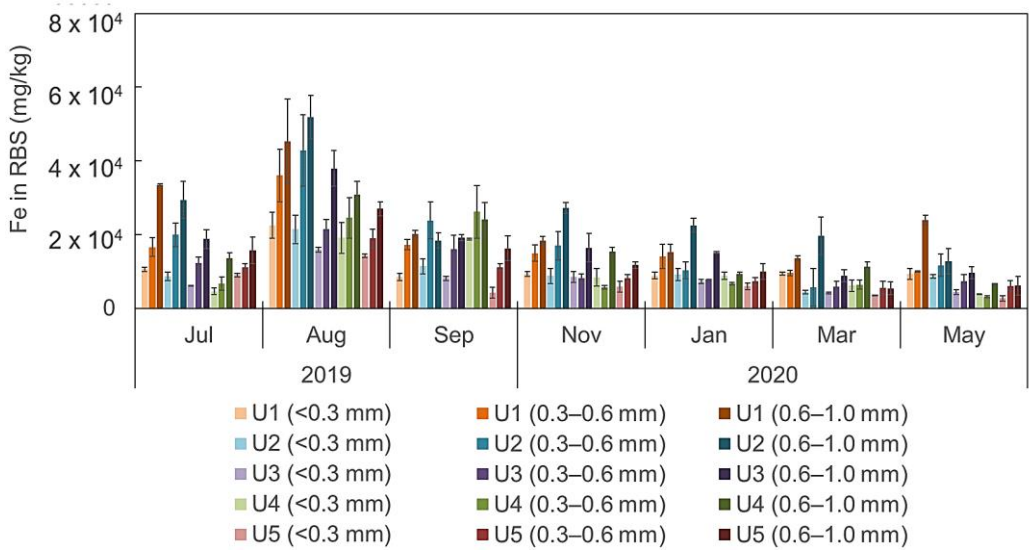

Figure 4.15 Fe concentrations in fractionated riverbed sediment of mainstream

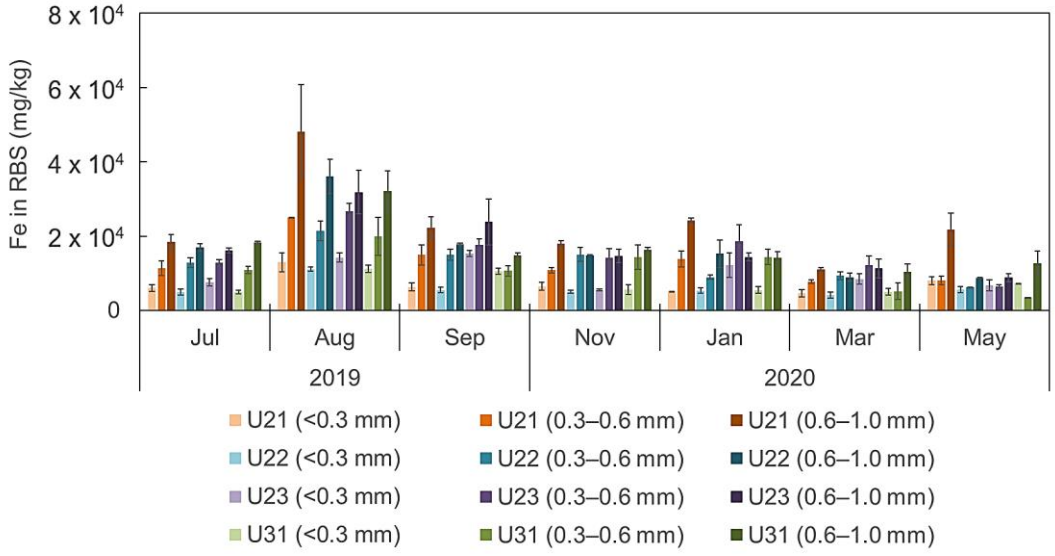

Figure 4.16 Fe concentrations in the fractionated riverbed sediment of the tributaries

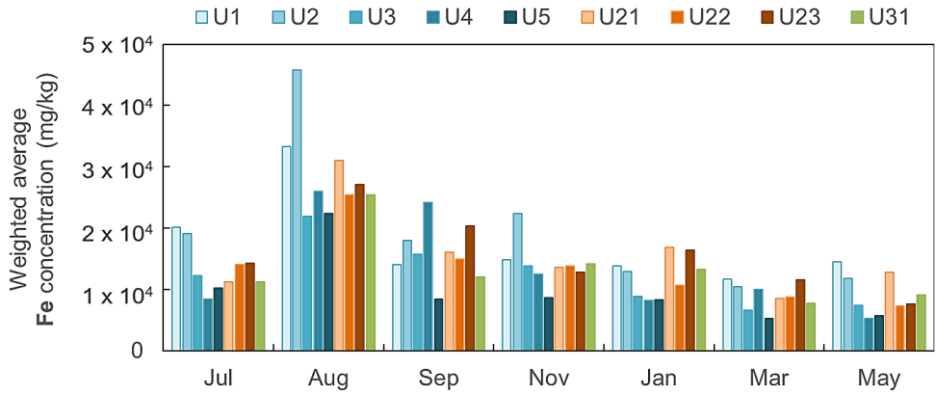

Figure 4.17 Weighted averaged Fe concentrations in the fractionated riverbed sediment

4.3.4 Spatial and temporal POC concentrations in the riverbed sediment

POC concentrations in fractionated riverbed sediments are depicted in Figure 4.18 (in mainstream of Umeda River), Figure 4.19 (in tributaries), and Figure 4.20 (for weighted average). It is revealed that the concentrations highly varied among seasons. However, the POC levels in September were also higher compared to other months, which similar observation also found in Zn levels. Similar to Zn and Fe, the POC also generally exhibit higher concentration in larger particles. According to Figure 4.20, the highest concentration was observed at U23 (in September), followed by U2 (in September). The spatial variability was clearly presented where the POC concentration decreased toward the downstream section in Umeda River. In contrast, generally the POC increased from upstream to downstream in the Sakai River.

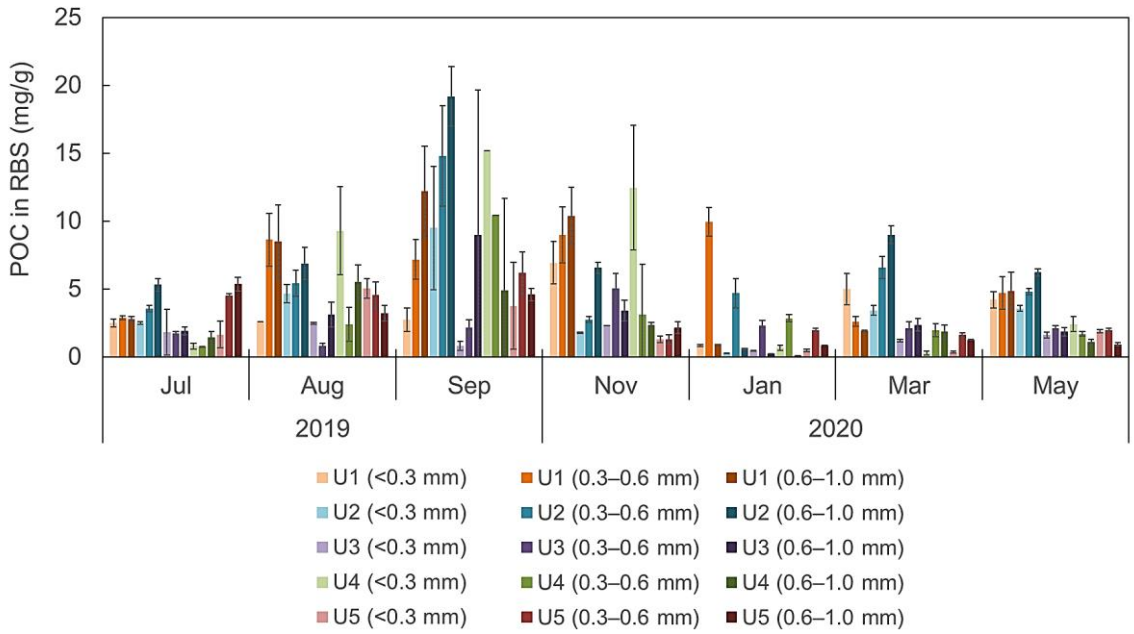

Figure 4.18 POC concentrations in the fractionated riverbed sediment

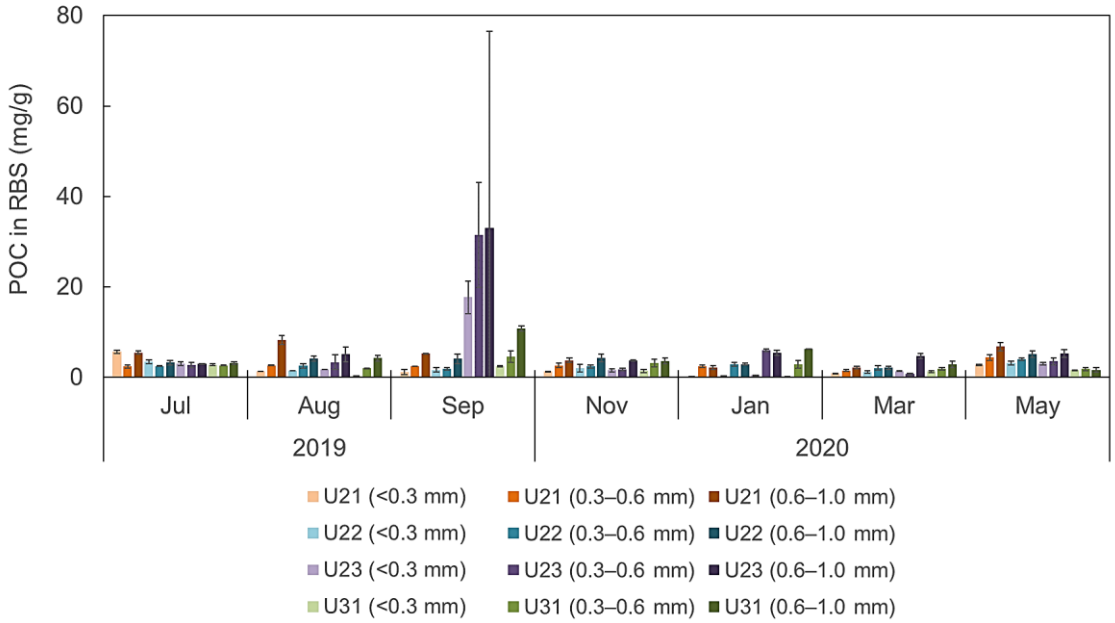

Figure 4.19 POC concentrations in the fractionated riverbed sediment of the tributaries

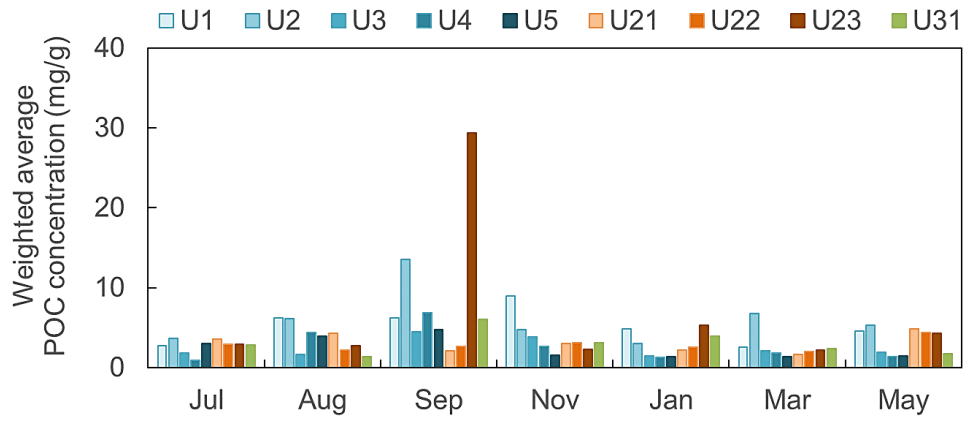

Figure 4.20 Weighted averaged POC concentrations in the fractionated riverbed sediment

Chapter 5 Assessment of Zn in surface water through high-resolution temporal survey in Umeda River

Summary

This chapter outlines Zn source identification and assessment by comparing measurement results in the baseflow (during weekday and weekend) and the stormflow in the Umeda River in Aichi Prefecture. High-resolution temporal sampling was used in both surveys, which were conducted on a fine day and during a rain event.

In the baseflow survey, the distinct differences in the Zn concentrations and loads between weekday and weekend indicated that the industrial wastewater impacted the elevated Zn concentrations on weekday. Meanwhile, the variations in the Fe concentrations on weekday were relatively similar. In February 2020, the total Zn concentrations on weekday (0.015–0.043 mg/L) at the most downstream point exhibited much higher concentrations than those during weekend (<0.0005–0.032 mg/L). Given the dissolved phase of these Zn levels (77 ± 11%), it is possible that industrial facilities discharged Zn concentrations into the Umeda River on weekdays.

In the stormflow survey, the Zn and Fe were mostly transported in the particulate form. The fluctuation of Zn concentrations (0.02–0.42 mg/L) followed the river discharges variation (3–89 m^3/s) except at the end of stormflow which the Zn finally declined despite the increasing discharge. The Zn sources in the river catchment might have been exhausted at the end of stormflow after the highest discharge peak. The non-point source might contribute to the riverine Zn levels in the stormflow. The highest Zn concentration at the respective discharge peak generally arrived before the discharge peak. Fe and SS variations were also in accordance with the river discharges. Only POC concentrations did not exhibit specific variations following the river discharges, except that the levels were slightly higher at the beginning than at the end of the stormflow.

5.1 Introduction

Dynamic diel variation in metal concentrations, particularly Zn, may be influenced by hydrological and biogeochemical processes (Rudall and Jarvis, 2012). The first to report a diel (diurnal) cycle of Zn concentrations in near-neutral and alkaline rivers were Bourg and Bertin (1996) and Brick and Moore (1996) followed by Nimick et al. (2003). Diel Zn cycles have previously been recorded in a number of near-neutral settings and rivers in the United States. (Barringer et al., 2008; Brick and Moore, 1996; Gammons et al., 2015; Kimball and Runkel, 2009; Kurz et al., 2013; Nimick et al., 2011), United Kingdom (Rudall and Jarvis, 2012), and France (Bourg and Bertin, 1996; Resongles et al., 2015; Superville et al., 2015). However, there are few comparisons of diel Zn concentrations throughout the weekday versus the weekend.

It is interesting to research if diurnal Zn variations may be found in Japanese rivers, particularly in the Aichi Prefecture. The sources of Zn might also be determined by focusing on activities that took place during the week and on weekends. As a result, the primary objective of this study was to examine the diel fluctuation and behavior of Zn in a near-neutral stream in Aichi Prefecture, Japan, during the weekday and weekend.

Only a few studies have examined metal contents in the baseflow and stormflow as the event continued using high-resolution temporal monitoring (Miller et al., 2003; Nicolau et al., 2012; Rothwell et al., 2007). The comparison of baseflow and stormflow surveys may identify potential Zn sources within the watershed [such as mineral weathering (Rothwell et al., 2007)], provide significant insights into the hydrology of metal transport (Miller et al., 2003), and provide an accurate load calculation across the year (Nicolau et al., 2012). Because of the washout of corroded materials, road deposit particle accumulation, and mineral weathering, Zn particulate load into rivers may be mobilized to a higher extent during rainfall periods. The influence of human activities on the geochemistry of river systems, particularly in metropolitan areas, has gotten a lot of attention recently (Rose and Shea, 2007). Behrendt (1993) used an emission method to estimate the point and non-point source loads of heavy metals. The most recent concerns in metal transportation, particularly in watershed draining mining regions, were extreme floods and severely low river flow; both possibly attributable to climate change (Barber et al., 2017; Byrne et al., 2020; Ciszewski and Grygar, 2016; Mayes et al., 2021). However, there is a scarcity of information about the origins and transport of Zn during baseflow and stormflow in rivers that drain small agricultural watersheds that may be polluted by industrial activity. Although industrial operations discharge a significant quantity of Zn, it is clear that the load from unknown sources during irrigation seasons is significantly larger than the load during non-irrigation months in another Japanese river (Andarani et al., 2020. As a result, the objectives of this article was how

Zn concentrations and loads varied in the baseflow and stormflow of a small agricultural river basin. Each event's potential sources of Zn contamination were identified.

5.2 Baseflow

5.2.1 Temporal variation of Zn

The diel concentrations of Zn in February 2020, during weekday and weekend over the 24 hours are shown in Figure 5.1a and b, respectively. The measurement results in October are illustrated in Figure 5.2. Table 5.1 (February) and Table 5.2 (October) describes the descriptive statistics of the hourly surveys on weekday and weekend.

In February, total Zn concentrations ranged from 0.015 to 0.043 mg/L (0.029 0.008 mg/L), whereas weekend total Zn values ranged from 0.0005 mg/L to 0.032 mg/L (0.010 0.007 mg/L). At 3:00, total Zn reached its maximum level (0.043 mg/L). The discharge peaked at 1.01 m^3/s in the afternoon, whereas total Zn levels dropped steadily until increasing slightly to 0.026 mg/L. The lowest concentration was recorded at 13:00 (0.015 mg/L) with a river flow of 0.96 m^3/s, which was considerably higher. The total Zn concentrations in February were considerably greater during the weekdays than on the weekends. Figure 5.1a also clearly indicates that the total Zn and D-Zn diel Zn fluctuations were synchronized with river flow changes. Due to dilution, larger river flows result in lower Zn concentrations, as reported by Nimick et al.(2003), Gozzard et al.(2011), and Resongles et al.(2015).

In February, the magnitude of the observed minimum to highest concentrations of D-Zn (the amplitude) increased by 293% (weekday) and 1778% (weekend). In October, the amplitude increased by 532% (weekday) and 342% (weekend). Other studies have discovered amplitudes of 140–326% for total Zn (Rudall and Jarvis, 2012), 800% for dissolved and colloidal Zn (Kimball and Runkel, 2009), and almost 1000% for D-Zn in the least buffered stream (Balistrieri et al., 2012). Gammons et al. (2015). outlined many potential mechanisms that increase diel fluctuation of Zn in a non-acidic stream.

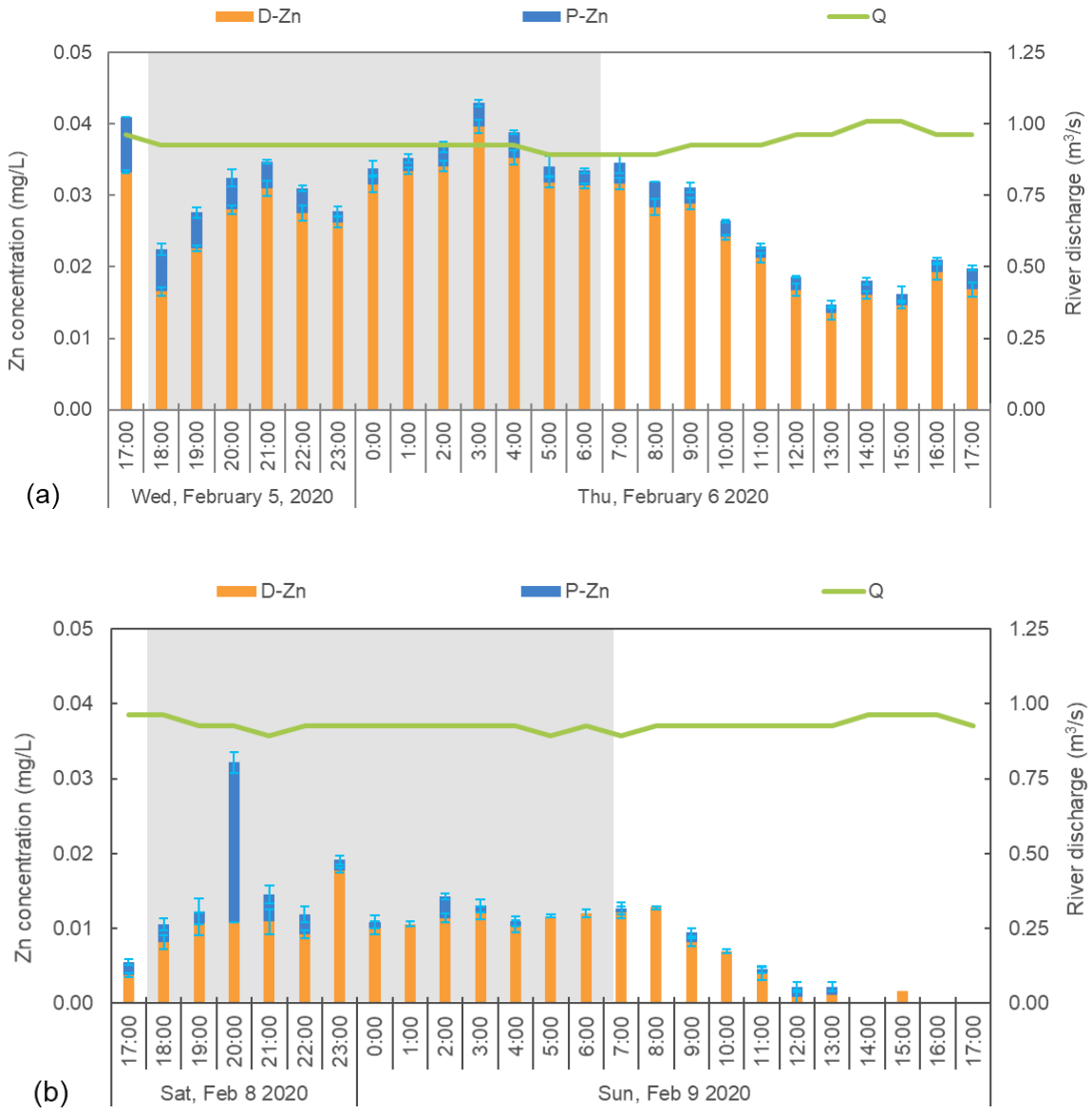

Figure 5.1 Diel Zn in the river water in February 2020: (a) on weekday and (b) on weekend

In October, the T-Zn concentrations varied from from 0.0046 to 0.0262 mg/L (0.0052 ± 0.0326 mg/L) during weekday, while during weekend, the total Zn ranged from 0.0052 to 0.0326 mg/L (0.0155 ± 0.0063 mg/L). Figure 5.2 shows that the total Zn reached its highest value (0.0262 mg/L) on Thursday at 8:00. The discharge peaked both at night and in the afternoon at 1.02 m^3/s, whereas the total Zn decreased gradually from early morning and reached the lowest at the afternoon (0.0039 mg/L on Thursday at 15:00) on weekday. In contrast to the February's results, the T-Zn concentration mean was slightly higher on weekday than on weekend. The T-Zn level fluctuation during the weekend also dominated by the particulate phase. The highest T-Zn was on

Saturday at 17:00 (0.0326 mg/L) while the lowest on Sunday at 18:00 (0.0052 mg/L). The diel pattern of T-Zn was not clearly seen during weekend. However, the D-Zn in October exhibited similar behavior to those in February.

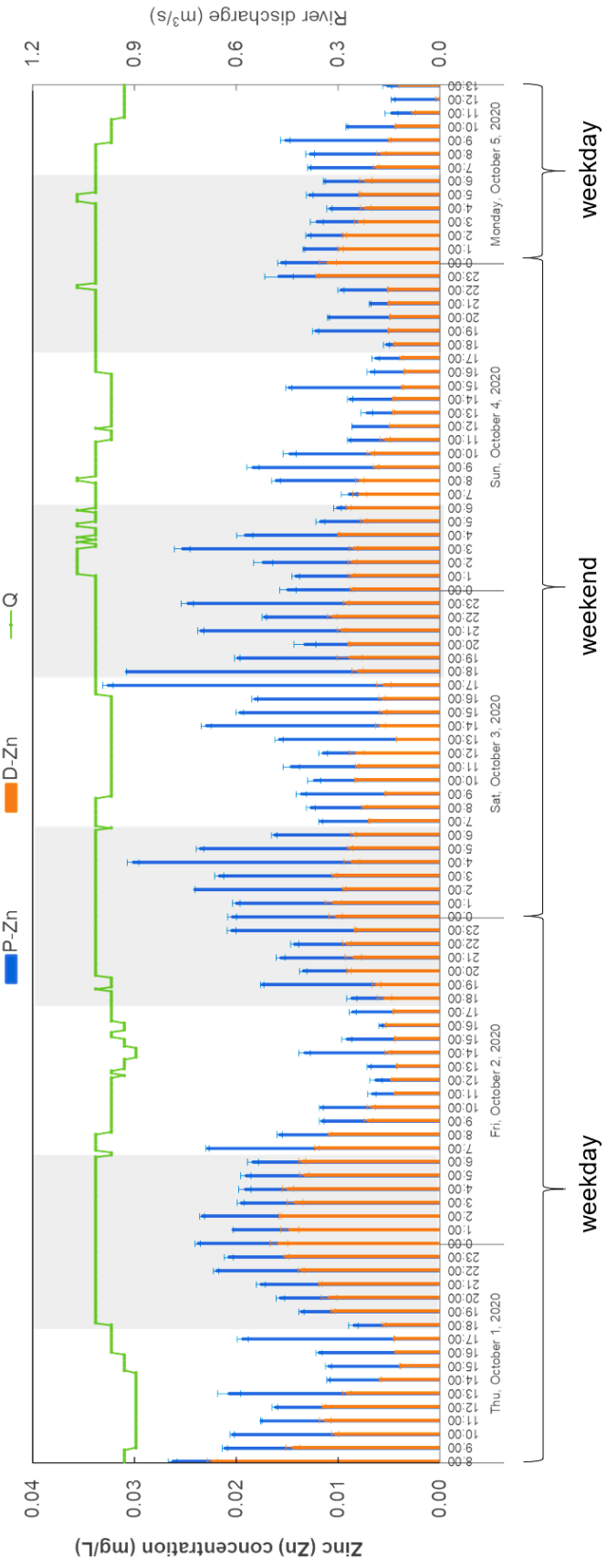

Figure 5.2 Diel Zn in the river water in October 2020

Table 5.1 Summary of water analysis results in the hourly survey in February 2020

	D-Zn (mg/L)	T-Zn (mg/L)	SS (mg/L)	D-Fe (mg/L)	T-Fe (mg/L)	POC (mg/g)	River discharge (m^3/s)
Weekday (n = 25)							
Minimum	0.014	0.015	5.5	0.034	0.104	112	0.89
Maximum	0.040	0.043	21.5	0.086	0.215	315	1.01
Mean	0.026	0.029	9.9	0.055	0.147	172	0.93
SD	0.007	0.008	3.5	0.014	0.028	50	0.03
CV	29%	27%	35%	26%	19%	29%	3%
Weekend (n = 25)							
Minimum	n.d.	n.d.	7.3	0.036	0.125	102	0.89
Maximum	0.0178	0.032	59.7	0.063	0.648	163	0.96
Mean	0.0079	0.010	14.1	0.051	0.180	131	0.93
SD	0.0049	0.007	10.0	0.007	0.101	17	0.02
CV	62%	73%	71%	14%	56%	13%	2%

n.d. : not detected (detection limit: 0.0005 mg/L for Zn and 0.01 mg/L for Fe)
CV : coefficient of variation

Table 5.2 Summary of water analysis results in the hourly survey in October 2020

	D-Zn (mg/L)	T-Zn (mg/L)	SS (mg/L)	D-Fe (mg/L)	T-Fe (mg/L)	POC (mg/g)	River discharge (m^3/s)
Weekday (n = 54)							
Minimum	n.d.	0.0046	4.4	0.034	0.095	140	0.90
Maximum	0.0224	0.0262	9.2	0.093	0.154	224	1.02
Mean	0.0088	0.0147	6.0	0.051	0.115	184	0.97
SD	0.0047	0.0059	1.1	0.012	0.014	21	0.04
CV	53%	40%	18%	23%	12%	11%	5%
Weekend (n = 54)							
Minimum	0.0035	0.0052	3.72	0.021	0.078	108	0.97
Maximum	0.0120	0.0326	14.84	0.059	0.170	285	1.07
Mean	0.0074	0.0155	5.5	0.038	0.103	209	1.01
SD	0.0021	0.0063	1.6	0.009	0.018	29	0.03
CV	29%	41%	30%	25%	17%	14%	3%

n.d. : not detected (detection limit: 0.0005 mg/L for Zn and 0.01 mg/L for Fe)
CV : coefficient of variation

Meanwhile, the diel D-Zn fluctuations exhibited a similar diel pattern during weekend, but with lower concentration values both in February and October. D-Zn concentration variations on weekends were similar to those on weekdays, although on a smaller scale. Weekend D-Zn fractions were smaller (56 ± 23%, 9–98% in February; 53 ± 17%, 17–89% in October) than weekday fractions (77 ± 11%, 57–98% in February; 59 ± 17%, 4–91% in October). Because of human operations, Zn was evidently introduced to the Umeda River's mainstream on weekday. Natural trace elements, including Zn, were also conveyed by suspended solids, according to Le Pape et al. (2012), but the dissolved phase contribution increased down the river in the lower reach, where the urbanization was located.

During the weekend in February, total Zn concentrations were still present during the day, but were below the detection limit (0.0005 mg/L) at 14:00, 16:00, and 17:00. In contrast, the total Zn concentrations in October exhibited slightly higher which might be due to the small rainfall occurred on Saturday morning. This also resulted in the slightly higher discharges over the weekend (see Table 5.2). It is also conceivable that a few industrial plants continued to operate on Saturday, although diel cycles may have happened when daytime concentrations were lower than nighttime concentrations.

The variations in concentrations might be attributed to the impact of the Zn point sources because these high temporally resolved samplings (weekday and weekend) were done in clear weather, especially in February's survey. The EQS for total Zn in Japan was set at 0.03 mg/L on an annual basis. In February, all Zn values throughout the weekend were low, with none exceeding 0.03 mg/L. Except for 23:00 (at midnight), Zn concentrations in Japan violated the EQS from 19:00 on Wednesday to 09:00 on Thursday. The EQS was only breached three times on weekends, according to an hourly survey conducted in October (Saturday at 04:00, 17:00, and 18:00). Although 0.03 mg/L is a standard for the annual average value, a breach within the 24-hour period might be expected. The time of water quality monitoring for river water quality evaluations should take this diel fluctuation of Zn into account.

5.2.2 Temporal variation of SS, Fe, and POC

The SS, Fe, and POC concentration variability in the baseflow is shown in Figure 5.3 (for SS in February), Figure 5.4 (for Fe in February), Figure 5.5 (for POC in February), Figure 5.6 (for SS in October), Figure 5.7 (for Fe in October), and Figure 5.8 (POC in October).

In February, the river discharges were relatively steady for both the weekday and weekend, varying from 0.89–1.01 m^3/s. The average in SS concentration (Figure 5.3) during the weekday was 9.9 ± 3.5 mg/L, ranging from 5.5–21.5 mg/L. During weekend, the SS concentration varied

from 7.3–19.0 mg/L, with a mean of 12 ± 9.97 mg/L, apart from an outlier (60 mg/L) because of unidentified source. The levels during weekend were slightly higher than those during the weekday, although the river discharges did not vary significantly.

On weekday, the average Fe concentration was 0.133 ± 0.015 mg/L (0.104–0.172 mg/L), whereas on weekend, it was 0.146 ± 0.053 mg/L (0.114–0.379 mg/L). Except for an outlier comparable to when the SS level was extraordinarily high, there was no substantial difference in Fe concentrations between weekdays and weekends. Both the SS and the Fe in this outlier example might have come from natural sources.

POC in February (Figure 5.5) also did not show a clear trend between weekday and weekend's levels, although the mean on weekday (172 ± 50 mg/L) was slightly higher than on weekend (131 ± 17 mg.L). The POC variation and concentrations were also slightly higher during weekday. POC during weekday varied from 112 to 315 mg/g, whereas on weekend, from 102 to 163 mg/g.

In October, the river discharges were relatively stable for both during weekday and weekend ranging from 0.90 to 1.07 m^3/s. SS concentrations in October (Figure 5.6) were generally higher than those in February. The SS levels varied from 4.4 to 9.2 mg/L on weekday (mean = 9.9 ± 3.5 mg/L) and from 3.72 to 14.84 mg/L on weekend (mean = 14.1 ± 10.0 mg/L). The Fe values in both the total and dissolved fractions are shown in Figure 5.7 (for the October survey). On weekdays (0.115 ± 0.014 mg/L, 0.095–0.154 mg/L) and weekends (0.103 ± 0.018 mg/L, 0.078–0.170 mg/L), there was no significant change in total Fe concentrations. Unlike the Zn concentrations, the Fe concentrations did not differ significantly between weekdays and weekends. Even though the Zn concentrations clearly showed a diel variation, the Fe concentrations showed no apparent change on weekdays or weekends. POC in October (Figure 5.8) also did not show an obvious trend between weekday and weekend. The POC varied from 140 to 224 mg/g on weekday and 108 to 285 mg/g on weekend.

In contrast to earlier research, the diurnal fluctuation in D-Fe concentrations owing to photoreduction was not seen in the Umeda River, which has a near-neutral pH (Kay et al., 2011; Sullivan and Drever, 2001). Different from Zn, the Fe in both sampling campaigns was mostly present in particulate phase.

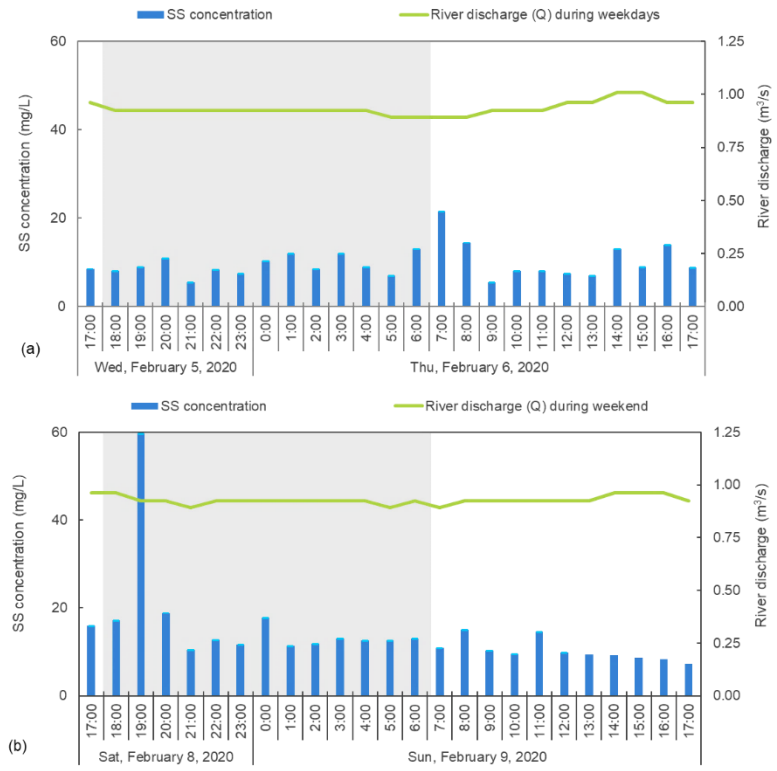

Figure 5.3 Diel SS in the river water in February 2020: (a) on weekday; (b) on weekend

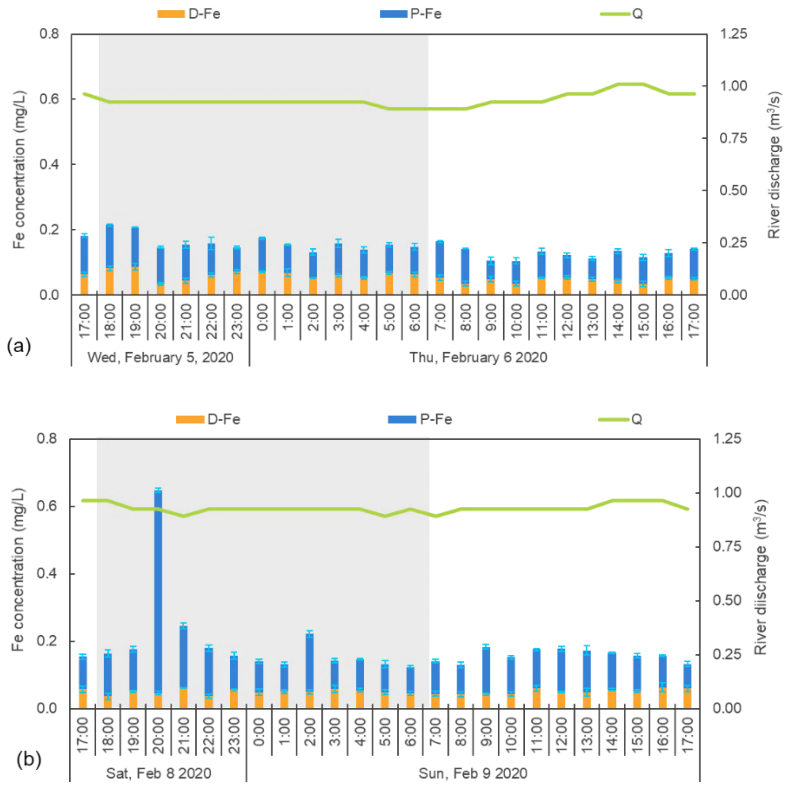

Figure 5.4 Diel Fe in the river water in February 2020: (a) on weekday and (b) on weekend

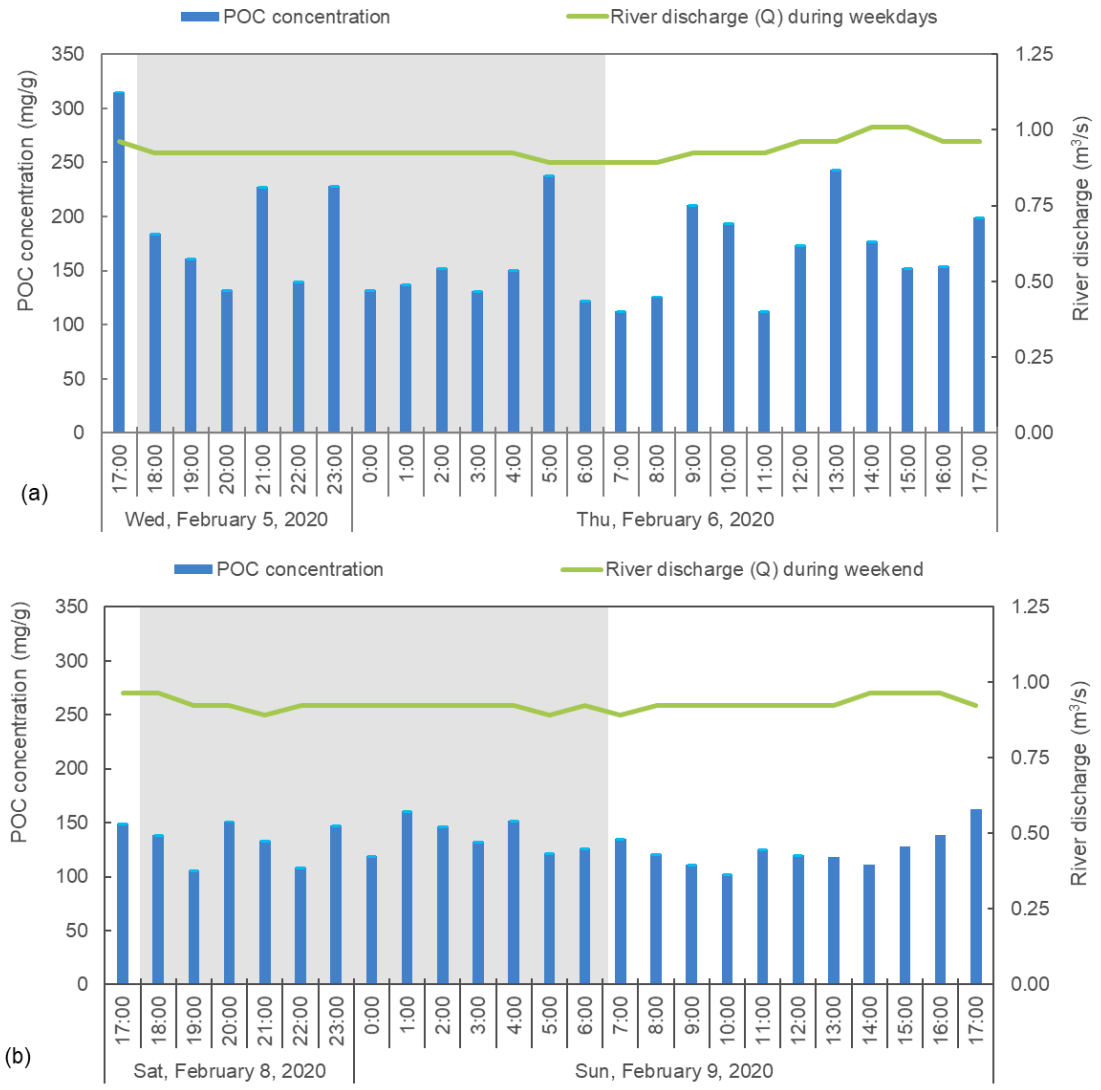

Figure 5.5 Diel POC in the river water in February 2020: (a) on weekday and (b) on weekend

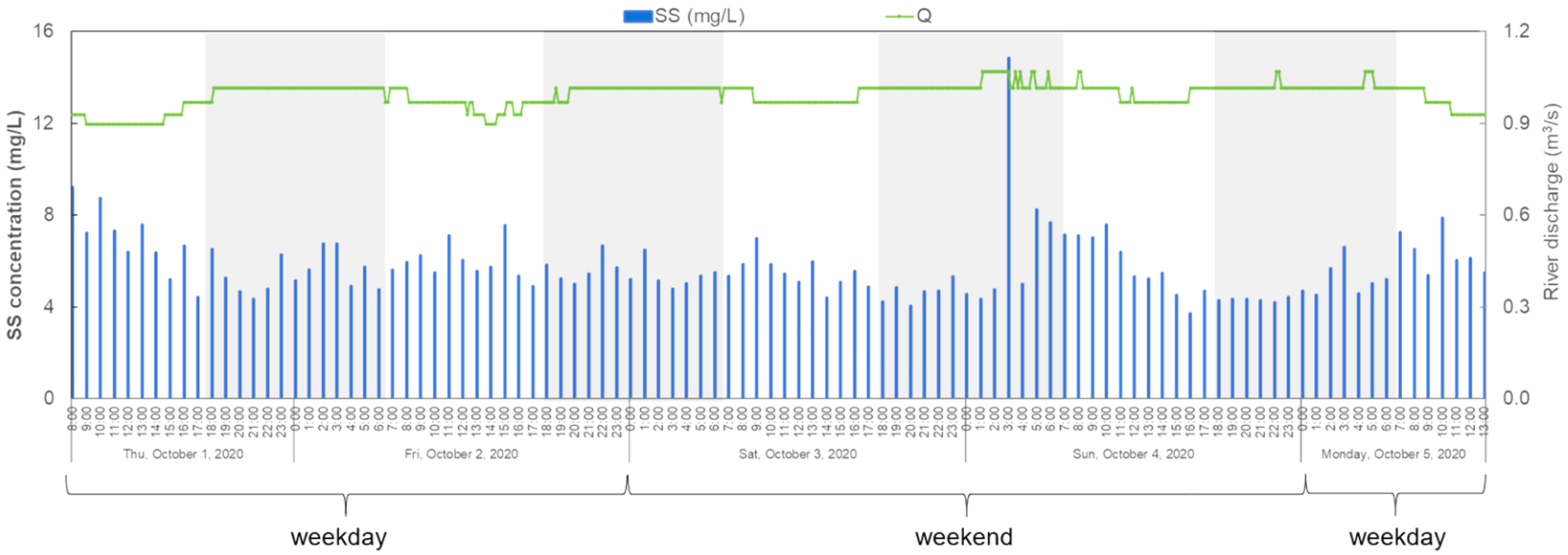

Figure 5.6 Diel suspended solids (SS) in the river water in October

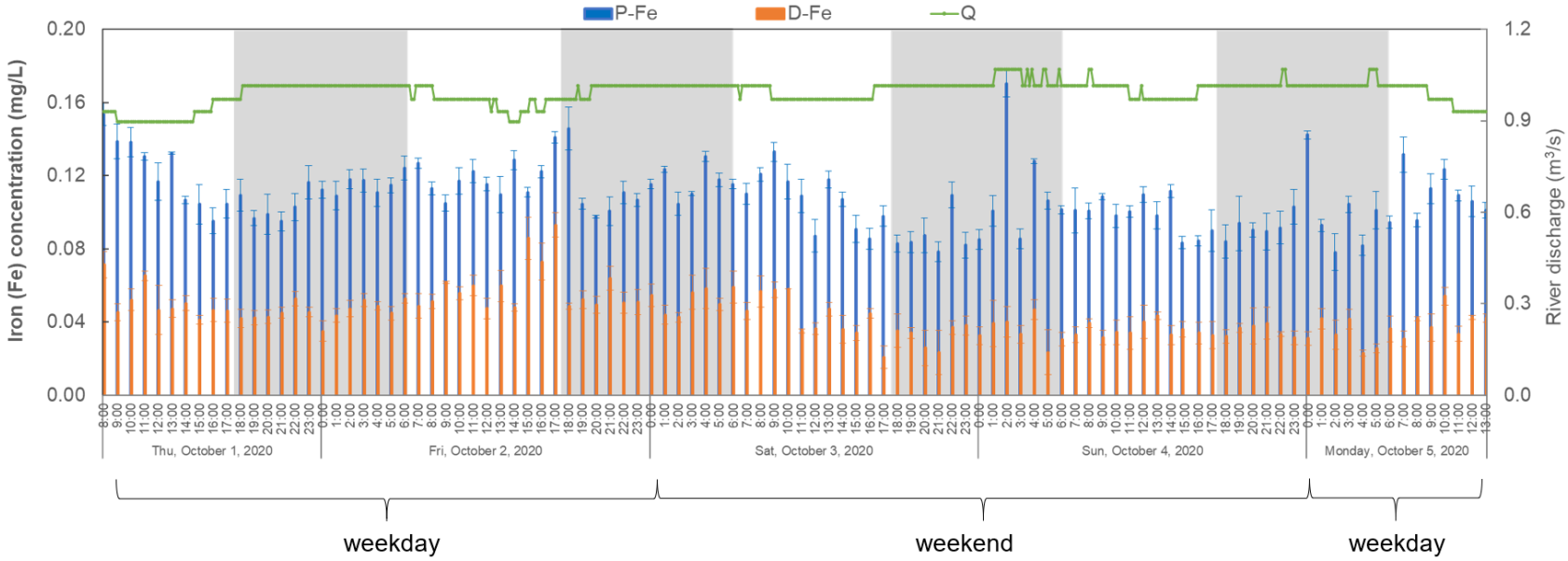

Figure 5.7 Diel Fe in the river water in October 2020

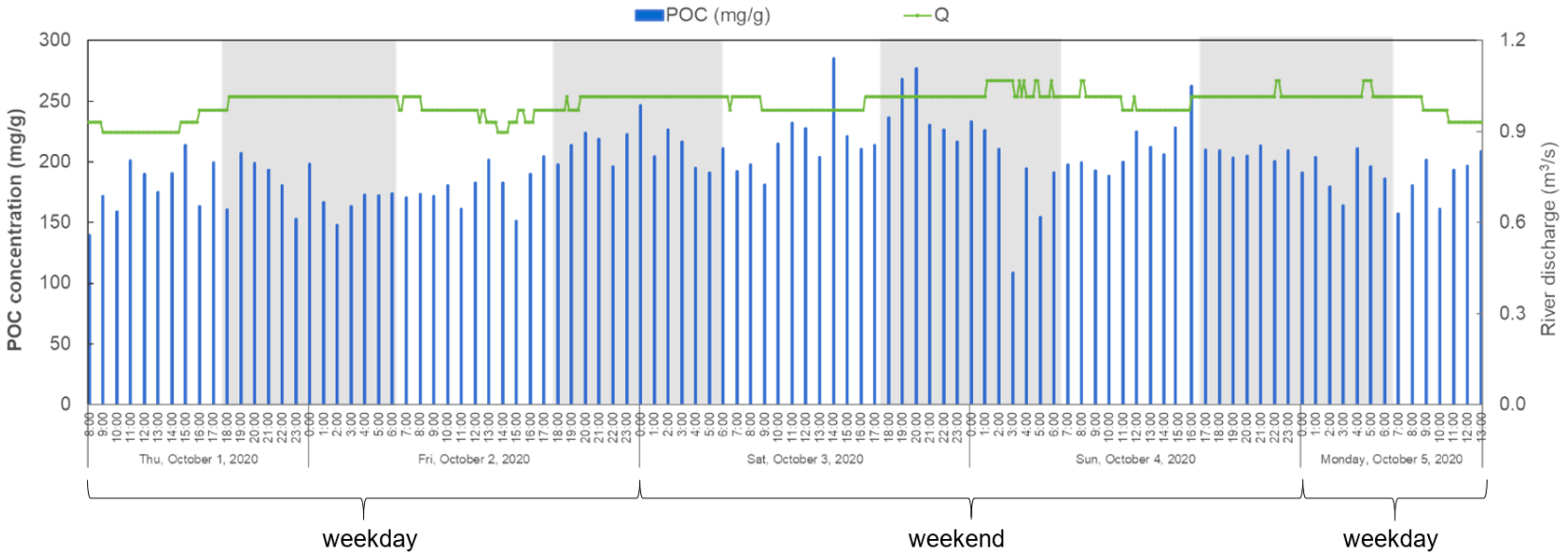

Figure 5.8 Diel particulate organic carbon (POC) in the river water in October 2020

5.3 Stormflow

From September 6 (Sunday) to September 8 (Tuesday), 2020, a rainy event consisted of four major discharge peaks in the Umeda River catchment (17, 27, 96, and 39 m^3/s). In contrast to the baseflow concentrations, instream Zn, SS, Fe, and POC concentrations generally followed river discharge during the rainy event, as illustrated in Figure 5.9, Figure 5.10, Figure 5.11, and Figure 5.12, respectively. According to these figures, it is obvious that the dissolved fraction of Zn and Fe remained low throughout the sampling event, with the exception of D-Zn at 18:30 on September 6, 2020 (0.117 mg/L).

5.3.1 Temporal variation of Zn

In comparison to the SS and Fe concentrations, the Zn concentrations in the stormflow showed a significant fluctuation. Just before the initial peak, the Zn level surged to the second-highest concentration (0.25 mg/L), then steadily dropped to around 0.04 mg/L in the steady flow at 3.47 m^3/s. The initial spike in Zn concentration (0.25 mg/L) might have been present in dissolved form as compared to the SS concentration level at 19:30 on September 6, 2020. Then the Zn concentrations began to fluctuate, corresponding with river flows, with the second high reaching 0.18 mg/L. Just before the third peak, the maximum concentration (0.42 mg/L) was reached, after which it gradually declined.

Given that this Zn peak occurred just before the discharge peak, the river system was flushed of any fine material present in its source prior to the highest discharge (Bradley and Lewin, 1982; Dawson and Macklin, 1998). A rainy event potentially generates easily soluble corrosion products in the first rain volume, frequently referred to as the first flush, that will be removed as runoff. It will then be followed by a more or less constant runoff rate during ongoing rain (He et al., 2001).

The amount of the initial flush may be affected by factors such as the length of dry periods and the extent of dry deposits, rain volume and intensity, and porous corrosion layers (He et al., 2001). Despite the fact that the fourth discharge peak was higher than the second, the Zn level only increased little when the fourth peak occurred, suggesting that the source had already been depleted. Furthermore, the decreased concentration at high flow might be due to a dilution effect caused by Zn-deficient water and particle intake. After the fourth peak, this was the case. EQS exceedances of 11% to 75% were quickly detected in a continuous low flow during the commencement of the storm event. The third ascending limb has the highest EQS exceedance (1,299%). Only after the Zn supply was depleted at the end of the storm episode (from 9 m^3/s), the concentrations did not exceed the EQS. It should be emphasized, however, that the EQS was established to evaluate the annual mean value.

Zn sources could be both point and non-point, and they can be natural or anthropogenic. Human activities such as atmospheric Zn deposition are examples of anthropogenic non-point sources (Naito et al., 2010; Sakata et al., 2005; Sakata and Marumoto, 2004); roof corrosion (Sage et al., 2016); sewage overflows (Gromaire-Mertz et al., 1999; Sakson et al., 2018); agricultural activities (Naito et al., 2010); road traffic activities, particularly tire wear, particle abrasion from tires, brakes, and road wear (Degaffe and Turner, 2011; Hjortenkrans et al., 2006; Legret and Pagotto, 1999; Wagner et al., 2018); and exhaust from vehicles (Hjortenkrans et al., 2006).

Municipal solid waste incineration plants were a substantial source of Zn particle deposition in the atmosphere in Tokyo Bay and France plants (Le Floch et al., 2003; Sakata et al., 2005). Wet deposition may also add to instream Zn levels in the Umeda River, especially at the start of the storm event. Furthermore, the Umeda River catchment region contains a significant number of agricultural activity, which might result in extra Zn in the soil as a result of fertilizer, pesticide (Banerjee et al., 2019), and livestock treatments (Itahashi et al., 2014; Mishima et al., 2005). According to Naito et al. (2010), the Zn emission to surface water in Japan due to leaching and runoff from agricultural land is 7 t/y.

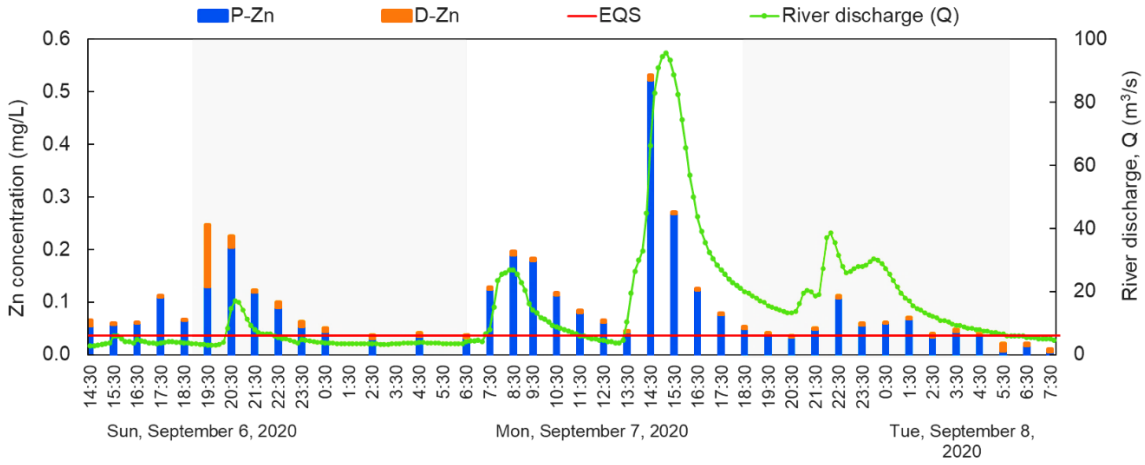

Figure 5.9 Zn concentrations in the stormflow

5.3.2 Temporal variation of SS, Fe, and POC

In the descending limb of the storm hydrograph, the SS concentration began to rise to 333 mg/L at the first peak. From 22:30 to 06:30, it gradually decreased in a constant flow. The SS concentration reached 590 mg/L just before the second peak, then dropped dramatically at the apex (401 mg/L), before rising to 456 mg/L and then steadily declining. After the third peak (1,309 mg/L), the SS concentration rose to its maximum level, exhibiting a similar occurrence to the first and fourth discharge peaks (438 mg/L).

The SS concentration peak occurred at the same time as the Fe pattern. However, all Fe concentration peaks (1.85, 2.68, 6.77, and 2.35 mg/L) occurred after the respective discharge maxima. Fe concentrations fluctuated in sync with river discharge, particularly from the storm's third peak until its end. The Fe concentration was more steady at the first and second discharge maxima. The Fe concentration levels were still quite high (1.39–2.68 mg/L) despite the decrease in discharges. Even after the discharge peaks, the SS and Fe variations revealed that the source was still present at the end of stormflow. The materials in the catchment's ground constantly flushed and flowed into the river body.

Compared to the POC concentrations in the baseflow, the POC in the stormflow was relatively lower varied from 28 to 76 mg/g. The fluctuation of POC in the stormflow did not follow the discharge variation, in contrast to the SS, Zn, and Fe. However, the POC level at the highest discharge peak shows relatively high concentration of 66 mg/g. During the stormflow, it can be observed that at the beginning of stormflow, the POC levels were relatively higher than those at the end of the stormflow.

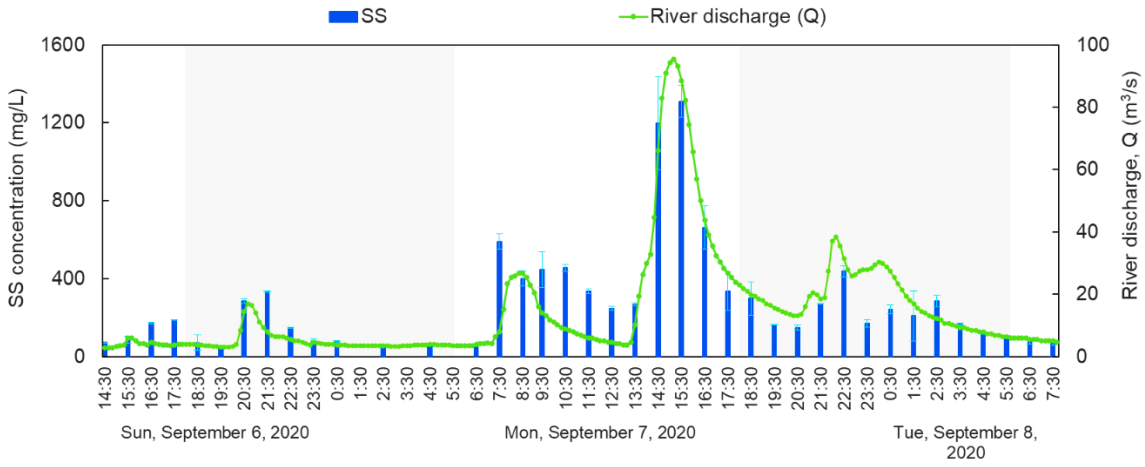

Figure 5.10 SS concentrations in the stormflow

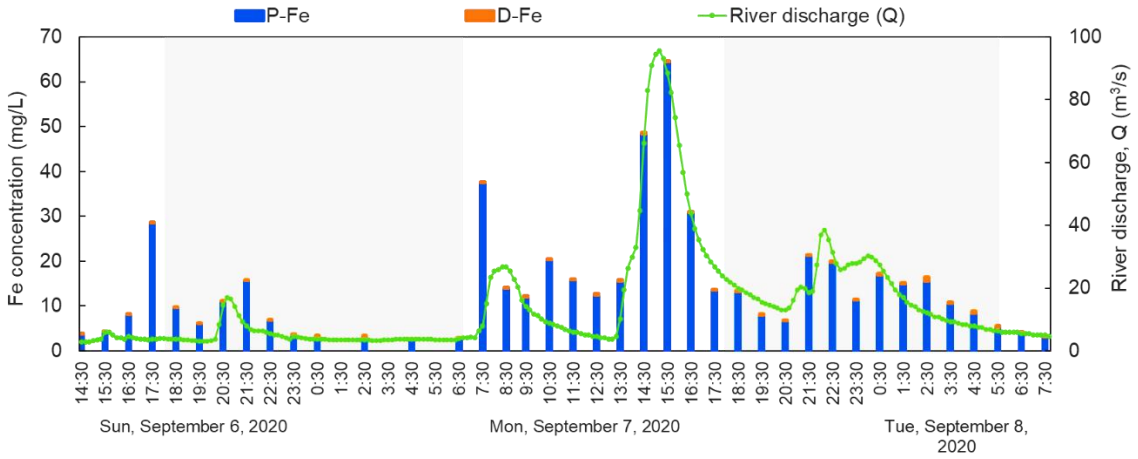

Figure 5.11 Fe concentrations in the stormflow

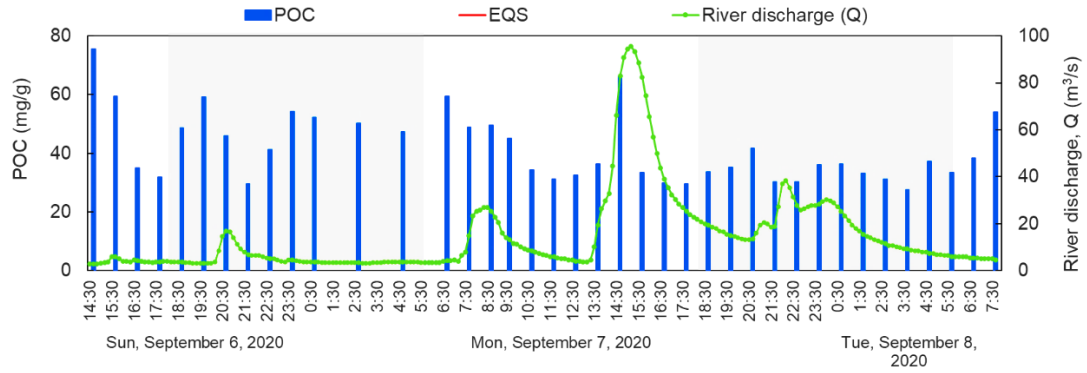

Figure 5.12 POC concentrations in the stormflow

Chapter 6 Zinc concentration and load assessment

Summary

By using the datasets presented in the previous chapters, ratio between particulate and dissolved phase, statistical analyses, load balances, and simple end member mixing analysis method (EMMA) were used to deeply analyze the data.

In Umeda River, the Zn was mainly transported in dissolved phase. However, the present study observed a low-moderate correlation between P-Zn and P-Fe during monthly and hourly (October) survey. Strong correlation between P-Zn and P-Fe was only found in the hourly baseflow survey in February. In this study, low and moderate correlation was observed between P-Zn and POC. There were also low-moderate correlations between Zn, Fe, and POC in the riverbed sediment.

Hierarchical cluster observation analysis enabled a classification using T-Zn and discharge (Q) datasets. Generally, the downstream area was the most polluted sites of Zn in Aizumame River and the Umeda River. The seasonal T-Zn and Q variation showed slightly different results between both rivers. Winter and spring were considered as the most polluted season in the Umeda River (summer and autumn grouped together), where in Aizumame River only winter has the most polluted season (autumn and spring grouped together). According to the cluster variables in Umeda River, the D-Zn was grouped together with pH, POC, and HCO_3^-. The cations and anions presence are generally less significant in term of metal transport and behavior compared to parameters such as pH, organic matter, and the presence of adsorbent (i.e., Fe hydroxides in this case).

The principal component factor loading analysis shows that the D-Zn (together with POC, pH, and Na^+) contributed to the Varifactor 3 which explains about 15% of total variance. This would confirmed that D-Zn may have been affected by POC which possibly explained by the adsorption of Zn to the organic matter. Meanwhile, P-Zn participated in Varifactor 5 which represents 8% of total variance. Varifactor 3 has a sampling location variability which may indicate an anthropogenic influence, whereas varifactor 4 has less influence on the sampling location.

In the Umeda River, the total daily Zn loading on weekday (T-Zn = 56 g/km^2/day; D-Zn = 50 g/km^2/day) was approximately three times higher than during weekend (T-Zn = 18 g/km^2/day; D-Zn = 15 g/km^2/day). These differences could originate from the industrial point sources. The industrial point sources may have contributed at least 67% of the total Zn loads (37 g/km^2/day)

and 70% of the D-Zn loads (35 g/km^2/day) on weekday. Meanwhile in the Aizumame River, the industrial point sources contributed approximately 68 g/km^2/day (57%).

After the greatest peak discharge, Zn levels, mostly in particle form, remained high, indicating that non-point Zn sources may be abundant in the catchment. However, the Zn was potentially more diluted than the SS and Fe, and its origin was depleted at the end of the storm episode. Using a simple EMMA with two tracers (Zn from point source and non-point source), it is estimated that the point sources accounted for 74% of the Zn loads while non-point sources accounted for 26%. The quantity of Zn emitted from point sources was greater than the amount of Zn emitted from non-point sources. To conserve aquatic organisms, river management in both baseflow and stormflow should be enhanced.

6.1 Introduction

The data was thoroughly analyzed using the datasets presented in the previous chapters. Several methods used were the hierarchical cluster observation analysis (HCA), principal component factor loading analysis (PCFA), flow analysis, ratio between particulate and dissolved phase, pearson correlation, and the simple end member mixing analysis method (EMMA). Comparing the Zn load between weekday and weekend was necessary to estimate the contribution of industrial wastewater into the river. The HCA of observations was firstly needed to classify the severity of Zn contamination. Then, the spatio-temporal variability of T-Zn loads was extensively analyzed in the flow analysis comparing each season as well as irrigation period. In order to assess the underlying factor affecting the Zn variation, several methods were used including ratio between particulate and dissolved, HCA of variables, and PCFA. Lastly, the EMMA was used to verify the Zn contribution from point sources by using both stormflow and baseflow loading comparisons.

6.2 Clustering the severity of Zn contamination in rivers

In the Chapter 3, the Zn concentrations and the river discharges are observed in both Aizumame River and Umeda River. A detail result explanation is provided, but it is not clear enough where and when the Zn pollution are severe or even considered as unpolluted. The average value of T-Zn concentrations and river discharges were used to classify the severity of Zn contamination in both rivers using hierarchical cluster analysis, specifically using cluster observation.

6.2.1 Cluster observations on Aizumame's dataset (T-Zn and Q)

In the Aizumame River, the most downstream sampling station (A5, 0.054 ± 0.020 mg/L) and slightly upper stations (A4, 0.059 ± 0.035 mg/L) has exceeded the EQS in 2017 for 12-month

average. It is obvious that both sites have severe Zn pollution. However, the classification was not clear enough for other sampling stations.

Hierarchical cluster observation analysis was implemented on the average value of T-Zn concentrations and river discharge at each sampling stations in Aizumame River water for 20 months. The results shown in Figure 6.a indicated that three clusters were formed. The first cluster (blue) shows the sampling locations located at the most upstream at the Aizumame River (A1) and followed by two tributaries, i.e. A11 and A21. This clearly indicated that the blue cluster is unpolluted sites. Meanwhile, in the second cluster (green), A2 and A3 were firstly clustered then followed by A4 and A5, respectively. This cluster revealed the polluted sites toward the downstream distance. Furthermore, A31 and A41, the tributaries of industrial areas, were grouped in the third cluster (red) of the Figure 6.a. This group shows extremely polluted sites.

Another cluster observation analysis was implemented to the average value of seasonal T-Zn concentrations and river discharge in the Aizumame River. Three distant groups were observed in Figure 6.b. Autumn and spring were grouped together which may indicate a moderate pollution of Zn. Meanwhile, summer and winter were separated which implies that winter has the highest T-Zn pollution period, whereas summer (blue) has relatively low pollution compared to the second (green) group and the winter (red) season.

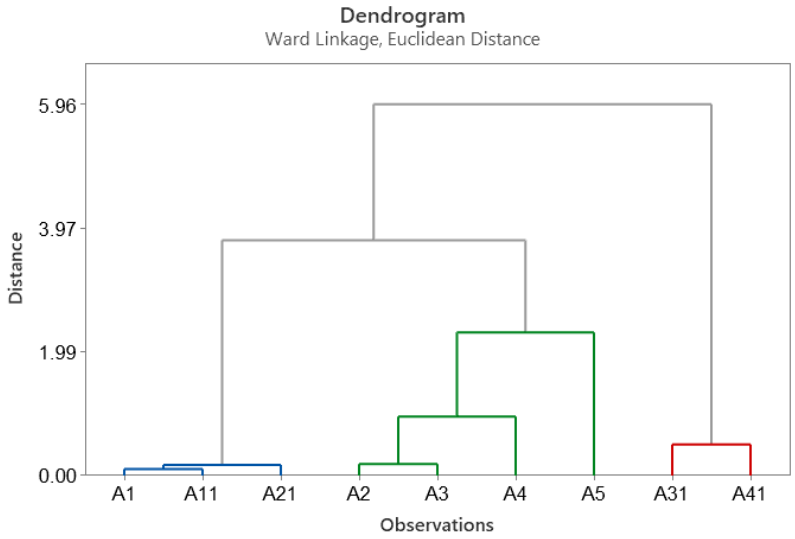

(a)

Figure 6.1 Hierarchical cluster observation analysis on the Aizumame's dataset (T-Zn and Q): (a) average value for 20 months survey; (b) seasonal variation

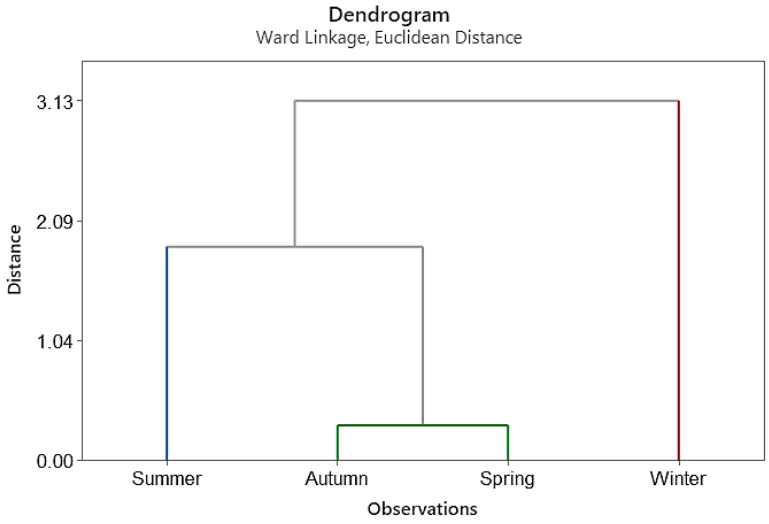

(b)

Figure 6.1 Hierarchical cluster observation analysis on the Aizumame's dataset (T-Zn and Q): (a) average value for 20 months survey; (b) seasonal variation *(Continued)*

6.2.2 Cluster observations on Umeda's dataset (T-Zn and Q)

In 2020, the annual means of T-Zn concentrations at U5 (0.031 mg/L) exceeded the EQS. The Chapter 3 also highlights that the downstream section of Umeda River were also relatively high (U3: 0.028 mg/L; U4: 0.029 mg/L). It is necessary to classify the location and period so that the degree of contamination can be determined. Using hierarchical cluster analysis, the classification can be easily undertaken.

Hierarchical cluster observations analysis was implemented to average T-Zn and Q of each sampling stations for 12 months of the monthly baseflow survey in the Umeda River. The dendograms in Figure 6.2a were grouping nine sampling stations into three clusters which indicated how severe the Zn pollution. Cluster-1 (red) mainly consists of U3, U4, and U5. This classification might reflect to the highly polluted sites influenced by anthropogenic activities. Moderate pollution was grouped into Cluster-2 (green), where it comprises U2 and U23 which firstly grouped together and then followed by U31 and U21 being one cluster. The least polluted sites (U1 and U22) were clustered together in the Cluster-3 (blue).

Different from those in the Aizumame River, the seasonal cluster observation in the Umeda River shows that summer and autumn were grouped in one cluster (blue), as illustrated in Figure 6.2b. This blue cluster indicates that both seasons are considered as the least polluted season in the Umeda River. Although winter and spring were not grouped together, both seasons exhibited an elevated T-Zn concentration which indicate Zn pollution. According to this dendogram, spring has relatively higher pollution than winter.

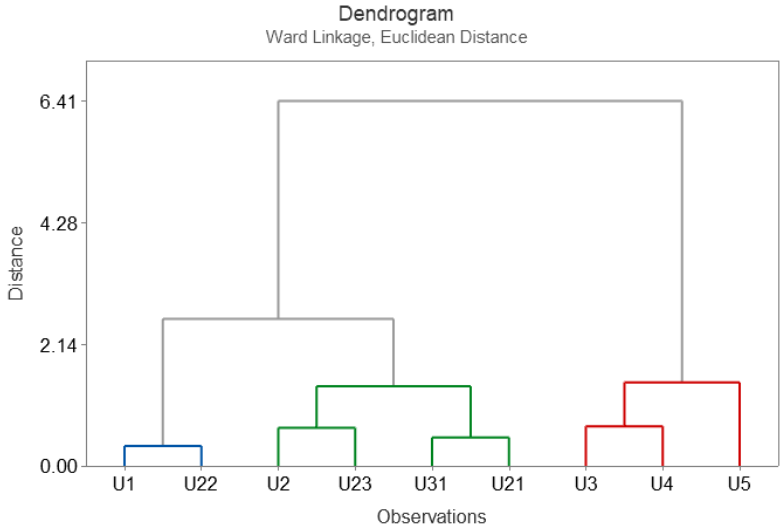

(a)

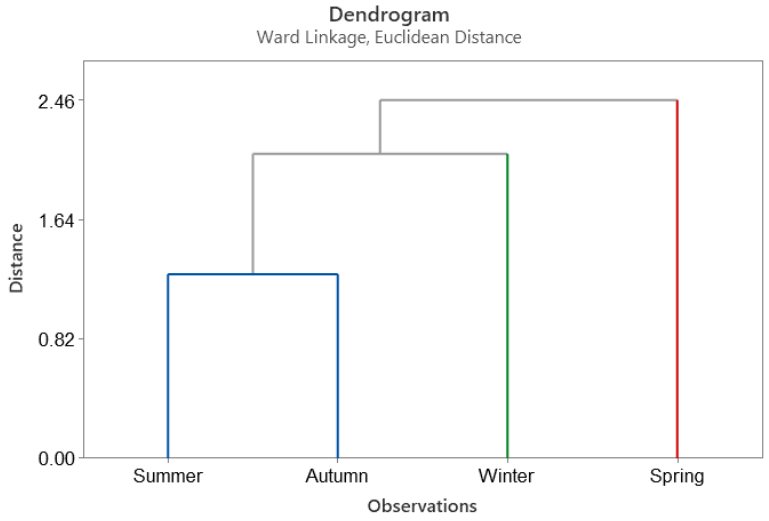

(b)

Figure 6.2 Hierarchical cluster observation analysis on the Umeda's dataset (T-Zn and Q): (a) average value for 20 months survey; (b) seasonal variation

6.2.3 Comparison of the clusters between the Aizumame River and the Umeda River

Both rivers had the same spatial T-Zn trend, where the downstream received the highest loading. The Zn source in the Aizumame was quite obvious, i.e. A31 and A41 where the industries discharging their wastewater. However, in the Umeda River, although U23 was affected by the industrial discharge, its cluster followed the moderate pollution instead of severely polluted sites.

Winter season is regarded as the period when the Zn exhibiting high concentrations in both rivers. By contrast, relatively low concentrations were found in summer. However, in the Umeda River, the winter was not included in the severely polluted season, despite the extremely high

concentrations in U5. This could be due to the river discharge which has the highest level in spring. A further analysis is thoroughly described in the Subsection 6.2.

The cluster observation analysis confirmed the tendency of observed trend and may have potential to be used as tool to analyze river section according to water quality. By using Q and T-Zn data, the cluster could be formed. However, it is difficult to identify which section of the river body receive considerable amount of T-Zn loading. Thus, flow analysis is necessary to understand the load dynamics from upstream to the downstream.

6.3 Flow analysis of T-Zn loadings based on the monthly baseflow survey

As discussed in the previous sections, the annual value of T-Zn concentrations exceeded in both Aizumame River and Umeda River. It is obvious that the human activities have impacted on the Zn levels in both rivers. Therefore, it is necessary to analyze the Zn loadings along the river. The highest contributing load might have the most significant influence on the instream Zn concentrations. The mass balance or flow analysis can be used to assess the flow along the river. To simplify the flow, the average concentrations of the respective periods was used. The periods used were seasons (summer, autumn, winter, and spring) and irrigation period (irrigation and non-irrigation). Moreover, the standard deviations are also provided on the Sankey diagram to show the variation within the period.

6.3.1 Seasonal Zn load variations

6.3.1.1 Seasonal Zn load variations in the Aizumame River

Seasonal river discharge variation can be seen in Figure 6.3 and T-Zn variability in Figure 6.4. The river discharge exhibited high to low value in: summer > spring > autumn > winter. Meanwhile the highest T-Zn load was found in autumn followed by summer, spring, and winter. The contribution of T-Zn did not coincide with river discharge which suggest that the point source affected the T-Zn input to the mainstream.

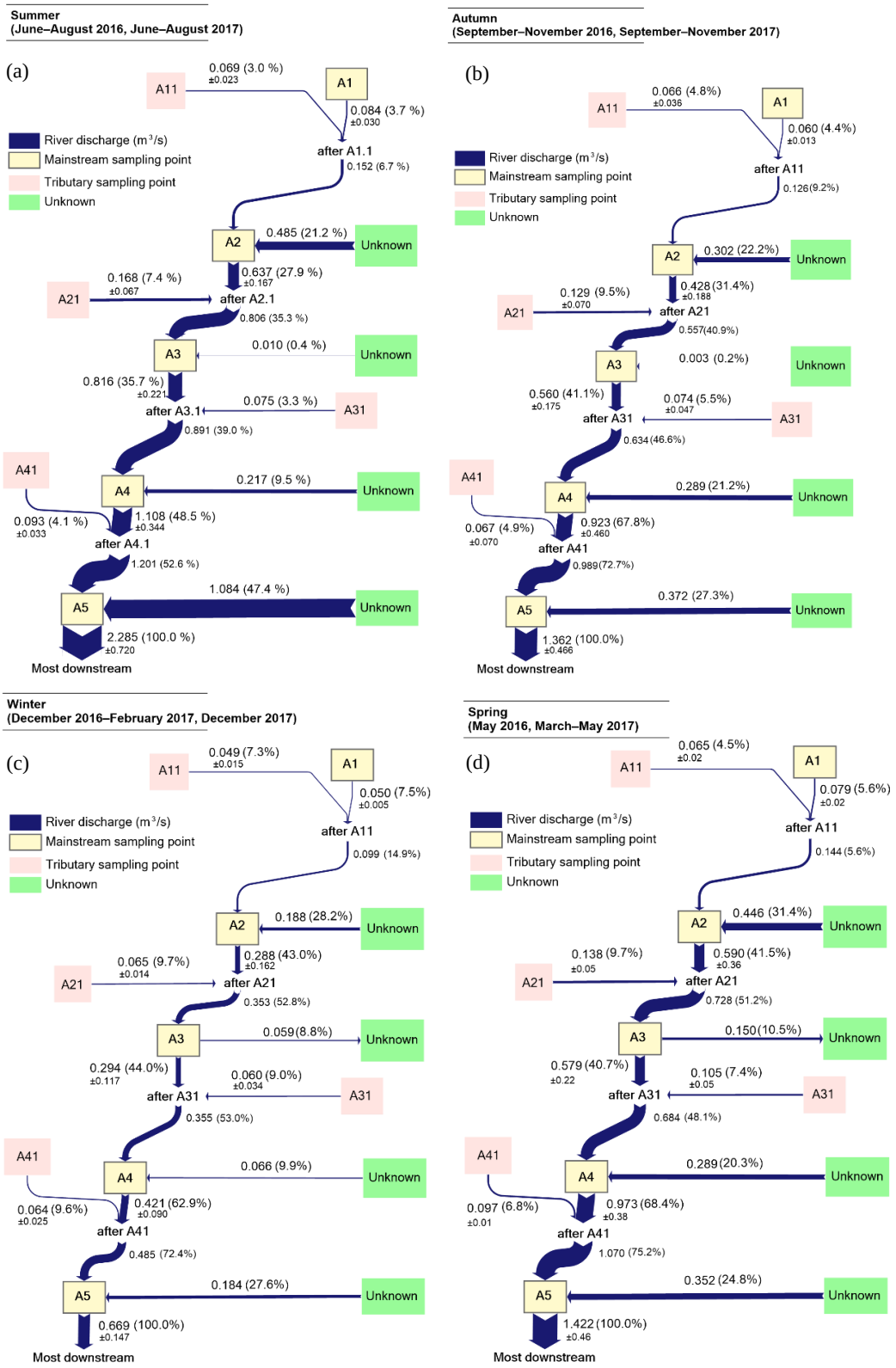

Figure 6.3 River discharge (Q) flow analysis in seasonal variation: (a) summer; (b) autumn; (c) winter; (d) spring in the Aizumame River. The values indicate mean (percentage relative to the output flow from A5 at each diagram) ± SD of the data series during the monthly survey.

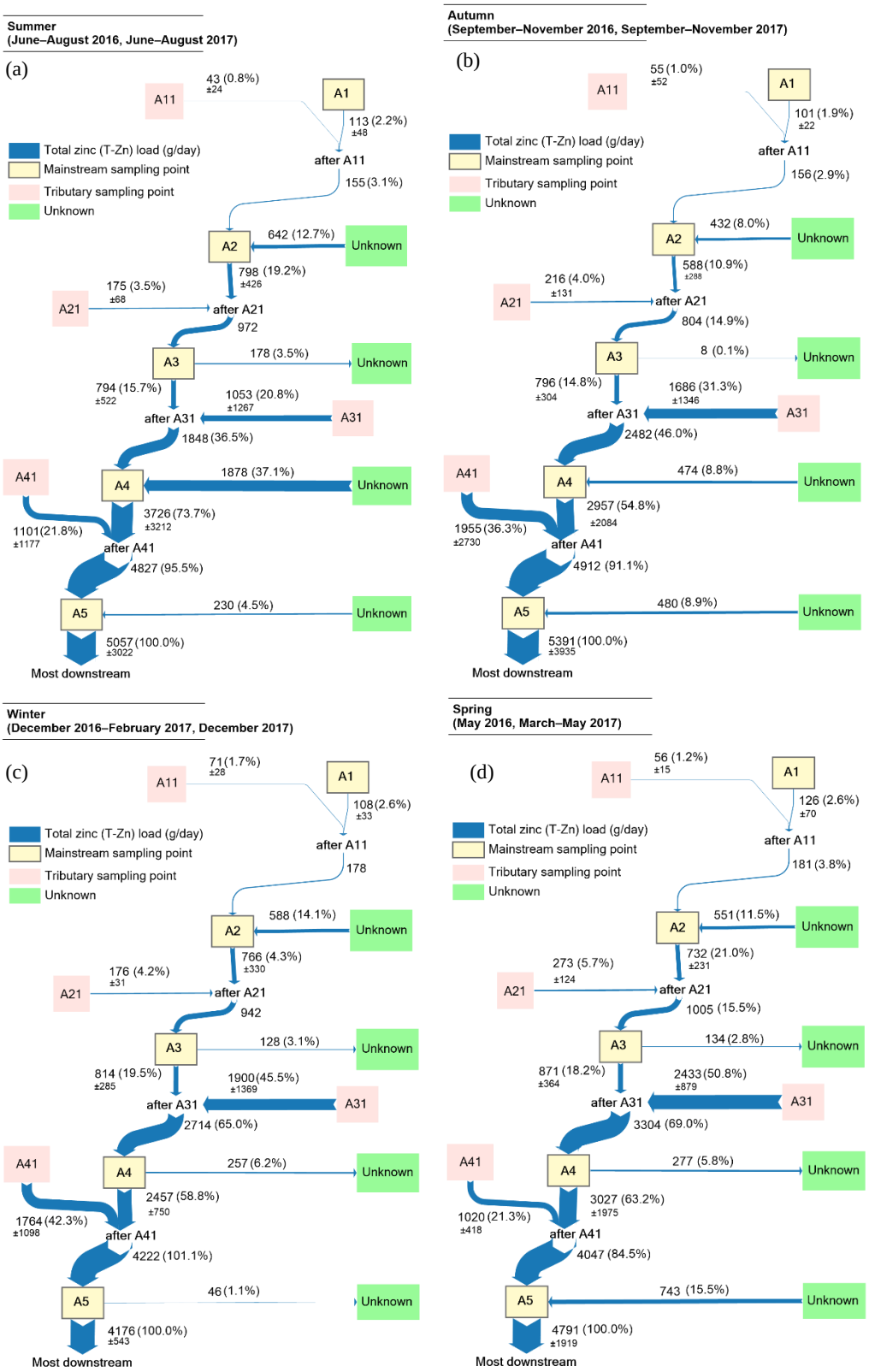

Figure 6.4 T-Zn load flow analysis in seasonal variations (a) summer; (b) autumn; (c) winter; (d) spring in the Aizumame River. The values indicate mean (percentage relative to the output flow from A5 at each diagram) ± SD of the data series during the monthly survey.

Generally, A31 contributed the highest proportion of T-Zn to the Aizumame River, except in summer. The A41 became the second highest contributor of T-Zn. Both A31 and A41 were located in the vicinity of many industrial areas that discharged the wastewater to the river body. The T-Zn loading input from A31 and A41 varied from 43% (summer) to 88% (winter). A21 also has smaller industrial area while A11 did not have any industrial area.

In summer, there was a high T-Zn input to A4 from unknown source, however the river discharge remained low. By contrast, the river discharge was high to A5 and the river discharge was low. This clearly indicates a dilution effect in the Aizumame River.

6.3.1.2 Seasonal Zn load variations in the Umeda River

The flow analysis of river discharge and T-Zn load can be seen in Figure 6.5 and Figure 6.6, respectively. The Umeda River did not have a significant variability of the river discharge during the sampling time. Indeed, the T-Zn seasonally varied which winter has the highest load of T-Zn, while summer exhibited the lowest load.

In winter, an elevated T-Zn input from unknown source to U5 was observed. Given that the river discharge contribution to U5 from unknown source is relatively low, it is likely that other point sources existed between U4 and U5. It is also possible that the changes in the water chemistry might cause the precipitates to become dissolved form. Therefore, a thorough investigation regarding the water quality is necessary. Obvious contribution from industrial wastewater in the vicinity of Sakai River was observed in spring, discharging about 1336 g/day.

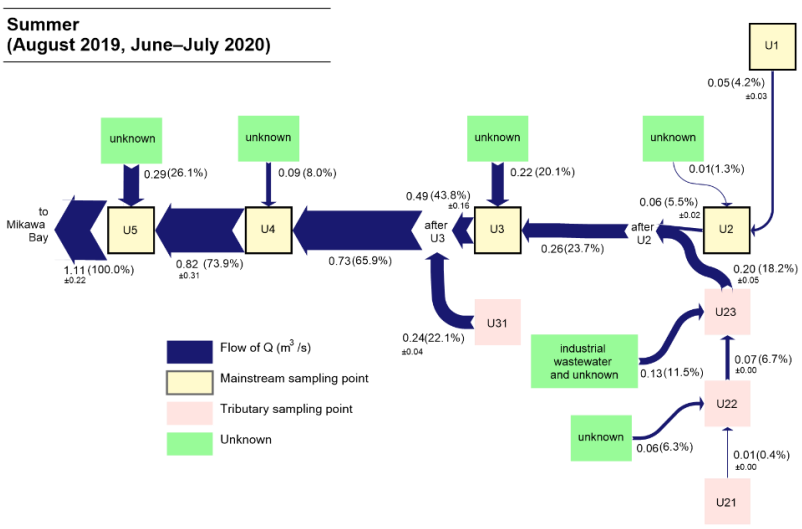

(a)

Figure 6.5 River discharge (Q) flow analysis in seasonal variations: (a) summer; (b) autumn; (c) winter; (d) spring in the Umeda River. The values indicate mean (percentage relative to the output flow from U5 at each diagram) ± SD of the data series during the monthly survey.

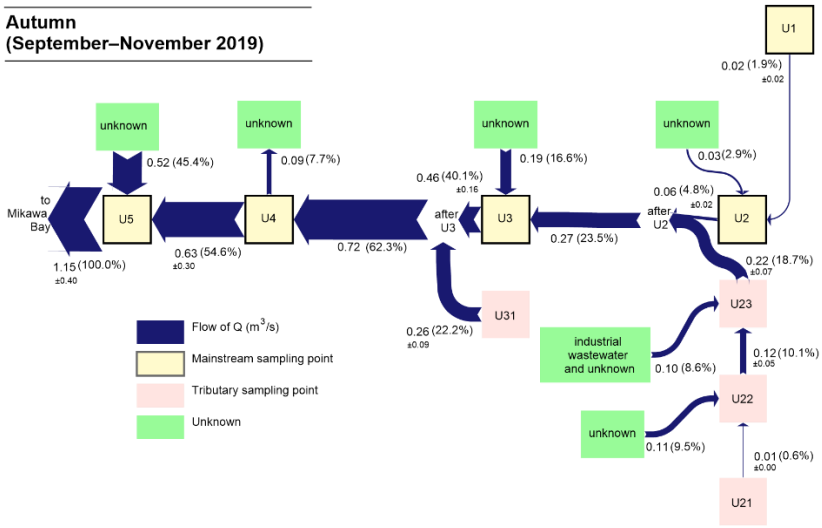

(b)

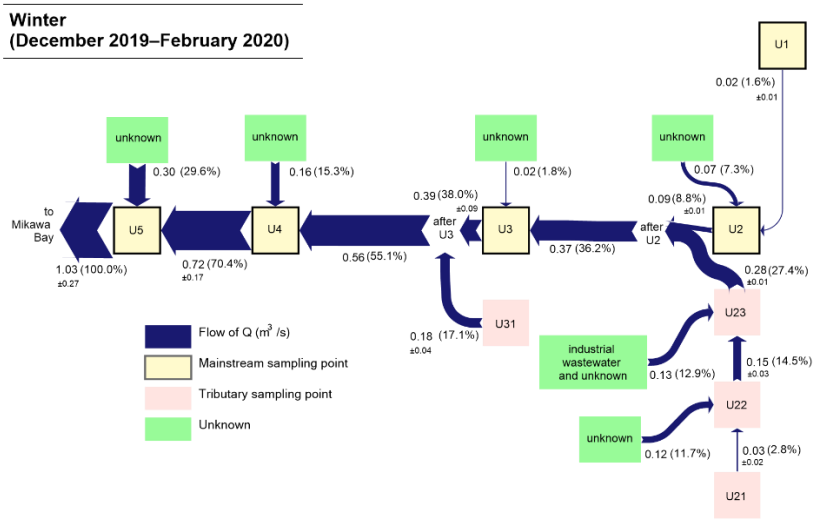

(c)

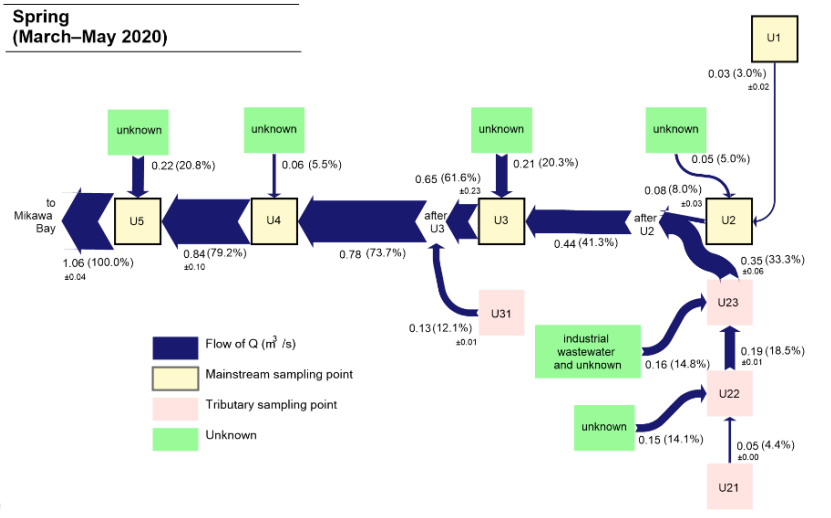

(d)

Figure 6.5 River discharge (Q) flow analysis in seasonal variations: (a) summer; (b) autumn; (c) winter; (d) spring in the Umeda River. The values indicate mean (percentage relative to the output flow from U5 at each diagram) ± SD of the data series during the monthly survey. *(Continued)*

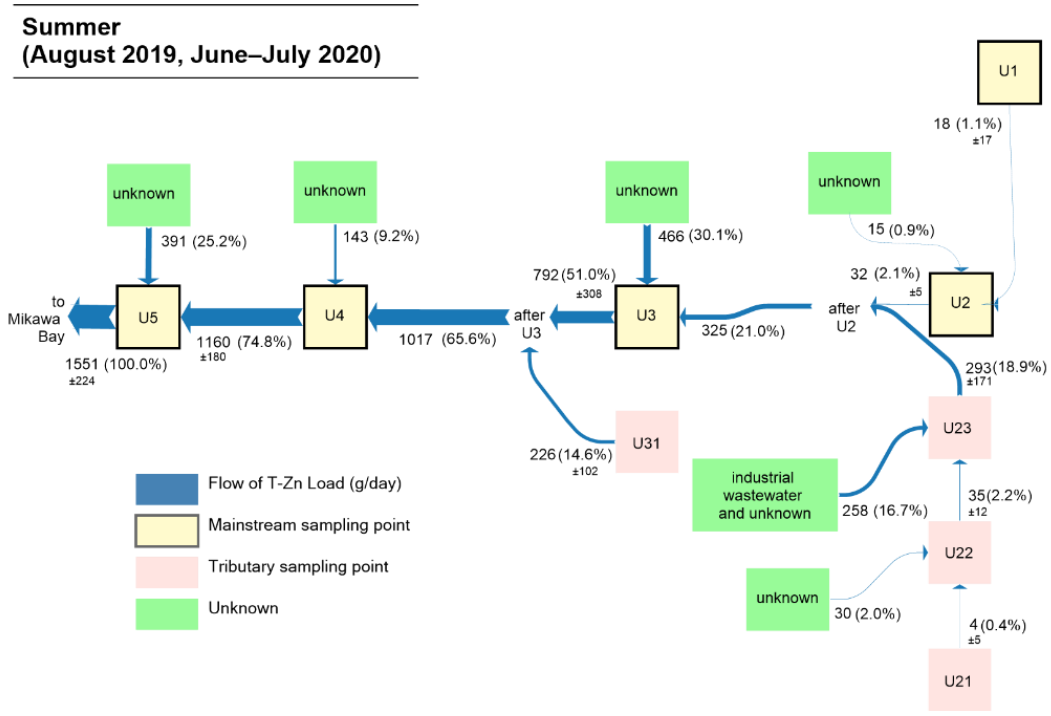

(a)

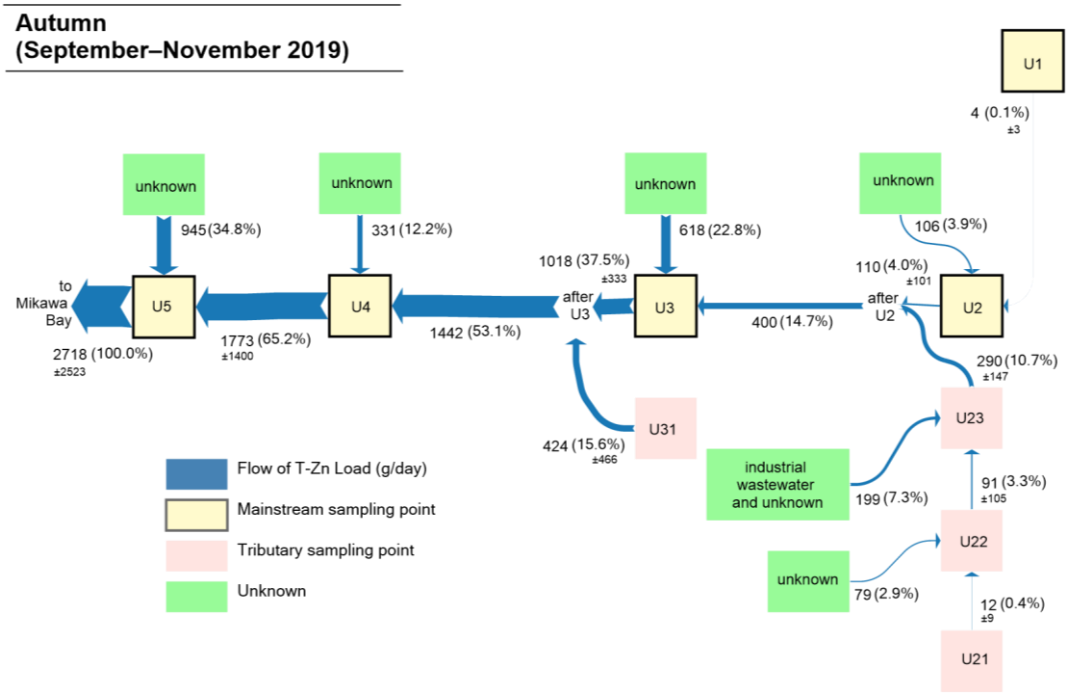

(b)

Figure 6.6 T-Zn load flow analysis in in seasonal variations: (a) summer; (b) autumn; (c) winter; (d) spring in the Umeda River The values indicate mean (percentage relative to the output flow from U5 at each diagram) ± SD of the data series during the monthly survey.

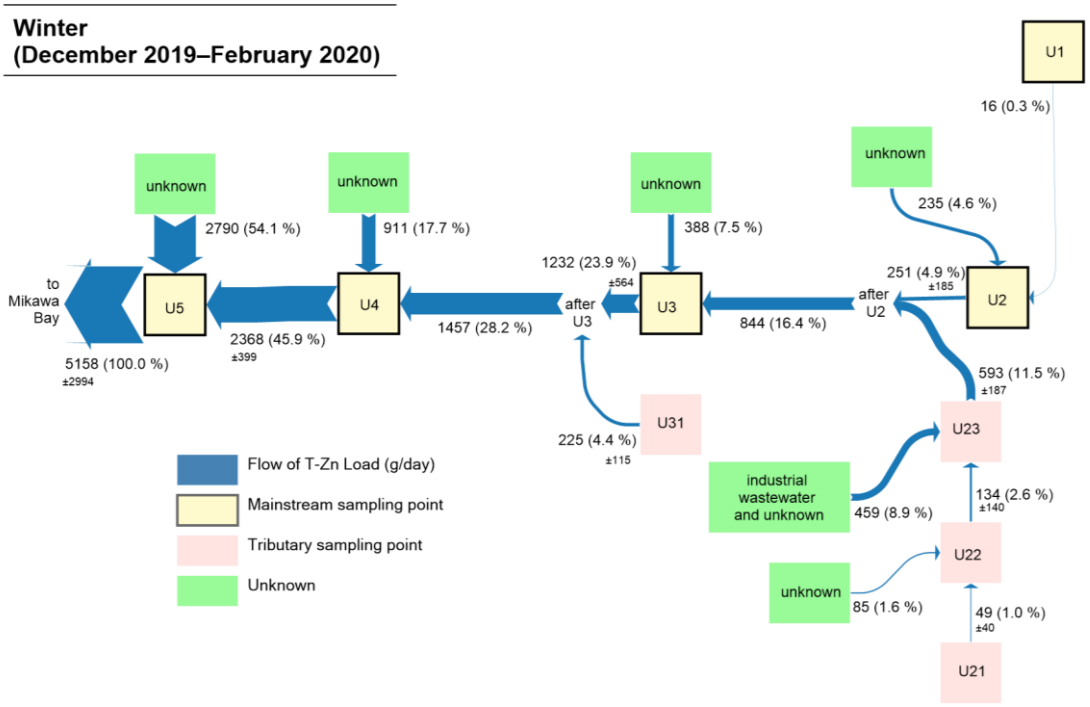

(c)

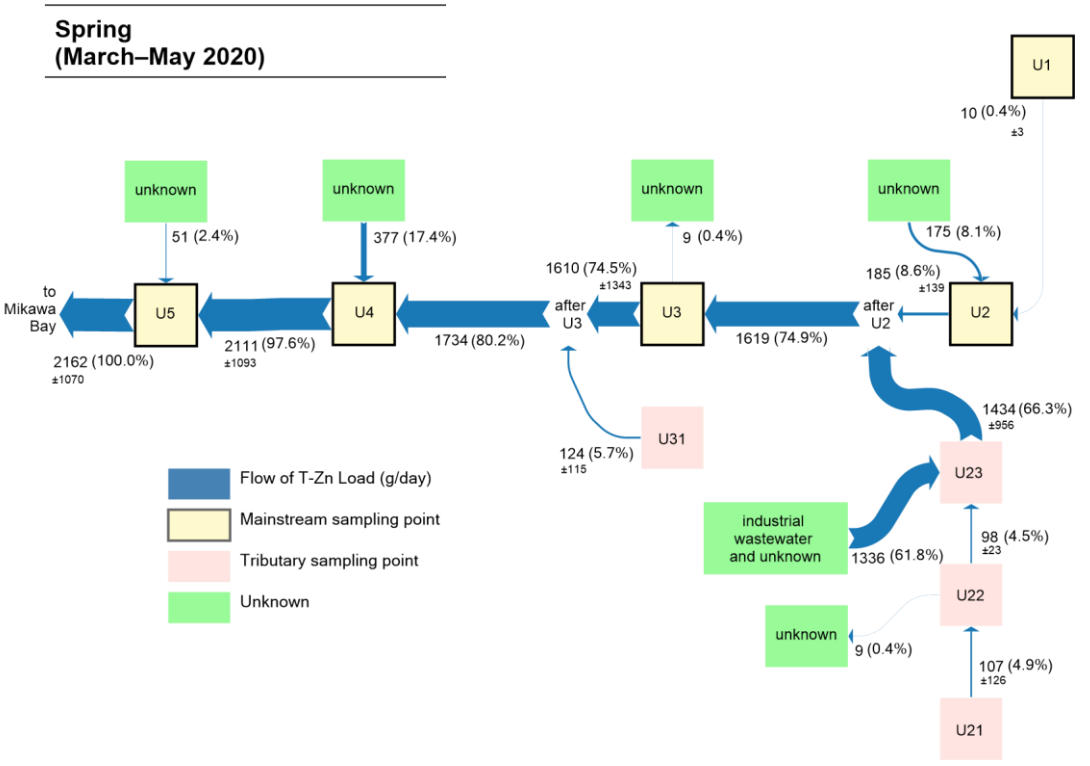

(d)

Figure 6.6 T-Zn load flow analysis in in seasonal variations: (a) summer; (b) autumn; (c) winter; (d) spring in the Umeda River The values indicate mean (percentage relative to the output flow from U5 at each diagram) ± SD of the data series during the monthly survey. (*Continued*)

6.3.1.3 Comparison of seasonal flow analyses between the Aizumame River and the Umeda River

Due to dissolution, precipitation, sorption, and complexation processes, Zn may experience many variations in speciation throughout the river (Abdel-Ghani and Elchaghaby, 2007; Akcay et al., 2003; Cooper, 2010; Dassenakis et al., 1998). Average mass flow analysis in a certain period were estimated in order to compare the Zn contribution in varying discharges due to seasonal changes during the monthly sampling events. The flow analysis is illustrated in a Sankey diagram. The overall input and output of each sample point were computed using the Sankey diagram.

The different land uses between the Aizumame River and the Umeda River may contribute the distinct results of T-Zn loads. In a catchment influenced by the paddy field area, the river discharge was largely affected by the irrigation activities, which is the case of the Aizumame River that has paddy field accounted for 12.4% of total watershed area while the crop land comprises 30.0%. The T-Zn load was the highest during the summer. However, it should be noted that the relatively high concentration was found in winter, apart from the outlier in June. By contrast, in Umeda River, the highest T-Zn load was observed in winter as well as the T-Zn concentrations. In Umeda River, the land uses were mostly affected by agriculture (5.8% paddy field and 43.0% crop land) while 29.6% is the urban area. It is different from the Aizumame River which has larger urban area (42.2%) than agriculture. The agricultural activities also comprise different crops, which in the Umeda River, the crop land (cabbage, tea, etc.) has the highest proportion compared to the paddy field. This may affect the river discharge variation between seasons.

In Aizumame River, the industrial discharge tributaries in the downstream section (A31 and A41) constantly contributed a considerable T-Zn loading (43% in summer to 88% in winter) to the mainstream which accounted for approximately 2,154–3,664 g/day. Although the maximum industrial input was in winter, the total T-Zn loading in the most downstream (A5) was highest during summer season. This is due to the contribution from unknown source to A4 (1,878 g/day). In Aizumame River, the T-Zn was obviously originated from the point source (mainly from industries) according to the load flow analyses.

By contrast, in Umeda River, the industrial wastewater input was clearly observed only in spring (61.8%, 1,336 g/day). Meanwhile, significantly lower industrial wastewater contributions were found in summer (16.7%), autumn (7.3%), and winter (8.9%). The unknown source of T-Zn loadings to U5 were quite high in autumn (34.8%) and winter (54.1%), despite its varying discharge (45.4% and 29.8%, respectively). Further analysis is needed which is discussed in the Subsection 6.4.1 about distinguishing the point sources and non-point sources in the Umeda River.

6.3.2 Irrigation and non-irrigation period

6.3.2.1 Comparison of loads during non-irrigation and irrigation period in the Aizumame River

T-Zn load and river discharge flow analysis using the sankey diagram during non-irrigation and irrigation period are illustrated in Figure 6.7 (river discharge) and Figure 6.8 (T-Zn). The loads of all mainstream sample stations during the irrigation period were higher than those during the non-irrigation period, in contrast to the concentration. River discharges were lower during the non-irrigation period than during the irrigation period. Because paddy field irrigation water discharge was minimal, the major source of Zn flow was wastewater from the industrial sector.

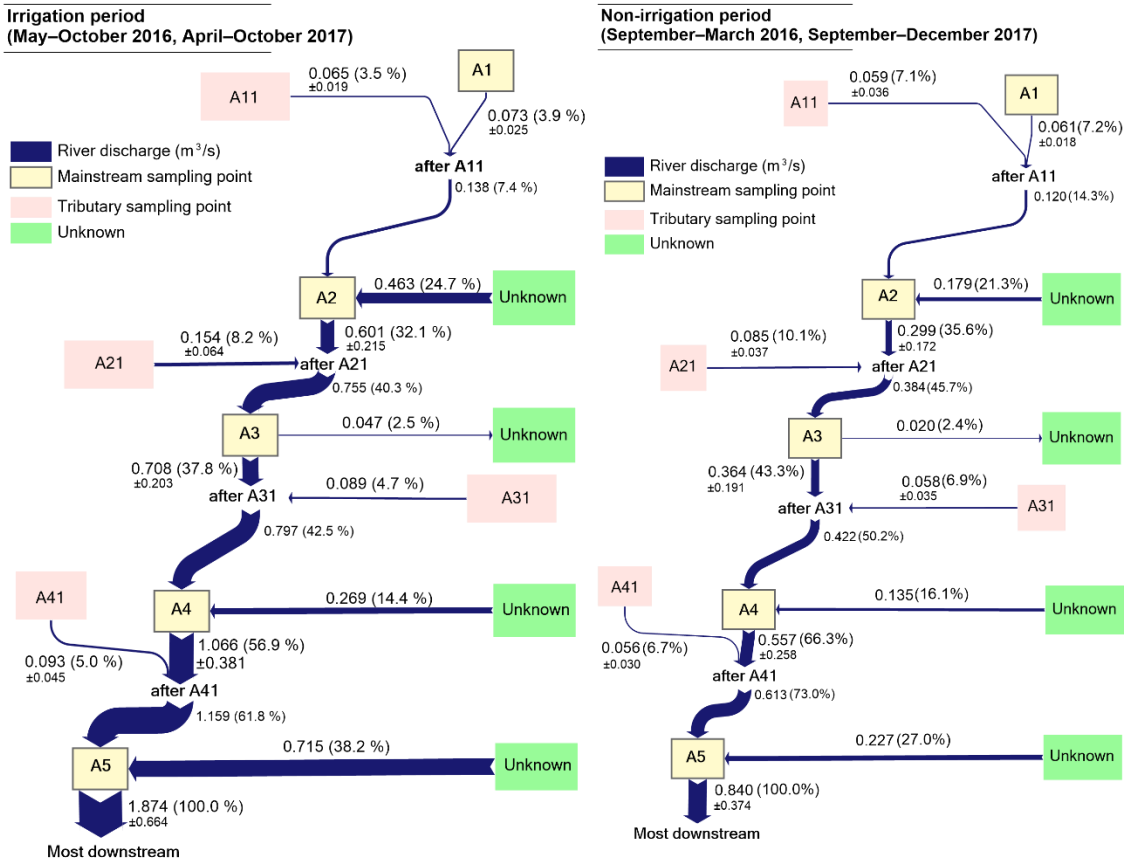

(a) (b)

Figure 6.7 River discharge (Q) flow analysis based on irrigation: (a) irrigation period; (b) non-irrigation period in the Aizumame River The values indicate mean (percentage relative to the output flow from A5 at each diagram) ± SD of the data series during the monthly survey.

As shown in Figure 6.7, the Zn of industrial discharge became more prominent during the non-irrigation period while the discharge to the mainstream remained low during both periods [0.089 m^3/s (A31) and 0.093 m^3/s (A41) in irrigation period and 0.058 m^3/s (A31) and 0.093 m^3/s (A41)]. According to Figure 6.8, the tributaries of the industrial area contributed about 3457 g/day and

3406 g/day to the mainstream in both the non-irrigation and irrigation periods, respectively. During the non-irrigation period, these values constituted 85% of total Zn introduced into the mainstream, but during the irrigation period, the contribution was as low as 62%. A31 and A41 were the primary contributors, with A31 contributing the most during the non-irrigation phase (1800 g/day) and slightly less during the irrigation period (1628 g/day). In comparison to the other tributaries, A41 delivered a higher load (e.g. 1536 g/day) into the main channel during irrigation.

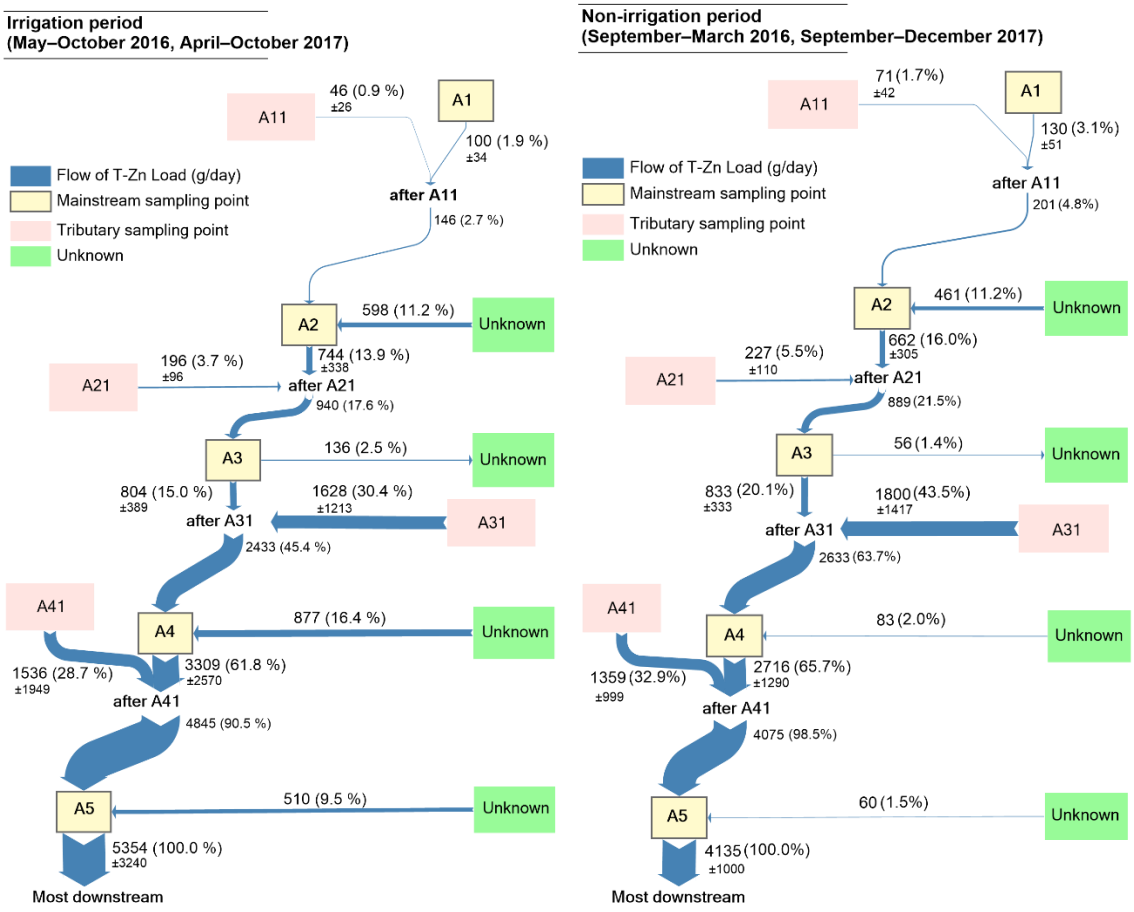

(a) (b)

Figure 6.8 T-Zn load flow analysis based on irrigation: (a) irrigation period; (b) non-irrigation period in the Aizumame River. The values indicate mean (percentage relative to the output flow from A5 at each diagram) ± SD of the data series during the monthly survey.

On the other hand, agricultural activities were most likely the source of the unknown source of A4 and A5, which was more than eight times higher during the irrigation period. The river discharges between irrigation and non-irrigation period were considerably different, particularly to A5 which contributed about 38.2% (irrigation, 0.715 m^3/s) and 27% (non-irrigation, 0.227 m^3/s).

Thus, the unknown sources are probably non-point sources. Moreover, the point sources were only identified from A11, A21, A31, and A41 during the extensive field survey.

6.3.2.2 Comparison of loads during irrigation and non-irrigation period in the Umeda River

The river discharges between irrigation and non-irrigation period were not much different in the Umeda River. As previously mentioned in Subsection 2.1.2, the Umeda River does not have a large proportion of paddy field. Figure 6.9 shows the river discharge balance in the Umeda River during both periods. However, the T-Zn loads exhibited different concentrations between irrigation and non-irrigation period, which the irrigation period has lower loads compared to those in the non-irrigation period. In this case, it is possible that the difference might be due to the seasonal variation, not primarily due to the irrigation activities.

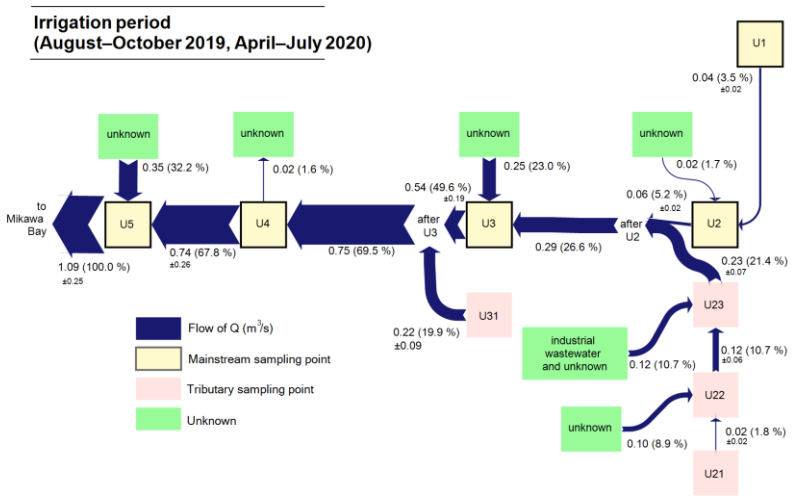

(a)

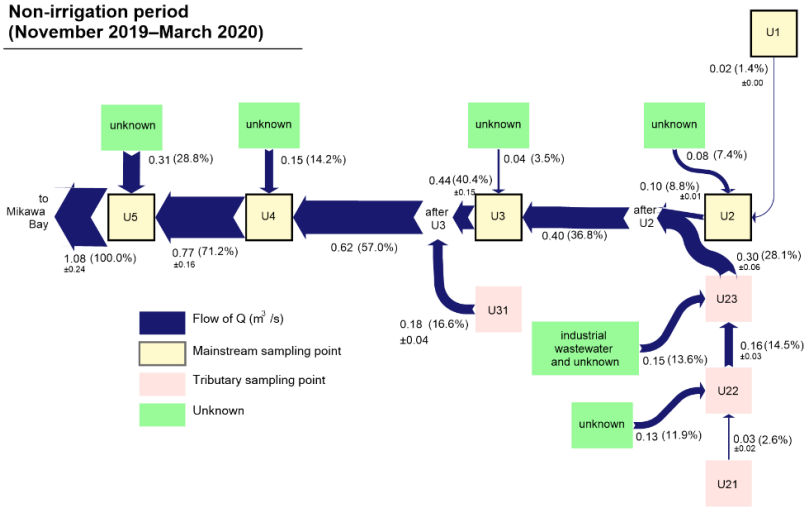

(b)

Figure 6.9 River discharge (Q) flow analysis based on irrigation: (a) irrigation period; (b) non-irrigation period in the Umeda River The values indicate mean (percentage relative to the highest flow of both periods) ± SD of the data series during the monthly survey.

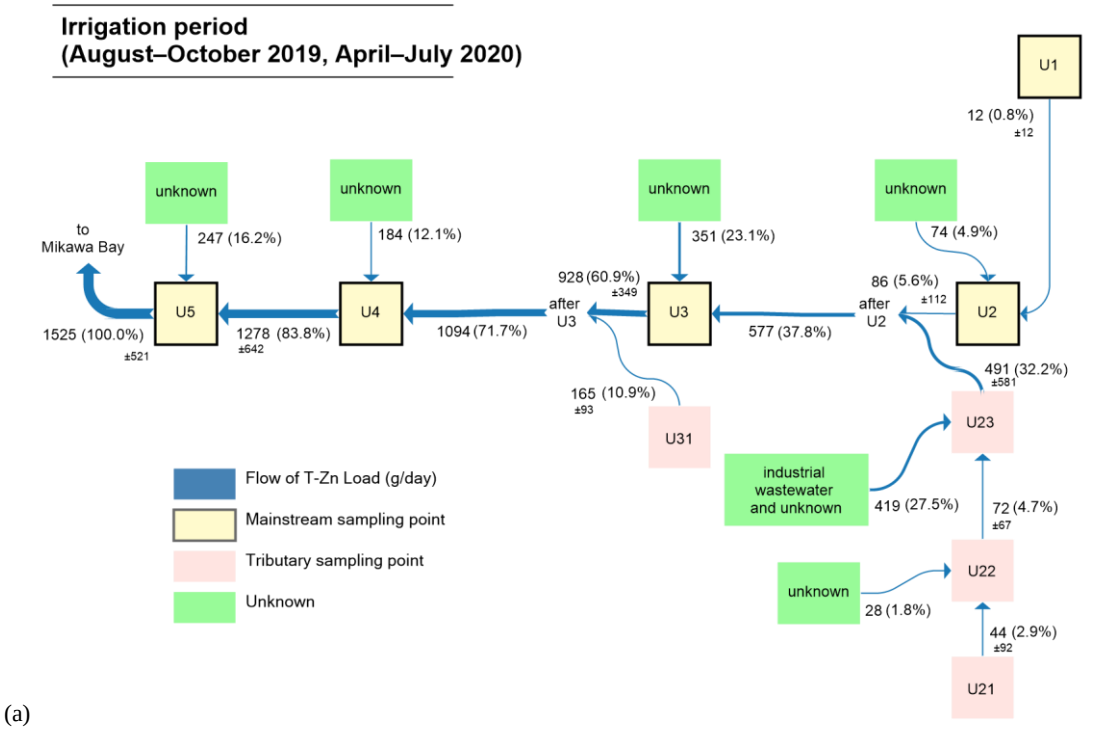

(a)

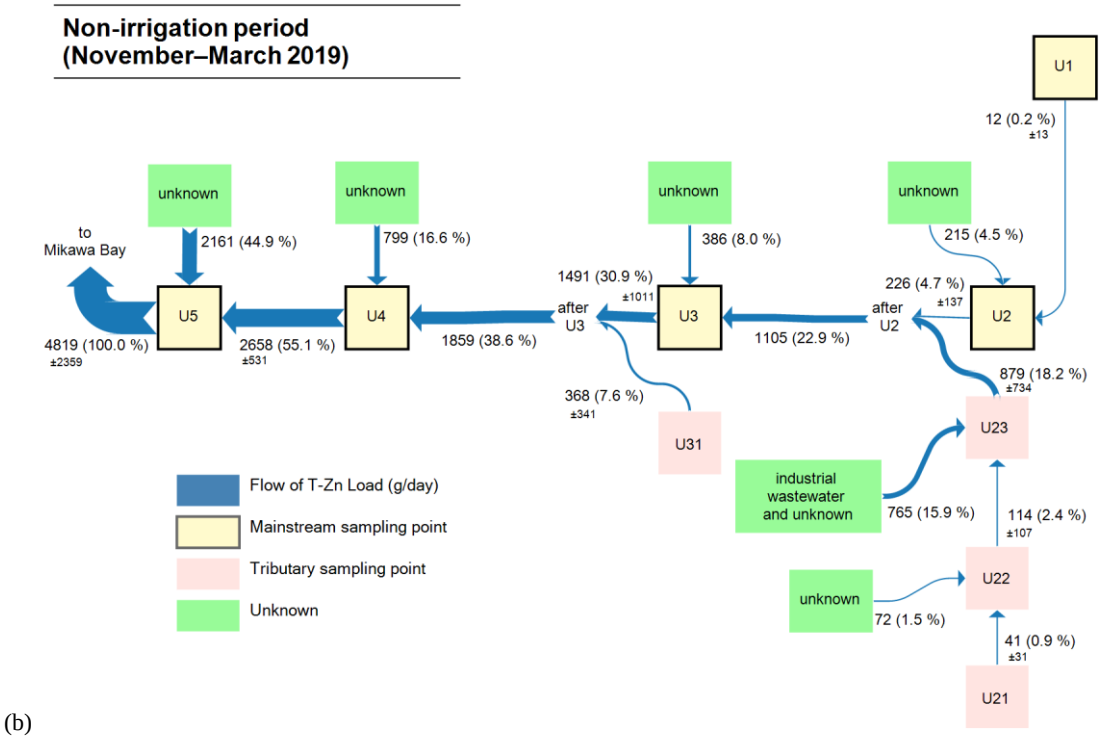

(b)

Figure 6.10 T-Zn load flow analysis based on irrigation: (a) irrigation period; (b) non-irrigation period in the Umeda River. The values indicate mean (percentage relative to the output flow from U5 at each diagram) ± SD of the data series during the monthly survey.

6.3.2.3 Comparison of irrigation period Zn variability between the Aizumame River and the Umeda River

The overall Zn burden to Japanese surface waters during normal water levels was 1,731 t/year according to Naito et al. (2010). In comparison, total Zn loads to the Aizumame River in Aichi Prefecture were 2.2 t/year or 0.049 t/km^2/year in the most downstream portion. Because of the high total Zn concentrations in the Aizumame River, the Zn loads to the Umeda River were lower (1.1 t/year or 0.024 t/km^2/year) than those to the Aizumame River. The distinct T-Zn loadings in each river might be due to the varied proportions of urban area.

Aizumame River and Umeda River have different characteristics of river catchment. The Aizumame River was influenced by the paddy field irrigation (12.8%), different from the Umeda River where the irrigation only accounted for 5.8%. Once again, the point sources were prominent in the Aizumame River, although the urban (42.2%) has slightly lower area than agricultural area (42.4%). Another evidence of point source contribution is thoroughly explained by the hourly survey in Chapter 6.4.1. Moreover, the Zn loadings in Aizumame River were generally higher during the irrigation period, in contrast to the Zn concentrations. Meanwhile, in Umeda River, the river discharge was slightly higher during non-irrigation period due to low proportion of paddy field. The T-Zn loadings in non-irrigation period were higher than in irrigation period. The urban area only comprises 29.8% of total land use in Umeda River catchment. The T-Zn loading differences between two periods could be affected by the seasonal variations rather than irrigation's. It is not apparent that the point sources are prominent in the Umeda River. Therefore, a further analysis is needed, which is described in Chapter 6.3 and 6.4.2.

6.4 Transport of Zn in the Umeda River

6.4.1 Ratio of Zn and Fe in suspended solids (SS) and water during monthly survey

A key parameter for assessing the possible migration of a pollutant in the dissolved phase when it comes into contact with riverbed sediment or SS is the ratio between particulate and dissolved phase levels (Sedeño-Díaz et al., 2020). Figure 6.11 shows the ratios of the metals at each sampling location. The ratio varied from 3.84 to 6.31 (CV: 10%) for Zn and from 4.45 to 6.80 (CV: 8%) for Fe. Generally the ratio were in accordance with the log ratio values in SS for the freshwater system which ranged from 3.5 to 6.9 (Allison and Allison, 2005), reflecting that a strong adsorption of the SS may occur (Gogoi et al., 2016). It can be seen clearly in the Figure 6.11 that the U22 had the highest ratio of Zn. Generally, the ratio decreased with increasing the distance from upstream in the Umeda River. Larger ratio values indicates higher adsorption capacity and less mobility in solution (Gogoi et al., 2016). It implies that the Zn has higher potential mobility in the water medium than Fe. It should be noted that the standard deviations

of U23 was relatively high, indicating that the ratio might have wide range. The lowest log ratio of Zn at U23 was in January, i.e., 4.2.

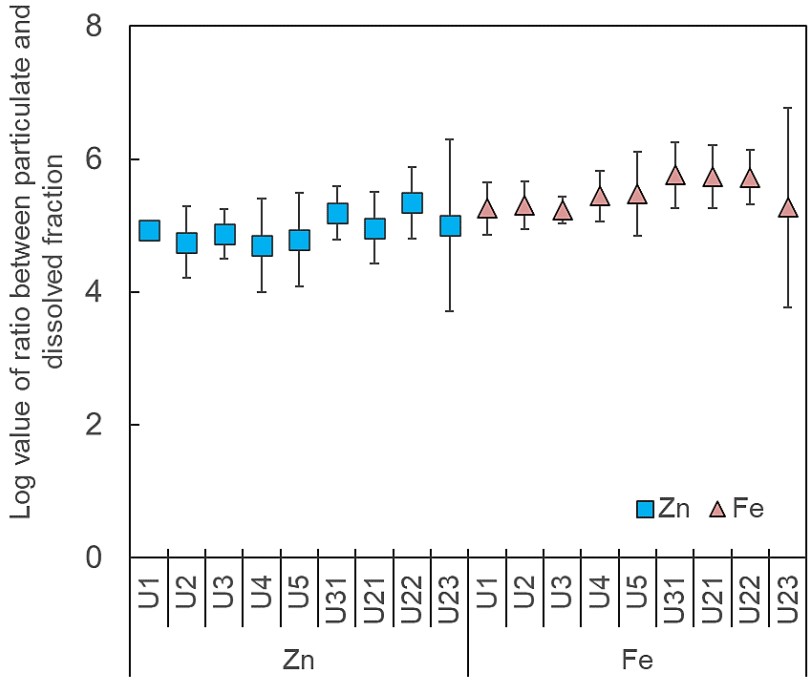

Figure 6.11 A plot illustrating mean values of log ratio between particulate and dissolved fraction of Zn and Fe during the 12-month

6.4.2 Correlation among P-Zn, P-Fe, and POC

6.4.2.1 Suspended solids (SS)

Although the Zn in the Umeda River was transported mainly in the dissolved form, the particulate form in the suspended solids (SS) might have correlated to Fe, as the inorganic part, and particulate organic carbon (POC), as the organic part. Figure 6.12 shows the correlation between Zn, P-Fe, and P-Zn at each sampling station. The data used in this correlation analysis was 12 (for monthly survey in one year).

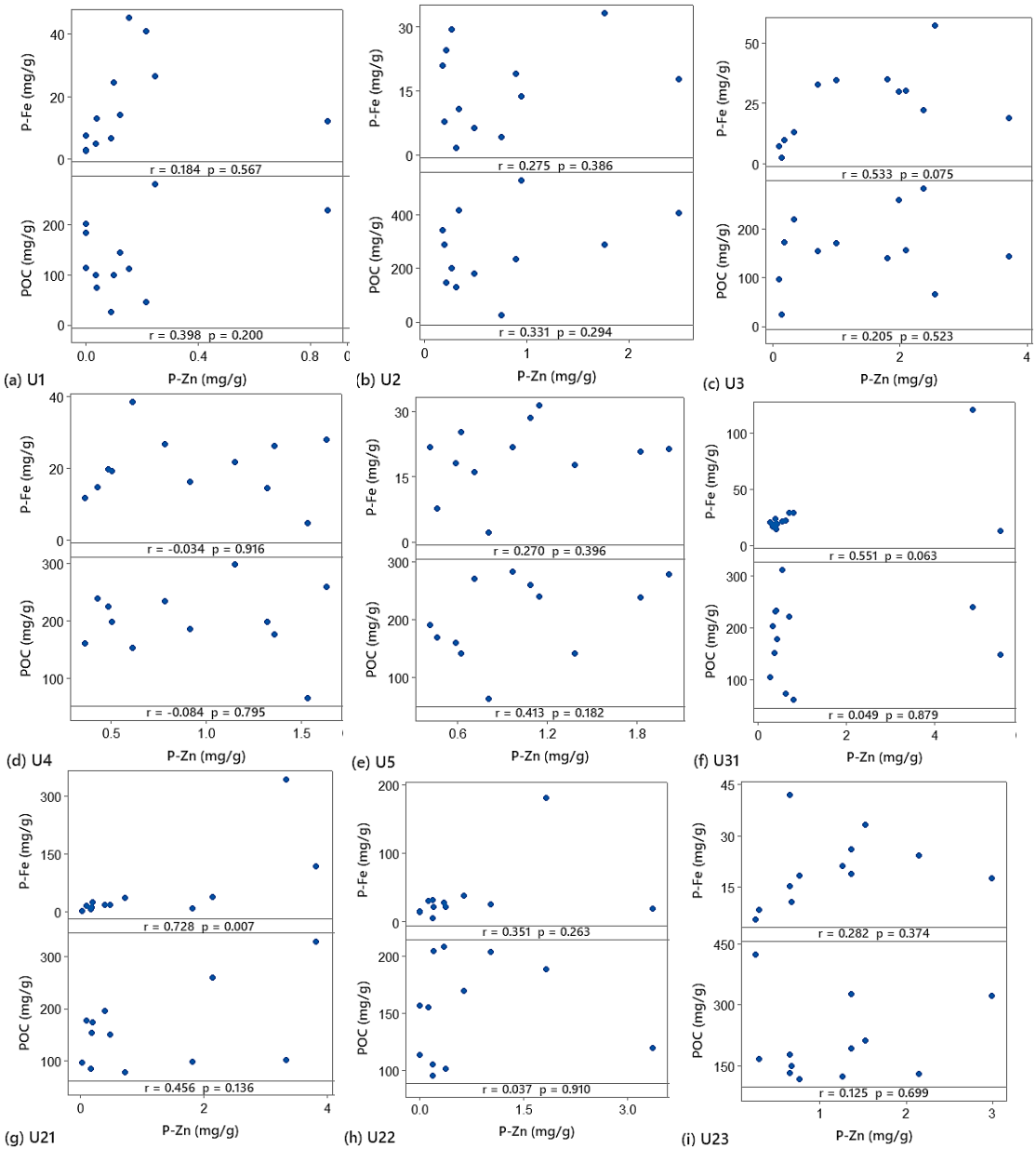

Figure 6.12 Correlation between P-Zn and POC and P-Fe in the monthly baseflow survey: from (a) to (i) are at U1, U2, U3, U4, U5, U31, U21, U22, and U23, respectively: the sample number (n) was 9 for each correlation.

According to the Figure 6.12, there were no consistent relation of P-Zn and POC in each sampling station. It should be also noted that the p-value was more than 0.05 indicating that the correlation could not draw conclusive evidence. However, a strong correlation ($r = 0.728$; $p < 0.05$) between P-Zn and P-Fe was found at U21, the most upstream sampling station in the Sakai River.

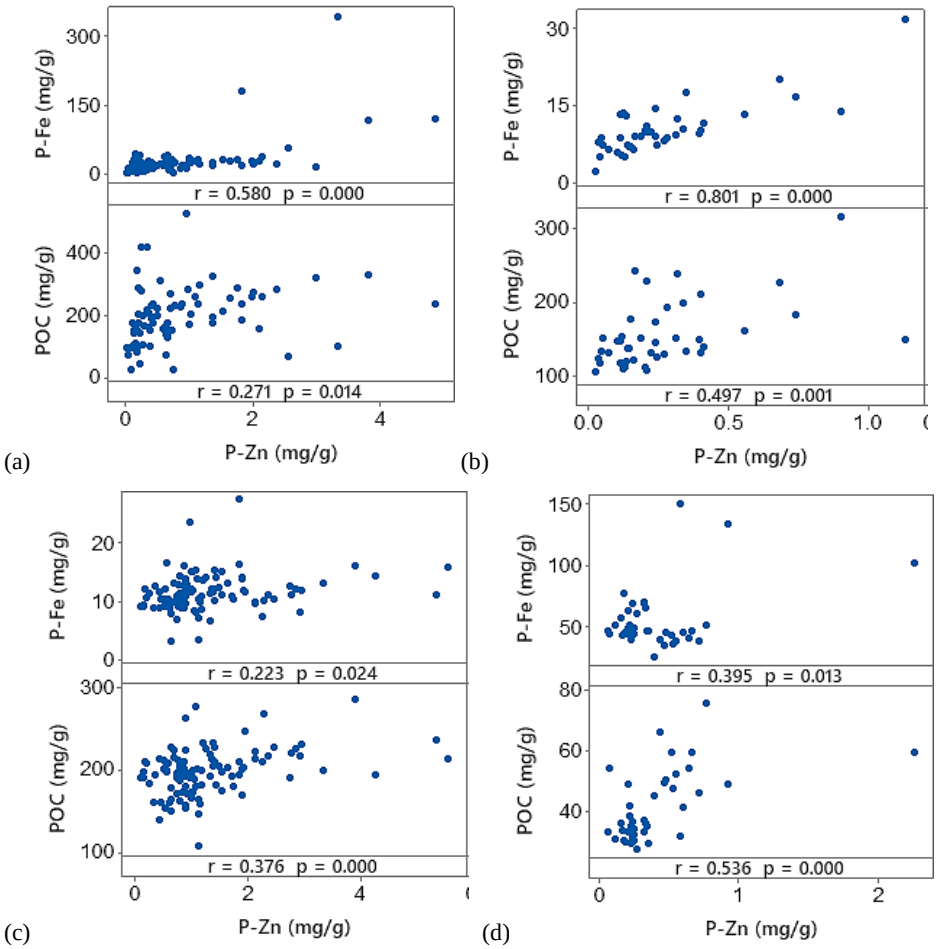

Figure 6.13 Correlation between P-Zn and POC; P-Zn and P-Fe: (a) in the monthly baseflow survey at all sampling stations of the Umeda River from August 2019 to July 2020 (n = 81); (b) in the hourly baseflow survey in February at U5 (n = 50); (c) in the hourly baseflow in October at U5 (n = 102); (d) in the hourly stormflow in September at U5 (n = 39)

Figure 6.13 illustrates positive correlations between P-Zn, P-Fe, and POC in monthly baseflow survey at all sampling stations, the hourly baseflow survey (both in February and October), and the hourly stormflow survey. In contrast to the correlation at each sampling station, P-Zn moderately correlated with P-Fe (r = 0.580; $p < 0.001$), as shown in Figure 6.13a. Low correlation was also confirmed between P-Zn and P-Fe in the baseflow survey in October (r = 0.223; $p < 0.05$) and the stormflow (r = 0.395; $p < 0.05$), as seen in Figure 6.13c and d. In February, a strong correlation was found between P-Fe and P-Zn (r = 0.801; $p < 0.001$) in the hourly baseflow survey. The correlation between P-Zn and POC generally showed a low-moderate correlation in the monthly survey (r = 0.271; $p < 0.05$), in February hourly survey (r = 0.497; $p < 0.01$), in October hourly survey (r = 0.376; $p < 0.001$), and in the stormflow survey (r = 0.536; $p < 0.001$).

6.4.2.2 Riverbed sediment

Figure 6.14 shows correlations among Zn, Fe, and POC in each particle size category. Significant correlations ($p < 0.05$) among Zn, Fe, and POC were confirmed in the riverbed sediment. A significant correlation indicates that concluding evidence can be derived from the dataset. Zn concentrations moderately correlated to Fe in each grain size category, namely 0.394 (for coarse sand), 0.437 (for medium sand), and 0.401 (for fine sand). Low-moderate correlations was found between Zn and POC.

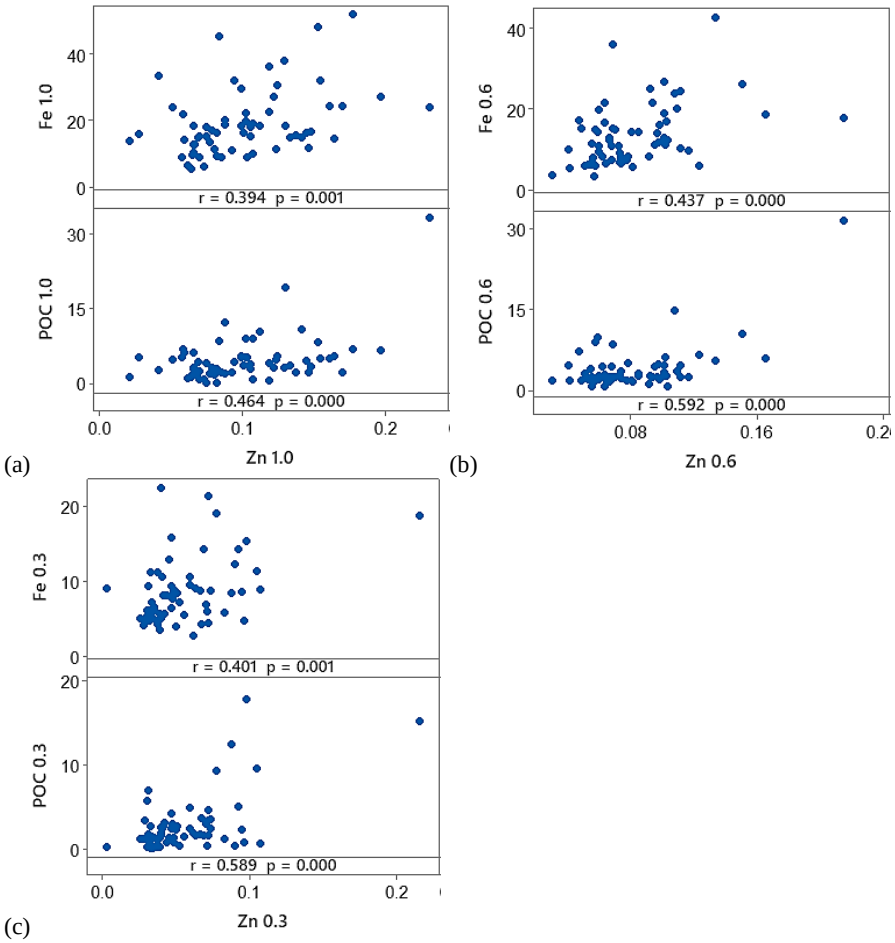

Figure 6.14 Correlation between Zn, Fe, and POC in each grain size category: (a) 1.0 (0.6–1.0 mm), (b) 0.6 denotes size of 0.3–0.6 mm; (c) 0.3 denotes size <0.3 mm. Sample number (n) for each correlation was 63.

Anthropogenic activities conducted during weekday could include industrial operations, mining, urban runoff, traffic emissions, atmospheric deposition, and agricultural runoff. Domestic activities performed every day could also have contributed to the elevated Zn (Naito et al., 2010) during both weekday and weekend. Interestingly, only the Zn concentrations on weekdays increased sharply in our research. Both natural and anthropogenic sources of Zn might be to blame

for the higher Zn levels, namely industrial operation (Andarani et al., 2020; Xu et al., 2017; Zhen et al., 2016), agricultural runoff (Ke et al., 2017; Xu et al., 2017; Yang et al., 2009), road runoff (Hüffmeyer et al., 2009), traffic emissions, and atmospheric deposition (Ministry of Environment of Japan, 2018; Sakata et al., 2005; Sörme and Lagerkvist, 2002), mining activities (Gozzard et al., 2011; Rudall and Jarvis, 2012; Wen et al., 2013), and natural occurrences (dos Reis et al., 2017).

The increased Zn may come from point sources because the hourly baseflow survey was undertaken in clear weather (no runoff discharges). Hence, there was no wet deposition or surface runoff introduced into the Umeda River. Sakata et al. (2005) found that the Zn loads substantially contributed to atmospheric depositions into Tokyo Bay. However, the majority of the Zn proportion in the Umeda River was dissolved, especially at night, thus the source was unlikely to be dry atmospheric deposition of particulate matter. The most downstream station in the Umeda River has the highest mean total Zn concentrations during 14 months from August 2019 to July 2020, according to the monthly baseflow survey. The Zn pollution in the Umeda River catchment might be due to wastewater point sources from manufacturing industries in the upper-middle stream region, given the land use of the watershed. A further evaluation of land uses surrounding the sampling stations is discussed in Subsection 6.2.3.

During the 12-month sampling period, three manufacturing industries discharged treated wastewater to the Sakai River, a tributary of the Umeda River, although Zn concentrations (0.036–0.079 mg/L) did not exceed the NES of 2.0 mg/L. However, following the confluence with the Sakai River, the instream Zn levels of the Umeda River were greater than those in the upper catchments.

Adsorption is a crucial chemical mechanism that limits the mobility of trace elements in natural water because of its kinetically rapid reactions (Gammons et al., 2015). According to earlier research (Gammons et al., 2015; Nimick et al., 2011), a suitable mineral or organic surface is required to induce trace elements, such as organic matter and hydrous metal oxides, to be adsorbed on the surface (Fe or Mn). Zn was primarily concentrated in the Fe-Mn oxide fraction in the case of Osaka Bay (Billah et al., 2019).

The present study also observed a low-moderate correlation between P-Zn and P-Fe during monthly and hourly (February and October) survey. Strong correlation between P-Zn and P-Fe was only found in the hourly baseflow survey in February as shown in Figure 6.13b. Other survey only exhibited low-moderate correlation between Fe and Zn. Association between P-Zn and P-Fe (r = 0.430; p < 0.05) was also confirmed in the downstream of Seyhan River's sediment (Davutluoglu et al., 2011).

The organic-rich SS in the riverine system might come from both aquatic species and anthropogenic sources (Huang et al., 2018). In a prior study, P-Zn and POC were shown to have a substantial positive relationship (Zeng and Han, 2020). In this study, low and moderate correlation was observed between P-Zn and POC in the monthly and hourly baseflow and hourly stormflow survey. At U5, During the monthly and hourly surveys, Zn was mostly found in a dissolved form (67 ± 20%). In comparison to industrial wastewaters, the D-Zn (61 ± 25%) had a greater proportion than the P-Zn. Nonetheless, both organic matter and Fe hydroxides may adsorb the particulate form of Zn.

6.4.3 Hierarchical cluster variables on Umeda aqueous phase dataset

Hierarchical cluster analysis was implemented to the dataset of aqueous phase, including pH, major cation, anion, dissolved Zn and Fe, particulate Zn and Fe, and POC in SS. The results were depicted in a dendogram for cluster variables (Figure 6.15).

The cluster variable dendrogram depicted three distinguished clusters among water parameters. Cluster-1 (depicted in red color) includes associations among EC, Na^+, $(SO_4)^{2-}$, K^+, and $(NO_3)^-$ suggesting that when EC increases, the dissolved constituents also increase. K^+ and $(NO_3)^-$ might origin from agricultural activities, namely fertilizer runoff when rainfall. Cluster-2 (depicted in green color) shows an association of Ca^{2+}, Mg^{2+}, and Cl^-. This cluster indicates that the possible sources are substantially from geochemical due to weathering of calcites and dissolution of magnesium dichloride. Cluster 3 is depicted in blue color which interestingly grouping all variables affecting the transport and phase of Zn concentrations. The Umeda River might be governed by rainwater chemistry followed by carbonate bearing rocks which suggested by the presence of HCO_3^-. It is further implied that cations and anions presence are generally insignificant in term of metal transport and behavior compared to parameters such as pH, organic matter, and the presence of adsorbent (i.e., Fe hydroxides in this case).

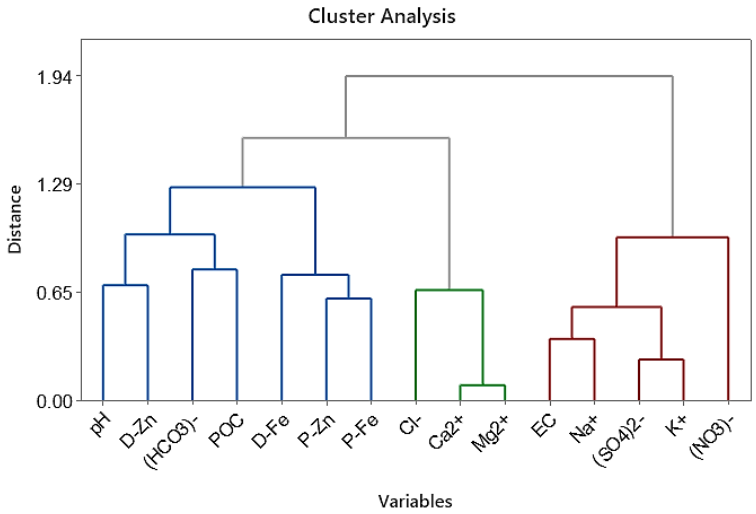

Figure 6.15 Dendogram obtained from the variable clustering

6.4.4 Identification of underlying factors and possible sources using principal component factor loading analysis (PCFA) on Umeda's water column dataset

The principal component was also used to identify the possible sources of Zn and its underlying factors by using the factor loading. This technique is used for dimension reduction, which reduces the number of random variables based on eigenvalue. A total of 81 samples and 16 variables were used in PCFA analysis. Prior to the PCFA, it is necessary to check the sampling adequacy and whether the factor loading analysis will reveal a meaningful conclusion by using the Kaiser-Meyer-Olkin (KMO) and Bartlett's test. The results are presented in Table 6.1. Because the KMO test are more than 0.5, the samples are adequate. The Bartlett's test of sphericity also shows a value of 821.380 for the Bartlett chi-square statistics ($p < 0.001$). This implies that variables are correlated and not orthogonal, hence, it is possible to explain the data variation with the principal component.

Table 6.1 Kaiser-Meyer-Olkin (KMO) and Bartlett's test

Kaiser-Meyer-Olkin Measure of Sampling Adequacy.		.669
Bartlett's Test of Sphericity	Approx. Chi-Square	821.380
	df	120
	Sig.	<.001

The factor loading with eigenvalue > 1 (the scree plot in Figure 6.16), explaining 70.918% of total variance, is presented in Table 6.2. PCA resolved five principal components (PCs). The factor loadings N > 0.225 were considered for the clear appearance of factor. Loadings of the five retained PCs can be seen in Table 6.3. Industrial discharges were first extracted component

explaining relatively high loading of Na^+, Ca^{2+}, Mg^{2+}, Cl^-, HCO_3^-, D-Zn, K^+, NO_3^-, SO_4^{2-}, Q, POC, P-Zn, and pH. It accounted 30% of total variance. Mostly the dissolved major fraction parameters, D-Zn, P-Zn, and POC were presented in the PC1. Loading factors of D-Zn were observed in PC1, PC3, PC4, and PC5. The second extracted PC (PC2) was groundwater and rock and soil weathering which showed maximum loading of Na^+, Ca^{2+}, Mg^{2+}, HCO_3, NO_3^-, SO_4^{2-}, D-Fe, and Q. The PC2 contributed 17% of total variance.

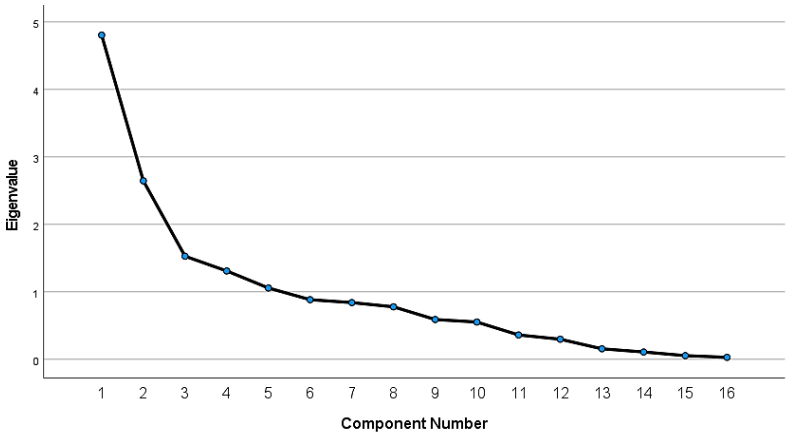

Figure 6.16 Scree plot of the principal components

Table 6.2 Total variance explained by the principal component analysis

Com-ponent	Initial Eigenvalues			Extraction Sums of Squared Loadings			Rotation Sums of Squared Loadings		
	Total	% of Variance	Cumulative %	Total	% of Variance	Cumulative %	Total	% of Variance	Cumulative %
1	4.806	30.038	30.038	4.806	30.038	30.038	3.272	20.452	20.452
2	2.645	16.533	46.571	2.645	16.533	46.571	2.747	17.168	37.620
3	1.528	9.551	56.122	1.528	9.551	56.122	2.460	15.372	52.992
4	1.310	8.187	64.309	1.310	8.187	64.309	1.665	10.409	63.401
5	1.057	6.609	70.918	1.057	6.609	70.918	1.203	7.517	70.918
6	.884	5.524	76.442						
7	.841	5.257	81.698						
8	.779	4.866	86.564						
9	.590	3.686	90.250						
10	.553	3.456	93.706						
11	.361	2.256	95.962						
12	.298	1.862	97.824						
13	.156	.974	98.798						
14	.109	.679	99.477						
15	.054	.340	99.817						
16	.029	.183	100.000						

D-Zn has moderate loading on PC3 (explaining 10% of total variance) which other parameters such as K^+, NO_3^-, SO_4^{2-}, SS, and POC also contributed from moderate to high loadings to PC3. The PC4 might represent fertilizers runoff accounted for 8% of total variance. From the maximum to minimum loading observed in PC4 are P-Fe, SS, P-Zn, Cl^-, D-Zn, POC, and HCO_3^-. Lastly, PC5 which accounted for 7% of total variance was correlated with pH, P-Fe, P-Zn, D-Zn, and Mg^{2+}.

The PC1 is extremely participated by most variables which prevent from drawing an interpretation. Variables of concern in this study, such as D-Zn and P-Zn, have high contribution to almost all PCs. Therefore, a rotation of principal components is necessary to achieve a simple representation of the underlying factors. This can be obtained by decreasing the low loading contribution of variables to PCs and enhancing the major contribution (Vega et al., 1998). The rotation modified the variance explained by each factor, but did not affect the goodness of fitting of the principal component solution (Vega et al., 1998).

Table 6.3 Unrotated component loading matrix

	PC1	PC2	PC3	PC4	PC5
D-Zn	**.576**	.157	**.365**	**-.309**	**-.262**
P-Zn	**.418**	.121	-.205	**.437**	**-.298**
D-Fe	-.164	**.642**	-.110	.014	.031
P-Fe	.031	-.219	-.077	**.539**	**-.448**
POC	**.475**	.121	**.654**	**.276**	.089
SS	.202	.133	**.690**	**.512**	.196
pH	**-.437**	-.084	-.095	.137	**.682**
HCO_3	**.687**	**.226**	.142	**-.261**	.208
Na	**.829**	**.372**	-.062	-.145	-.023
Ca	**.812**	**-.431**	-.042	.015	.205
Mg	**.803**	**-.389**	-.191	.031	**.229**
Cl	**.710**	-.164	.067	**-.379**	-.144
K	**.463**	**.687**	**-.361**	.209	.112
NO_3	**.483**	**-.670**	**-.252**	.146	.025
SO_4	**.513**	**.655**	**-.368**	.193	.099
Q	**-.368**	**.452**	.162	-.195	-.066

Bold value represents factor loading higher than 0.225

PC : principal component (unrotated principal component)

The rotation was done by using varimax with Kaiser normalization which generates 5 retained rotated PCs (hereafter referred to as varifactors, VFs). Varifactor 1 (VF1) represents a lesser amount of variance compared to PC1 (20%) highly contributed by Mg, Ca, NO_3^-, Q, D-Fe and

moderately participated by Cl^-, Na^+, HCO_3^-. This can be interpreted as a mineral component of the river water. The mineral weathering such as calcite, limestone, and magnesium dichloride might potentially happened and being a considerable amount of discharge to the river water system. VF2 represents 17% of total variance which highly participated by K^+, SO_4^{2-}, and Na^+. Moderate loadings of D-Fe, P-Zn, HCO_3^-, and Mg^{2+} to VF2 are also observed. Agricultural activities such as fertilizers application may have contributed to the K^+ and SO_4^{2-}. The fertilizers could contain trace amount of Zn. VF3 contains 15% of the total variance which includes D-Zn, pH, Cl^-, and Na^+. While moderate loadings are participated by HCO_3^-, POC, Ca^{2+}, and Mg^{2+}. The VF3 may indicate the contribution of industrial point source which eventually reacts with the water components, mainly by pH and POC according to the previous cluster variable analysis.

Table 6.4 Rotated component loading matrix using varimax with Kaiser normalization

	VF1	VF2	VF3	VF4	VF5
D-Zn	.053	.089	**.761**	**.236**	-.085
P-Zn	.195	**.412**	.138	.087	**.527**
D-Fe	**-.502**	**.433**	-.074	-.032	-.073
P-Fe	.125	-.070	-.062	.059	**.720**
POC	.108	.085	**.289**	**.806**	.013
SS	-.021	.026	-.038	**.908**	.084
pH	.013	-.054	**-.737**	.049	**-.379**
HCO_3	**.265**	**.393**	**.488**	**.241**	**-.366**
Mg	**.877**	**.237**	**.225**	.073	-.063
Ca	**.866**	.136	**.290**	.173	-.073
NO_3	**.842**	-.093	.040	-.089	.200
K	-.038	**.929**	.080	.044	.036
SO_4	.010	**.926**	.118	.036	.040
Na	**.253**	**.635**	**.597**	.128	-.108
Cl	**.453**	.070	**.687**	-.009	-.134
Q	**-.617**	.016	.022	-.016	-.164

Bold value represents factor loading higher than 0.225

VF : varifactor (rotated principal component)

The bicarbonate plays an important role as the buffer capacity in the river system. VF4 represents 10% of total variance has a high load of SS and POC. The VF4 can be explained by the particulate organic matter in SS. VF5 which has 8% of variance includes high loading of P-Fe and P-Zn and moderate loading of HCO_3^- and pH. This may indicate the correlation of inorganic fraction of Fe and Zn are influenced by the pH.

Figure 6.17 clearly shows the land uses surrounding each sampling stations. Moreover, boxplots of VF1–VF5 scores in the nine sampling stations are illustrated in Figure 6.18. An obvious spatial variation can be seen in the VF1, VF2, and VF3. These varifactors may indicate a contribution from land uses. In particular, the VF2 (agriculture) and VF3 (industrial point source) might indicate that the Zn was released from anthropogenic sources. Meanwhile, VF1 may indicate natural occurrences due to mineral weathering. The large spread around the median in VF1 (U31), VF2 (U3 and U23), VF3 (all except U31), VF4 (U1, U2, U5, U21–U23) may indicate a key role of sampling time to the variance of the respective VFs. Exceptionally low spatial variation was only observed in the VF4 and VF5, revealing that these varifactors has small effect of spatial variation, which may originate from natural sources. However, the spread around median still gives a clue about the seasonal variation that the downstream section of Umeda River generally had smaller seasonal variation.

The VF1–3 might be affected by the land uses. In the Umeda River, the urban area represents second highest proportion of total land use area from U2 to U5. It can be seen in the boxplot of VF3 that these sampling stations has a distinct value from U1, indicating D-Zn pollution to some extent in this area which also been confirmed with the cluster analysis.

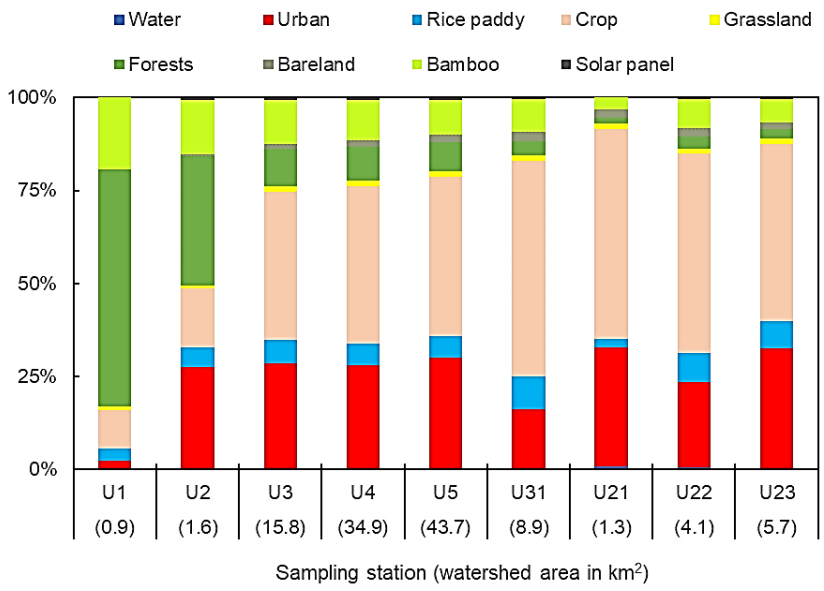

Figure 6.17 Land uses in the vicinity of Umeda River

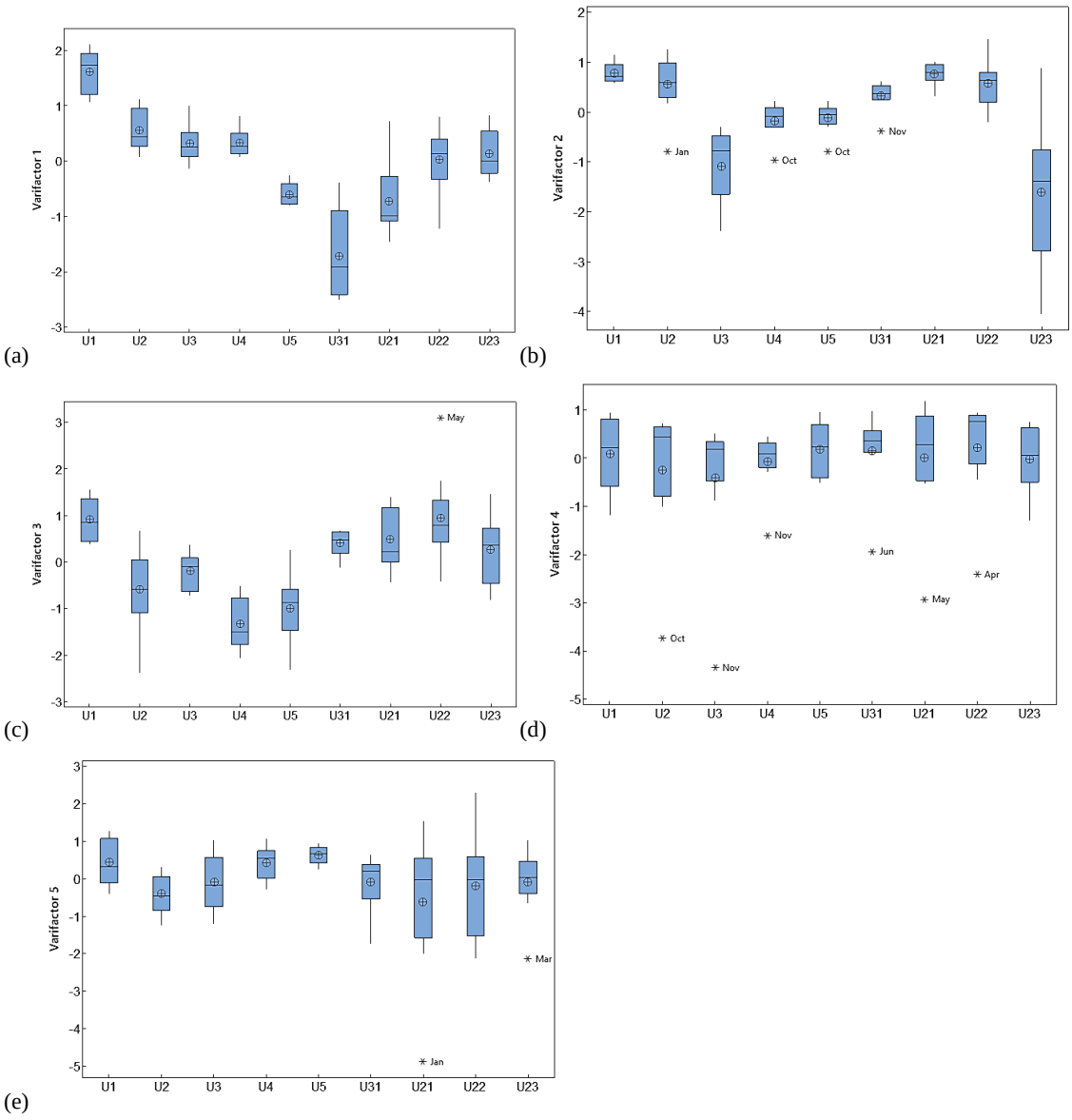

Figure 6.18 Varifactor scores for each sampling point

6.5 Zn possible sources

6.5.1 Estimation of industrial point sources contribution by comparing weekday and weekend loads in the Aizumame River and the Umeda River

The Zn loads comparison was performed only during the February's survey because the weekday Zn levels were considerably higher than weekend Zn levels. The total and D-Zn loads varied greatly over 24 hours during both time events (Figure 6.19). On weekdays, the mean total Zn load (97.15 ± 25.43 g/h) and D-Zn load (87.45 ± 23.61 g/h) were significantly greater than on weekends (32.20 ± 23.30 g/h and 36.17 ± 7.78 g/h, respectively). The greatest total Zn load (142.72 g/h) occurred at 3:00 on weekdays, while the lowest (50.94 g/h) occurred at 13:00

throughout the day and in the presence of a greater river discharge. During the weekend, a similar pattern of decreasing loads during the day was observed. The volatility was, however, smaller than it had been during the weekend. The overall Zn load peaked at 106.93 g/h and then declined until it was below the detection limit at 14:00, but the D-Zn load was already low since 12:00. Due to increasing P-Zn concentrations, two peaks of total Zn emerged over the weekend. Suspended particles may have contributed to the high Zn, which contained Fe, at 20:00. Meanwhile, the D-Zn had a substantial impact on the overall Zn burden at 23:00. On weekdays (T-Zn = 56 g/km^2/day; D-Zn = 50 g/km^2/day), the total daily Zn loading was about three times greater than on weekends (T-Zn = 18 g/km^2/day; D-Zn = 15 g/km^2/day). These discrepancies might be the result of industrial point sources. On weekdays, industrial point sources are thought to have generated at least 67% of total Zn loads (37 g/km^2/day) and 70% of D-Zn loads (35 g/km^2/day).

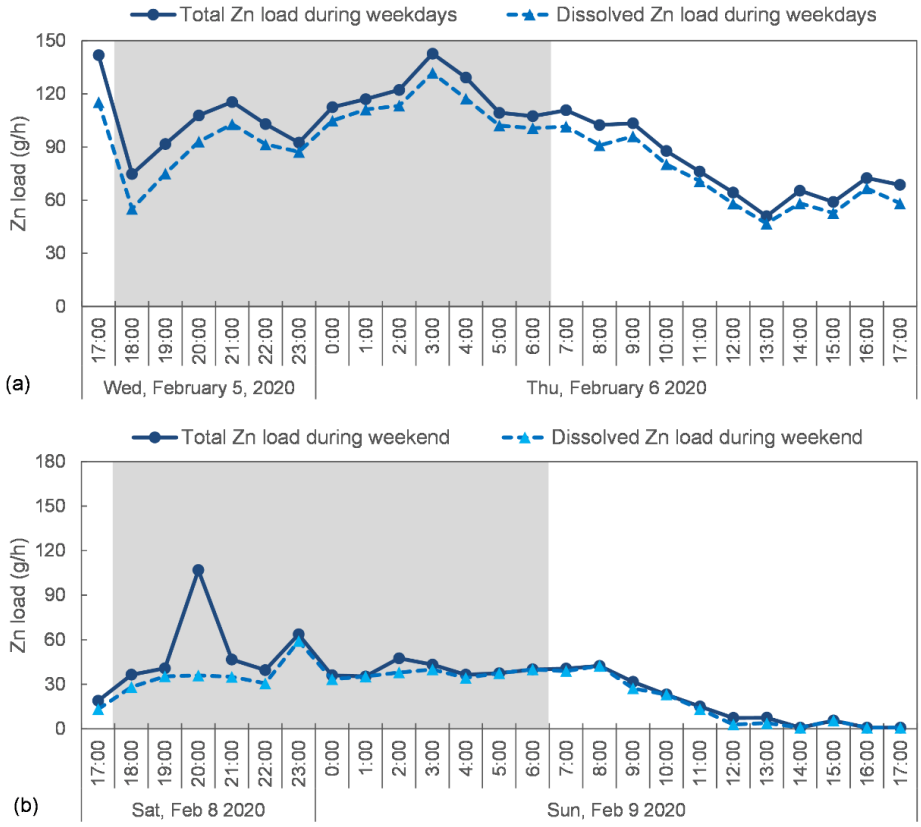

Figure 6.19 Total and dissolved Zn load in the Umeda River during the hourly baseflow survey: (a) on weekday and (b) on weekend. The gray shaded area indicates night-time hours (from 18:00 to 06:00).

The Aizumame River also showed a distinct variation of T-Zn loads between weekday and weekend. The T-Zn varied from 127.41 g/h to 359.62 g/h (217.73 ± 44.43 g/h) on weekday and

from 43.34 to 135.27 g/h (92.88 ± 18.18 g/h) on weekend. The fluctuation of T-Zn did not have a particular pattern while the Umeda River had a pattern in which the nighttime has relatively higher concentration. The pattern between weekday and weekend in the Aizumame River was also different. The T-Zn peak loading occurred at 11:00 while the lowest at 15:00 on weekday. Meanwhile, the highest T-Zn load exhibited at 09:00 and the lowest T-Zn load at 17:00. The difference between weekday and weekday in Aizumame River was lower than those in Umeda River. Based on the hourly survey, the total daily T-Zn loading in the Aizumame River was 118 g/km^2/day on weekday and 50 g/km^2/day during weekend. The industrial point sources contributed approximately 2996 g/day (57%) in the Aizumame River. The Zn yields from the industrial point sources accounted for approximately 68 g/km^2/day.

According to a survey conducted between July 2007 (flood season) and January 2008 by Wen et al.(2013), non-mining industrial operations contributed 3.8 g/km^2/day (Chongqing region) and 0.3 g/km^2/day (Wuhan region) of D-Zn to the Yangtze River (dry season). In the Rhine catchment region in Germany, Zn input from industrial discharges was 1.0 g/km^2/day in 2000 (Fuchs et al., 2002). Thus, the Japanese river catchments (Aizumame and Umeda) have a greater Zn output from industrial areas than other rivers (Yangtze and Rhine), which have a much wider catchment area.

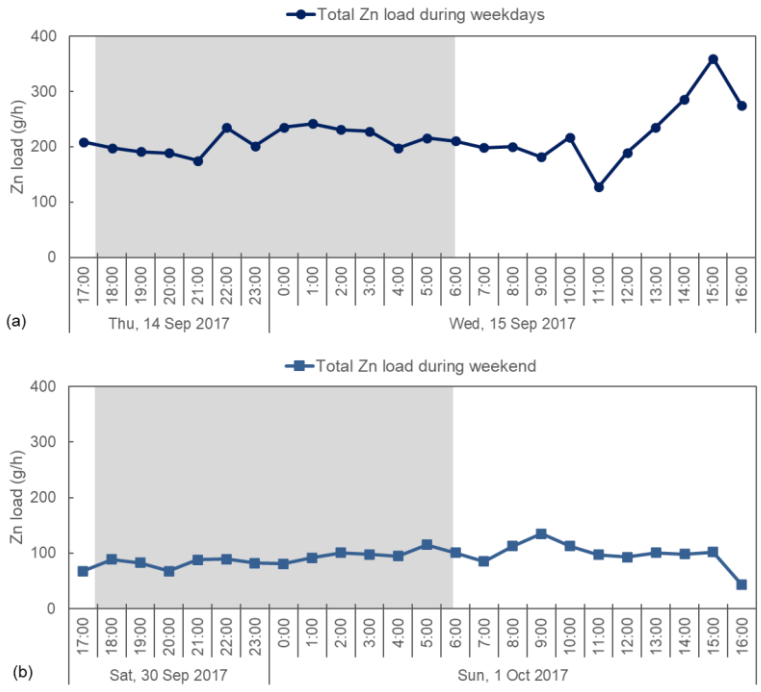

Figure 6.20 Total Zn loads in the Aizumame River: (a) on weekday and (b) during weekend. The gray shaded area indicates night-time hours (from 18:00 to 05:30).

6.5.2 Estimation of point and non-point sources by comparing baseflow and stormflow loadings

6.5.2.1 Correlations among SS, Fe, and Zn levels in the stormflow and baseflow hourly survey

Figure 6.21 shows the Pearson correlation data plots for T-Zn, T-Fe, and SS concentrations. The correlation between SS and Zn concentrations in the baseflow and stormflow was substantially positive (r = 0.797, p < 0.001), but the association between SS and Fe concentrations was quite substantial (r = 0.965, p < 0.001). During the storm, Zn and Fe were clearly transported into the river in particle form. The SS and Zn concentrations had no significant association in the baseflow, whereas the SS–Fe correlation had a very strong significant and positive correlation (r = 0.911, p < 0.001). Consequently, most Fe in the baseflow is expected to be in particulate form. During baseflow, particular point sources of Zn (dominated by the dissolved component) might well be present.

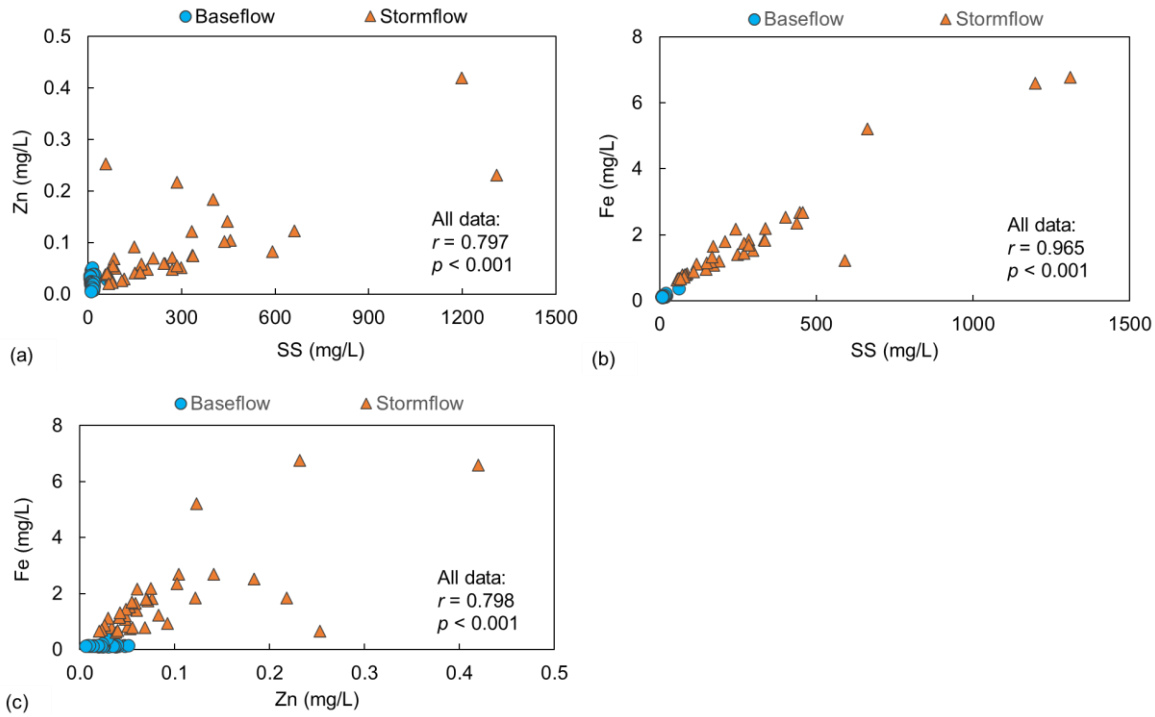

Figure 6.21 The correlations between parameters: (a) SS–Zn; (b) SS–Fe; (c) Zn–Fe

For both stormflow and baseflow, there was a strong and positive relationship between Zn and Fe (r = 0.798, p < 0.001). The Zn in storm water might be adsorbed on the Fe–oxyhydroxide coats of the SS in a near-neutral river like the Umeda River. Zn in particulate form is often absorbed by organic matter or Fe–Mn oxyhydroxides, according to prior study (Dali-youcef et al., 2006; Dawson and Macklin, 1998; Gammons et al., 2015; Nimick et al., 2011; Rose et al., 2001). The association between Zn and Fe, on the other hand, was significantly smaller and not significant

during the baseflow. The weak association with SS suggests that a large portion of the baseflow Zn was dissolved.

For all data from both flows, the loads of SS, Fe, and Zn (g/s) were determined by multiplying the concentration (mg/L) by the discharge (m^3/s). Empirical L-Q equation (Equation 2.2) were developed using non-linear regression (Kunimatsu et al., 2006). The n coefficient, as shown in Figure 6.22, compensated for more than n > 1, indicating the origin was primarily non-point pollution and washout-type runoff (Yamada et al., 2009). The SS load had the greatest n coefficient (n = 1.98), whereas the n values of Fe and Zn were lower, at 1.76 and 1.62, respectively. Although the Zn was likely from non-point sources based on the L-Q model, several data points did not fit to the prediction interval of the regression line.

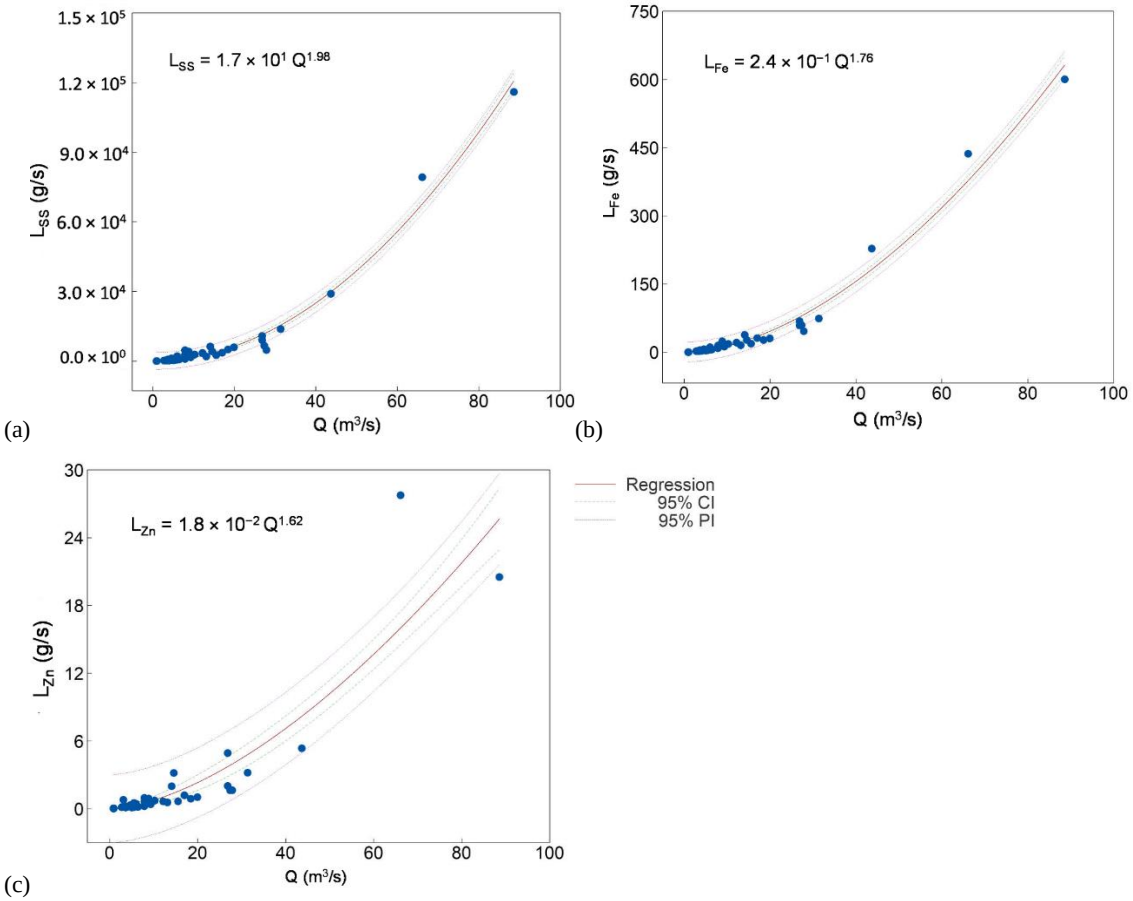

Figure 6.22 Load and discharge curve (the L-Q model): (a) SS; (b) Fe; (c) Zn

6.5.2.2 End member mixing analysis with two tracers (Zn from point source and Zn non-point source)

During the sample event, the total loadings of SS, Fe, and Zn in the baseflow and stormflow were determined. The daily load of each parameter in both events is shown in Table 6.5. The daily load in the baseflow for SS, Fe, and Zn was 2.4×10^{1} t/day for SS, 2.8×10^{-1} t/day for Fe, and 4.7 ×

10^{-2} t/day, respectively. The overall loadings of SS (1.7×10^4 t/day), Fe (9.8×10^1 t/day), and Zn (4.4 t/day) in the stormflow were significantly greater than in the baseflow.

The load ratios in the baseflow and stormflow (Table 6.5) suggest that there were distinct load magnitudes between the two flows, with the stormflow loads being significantly greater than the baseflow loads, especially for SS. With a discharge mean ratio of 16, the SS ratio was 692, indicating that the loads were over 700 times higher than those in the baseflow. The Fe (350) and Zn (93) loading ratios, on the other hand, were significantly lower than the SS ratio. In this investigation, the Fe ratio included both dissolved and particulate fraction.

Table 6.5 Total daily load of suspended solids (SS), Fe, and Zn

	Q (m^3/day)	**SS (t/day)**	**Fe (t/day)**	**Zn (t/day)**
Baseflow	8.4×10^4	2.4×10^1	2.8×10^{-1}	4.7×10^{-2}
Stormflow	1.3×10^6	1.7×10^4	9.8×10^1	4.4
$\frac{\textbf{stormflow}}{\textbf{baseflow}}$	15	692	350	93

Fe and Zn were most likely diluted amid the river's comparatively unpolluted particulate matter and water. The diluting effect was also found at the stormflow, where the concentration of the metal transported in solution and bound to the SS reduced due to mixing with comparatively clean sediment and water, according to previous studies (Bradley and Lewin, 1982; Dawson and Macklin, 1998). The duration and extent of the dry period might just have allowed SS, Zn, and Fe to accumulate in the watershed. The impermeable surfaces of the urban region, which account for 21.8% of land use in the Umeda River watershed, would be particularly vulnerable to this accumulation. The Zn load ratio was only 93, indicating that Zn was diluted more than Fe. This result is proven by the fact that the concentration of Zn at the last discharge peak, which occurred at the end of the storm period, was lower.

Using equations (2.3) and (2.4), the end member mixing analysis (EMMA) was used to determine the Zn point source (PS) and non-point or diffuse source (NPS) contributions. Because the Zn concentrations from PS were essentially comparable in both the baseflow and the stormflow, the ratio of Zn ($\frac{\text{stormflow}}{\text{baseflow}}$) from PS was 1. The ratio of Zn from non-point sources (R_{Zn_PS}) was the same as the Fe ratio (350), whereas the overall Zn ratio was 93 (see Table 6.5). The PS proportion was 74%, whereas the NPS fraction was just 26%, according to this estimate (Figure 6.23). The amount of Zn released by PS was three times that of NPS. During the stormflow, Zn discharge

was 93 times greater than during the baseflow, when the major sources were PS, which accounted for around 3.2 t/day. In the stormflow, NPS generated approximately 1.2 t/day.

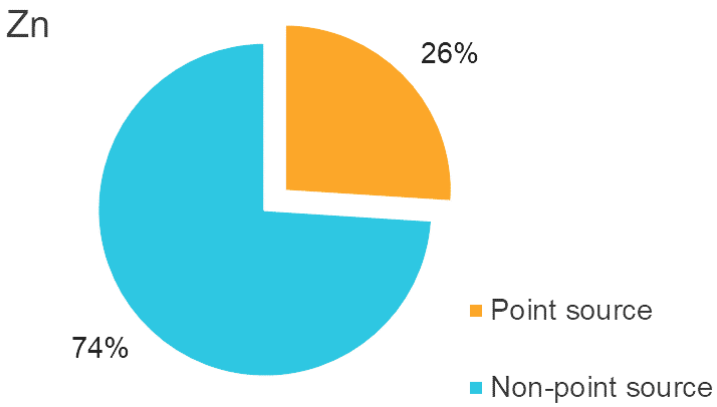

Figure 6.23 The estimation of Zn input proportion from point and non-point sources

This research shows that river management is required for both point and non-point Zn sources to ensure that Zn discharged into river water does not harm aquatic species. Because the Zn input from NPS was greater during the stormflow, stormwater runoff from human activities should be managed effectively. The particulate fraction in the stormflow was significantly greater than the dissolved fraction. Particulates of zinc can come from both human and natural sources. Tire wear particles, which may be highly bioavailable, are a possible anthropogenic non-point source (Wagner et al., 2018). Other particles might come from farming areas (which comprise the majority of land usage surrounding the Umeda River) and atmospheric deposition. It is also conceivable that Zn-contaminated riverbed sediment was re-suspended. The natural weathering process of the river basin might provide Zn (Chu et al., 2021). To avoid excessively high levels of particulate Zn, monitoring of particle discharge discharged into the river is necessary. An infiltration-based stormwater control system is one option for regulating this outflow (Behroozi et al., 2021).

The concentrations were greater at night, according to the baseflow study, therefore this should be reflected into the monitoring protocols. With greater proportions of dissolved Zn, particularly ZnCl2, the toxicity of Zn may rise (Pagano et al., 2017; Wagner et al., 2018). To keep Zn levels below the National Effluent Standards (NES) of 2.0 mg/L, wastewater treatment is unquestionably necessary. The annual wastewaters released to the Umeda River's tributary (the Sakai River) were all below the NES, according to earlier study, yet riverine Zn concentrations in the downstream portion remained exceptionally high during the winter season, when river

discharges were generally low (Andarani et al., 2021). As a result, the Zn loading released by PS (especially from human sources such as industrial plants) must be carefully regulated.

Chapter 7 Concluding remarks

7.1 Recall of the thesis objectives

The aim of this study was to assess the spatial and temporal variation and source identification of Zn in near-neutral rivers located in Aichi Prefecture, Japan. According to the Figure 1.5, designated surveys were conducted. The conclusions are drawn based on the several analysis methods discussed in the Chapter 6. Figure 7.1 shows a schematic conclusion described in the Chapter 7.2.

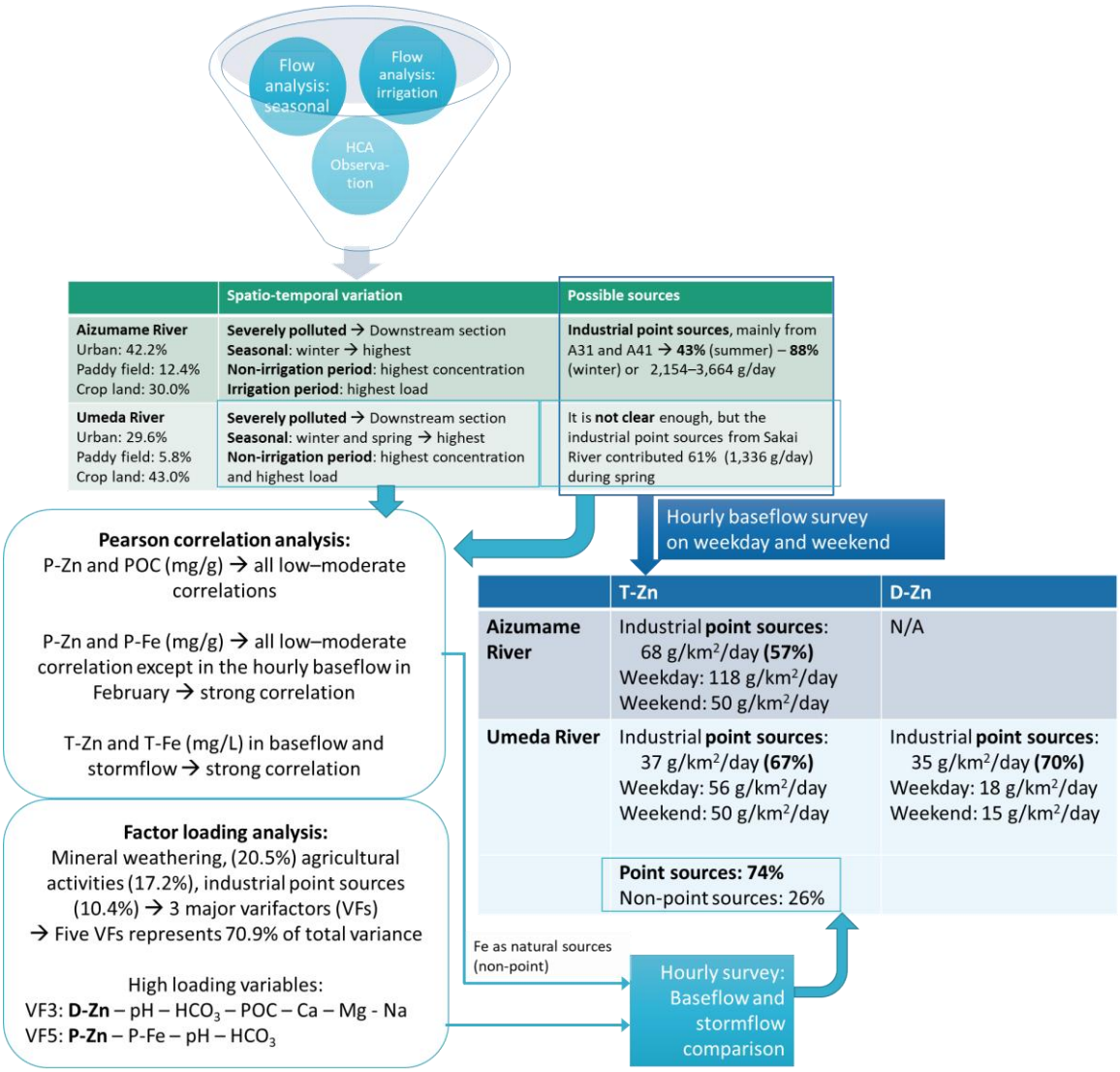

Figure 7.1 Schematic conclusions

7.2 Concluding remarks

Zn is a heavy metal that can be found in large quantities in the earth's crust. Regulators have imposed a strict environmental quality standard (EQS) for Zn (0.03 mg/L) due to its toxicity to aquatic life. Because multiple Japanese rivers still exceeded the EQS, it is inevitable to assess the Zn variability and identify its source in rivers.

The first study of Zn was conducted in the Aizumame River, Aichi Prefecture, which has a well-developed industrial area (42.2% of total catchment area). The EQS was breached in 2017 at the two downstream sampling stations (A4 = 0.059 mg/L; A5 = 0.055 mg/L) and tributaries (A31 = 0.284 mg/L and A41 = 0.232 mg/L). During the irrigation period, the average Zn concentration was lower than during the non-irrigation period. During the irrigation time, however, the load was greater. River flows were greater during irrigation, resulting in a lower concentration. Industrial regions were found to be the primary source of Zn, contributing anywhere from 2,154 g/day (43% in summer) to 3,664 g/day (88% in winter) into the mainstream. During the non-irrigation period, when only industrial discharges released Zn load to the mainstream, these contributions became more apparent.

The second assessment were conducted in the Umeda River, Aichi Prefecture. The study was performed through three survey types, i.e. the monthly baseflow, hourly baseflow (in February and October), and the hourly stormflow. Throughout the year, total Zn concentrations along the Umeda River fluctuated in spatial and temporal. During the spring and winter seasons, the greatest levels were observed, with concentrations typically increasing downstream. In February, during the winter season, all sample locations exhibited relatively high values ranging from 0.021 mg/L to 0.062 mg/L. At the most downstream part of the Umeda River, the annual mean concentration value of 0.031 mg/L has exceeded the EQS. Meanwhile, the middle-lower reach (U3, U4, and U23) almost exceeded the EQS. These sampling stations were located after the input of industrial discharges in Sakai River. It is likely that anthropogenic activities impacted Zn concentrations in the Umeda River.

In Aizumame River, the total Zn was obviously originated from the point source (mainly from industries) according to the load flow analyses. By contrast, in Umeda River, the industrial wastewater input was clearly observed only in spring (61.8%, 1,336 g/day), thus, further investigation was conducted. The hourly study in the Umeda River was carried out to assess the impact of human activities carried out during the week. The February survey has remarkably difference of total and dissolved Zn between weekday and weekend levels. The discrepancies in Zn concentrations and loads between weekday and weekend suggested that the increased Zn levels on weekday were influenced by industrial effluent. This difference between total fraction

of Zn concentrations on weekday and weekend was not observed in the October's survey. However, it is confirmed that the diel dissolved Zn occurred where the dissolved Zn has relatively higher level at night than during the daytime. The dissolved Zn concentrations were slightly higher on the weekday than those on weekend in the October hourly survey. Meanwhile, the variations in the Fe concentrations on weekday were relatively similar to those during weekend for both February and October, indicating that the source was mainly from the natural origins. A strong correlation between particulate Zn, particulate Fe, and POC concentrations at the most downstream sampling station (U5) suggested that organic matter and hydrous Fe oxides might have adsorbed Zn in the riverine system.

Aizumame River and Umeda River have different characteristics of river catchment. The Aizumame River was influenced by the paddy field irrigation (12.4%), different from the Umeda River where crop lands (30.0%) dominated the catchment area. Once again, the point sources were prominent in the Aizumame River, as the urban (42.2%) has slightly higher area than agricultural area. It is obvious that the total Zn levels in the Aizumame River were originated from the industrial point sources based on the hourly weekday and weekend survey. The total Zn loads were also affected by the irrigation so that the irrigation period has a higher load compared to non-irrigation period, in contrast to the total Zn concentration which has higher value in the non-irrigation period. The seasonal variation also showed that the highest total Zn load in Aizumame River was found in autumn followed by summer, spring, and winter. Meanwhile, in Umeda River the highest total Zn concentration and load was in non-irrigation period and winter. It should be noted that due to a small influence from paddy field (agricultural area comprises crop land 43.0% and paddy field 5.8%, whereas urban 29.6% of total watershed area), the river discharge in the Umeda River did not significantly differ between irrigation period and non-irrigation period. The contribution amount of total Zn loading from the industrial point sources in the Aizumame River was 68 g/km^2/day (57%), whereas in the Umeda River was 37 g/km^2/day (67%). Moreover, the dissolved phase in the Umeda River had higher input proportion to the riverine Zn levels (70%, 35 g/km^2/day).

Based on the comparison of baseflow and stormflow loadings in Umeda River, Zn possible sources were identified according to the type (point or non-point source). Both surveys were undertaken by high-resolution temporal sampling during a sunny day (baseflow) and during a rainy event (stormflow). The results revealed that in the baseflow, the primary sources were point sources, whereas in the stormflow, diffuse (non-point) sources were responsible for the extremely high concentrations of Zn in the Umeda River. Zn levels, mainly in particulate form, remained high even after the highest peak discharge occurred, indicating that non-point Zn sources may be abundant in the catchment. However, compared to suspended solid and Fe, the Zn were potentially

more diluted, and its source was exhausted at the end of storm event. As previously mentioned, the Fe in the baseflow and stormflow was primarily released from natural non-point sources. Using a simple end member mixing analysis with two tracers (Zn from point source and non-point source), approximately 74% of the Zn loads came from point sources and 26% originated from non-point sources. River management can be improved if Zn point sources are adequately managed. Given that Zn concentrations in wastewater were still below the national effluent standards, all of Zn loading inputs to the river should also be considered. During a storm event, it is also important to control the particulate Zn released into the river.

References

Abdel-Ghani, N.T., Elchaghaby, G.A., 2007. Influence of operating conditions on the removal of Cu, Zn, Cd and Pb ions from wastewater by adsorption. Int. J. Environ. Sci. Technol. 4, 451–456.

Akcay, H., Oguz, A., Karapire, C., 2003. Study of heavy metal pollution and speciation in Buyak Menderes and Gediz river sediments. Water Res. 37, 813–822. https://doi.org/10.1016/S0043-1354(02)00392-5

Allison, J.D., Allison, T.L., 2005. Partition coefficients for metals in surface water, soil, and waste. Washington, DC.

Alomary, A.A., Belhadj, S., 2007. Determination of heavy metals (Cd, Cr, Cu, Fe, Ni, Pb, Zn) by ICP-OES and their speciation in Algerian Mediterranean Sea sediments after a five-stage sequential extraction procedure. Environ. Monit. Assess. 135, 265–280. https://doi.org/10.1007/s10661-007-9648-8

Amoatey, P., Baawain, M.S., 2019. Effects of pollution on freshwater aquatic organisms. Water Environ. Res. 91, 1272–1287. https://doi.org/10.1002/wer.1221

Andarani, P., Alimuddin, H., Suzuki, R., Yokota, K., Inoue, T., 2021. Zinc contamination in surface water of the Umeda River, Japan. IOP Conf. Ser. Earth Environ. Sci. 623, 012064. https://doi.org/10.1088/1755-1315/623/1/012064

Andarani, P., Yokota, K., Saga, M., Inoue, T., Matsumoto, Y., 2020. Study of zinc pollution in river water: Average mass balance based on irrigation schedule. River Res. Appl. 36, 1286–1295. https://doi.org/10.1002/rra.3632

APHA (American Public Health Association), 2018. 2320 Alkalinity, in: Standard Methods For the Examination of Water and Wastewater. https://doi.org/10.2105/SMWW.2882.023

Autrup, H., Calow, P., Dekant, W., Greim, H., Wojciech, H., Janssen, C., Jansson, B., Komulainen, H., Ladefoged, O., Linders, J., Mangelsdorf, I., Nuti, M., Steenhout, A., Tarazona, J., Testai, E., Vighi, M., Viluksela, M., 2007. Risk Assessment Report on Zinc: Environmental Part, Scientific Committee on Health and Environmental Risks. Brussels.

Balistrieri, L.S., Nimick, D.A., Mebane, C.A., 2012. Assessing time-integrated dissolved concentrations and predicting toxicity of metals during diel cycling in streams. Sci. Total Environ. 425, 155–168. https://doi.org/10.1016/j.scitotenv.2012.03.008

Banerjee, K.S., Jittan, L., Ramkalawan, S., 2019. Spatial variational characteristics analysis of heavy metals pollution in the water of the Caroni River system: Case study from a tropical river. Water Sci. Technol. Water Supply 19, 2288–2297. https://doi.org/10.2166/ws.2019.110

Barber, L.B., Paschke, S.S., Battaglin, W.A., Douville, C., Fitzgerald, K.C., Keefe, S.H., Roth, D.A., Vajda, A.M., 2017. Effects of an Extreme Flood on Trace Elements in River Water - From Urban Stream to Major River Basin. Environ. Sci. Technol. 51, 10344–10356. https://doi.org/10.1021/acs.est.7b01767

Barringer, J.L., Wilson, T.P., Szabo, Z., Bonin, J.L., Fischer, J.M., Smith, N.P., 2008. Diurnal variations in, and influences on, concentrations of particulate and dissolved arsenic and metals in the mildly alkaline Wallkill River, New Jersey, USA. Environ. Geol. 53, 1183–1199. https://doi.org/10.1007/s00254-007-0708-8

Barthold, F.K., Tyralla, C., Schneider, K., Vaché, K.B., Frede, H.G., Breuer, L., 2011. How many

tracers do we need for end member mixing analysis (EMMA)? A sensitivity analysis. Water Resour. Res. 47, 1–14. https://doi.org/10.1029/2011WR010604

Bass, J. a B., Blust, R.J., Clarke, R.T., Corbin, T. a, Davison, W., De Schamphelaere, K. a C., Janssen, C.R., Kalis, E.J.J., Kelly, M.G., Kneebone, N.T., Lawlor, a J., Lofts, S., Temminghoff, E.J.M., Thacker, S. a, Tipping, E., Vincent, C.D., Warnken, K.W., Zhang, H., 2008. Environmental Quality Standards for Trace Metals in the Aquatic Environment, Environment. Environment Agency, Bristol.

Behrendt, H., 1993. Separation of point and diffuse loads of pollutants using monitoring data of rivers. Water Sci. Technol. 28, 165–175. https://doi.org/10.2166/wst.1993.0416

Behroozi, A., Arora, M., Fletcher, T.D., Western, A.W., Costelloe, J.F., 2021. Understanding the Impact of Soil Clay Mineralogy on the Adsorption Behavior of Zinc. Int. J. Environ. Res. https://doi.org/10.1007/s41742-021-00334-0

Bhatti, S.S., Sambyal, V., Nagpal, A.K., 2018. Analysis of Genotoxicity of Agricultural Soils and Metal (Fe, Mn, and Zn) Accumulation in Crops. Int. J. Environ. Res. 12, 439–449. https://doi.org/10.1007/s41742-018-0103-1

Billah, M.M., Kokushi, E., Uno, S., 2019. Distribution, Geochemical Speciation, and Bioavailable Potencies of Cadmium, Copper, Lead, and Zinc in Sediments from Urban Coastal Environment in Osaka Bay, Japan. Water. Air. Soil Pollut. 230. https://doi.org/10.1007/s11270-019-4196-8

Bodar, C.W.M., Pronk, M.E.J., Sijm, D.T.H.M., 2005. The European Union risk assessment on zinc and zinc compounds: the process and the facts. Integr. Environ. Assess. Manag. 1, 301–319. https://doi.org/10.1897/1551-3793(2005)1[301:TEURAO]2.0.CO;2

Bourg, A.C.M., Bertin, C., 1996. Diurnal variations in the water chemistry of a river contaminated by heavy metals: Natural biological cycling and anthropic influence. Water. Air. Soil Pollut. 86, 101–116. https://doi.org/10.1007/BF00279148

Bradley, S.B., Lewin, J., 1982. Transport of heavy metals on suspended sediments under high flow conditions in a mineralised region of wales. Environ. Pollution. Ser. B, Chem. Phys. 4, 257–267. https://doi.org/10.1016/0143-148X(82)90012-X

Brick, C.M., Moore, J.N., 1996. Diel variation of trace metals in the upper Clark Fork River, Montana. Environ. Sci. Technol. 30, 1953–1960. https://doi.org/10.1021/es9506465

Britannica, Acrisol. Encyclopedia Britannica. URL https://www.britannica.com/science/Acrisol (accessed 7.27.21).

Byrne, P., Onnis, P., Runkel, R.L., Frau, I., Lynch, S.F.L., Edwards, P., 2020. Critical Shifts in Trace Metal Transport and Remediation Performance under Future Low River Flows. Environ. Sci. Technol. 54, 15742–15750. https://doi.org/10.1021/acs.est.0c04016

Carolin, C.F., Kumar, P.S., Saravanan, A., Joshiba, G.J., Naushad, M., 2017. Efficient techniques for the removal of toxic heavy metals from aquatic environment: A review. J. Environ. Chem. Eng. 5, 2782–2799. https://doi.org/10.1016/j.jece.2017.05.029

Chasapis, C.T., Spiliopoulou, C.A., Loutsidou, A.C., Stefanidou, M.E., 2012. Zinc and human health: An update. Arch. Toxicol. 86, 521–534. https://doi.org/10.1007/s00204-011-0775-1

Chu, X., Wang, H., Zheng, F., Huang, C., Xu, C., Wu, D., 2021. Spatial Distribution Characteristics and Sources of Nutrients and Heavy Metals in the Xiujiang River of Poyang Lake Basin in the Dry Season. Water 13, 1654. https://doi.org/10.3390/w13121654

Ciszewski, D., Grygar, T.M., 2016. A Review of Flood-Related Storage and Remobilization of Heavy Metal Pollutants in River Systems. Water. Air. Soil Pollut. 227.

https://doi.org/10.1007/s11270-016-2934-8

Comber, S.D.W., Merrington, G., Sturdy, L., Delbeke, K., van Assche, F., 2008. Copper and zinc water quality standards under the EU Water Framework Directive: The use of a tiered approach to estimate the levels of failure. Sci. Total Environ. 403, 12–22. https://doi.org/10.1016/j.scitotenv.2008.05.017

Cooper, M., 2010. Advanced Bash-Scripting Guide An in-depth exploration of the art of shell scripting Table of Contents. Okt 2005 Abrufbar uber httpwww tldp orgLDPabsabsguide pdf Zugriff 1112 2005 2274, 2267–2274. https://doi.org/10.1002/hyp

Councell, T.B., Duckenfield, K.U., Landa, E.R., Callender, E., 2004. Tire-Wear Particles as a Source of Zinc to the Environment. Environ. Sci. Technol. 38, 4206–4214. https://doi.org/10.1021/es034631f

Dalai, T.K., Rengarajan, R., Patel, P.P., 2004. Sediment geochemistry of the Yamuna River System in the Himalaya: Implications to weathering and transport. Geochem. J. 38, 441–453. https://doi.org/10.2343/geochemj.38.441

Dali-youcef, N., Ouddane, B., Derriche, Z., 2006. Adsorption of zinc on natural sediment of Tafna River (Algeria). J. Hazard. Mater. 137, 1263–1270. https://doi.org/10.1016/j.jhazmat.2006.03.068

Dassenakis, M., Scoullos, M., Foufa, E., Krasakopoulou, E., Pavlidou, A., Kloukiniotou, M., 1998. Effects of multiple source pollution on a small Mediterranean river. Appl. Geochemistry 13, 197–211. https://doi.org/10.1016/S0883-2927(97)00065-6

Davutluoglu, O.I., Seckin, G., Ersu, C.B., Yilmaz, T., Sari, B., 2011. Assessment of Metal Pollution in Water and Surface Sediments of the Seyhan River, Turkey, Using Different Indexes. Clean - Soil, Air, Water 39, 185–194. https://doi.org/10.1002/clen.201000266

Dawson, E.J., Macklin, M.G., 1998. Speciation of heavy metals on suspended sediment under high flow conditions in the River Aire, West Yorkshire, UK. Hydrol. Process. 12, 1483–1494.https://doi.org/10.1002/(SICI)1099-1085(199807)12:9<1483::AID-HYP651>3.0.CO ;2-W

Degaffe, F.S., Turner, A., 2011. Leaching of zinc from tire wear particles under simulated estuarine conditions. Chemosphere 85, 738–743. https://doi.org/ 10.1016/j.chemosphere.2011.06.047

dos Reis, D.A., da Fonseca Santiago, A., Nascimento, L.P., Roeser, H.M.P., 2017. Influence of environmental and anthropogenic factors at the bottom sediments in a Doce River tributary in Brazil. Environ. Sci. Pollut. Res. 24, 7456–7467. https://doi.org/10.1007/s11356-017-8443-5

Driessen, P., Deckers, J., 2001. Mineral Soils conditioned by Limited Age, Lect. Notes Major Soils world. URL http://www.fao.org/3/Y1899E/y1899e08.htm#P2_46 (accessed 7.27.21).

Fu, J., Zhao, C., Luo, Y.Y., Liu, C., Kyzas, G.Z., Luo, Y.Y., Zhao, D., An, S., Zhu, H., 2014. Heavy metals in surface sediments of the Jialu River, China: Their relations to environmental factors. J. Hazard. Mater. 270, 102–109. https://doi.org/ 10.1016/j.jhazmat.2014.01.044

Fuchs, S., Scherer, U., Hillenbrand, T., Marscheider-Weidemann, F., Behrendt, H., Opitz, D., 2002. Emissions of Heavy Metals and Lindane into River Basins of Germany. Federal Environmental Agency (Umweltbundesamt), Berlin.

Gammons, C.H., Nimick, D.A., Parker, S.R., 2015. Diel cycling of trace elements in streams draining mineralized areas-A review. Appl. Geochemistry 57, 35–44. https://doi.org/10.1016/j.apgeochem.2014.05.008

Geological Survey of Japan, 2021. 1/50,000 geological map of Japan. URL https://gbank.gsj.jp/geonavi/geonavi.php#13,34.73110,137.46215 (accessed 7.27.21).

Gogoi, A., Tushara Chaminda, G.G., An, A.K.J., Snow, D.D., Li, Y., Kumar, M., 2016. Influence of ligands on metal speciation, transport and toxicity in a tropical river during wet (monsoon) period. Chemosphere 163, 322–333. https://doi.org/10.1016/j.chemosphere.2016.07.105

Gozzard, E., Mayes, W.M., Potter, H.A.B., Jarvis, A.P., 2011. Seasonal and spatial variation of diffuse (non-point) source zinc pollution in a historically metal mined river catchment, UK. Environ. Pollut. 159, 3113–3122. https://doi.org/10.1016/j.envpol.2011.02.010

Gromaire-Mertz, M.C., Garnaud, S., Gonzalez, A., Chebbo, G., 1999. Characterisation of urban runoff pollution in Paris. Water Sci. Technol. 39, 1–8. https://doi.org/10.1016/S0273-1223(99)00002-5

GSC (Geological Survey of Canada), 1995. National geochemical reconnaissance data. Ottawa, Natural Resources Canada, Government of Canada.

Guan, Q., Wang, L., Pan, B., Guan, W., Sun, X., Cai, A., 2016. Distribution features and controls of heavy metals in surface sediments from the riverbed of the Ningxia-Inner Mongolian reaches, Yellow River, China. Chemosphere 144, 29–42. https://doi.org/10.1016/j.chemosphere.2015.08.036

Guo, H., Barnard, A.S., 2013. Naturally occurring iron oxide nanoparticles: Morphology, surface chemistry and environmental stability. J. Mater. Chem. A 1, 27–42. https://doi.org/10.1039/c2ta00523a

Guo, X., Zhong, J., Song, Y., Tian, Q., 2010. Substance flow analysis of zinc in China. Resour. Conserv. Recycl. 54, 171–177. https://doi.org/10.1016/j.resconrec.2009.07.013

Gyorffy, E.J., Chan, H., 1992. Copper deficiency and microcytic anemia resulting from prolonged ingestion of over-the-counter zinc. Am. J. Gastroenterol. 87, 1054–1055.

Han, S., Naito, W., Hanai, Y., Masunaga, S., 2013. Evaluation of trace metals bioavailability in Japanese river waters using DGT and a chemical equilibrium model. Water Res. 47, 4880–4892. https://doi.org/10.1016/j.watres.2013.05.025

Hatakeyama, S., 1989. Effect of copper and zinc on the growth and emergence of Epeorus latifolium (Ephemeroptera) in an indoor model stream. Hydrobiologia 174, 17–27. https://doi.org/10.1007/BF00006054

He, W., Odnevall Wallinder, I., Leygraf, C., 2001. A laboratory study of copper and zinc runoff during first flush and steady-state conditions. Corros. Sci. 43, 127–146. https://doi.org/10.1016/S0010-938X(00)00066-4

Heijerick, D.G., De Schamphelaere, K.A.C., Janssen, C.R., 2002. Predicting acute zinc toxicity for Daphnia magna as a function of key water chemistry characteristics: Development and validation of a biotic ligand model. Environ. Toxicol. Chem. 21, 1309–1315. https://doi.org/10.1002/etc.5620210628

Hein, M.S., 2003. Copper deficiency anemia and nephrosis in zinc-toxicity: a case report. S. D. J. Med. 56, 143–147.

Hem, J.D., 1972. Chemistry and occurrence of cadmium and zinc in surface water and groundwater. Water Resour. Res. 8, 661–679. https://doi.org/10.1029/WR008i003p00661

Hjortenkrans, D., Bergbäck, B., Häggerud, A., 2006. New metal emission patterns in road traffic environments. Environ. Monit. Assess. 117, 85–98. https://doi.org/10.1007/s10661-006-7706-2

Hogstrand, C., 2011. Fish Physiology: Homeostasis and Toxicology of Essential Metals, Volume 31A. Academic Press, Canada.

Huang, G., Zhang, M., Liu, C., Li, L., Chen, Z., 2018. Heavy metal(loid)s and organic contaminants in groundwater in the Pearl River Delta that has undergone three decades of urbanization and industrialization: Distributions, sources, and driving forces. Sci. Total Environ. 635, 913–925. https://doi.org/10.1016/j.scitotenv.2018.04.210

Hüffmeyer, N., Klasmeier, J., Matthies, M., 2009. Geo-referenced modeling of zinc concentrations in the Ruhr river basin (Germany) using the model GREAT-ER. Sci. Total Environ. 407, 2296–2305. https://doi.org/10.1016/j.scitotenv.2008.11.055

International Zinc Association, 2014. Zinc in the Environment: an Introduction. URL https://www.zinc.org/wp-content/uploads/sites/4/2015/01/Zinc-in-the-Environment-Understanding-the-Science_web.pdf

Itahashi, S., Kasuya, M., Suzuki, R., Abe, K., Banzai, K., 2014. Assessment of potential risk to aquatic organisms by zinc originating from swine farm effluent in a rural area of Japan. Japan Agric. Res. Q. 48, 291–298. https://doi.org/10.6090/jarq.48.291

Jacquat, O., Voegelin, A., Kretzschmar, R., 2009. Local coordination of Zn in hydroxy-interlayered minerals and implications for Zn retention in soils. Geochim. Cosmochim. Acta 73, 348–363. https://doi.org/10.1016/j.gca.2008.10.026

Jain, C.K., Ram, D., 1997. Adsorption of lead and zinc on bed sediments of the River Kali. Water Res. 31, 154–162. https://doi.org/10.1016/S0043-1354(96)00232-1

Jain, C.K., Singhal, D.C., Sharma, M.K., 2004. Adsorption of zinc on bed sediment of River Hindon: Adsorption models and kinetics. J. Hazard. Mater. 114, 231–239. https://doi.org/10.1016/j.jhazmat.2004.09.001

Japan Meteorological Agency, 2021. Past weather data in Toyohashi City, Aichi Prefecture. URL https://www.data.jma.go.jp/obd/stats/etrn/index.php?prec_no=51&block_no=0470&year=2008&month=12&day=&view=p1 (accessed 7.27.21).

JAXA (Japan Aerospace Exploration Agency), 2021. ALOS2-2/ALOS Science Project. URL https://www.eorc.jaxa.jp/ALOS/en/lulc/lulc_jpn.htm (accessed 5.5.21).

Jensen, J., Larsen, M.M., Bak, J., 2016. National monitoring study in Denmark finds increased and critical levels of copper and zinc in arable soils fertilized with pig slurry. Environ. Pollut. 214, 334–340. https://doi.org/10.1016/j.envpol.2016.03.034

Jones, F., Bankiewicz, D., Hupa, M., 2014. Occurrence and sources of zinc in fuels. Fuel 117, 763–775. https://doi.org/10.1016/j.fuel.2013.10.005

Kanda, T., Takata, Y., Kohyama, K., Ohkura, T., Maejima, Y., Wakabayashi, S., Obara, H., 2018. New soil maps of Japan based on the comprehensive soil classification system of Japan - First approximation and its application to the world reference base for soil resources 2006. Japan Agric. Res. Q. 52, 285–292. https://doi.org/10.6090/jarq.52.285

Kay, R.T., Groschen, G.E., Cygan, G., Dupré David H., D.H., 2011. Diel cycles in dissolved barium, lead, iron, vanadium, and nitrite in a stream draining a former zinc smelter site near Hegeler, Illinois. Chem. Geol. 283, 99–108. https://doi.org/10.1016/j.chemgeo.2010.10.009

Ke, X., Gui, S., Huang, H., Zhang, H., Wang, C., Guo, W., 2017. Ecological risk assessment and source identification for heavy metals in surface sediment from the Liaohe River protected area, China. Chemosphere 175, 473–481. https://doi.org/10.1016/j.chemosphere.2017.02.029

Kimball, B.A., Runkel, R.L., 2009. Spatially detailed quantification of metal loading for decision

making: Metal mass loading to American fork and Mary Ellen Gulch, Utah. Mine Water Environ. 28, 274–290. https://doi.org/10.1007/s10230-009-0085-5

Kögel-Knabner, I., Amelung, W., 2014. 12.7 - Dynamics, Chemistry, and Preservation of Organic Matter in Soils, in: Holland, H.D., Turekian, K.K. (Eds.), Treatise on Geochemistry (Second Edition). Elsevier, Oxford, pp. 157–215. https://doi.org/10.1016/B978-0-08-095975-7.01012-3

Kunimatsu, T., Otomori, T., Osaka, K., Hamabata, E., Komai, Y., 2006. Evaluation of nutrient loads from a mountain forest including storm runoff loads. Water Sci. Technol. 53, 79–91. https://doi.org/10.2166/wst.2006.041

Kurz, M.J., de Montety, V., Martin, J.B., Cohen, M.J., Foster, C.R., 2013. Controls on diel metal cycles in a biologically productive carbonate-dominated river. Chem. Geol. 358, 61–74. https://doi.org/10.1016/j.chemgeo.2013.08.042

Le Floch, M., Noack, Y., Robin, D., 2003. Emission sources identification in a vinicity of the municipal solid waste incinerator of Toulon in the South of France. J. Phys. IV Fr. 107, 727–730. https://doi.org/10.1051/jp4:20030404

Le Pape, P., Ayrault, S., Quantin, C., 2012. Trace element behavior and partition versus urbanization gradient in an urban river (Orge River, France). J. Hydrol. 472–473, 99–110. https://doi.org/10.1016/j.jhydrol.2012.09.042

Legret, M., Pagotto, C., 1999. Evaluation of pollutant loadings in the runoff waters from a major rural highway. Sci. Total Environ. 235, 143–150. https://doi.org/10.1016/S0048-9697(99)00207-7

Levard, C., Basile-Doelsch, I., 2016. Chapter 3 - Geology and Mineralogy of Imogolite-Type Materials, in: Yuan, P., Thill, A., Bergaya, F. (Eds.), Nanosized Tubular Clay Minerals, Developments in Clay Science. Elsevier, pp. 49–65. https://doi.org/10.1016/B978-0-08-100293-3.00003-0

Levenberg, K., Arsenal, F., 1943. A Method for the Solution of Certain Non-Linear Problems in Least Squares. Q. Appl. Math. 1, 536–538.

Li, Y.N., Duan, Z., Li, J., Shao, Z., Mo, J., Wu, J., Ling, S., Liu, Z., Chen, C., 2020. Quantitative analysis of trace metals in the Raritan River with inductively coupled plasma mass spectrometer. Water Sci. Technol. Water Supply 20, 3183–3193. https://doi.org/10.2166/ws.2020.206

Liao, J., Chen, J.J., Ru, X., Chen, J.J., Wu, H., Wei, C., 2017. Heavy metals in river surface sediments affected with multiple pollution sources, South China: Distribution, enrichment and source apportionment. J. Geochemical Explor. 176, 9–19. https://doi.org/10.1016/j.gexplo.2016.08.013

Lough, G.C., Schauer, J.J., Park, J.-S., Shafer, M.M., DeMinter, J.T., Weinstein, J.P., 2005. Emissions of Metals Associated with Motor Vehicle Roadways. Environ. Sci. Technol. 39, 826–836. https://doi.org/10.1021/es048715f

Maanan, Mohamed, Saddik, M., Maanan, Mehdi, Chaibi, M., Assobhei, O., Zourarah, B., 2015. Environmental and ecological risk assessment of heavy metals in sediments of Nador lagoon, Morocco. Ecol. Indic. 48, 616–626. https://doi.org/10.1016/j.ecolind.2014.09.034

Manceau, A., Marcus, M.A., Tamura, N., 2002. Quantitative Speciation of Heavy Metals in Soils and Sediments by Synchrotron X-ray Techniques. Rev. Mineral. Geochemistry 49, 341–428. https://doi.org/10.2138/gsrmg.49.1.341

Mansoor, S.Z., Louie, S., Lima, A.T., Van Cappellen, P., MacVicar, B., 2018. The spatial and temporal distribution of metals in an urban stream: A case study of the Don River in Toronto,

Canada. J. Great Lakes Res. 44, 1314–1326. https://doi.org/10.1016/j.jglr.2018.08.010

Mansoorian, H.J., Mahvi, A.H., Jafari, A.J., 2014. Removal of lead and zinc from battery industry wastewater using electrocoagulation process: Influence of direct and alternating current by using iron and stainless steel rod electrodes. Sep. Purif. Technol. 135, 165–175. https://doi.org/10.1016/j.seppur.2014.08.012

Marquardt, D.W., 1963. An Algorithm for Least-Squares Estimation of Nonlinear Parameters. J. Soc. Ind. Appl. Math. 11, 431–441. https://doi.org/10.1137/0111030

Maslennikova, S., Larina, N., Larin, S., 2012. The effect of sediment grain size on heavy metal content. Lakes, Reserv. ponds 6, 43–54.

Matsuyama, N., Saigusa, M., Abe, T., 1994. Distributions of Allophanic Andosols and Nonallophanic Andosols in Kanto and Chubu Districts. Japanese J. Soil Sci. Plant Nutr. 65, 304–312. https://doi.org/10.20710/dojo.65.3_304

Matsuzaki, K., 2011. Validation trial of Japan's zinc water quality standard for aquatic life using field data. Ecotoxicol. Environ. Saf. 74, 1808–1823. https://doi.org/10.1016/j.ecoenv.2011.07.003

Mayes, W.M., Perks, M.T., Large, A.R.G., Davis, J.E., Gandy, C.J., Orme, P.A.H., Jarvis, A.P., 2021. Effect of an extreme flood event on solute transport and resilience of a mine water treatment system in a mineralised catchment. Sci. Total Environ. 750, 141693. https://doi.org/10.1016/j.scitotenv.2020.141693

Miller, C. V., Foster, G.D., Majedi, B.F., 2003. Baseflow and stormflow metal fluxes from two small agricultural catchments in the Coastal Plain of the Chesapeake Bay Basin, United States. Appl. Geochemistry 18, 483–501. https://doi.org/10.1016/S0883-2927(02)00103-8

Ministry of Environment of Japan, 2021. Pollution Release and Transfer Register for all substances in 2019 (in Japanese). URL http://www2.env.go.jp/chemi/ prtr/prtrinfo/contents/openPrtr2.do# (accessed 7.27.21).

Ministry of Environment of Japan, 2018. Pollutant Release and Transfer Register (PRTR) Data Page (in Japanese). URL http://www2.env.go.jp/chemi/prtr/prtrinfo/index.html (accessed 11.30.20).

Ministry of the Environment of Japan: Water and Air Environment Bureau, 2020. Results of water quality measurement of public water bodies in the first year of Reiwa (in Japanese). URL https://www.env.go.jp/water/suiiki/index.html (accessed 7.27.21).

Mishima, S., Taniguchi, S., Kawasaki, A., Komada, M., 2005. Estimation of Zinc and Copper Balance in Japanese Farmland Soil Associated with the Application of Chemical Fertilizers and Livestock Excreta. Soil Sci. Plant Nutr. 51, 437–442. https://doi.org/10.1111/j.1747-0765.2005.tb00050.x

Mohiuddin, K.M., Otomo, K., Ogawa, Y., Shikazono, N., 2012. Seasonal and spatial distribution of trace elements in the water and sediments of the Tsurumi River in Japan. Environ. Monit. Assess. 184, 265–279. https://doi.org/10.1007/s10661-011-1966-1

Montalvo, D., Degryse, F., da Silva, R.C., Baird, R., McLaughlin, M.J., 2016. Agronomic Effectiveness of Zinc Sources as Micronutrient Fertilizer, Advances in Agronomy. Elsevier Inc. https://doi.org/10.1016/bs.agron.2016.05.004

Morrill, J.C., Bales, R.C., Conklin, M.H., 2001. The relationship between air temperature and stream temperature, in: American Geophysical Union, Spring Meeting.

Naito, W., Kamo, M., Tsushima, K., Iwasaki, Y., 2010. Exposure and risk assessment of zinc in Japanese surface waters. Sci. Total Environ. 408, 4271–4284.

https://doi.org/10.1016/j.scitotenv.2010.06.018

Nicolau, R., Lucas, Y., Merdy, P., Raynaud, M., 2012. Base flow and stormwater net fluxes of carbon and trace metals to the Mediterranean sea by an urbanized small river. Water Res. 46, 6625–6637. https://doi.org/10.1016/j.watres.2012.01.031

Nimick, D.A., Gammons, C.H., Cleasby, T.E., Madison, J.P., Skaar, D., Brick, C.M., 2003. Diel cycles in dissolved metal concentrations in streams: Occurrence and possible causes. Water Resour. Res. 39, 1247. https://doi.org/10.1029/2002WR001571

Nimick, D.A., Gammons, C.H., Parker, S.R., 2011. Diel biogeochemical processes and their effect on the aqueous chemistry of streams: A review. Chem. Geol. 283, 3–17. https://doi.org/10.1016/j.chemgeo.2010.08.017

Oguntade, O.A., Adetunji, M.T., Azeez, J.O., 2015. Uptake of manganese, iron, copper, zinc and chromium by Amaranthus cruentus L. irrigated with untreated dye industrial effluent in low land field. J. Environ. Chem. Eng. 3, 2875–2881. https://doi.org/10.1016/j.jece.2015.10.022

Pagano, M., Porcino, C., Briglia, M., Fiorino, E., Vazzana, M., Silvestro, S., Faggio, C., 2017. The Influence of Exposure of Cadmium Chloride and Zinc Chloride on Haemolymph and Digestive Gland Cells from Mytilus galloprovincialis. Int. J. Environ. Res. 11, 207–216. https://doi.org/10.1007/s41742-017-0020-8

Parizanganeh, A., 2008. Grain size effect on trace metals in contaminated sediments along the Iranian coast of the Caspian Sea, in: The 12th World Lake Conference. pp. 329–336.

Parker, S.R., Gammons, C.H., Jones, C.A., Nimick, D.A., 2007. Role of hydrous iron oxide formation in attenuation and diel cycling of dissolved trace metals in a stream affected by acid rock drainage. Water. Air. Soil Pollut. 181, 247–263. https://doi.org/10.1007/s11270-006-9297-5

Priadi, C., Bourgeault, A., Ayrault, S., Gourlay-Francé, C., Tusseau-Vuillemin, M.-H., Bonté, P., Mouchel, J.-M., 2011. Spatio-temporal variability of solid{,} total dissolved and labile metal: passive vs. discrete sampling evaluation in river metal monitoring. J. Environ. Monit. 13, 1470–1479. https://doi.org/10.1039/C0EM00713G

Resongles, E., Casiot, C., Freydier, R., Le Gall, M., Elbaz-Poulichet, F., 2015. Variation of dissolved and particulate metal(loid) (As, Cd, Pb, Sb, Tl, Zn) concentrations under varying discharge during a Mediterranean flood in a former mining watershed, the Gardon River (France). J. Geochemical Explor. 158, 132–142. https://doi.org/10.1016/j.gexplo.2015.07.010

Richardson, G.M., Garrett, R., Mitchell, I., Mah-Poulson, M., Hackbarth, T., 2001. Critical review on natural global and regional emissions of six trace metals to the atmosphere, Research Organisation, the International Copper Association, and the Nickel Producers Environmental Research Association. Canada. URL https://www.echa.europa.eu/documents/10162/13630/vrar_appendix_p2_en.pdf (accessed 9.27.20).

Rose, S., Crean, M.S., Sheheen, D.K., Ghazi, A.M., 2001. Comparative zinc dynamics in Atlanta metropolitan region stream and street runoff. Environ. Geol. 40, 983–992. https://doi.org/10.1007/s002540100285

Rose, S., Shea, J.A., 2007. Chapter 6 Environmental geochemistry of trace metal pollution in urban watersheds. Dev. Environ. Sci. 5, 99–131. https://doi.org/10.1016/S1474-8177(07)05006-1

Rothwell, J.J., Evans, M.G., Daniels, S.M., Allott, T.E.H., 2007. Baseflow and stormflow metal concentrations in streams draining contaminated peat moorlands in the Peak District

National Park (UK). J. Hydrol. 341, 90–104. https://doi.org/10.1016/j.jhydrol.2007.05.004

Rudall, S., Jarvis, A.P., 2012. Diurnal fluctuation of zinc concentration in metal polluted rivers and its potential impact on water quality and flux estimates. Water Sci. Technol. 65, 164–170. https://doi.org/10.2166/wst.2011.834

Sage, J., El Oreibi, E., Saad, M., Gromaire, M.C., 2016. Modeling the temporal variability of zinc concentrations in zinc roof runoff—experimental study and uncertainty analysis. Environ. Sci. Pollut. Res. 23, 16552–16566. https://doi.org/10.1007/s11356-016-6827-6

Sakata, M., Marumoto, K., 2004. Dry Deposition Fluxes and Deposition Velocities of Trace Metals in the Tokyo Metropolitan Area Measured with a Water Surface Sampler. Environ. Sci. Technol. 38, 2190–2197. https://doi.org/10.1021/es030467k

Sakata, M., Narukawa, M., Marumoto, K., 2005. Atmospheric and riverine inputs of trace substances to Tokyo Bay, Report of Central Research Institute of Electric Power Industry (CRIEPI).

Sakson, G., Brzezinska, A., Zawilski, M., 2018. Emission of heavy metals from an urban catchment into receiving water and possibility of its limitation on the example of Lodz city. Environ. Monit. Assess. 190, 281. https://doi.org/10.1007/s10661-018-6648-9

Schroeder, H.A., Nason, A.P., Tipton, I.H., Balassa, J.J., 1967. Essential trace metals in man: Zinc. Relation to environmental cadmium. J. Chronic Dis. 20, 179–210. https://doi.org/10.1016/0021-9681(67)90002-1

Sedeño-Díaz, J.E., López-López, E., Mendoza-Martínez, E., Rodríguez-Romero, A.J., Morales-García, S.S., 2020. Distribution coefficient and metal pollution index in water and sediments: Proposal of a new index for ecological risk assessment of metals. Water (Switzerland) 12. https://doi.org/10.3390/w12010029

Seto, M., Wada, S., Suzuki, S., 2013. The effect of zinc on aquatic microbial ecosystems and the degradation of dissolved organic matter. Chemosphere 90, 1091–1102. https://doi.org/10.1016/j.chemosphere.2012.09.014

Shikazono, N., Zakir, H.M., Sudo, Y., 2008. Zinc contamination in river water and sediments at Taisyu Zn-Pb mine area, Tsushima Island, Japan. J. Geochemical Explor. 98, 80–88. https://doi.org/10.1016/j.gexplo.2007.12.002

Shope, C.L., Xie, Y., Gammons, C.H., 2006. The influence of hydrous Mn-Zn oxides on diel cycling of Zn in an alkaline stream draining abandoned mine lands. Appl. Geochemistry 21, 476–491. https://doi.org/10.1016/j.apgeochem.2005.11.004

Simon-Hertich, B., Wibbertmann, A., Wagner, D., Tomaska, L., Malcolm, H., 2001. Environmental Health Criteria 221 ZINC, Environmental Health Criteria. Geneva.

Singh, A.K., Hasnain, S.I., Banerjee, D.K., 1999. Grain size and geochemical partitioning of heavy metals in sediments of the Damodar River - A tributary of the lower Ganga, India. Environ. Geol. 39, 90–98. https://doi.org/10.1007/s002540050439

Smith, J.C., Mcdaniel, E.G., Fan, F.F., Halsted, J.A., 1973. Zinc: A trace element essential in vitamin A metabolism. Science 181. 954–955. https://doi.org/10.1126/science.181.4103.954

Sörme, L., Lagerkvist, R., 2002. Sources of heavy metals in urban wastewater in Stockholm. Sci. Total Environ. 298, 131–145. https://doi.org/10.1016/S0048-9697(02)00197-3

Sullivan, A.B., Drever, J.I., 2001. Spatiotemporal variability in stream chemistry in a high-elevation catchment affected by mine drainage. J. Hydrol. 252, 237–250. https://doi.org/10.1016/S0022-1694(01)00458-9

Superville, P.J., Prygiel, E., Mikkelsen, O., Billon, G., 2015. Dynamic behaviour of trace metals in the DeÛle River impacted by recurrent polluted sediment resuspensions: From diel to seasonal evolutions. Sci. Total Environ. 506–507, 585–593. https://doi.org/10.1016/j.scitotenv.2014.11.044

Tabayashi, H., Daigo, I., Matsuno, Y., Adachi, Y., 2009. Development of a dynamic substance flow model of zinc in Japan 49, 1265–1271.

Tachibana, J., Hirota, K., Goto, N., Fujie, K., 2008. A method for regional-scale material flow and decoupling analysis: A demonstration case study of Aichi prefecture, Japan. Resour. Conserv. Recycl. 52, 1382–1390. https://doi.org/10.1016/j.resconrec.2008.08.003

Tansel, B., Rafiuddin, S., 2016. Heavy metal content in relation to particle size and organic content of surficial sediments in Miami River and transport potential. Int. J. Sediment Res. 31, 324–329. https://doi.org/10.1016/j.ijsrc.2016.05.004

Tessier, A., Campbell, P.G.C., Bisson, M., 1982. Particulate trace metal speciation in stream sediments and relationships with grain size: Implications for geochemical exploration. J. Geochemical Explor. 16, 77–104. https://doi.org/10.1016/0375-6742(82)90022-X

Tsushima, K., Naito, W., Kamo, M., 2010. Assessing ecological risk of zinc in Japan using organism- and population-level species sensitivity distributions. Chemosphere 80, 563–569. https://doi.org/10.1016/j.chemosphere.2010.04.031

US-EPA, 1980. Ambient Water Quality Criteria for Zinc, EPA 440/5-80-079. United States.

US-EPA, 2006. Data Quality Assessment: Statistical Methods for Practitioners. United States.

Vega, M., Pardo, R., Barrado, E., Debán, L., 1998. Assessment of seasonal and polluting effects on the quality of river water by exploratory data analysis. Water Res. 32, 3581–3592. https://doi.org/10.1016/S0043-1354(98)00138-9

Viers, J., Dupré, B., Gaillardet, J., 2009. Chemical composition of suspended sediments in World Rivers: New insights from a new database. Sci. Total Environ. 407, 853–868. https://doi.org/10.1016/j.scitotenv.2008.09.053

Vu, C.T., Lin, C., Shern, C.C., Yeh, G., Le, V.G., Tran, H.T., 2017. Contamination, ecological risk and source apportionment of heavy metals in sediments and water of a contaminated river in Taiwan. Ecol. Indic. 82, 32–42. https://doi.org/10.1016/j.ecolind.2017.06.008

Wagner, S., Hüffer, T., Klöckner, P., Wehrhahn, M., Hofmann, T., Reemtsma, T., 2018. Tire wear particles in the aquatic environment - A review on generation, analysis, occurrence, fate and effects. Water Res. 139, 83–100. https://doi.org/10.1016/j.watres.2018.03.051

Wahaab, R.A., Alseroury, F.A., 2019. Wastewater treatment: a case study of electronics manufacturing industry. Int. J. Environ. Sci. Technol. 16, 47–58. https://doi.org/10.1007/s13762-017-1529-2

Water Framework Directive, 2015. The Water Framework Directive (Standards and Classification) Directions (England and Wales), Water Framework Directive.

Water Framework Directive, 2010. The River Basin Districts Typology, Standards and Groundwater threshold values (Water Framework Directive) (England and Wales) Directions.

Wen, Y., Yang, Z., Xia, X., 2013. Dissolved and particulate zinc and nickel in the Yangtze River (China): Distribution, sources and fluxes. Appl. Geochemistry 31, 199–208. https://doi.org/10.1016/j.apgeochem.2013.01.004

Whitney, P.R., 1975. Relationship of manganese-iron oxides and associated heavy metals to grain size in stream sediments. J. Geochemical Explor. 4, 251–263. https://doi.org/10.1016/0375-

6742(75)90005-9

Xu, F.F., Liu, Z., Cao, Y., Qiu, L., Feng, J., Xu, F.F., Tian, X., 2017. Assessment of heavy metal contamination in urban river sediments in the Jiaozhou Bay catchment, Qingdao, China. Catena 150, 9–16. https://doi.org/10.1016/j.catena.2016.11.004

Yamada, T., Inoue, T., Tsushima, K., Nagai, M., Kiso, Y., 2009. Nutrient Loss from a Tea Plantation Area in Japan. J. Water Environ. Technol. 7, 331–340. https://doi.org/10.2965/jwet.2009.331

Yamagata, H., Yoshizawa, M., Minamiyama, M., 2010. Assessment of current status of zinc in wastewater treatment plants to set effluent standards for protecting aquatic organisms in Japan. Environ. Monit. Assess. 169, 67–73. https://doi.org/10.1007/s10661-009-1151-y

Yang, Y., He, Z., Lin, Y., Phlips, E.J., Stoffella, P.J., Powell, C.A., 2009. Temporal and Spatial Variations of Copper, Cadmium, Lead, and Zinc in Ten Mile Creek in South Florida, USA. Water Environ. Res. 81, 40–50. https://doi.org/10.2175/106143008x296479

Yokota, K., Inoue, T., Yokokawa, M., Shimoyama, R., Okubo, Y., 2013. Evaluation of nitrogen and phosphorus runoff load in rivers based on high-frequency surveys. Environ. Sci. 26, 140 (in Japanese).

Yoshimura, C., Omura, T., Furumai, H., Tockner, K., 2005. Present state of rivers and streams in Japan. River Res. Appl. 21, 93–112. https://doi.org/10.1002/rra.835

Zeng, J., Han, G., 2020. Tracing zinc sources with Zn isotope of fluvial suspended particulate matter in Zhujiang River, southwest China. Ecol. Indic. 118, 106723. https://doi.org/10.1016/j.ecolind.2020.106723

Zhang, G., Bai, J., Xiao, R., Zhao, Q., Jia, J., Cui, B., Liu, X., 2017. Heavy metal fractions and ecological risk assessment in sediments from urban, rural and reclamation-affected rivers of the Pearl River Estuary, China. Chemosphere 184, 278–288. https://doi.org/10.1016/j.chemosphere.2017.05.155

Zhen, G., Li, Y., Tong, Y., Yang, L., Zhu, Y., Zhang, W., 2016. Temporal variation and regional transfer of heavy metals in the Pearl (Zhujiang) River, China. Environ. Sci. Pollut. Res. 23, 8410–8420. https://doi.org/10.1007/s11356-016-6077-7